

A Study on the Failure Mechanics of the Side Structure of a Struck
Ship due to Impact Forces

Thesis submitted for the
Degree of Master of Science
in the Faculty of Engineering
of the University of Glasgow

By

William Alifrangis

Department of Naval Architecture and Ocean Engineering
University of Glasgow

October 1999

© William Alifrangis, 1999

ProQuest Number: 13818936

All rights reserved

INFORMATION TO ALL USERS

The quality of this reproduction is dependent upon the quality of the copy submitted.

In the unlikely event that the author did not send a complete manuscript and there are missing pages, these will be noted. Also, if material had to be removed, a note will indicate the deletion.



ProQuest 13818936

Published by ProQuest LLC (2018). Copyright of the Dissertation is held by the Author.

All rights reserved.

This work is protected against unauthorized copying under Title 17, United States Code
Microform Edition © ProQuest LLC.

ProQuest LLC.
789 East Eisenhower Parkway
P.O. Box 1346
Ann Arbor, MI 48106 – 1346

GLASGOW
UNIVERSITY
LIBRARY

11788 (copy 1)

This thesis is dedicated to my Family

Evangelos and Amalia

and Dimitris

and to my fiancée

Maria

DECLARATION

Except where reference is made to the work of others,
this thesis is believed to be original

Table of Contents

Aknowledgements.....	1
Notation.....	3

Chapter 1 Introduction and Literature Review

Introduction.....	6
1.1 Collision Statistics.....	8
1.2 Protection against Collision.....	10
1.3 Assumptions used in Collision Evaluation.....	12
1.4 Dynamic Effects.....	15
1.4.1 Inertia Force.....	15
1.4.2 Strain Hardening Effect.....	15
1.5 External and Internal Mechanics of Collision.....	16
1.6 Literature Review.....	17
1.6.1 Minor Collision Methods.....	17
1.6.2 Major Collision Methods.....	20
1.7 Conclusions.....	27
1.8 Aim of the Thesis.....	28
1.9 Layout of the Thesis.....	29
Figures.....	31

Chapter 2 Internal Mechanics of Ship to Ship Collisions

Introduction.....	42
2.1 Internal Mechanics of Ship to Ship Collisions.....	43
2.2 Methods of Treatment.....	44
2.3 Structural Members involved in Collision.....	45
2.4 Mathematical Modelling of the Internal Collision Mechanics.....	46
2.5 Difficulties arising due to New Structures.....	48
2.6 Analytical Presentation of the Failure Modes of Individual Structural Members and their Role in Collision.....	50
2.7 Conclusions.....	55
Figures.....	58

Chapter 3 Assessment of Collision Resistance of Ships

Introduction.....	66
3.1 Proposed Method – Hegazy (1980).....	68
3.2 Assumptions.....	70
3.3 Theoretical Analysis of the Various Components of Energy Absorption.....	72
3.3.1 Determination of the Critical Indentation.....	73
3.4 Energy Absorbed by Different Parts of the Ship's Structure.....	75
3.4.1 Energy absorbed due to membrane tension in the stiffened side plating of the struck ship.....	75
3.4.2 Energy absorbed due to membrane tension in the decks of the struck ship.....	77
3.4.3 Energy absorbed due to buckling of the decks of the struck ship.....	78
3.4.4 Energy absorbed due to buckling of deck transverses in the decks of the struck ship.....	79

3.4.5 Energy absorbed due to the collapse of side transverses of the struck ship.....	80
3.4.6 Rupture of hull and deck plating of the struck ship.....	81
3.4.7 Energy absorbed due to wedge splitting of decks.....	84
3.4.8 Energy dissipated in crushing the bow of the striking ship.....	87
3.5 Minor and Major Collisions.....	89
3.5.1 Minor Collisions.....	89
3.5.2 Major Collisions.....	90
3.6 Conclusions.....	91
3.7 Development of Fortran Code based on Hegazy's Method.....	92
3.8 Application on a Small Oil Tanker design.....	94
3.9 Results and Conclusions.....	96
Figures.....	99

Chapter 4 Buckling Strength of the Decks

Introduction.....	117
4.1 Orthotropic and Discrete Beam Method.....	119
4.2 Parameters affecting Stiffened Plating Strength.....	121
4.3 Proposed Method – Pu and Das (1994).....	122
4.4 Incorporation of the Proposed Method to the Program.....	126
4.5 Comparison of the Results and Conclusions.....	127
Figures.....	129

Chapter 5 Estimation of the Crashworthiness of a Double-Hull Vessel

Introduction.....	142
5.1 Introduction of the Method to a Double-Hull Design.....	143
5.2 Mathematical model for the Double-Hull Tanker.....	144
5.3 Assumptions.....	148
5.4 Collision Scenarios.....	151
5.4.1 Estimation of the Drafts.....	152
5.5 Results and Conclusions.....	153
Figures.....	160

Chapter 6 Estimation of the Crashworthiness of a Single-Hull Tanker

Introduction.....	186
6.1 Single-skin Tanker.....	187
6.2 Application of the Proposed Method.....	188
6.3 Results and Conclusions.....	189
6.4 Comparison of the Crashworthiness of the double and single- skinned tankers.....	192
Figures.....	194

Chapter 7 Parametric Optimisation of the Double-Hull Tanker Structure

Introduction.....	207
7.1 Web Frames Spacing.....	209
7.2 Distance between the outer and inner hull.....	209
7.3 Double bottom height.....	210
7.4 Addition of Material to the Structure.....	210
7.5 Conclusions.....	213
Figures.....	215

Chapter 8 Conclusions and Proposals

8.1 Assessment and Conclusions of the Work.....	223
8.2 Proposals.....	228
 List of References.....	 230
 Appendix A Mid-ship section design Calculations	
Appendix B Energy absorbed due to membrane tension in the stiffened hull of the struck ship	
Appendix C Energy absorbed due to membrane tension in the stiffened decks of the struck ship	
Appendix D Buckling Strength of Deck Structures	
Appendix E Limiting Value of the Indentation beyond which rupture of the hull occurs	

Acknowledgements

This thesis was conducted in the Department of Naval Architecture and Ocean Engineering at the University of Glasgow during the last year. A number of people contributed in many ways in order this work to come to a successful end.

First of all I would like to thank my father and my mother for providing me with the financial and moral support, which was required for the conduction of a Master degree.

Furthermore, I would like to thank my supervisor, Dr. P.K. Das and the head of the department Prof. Nigel Barltrop for their assistance throughout my M.Sc. The weekly discussions with Dr. Das were one of the reasons that the present work became feasible in this amount of time. His consistent supervision, the lengthy discussions and the moral encouragement that he provided to me were invaluable.

I wish to express my gratitude to Prof. Nigel Barltrop for the interest he showed for me from the early days that I arrived in Glasgow. I received from him brilliant guidelines required for the completion of my project.

I would also like to thank Dr S. Day for the discussions we had regarding several parts of my project.

I am indebted to Maureen McGrady, the secretary of the department for helping me in every problem I faced regarding or not the University.

I wish to express my thanks to Dr. Alexandros Glykas, who helped me to join the department and brought me in contact with Prof. N., Barltrop, while he was finishing his Ph.D. in Glasgow University.

Special thanks to Trym Tveitnes and John Tsarouchas for the help and the very nice time we had in the department's office and out of it. I would like to thank also Lee Yu for his help on various aspects of my work.

I wish to thank also my fiancée Maria Balta for the moral support and the patience she showed.

I finally would like to thank Mr Griffith Roberts, technical manager of Nomikos Ltd, which provide me some midship section designs and also a recent copy of the ABS regulations.

Last but not least I would like to thank my brother Dimitri Alifrangi for his encouragement and support and my other roommate Panagioti Moraiti for their patience, when the pressure of the work did not make me the perfect company. Also thanks to Pari, Niko, Christo, Alexi and Stelio.

Notation

σ'_0 : dynamic flow stress

$\left(\dot{\epsilon}\right)$: strain rate

E_T : (eq.(1.6.1.1)) total energy absorbed by the struck's ship structure

σ_y : yield stress of the material

R_T : volume of the damaged material

$E_{(a,b)}$: (eq(1.6.1.3)) energy absorbed by the side structure for strike other than a mid-span strike.

E_{CL} : (eq(1.6.1.3)) energy absorbed considering a mid-span strike.

M_B, V_B : mass and velocity at impact of striking vessel

M_A, V_A : mass and velocity of the struck vessel

K_T : kinetic energy lost in collision

dm: added mass accounting for the hydrodynamic resistance of the surrounding water

L: half distance between web frames

$2b_e$: effective width of deck plating = $2 \cdot C \cdot t_d \cdot \sqrt{\frac{E}{\sigma_y}}$, by Timoshenko

E= modulus of elasticity

C= experimental constant varying with the proportions of the plate. $C \approx 1.0$.

$\gamma = \sigma_{\alpha} / \sigma_y$

t_d = thickness of deck plating.

σ_{α} = buckling stress of the frame alone (for calculating σ_{α} the span of deck transverse is taken as the distance between ship's side and the nearest heavy longitudinal girder).

A= cross sectional area of the frame alone.

H= vertical depth of damage in the struck ship

t_s : thickness of the side plating (equivalent thickness allowing for stiffeners)

n : number of decks involved in collision in the struck ship

q : intensity of the uniformly distributed load acting on a side transverse

q_c : uniformly distributed load to cause collapse of a side transverse

s : frame spacing

y : wedge penetration into the deck of the struck ship

A_d : Cross-sectional area of stiffened decks in the bow structure of the striking vessel involved in collision

A_s : Cross-sectional area of stiffened side shell plating of the striking bow

D : distance between decks

E_1 : energy absorbed due to membrane tension in the stiffened side shell plating of the struck ship

E_2 : energy absorbed due to membrane tension in the decks of the struck ship

E_3 : energy absorbed due to buckling of the decks of the struck ship.

E_4 : energy absorbed due to the collapse of the deck transverses in the struck ship

E_5 : energy absorbed due to the collapse of the side transverses in the struck ship

E_6 : energy absorbed due to wedge splitting of the decks of struck ship

E_b : energy absorbed by the bow structure of the striking ship

E_{minor} , E_o : energy absorbed by the struck ship prior to the rupture of hull plating

E_s : energy absorbed by the struck ship

E_T : total energy absorbed by the structures of the colliding vessels

F : sum of the membrane tension forces in side and deck plating as well as the buckling force in the latter, calculated on one side only of the incursion line

I : second moment of area of side transverse about axis of bending

M_p : fully plastic moment

M_y : yield moment

P : force required to push the striking bow into the deck plating of the struck ship

P_b : force acting on the bow structure of the striking ship during collision

P_c : Collapse load of a deck transverse flanking the strike

R : reaction force at deck transverse in the struck ship flanking the strike as a result of the impact force

R_{T1} : volume of the deformed portion of side shell plating of the struck ship due to membrane force.

R_{T2} : volume of the distorted portion of deck plating of the struck ship due to membrane tension force

R_{T3} : volume of the displaced portion of deck plating of the struck ship due to buckling

R_{T4} : volume of the damaged parts of deck transverses in the struck ship

R_{T5} : volume of the damaged portion of the deck plating due to the penetration of the striking bow

R_{Tb} : volume of the damaged material in the bow structure of the striking ship

S : height of the side transverses (i.e. distance between decks or between deck and bottom)

W = indentation at the incursion line

W_o : critical indentation, indentation at the incursion line at which the deck transverses flanking the strike start to buckle

$W1$ = indentation at frame No. 1

W_L : limiting indentation, indentation beyond which rupture of the hull plating occurs

Y : longitudinal length of damage in the struck ship

Z : longitudinal length of damage in the bow structure of the striking ship

ϵ_u : maximum (ultimate) strain at plating rupture

θ : striking ship's stem half angle

σ_m : average compressive stress at collapse = $\Phi \sigma_y$

Φ : ultimate strength factor = σ_m / σ_y

Φ_b, Φ_d : ultimate strength of bow and deck structure respectively

ψ : angle between the position of side plating before and after collision.

Chapter 1

Introduction and Literature Review

Introduction

The study of the collisions between ships constitutes an imperative requirement in the recent years. The reason for this, is the continuously rising attention that government of most countries, the media and as a result the public opinion, attracted for the contamination of the environment and the protection of human life.

During the last half century, protection of the environment has been of major concern. It is evident, that the technological achievements have caused damage to nature resulting from either continuous processes or accidents. The pollution of the marine environment has become of major concern due to the large amount of accidents occurring at sea. Marine pollution is defined as the addition of any substance to the marine environment as a result of man's activities, with a big and generally detrimental effect on it. The pollution of the marine environment is stemming from different sources, such as from pollutants released from shore, the atmosphere and of course marine structures. It has been estimated by Tsokalis et al. (1994) that annually 2.3 million tons of petroleum are released into the sea and that 5% of this amount is attributed to tanker accidents.

The percentage of total and partial losses attributed to collision accidents on the total amount of total and partial losses is being recorded every year from the Institute of

London Underwriters. Every year's edition contains a lot of statistical data on casualties. The above – mentioned percentage for the years 1985 – 1996 is varying from 15 – 20%. Moreover, collisions have been identified as being the most frequent accidents resulting to oil – spills. ISSC (1997) published a table (Table 1.1) from a work carried out by Ventikos, which shows that tankers caused the 1/3 of the oil – spills in 1994.

The need for studying collisions becomes quite clear, when specific cases are coming in mind. A lot of accidents occur every year but some of them are of great importance due to their adverse results. There are cited below two examples of collisions that occurred in 1994. The first one occurred in Yangtze River on the first of February 1994 between the vessels “Chuanyun 21” and “Changjiang 2023”. The struck vessel “Chuanyun 21”, which was a passenger ship sank subsequently after the impact. Ninety-eight people were missing and never found. The other one occurred at Bosphorus on the thirteenth of March 1994 between the vessels “Nassia” and “Shipbroker”. The struck vessel “Nassia” was blown up as a result of the collision. Twenty-nine people were killed by the explosion and two more were seriously injured.

As it can be seen, except the contamination of the marine environment, marine accidents often result in loss of lives. Collisions are high – risk accidents that may cost the life of many people. It is thus important not only to try to prevent such accidents but also to deal with the residual strength of the structure after the occurrence of the accident in order to prepare for safe salvage operations.

Except the pollution of the marine environment and the loss of lives, which remain two very ruinous consequences of collisions, loss of property and costly salvage and cleaning-up operations are as well to be considered. It is well known that an enormous

amount of certificates are required for a tanker to sail in the United States Coastal Waters. A tanker causing a large oil spill accident could easily result in a bankruptcy crisis for its shipping company.

The researchers, realizing of the role that the accidents of ships play in pollution and loss of lives, were motivated to conduct a vast amount of work with the final aim of protecting the marine environment, the lives at sea and the affected areas and population.

The environmental pollution is not the only problem. Many times this pollution affects the population in the vicinity of the pollution. For example, due to storms in the Sea of Japan, a Russian tanker carrying 19000 tons of heavy fuel oil broke into the fore part and the aft part of the hull and a large amount of oil was spilled, which caused huge damage to the local fishing industry. For this reason, a lot of research work has been carried out in the various aspects concerning ship accidents.

The first samples of research work in the field of ship collisions were presented in the early fifties. The bulk of the research work from the early fifties to the early seventies was devoted to the reactor and nuclear spaces of nuclear powered ships. From the early seventies until now, the attention of the researchers has been paid to the development of methodologies for designing hull structures, which can sustain the impact induced by a striking vessel without rupturing. This is particularly important in the case of oil tankers, LNG and LPG carriers or other similar types of ships.

1.1 Collision Statistics

The statistical data cited in this chapter were collected from the annual editions of the Institute of London Underwriters “Casualty Statistics 1996”, the annual editions of Lloyd’s Register “World Casualty Statistics”, and the report of ISSC 1997.

The annual edition of Institute of London Underwriters reports every ship accident (collisions, grounding, fire and explosion, machinery and others), which result in total loss of the ship. The ships recorded are only those with capacity over 500 gross tons.

The accidents are classified as actual total losses and constructive total losses. Moreover, the accidents are classified according to the type of the vessel, their capacity, the cause of accident and the age of each vessel.

A ship is considered “total loss”, when the cost of repair is out of rational limits and of course when is impractical for the ship to be repaired. The term “total loss” is attributed to ships, which after the occurrence of an accident are yielded to scrap or ships that sank during the accident. The “total losses” are subdivided to actual and constructive total losses. The term “actual total loss” is attributed to a ship that sank during the accident or was totally destroyed. On the other hand, the term “constructive total loss” is attributed to a ship, for which the insurance decided that its repair is out of cost bounds.

As it can be seen from Figures 1.1, 1.2, 1.3, the percentage of collisions that resulted in total loss of the vessel as defined above, on the total losses of all kinds of accidents is for tankers 5.3%, for bulk carriers 28.6%, for general cargo ships 14% and for other types of ships 10.5%.

Daidola (1995) presented a table (Table 1.2) listing 50 major oil spills from tankers and combined carriers. The table contains the name of the ship, its size, the volume of the oil spill and the location and cause of the accident. The data collected reveal that from the fifty recorded oil spills eleven occurred due to collision.

A lot of aspects must be examined through statistics. This will give a clearer image of the collision problem and what should be done. Statistics about the geographical location

of the collisions, the weather conditions, the time of the accident, could be provided. This kind of statistical analysis will motivate the authorities to establish new regulations.

1.2 Protection against Collision

In order to reduce the consequences of ship collisions, classification societies, researchers and government of countries have tried to adopt adequate measures. These measures are mostly consisting of new regulations. The aim of the rules established is to prevent loss of lives at sea, to reduce or prevent marine pollution and finally to prevent loss of property.

There are two goals that should be achieved. The first one is to adopt preventive measures so that the collision accidents do not occur. The second one is to reduce the consequences of collision accidents, when they occur.

The first goal is called “Prevention”. Prevention of collisions could be achieved by the installation of proper navigational aids on the ships. The rules established enjoin the use of such navigational aids. Crew also plays a very important role on the prevention of the accidents. From statistical analysis of the accidents, it became clear that most of the accidents occurred during the night or during the lunch break of the crew. Apparently, because of the involvement of human factor, accidents will continue to occur.

The second goal is called “Mitigation”. Most accidents are caused by human factors such as operational mistakes. The complete removal of these factors is impossible and accidents will happen. That is the point that “mitigation” comes in scene. The aim is to modify the structure of the ships in such a way that the damage, which occurs during

collision, would not result in the sinking of the vessel or in the outflow of hazardous cargo. The 13th ISSC (1997) in the chapter “Structural design against Collision and Grounding” reported some new design concepts and compared them in terms of prevention of oil outflow. The increased efficiency of these designs is either through improvements in compartmentation of cargo and ballast spaces, or through improvement crashworthiness against groundings and collisions.

There have been developed a lot of designs in order to reduce the oil outflow, some of them are shown in Figures 1.5, 1.6, 1.7. Many ideas are good and effective but they are not cost effective. The cost is a very important restrictive factor, which counts the feasibility of the designs. Bearing these in mind, it is needless to say that wider double sides, deeper double bottoms, smaller cargo tanks, increased scantlings of structural members, and improved material properties of materials enhance the crashworthiness and minimize the oil outflow. However, the economic pressure and the ups and downs of the shipping market make the fully incorporation of these features to ship design unacceptable. Therefore, there is a need for innovative and jointly practical design ideas to be developed.

It is obvious that both of the above-cited goals can not be achieved totally. Accidents will continue to occur whatever the navigational aids are and also oil will continue to outflow into the sea whatever the structural configuration of a ship is. So the goal to be achieved is to find the golden section and maximize the effect of prevention and mitigation.

The part that “prevention” can play is through regulations. The authorities by keeping in hand the results of statistical analysis can identify the high-risk areas and impose limits on the speed of the vessels, which sail in these high-risk areas.

On the other hand, the part that “mitigation” can play is through modifying the structural configuration of vessels. The aim is to accomplish the best structural configuration in terms of energy absorption before the rupture of the hull, which will obviously differ from ship to ship. The tools for this work are the methods provided by the researchers and predict the capacity of energy absorption by a ship design. A vast amount of research work has been carried out in this direction. The object of research is to develop a method, which could accurately predict the energy absorbed during a collision.

1.3 Assumptions used in Collision Evaluation

The collision between ships is only one of the possible collision scenarios that have been recorded during the years. The others possible scenarios are:

- Supply vessel to offshore structure.
- Ship to rigid pier or bridge.
- Ship to artificial island.

The present thesis examines the ship to ship collision and does not deal with the other scenarios. Focusing more in any of these collision scenarios, the nature of those is usually described as being right angle or oblique, referring to the relative position of the struck ship center line to the vector the vector of velocity of the striking ship/object.

Ship to ship collision scenario consisting of a striking ship and a struck ship. The striking ship travelling with a certain speed is impacting a struck ship, either stationary or a moving one. The impact force is a function of the stiffness of the structure of the two ships in the contacted area. The load to penetration relationship is different from ship to

ship collision. The shape of both the striking and struck ship at the end of the collision is highly depended on the relative stiffness of the two structures, their geometry and a large number of other parameters. The key elements associated with ship to ship collisions are:

- nature of collision: oblique or right angle
- intensity of collision: speed, displacement, bow shape, draft
- condition of struck vessel: displacement, draft, speed, relative orientation, environmental conditions and structural resistance to collision.

In order to study collisions, which is a very complicated phenomenon, investigators are obliged to adopt a number of simplifying assumptions to make the problem solvable. The most used assumptions that are made are:

1. Collision between ships is an entirely inelastic process.
2. The structural response of ship's structures during collision can be estimated using static analysis.
3. Structural behaviour can be disconnected from the rigid body response.
4. The behaviour of the material is ductile.
5. The main energy absorption mechanism prior to fracture of the side shell is membrane tension.

These assumptions are more or less used in most of the literature dealing with the study of collisions. Some of them have been confirmed through experimental tests, while others are still being argued.

Assumption (1) is well confirmed from many researchers. It has been proved that the energy dissipated in the elastic process is negligible compared to the total energy absorbed in a collision.

Assumption (2) is still under consideration. The static analysis can be applied only if the dynamic effects, such as inertia force of the colliding ships and strain-rate sensitivity of the material, can be neglected. It is evident that all impacts involve some dynamic effects. Therefore, it is needed to determine when a static approach is adequate and when a dynamic approach is more suitable. Jones (1976) proposed a criterion for the transition from static to dynamic loading. If the duration of impact is longer than the corresponding natural period of elastic vibration of the hull plating, then a static analysis is adequate; otherwise a dynamic approach is required.

Assumption (3) was found to be very rational. McDermott et al. (1974) through simplified approaches identified the elastic and hydrodynamic (energy absorbed due to the hydrodynamic resistance of the surrounding water) energies and concluded that they are small compared with the potential plastic energy absorbed in minor collisions that terminate just prior to the rupture of the hull plating of the struck ship.

Assumption (4) is used in most of the methods developed through the years. On the other hand, Akita et al. (1972) have detected, in the experimental tests that have conducted, two distinctly different failure types in transversely framed side structures, when penetrated statically by a rigid bow. The one is a deformation type failure, which is characterized by buckling of decks and stiffeners and a large portion of the external load is supported by membrane tension prior to the rupture of the side shell. The other one is a crack type failure, which is characterized by a local penetration of a rigid bow, which ruptures the side shell and decks as indicated in Figure 1.11.

Finally, assumption (5) has been verified theoretically and experimentally. When the penetration overcomes 0.75-1.0 times the thickness of the side shell plating then the membrane effect becomes the dominant energy absorption mechanism, until the rupture of the shell plating.

1.4 Dynamic Effects

Although assumption number (2) is extensively used in the theoretical simplified methods, it is clear that all impacts will involve some dynamic effects. When the dynamic effects are to be taken into account, two important aspects should be considered. The first is inertia force and the second is strain-rate sensitivity.

1.4.1 Inertia force

The dynamic effects that collisions involve are described in the term of the “inertia force”. When the two ships hit each other a lot of dynamic effects take place as overall vibrations of the ships structure and local vibrations of the structural elements. The error could be considerable when the duration of impact is less than the natural period of the plating as Jones(1973) has shown.

1.4.2 Strain Hardening Effect

It is well known that the post-yield plastic flow of iron and mild steel is considerably affected by the rate of straining. Mild steel is of great importance in naval architecture and ocean engineering because it is extensively used in marine structures.

The most widely used formulation for the dynamic flow stress σ'_0 as a function of the strain rate $\left(\dot{\varepsilon}\right)$ is known as the Cowper-Symonds relation:

$$\frac{\sigma'_0}{\sigma_0} = 1 + \left(\frac{\dot{\varepsilon}}{D}\right)^{\frac{1}{q}}$$

The constants D and q have been investigated but particularly from dynamic tests on materials with small strains, whereas the strains in many impact problems in naval architecture can be considerably larger and may even reach the rupture strain.

Marsch and Campbell (1963) have shown that the strain rate sensitivity of mild steel decreases with increasing strain. The Cowper-Symonds equation ignores this observation and might exaggerate the influence of strain rate effects when large strains are involved in the calculations.

McDermott et al. (1974) in order to take into account the strain hardening effect proposed that in the calculations of the energy absorbed instead of the yield stress of the material (σ_y) could be used the value $\frac{\sigma_y + \sigma_u}{2}$.

Hegazy (1980) adopted the proposition of McDermott et al. (1974), which seems to work for the approximate theoretical methods.

1.5 External and Internal Mechanics of Collision.

The analysis of a ship to ship collision is usually separated into the external mechanics and the internal mechanics. The external collision dynamics deals with the rigid body motions of the colliding vessels. The inner collision dynamics involve the evaluation of the force – indentation responses of the striking ship and the struck ship during the collision. The internal dynamics represent the structure dynamics while the outer dynamics incorporate the virtual impact dynamics and the hydrodynamics. In “internal dynamics” the stresses and deformations to both ships are derived on the mere basis of the total impact energy and of the initial kinematic configuration of the impact. In “outer dynamics” the total impact energy is computed using the working hypotheses of added masses accounting for the water resistance.

To the knowledge of the author two methods have been presented in the external collision dynamics field. The first one is coming from Woisin (1987) and the second one is from Hegazy (1979), conducted at the University of Newcastle.

The field of inner collision dynamics is swarming with methods. The pioneering method was presented by Minorsky (1959) and was followed by a lot of researchers. A vast amount of work has been carried out since then, which will be reviewed in the following subsection.

1.6 Literature Review

The methods used for the collision resistance of ships are usually classified as minor collision methods and major collision methods. A minor collision (or low energy collision) is defined as a collision, which take place at relatively low speed where the shell of the struck ship is deformed but not ruptured. On the other hand, a major collision (or high-energy collision) is defined as a collision, which is associated with high impact speed and tend to cause rupture of the hull.

1.6.1 Minor Collision Methods

McDermott et al. (1974)

McDermott et al. (1974) presented an analytical procedure to evaluate the structure of a tank ship from the viewpoint of the actual protection it affords the cargo during minor collision.

This research work considers the energy absorption characteristic of the individual components and also separates the elastic, plastic and hydrodynamic energies of collision.

The authors conclude that elastic and hydrodynamic energies are small compared with the potential plastic energy available and can be neglected when estimating the energy absorbed in minor collisions that terminate just prior to cargo tank rupture.

The method pertains to the approximate theoretical methods and consists from the following described mathematical model. Three phenomena are assumed to produce plastic deformations:

- longitudinal plastic bending of the stiffened hull plating
- plastic membrane tension in the stiffened hull plating and deck
- yielding or buckling of the web-frames (and/or swash bulkheads)

The stiffened hull of the struck ship is analysed as a series of independent longitudinal “T-beam” units, each consisting of one longitudinal stiffener and the portion of hull plating that may be assumed to act monolithically with that stiffener. The force transferred from each “T-beam” unit to the flanking web-frames is calculated for every indentation in order to be discovered if the flanking web-frames collapse. The total energy absorbed is finally calculated by adding the plastic bending energy of the stiffened hull, the membrane-tension plastic energy and energy absorbed due to the collapse of the web-frames.

Jones (1978)

Jones (1978) in order to extend Minorsky’s method to minor collision problems developed the following method. This method pertains to the so called global methods or simple design methods, because it establish a simple relationship between the amount of energy absorbed from the colliding ships’ structures to values of the volume and area of the damaged material.

Considering a rigid perfectly plastic beam with fully clamped supports across a span $2L$ which is subjected to a concentrated load P at the mid span, Jones presented the following formula for the energy absorbed by the struck ship's structure:

$$E_T = 0.030288 \cdot \sigma_y \cdot R_T \cdot \left(\frac{W}{L}\right)^2 \quad (1.6.1.1)$$

$$R_T = \frac{2 \cdot L \cdot B \cdot H}{144} \quad (1.6.1.2)$$

where E_T is the total energy absorbed (ton-knots²), σ_y is the yield stress (lb/in²), W is the final deflection and R_T is the volume of the side shell plating assumed to be involved in membrane mechanism (ft²in) (see equation 1.6.1.2), B is the beam breadth, and H is the beam thickness.

This formula (equation 1.6.1.1 with $\sigma_s = 30000$ lb/in²) for various values of $W/2L$ was compared with Minorsky's empirical relation (see Figure 1.9), which gives a family of lines radiating from the origin of Fig. in which minor or low energy collision was contained.

Van Mater (1978)

Van Mater (1978) proposed an extension to Jones formula so that the latter could be applied to an off centre hit. The geometrical model of the method is shown in Figure 1.10.

Considering the effect of a concentrated load at variable location on a fully clamped beam, Van Mater concluded to the following formula:

$$E_{(a,b)} = E_{CL} \cdot \frac{L}{2} \cdot \left(\frac{1}{a} + \frac{1}{b}\right) \quad (1.6.1.3)$$

where E_{CL} is the absorbed energy for mid span strike as introduced by Jones (1978).

Van Mater used the failure criterion proposed by McDermott (1974) to approximate the limiting indentation beyond which rupture of the hull occurs. By introducing the result in the equation (1.6.1.3) the equation reduces to:

$$E_{(a,b)} = E_{CL} \cdot \frac{a}{b} \quad (1.6.1.4)$$

It is evident that this result contains many oversimplifications but it shows clearly that a stiffened panel between bulkheads will absorb much less energy before rupture as the strike point moves away from the centre span.

The approach taken by both Jones and Van Mater is an oversimplification of circumstances that would prevail in an actual collision. The point that these methods wish to make clear is that there is hope for the development of a simple Minorsky type relationship, which would permit the prediction of the depth of incursion at shell rupture for a given input in collision kinetic energy within reasonable upper bound error.

1.6.2 Major Collision Methods

Three methods have been well known for calculating the work done in major collisions, the first by Minorsky (1959), the second by the structural group at the Naval Construction Research Establishment (N.C.R.E.) (1967) and the third by Akita and Kitamura (1972). The common objective of these methods was to estimate the energy absorbing characteristics of ships' structures with basic consideration the safe designing of

nuclear ships. Due to the increased need for safe ships which carry hazardous cargo the methods were applied during the years to tankers and LNG carriers.

Minorsky (1959)

Minorsky (1959) in his pioneering paper on ship collision developed a semi-empirical procedure based on the overall damage and kinetic energy lost in collision. Twenty-six serious collisions in the period until 1959 were analysed for the kinetic energy absorbed in the collision and for the extent of the damage. Data were provided by the U.S. Coast Guard.

The collision scenario is assumed as a striking ship travelling with a speed V_B and impacting a stationary ship at right angles.

Defining:

M_B, V_B as the mass and velocity at impact of striking vessel,

M_A, V_A as the mass and velocity of the struck vessel ($V_A = 0$)

U as the final common velocity in the direction of the striking vessel,

dm as the virtual increase in mass of the struck vessel due to water entrained.

According to the conservation of momentum and energy principal, it is evident:

$$U \cdot (M_B + M_A + dm) = M_A \cdot V_A + M_B \cdot V_B \quad (1.6.2.1)$$

$$K_T = \frac{1}{2} M_B V_B^2 - \frac{1}{2} (M_B + M_A + 0.4M_A) \cdot U^2 \quad (1.6.2.2)$$

The equation (1.6.2.2) gives the kinetic energy lost in collision, K_T , which is the difference between the initial kinetic energy and the final energy remaining in the system after impact. As it can be seen from the above-mentioned equations the added mass was estimated by Minorsky to be $0.4M_A$.

The second part of the study consisted in selecting a function of the energy-absorbing strength members of the colliding ships so that a satisfactory correlation could be established between the structural damage and the lost kinetic energy. The members that can absorb energy in collision were argued to be those members having depth in the direction of penetration. Such members are the decks, flats and inner and outer bottoms of both vessels. Therefore, a “resistance factor” R_T was calculated based on these members.

Through calculation, the function that was obtained was:

$$E_T = 414.5 \cdot R_T + 121900(\text{ton} - \text{knots}^2) \quad (1.6.2.3)$$

The result was a straight line except an area near the origin, where the relationship between K_T and R_T could not be established due to the considerable scattering of the points (see Figure 1.8). This means that the Minorsky formula is only applicable in major collisions.

Woisin (1979) based on the experimental results of GKSS (Hamburg), proposed a modification on Minorsky’s formula as follows:

$$K_T = 47 \cdot R_T + 0.5 \sum h_s t_s^2 \text{ (MJ)} \quad (1.6.2.4)$$

where, K_T is the loss of kinetic energy, R_T represents the volume of the damaged material, h_s is the height of broken or heavily deformed longitudinal member, and t_s is its thickness.

N.C.R.E. (1967)

A simple theoretical method was developed and presented by NCRE (1967). The formula was confirmed by static tests on a series of models. The striking vessel is assumed to have a wedge shaped rigid bow. The formula takes into account only the contribution of the decks of the struck ship. The striking wedge was assumed being resisted by a direct crippling stress in the deck, normal to the wedge, and a frictional force tangential to the wedge. The crippling stress was found experimentally to be 90 per cent of the corresponding 0.3 per cent proof stress for the material of the structure.

With these assumptions, some very simple expressions were derived for the penetrating force and the work done:

$$\text{Penetrating Force} = 2 \cdot \sigma \cdot A \cdot \left(\sin \frac{a}{2} + \mu \cdot \cos \frac{a}{2} \right) = 2 \cdot k \cdot \sigma \cdot t \cdot \left(\tan \frac{a}{2} + \mu \right) \cdot x \quad (1.6.2.5)$$

$$\text{Work Done} = \int F \cdot dx = k \cdot \sigma \cdot t \cdot \left(\tan \frac{a}{2} + \mu \right) \cdot x^2 \quad (1.6.2.6)$$

where:

A = effective area of contact on each side of wedge

a = wedge angle

k = (effective area of contact)/(area of plating) = A/A_p

t = thickness of plating

μ = coefficient of friction

x = depth of penetration

Considering the outcome of the experiments for the crippling stress and that the coefficient of friction was experimentally deduced to be 0.25, then the equation (1.6.2.6) concludes to:

$$\text{Work done} = 0.9 \cdot \sigma_y \cdot t \cdot (\tan\theta + 0.25) \cdot x^2 \quad (1.6.2.7)$$

Equation (1.6.2.7) is a very simple Minorsky type formula. The basic limitation to its use is that only an infinitely rigid bow was considered. However, Belli (1970) summarized the experimental work which had been conducted in Naples since 1961 and found that the NCRE method gave good predictions provided appropriate allowance was made for the rigid bow assumption.

Akita et al. (1971, 1972)

Akita et al. (1971) conducted a very large amount of work consisting by experiments and theoretical analysis of collisions. The experimental results obtained from eight idealized ship side models penetrated statically by rigid bows. The ship side models consisted of a side shell, two decks and transverse framing. Also the behaviour of eleven other side structural designs was examined.

The authors observed that there were two major types of failure in transversely framed side structures, which were penetrated statically with rigid bows. A deformation failure mode is characterized by buckling of decks and stiffeners over a relatively large area of the side shell and a large portion of the external load is supported by membrane tension prior

to the rupture of the side shell. A crack type failure is characterized by a local penetration of a rigid bow, which ruptures the side shell and decks as it can be seen in Figure 1.11. The deformation type of failure occurred when the strain directly below the bow was less than about 0.3, while crack type failure were associated with larger strains.

It appears from some dynamic tests on similar structural arrangements, which were reported by Akita et al. (1971), that the energy absorbing mechanisms and fracture types were similar to those observed in the corresponding static tests. However, the energy absorbed in a dynamic test was larger than that which was absorbed in the corresponding static tests, a circumstance that was attributed to the influence of material strain-rate sensitivity. It should be remarked that this increase in capacity might not be realized in a ship during a collision because this is a highly nonlinear phenomenon, which is very sensitive to size. Moreover, Duffey (1971) has shown that the influence of material strain-rate sensitivity cannot be properly scaled up from a model to a full sized structure, when they are made of identical materials.

Akita et al. (1971, 1972) have also developed an approximate and simple formula for calculating the amount of energy absorbed by the decks of a struck ship during collision. The developed formula is based on the same principles as the formula developed by NCRE (1967), except that the frictional forces between the deck plating of the striking bow were neglected and the value of the crippling stress was taken as 80 per cent of the yield strength of the material. Besides, the formula can also take account of the energy absorbed by the striking bow during a collision. This was done by introducing a correction factor relative to absorbed energy by a rigid stem and depends on the strength ratio of stem to side structures.

The proposed formula, when the relation between the absorbed energy and penetration by a rigid stem falls into a crack-type fracture, is:

$$E_s(w) = N \cdot t_d \cdot \sigma_o \cdot \tan \vartheta \cdot w^2 \quad (1.6.2.8)$$

The relation between the absorbed energy and penetration by a soft stem can be expressed:

$$E = \beta(\lambda) \cdot N \cdot t_d \cdot \sigma_o \cdot \tan \vartheta \cdot w_A^2 \quad (1.6.2.9)$$

where:

N = number of deck layers,

t_d = deck plate thickness

σ_o = material constant (use 80% of yield point)

θ = half of stem angle

w = sum of penetrations for both stem and side. When a rigid stem is assumed, penetration of side only.

w_A = dent in the side of a struck vessel

$\beta(\lambda)$ = correction factor relative to absorbed energy by a rigid stem.

λ = strength ratio of stem to side structure.

The strength ratio of the stem-side (λ) as well as the correction factor of absorbed energy are obtained by using a buckling load for the stem and a rupture for the side, which can be obtained either as experimental or calculated values.

1.7 Conclusions

In the minor collisions' field the methods, which are known were developed by Rosenblatt (1971, 1972), McDermott et al. (1974), Jones (1978) and Van Mater (1978). The first two methods pertain to the approximate theoretical methods. The plastic energy absorbed from the side of a struck ship is estimated using plasticity theory and various empirical relations from several sources for the load-deflection and energy-absorbing characteristics of the structural members, which were deformed during collision. The other two methods, which are actually one method and its extension to variable location collision cases, pertain to the so-called global methods. The global methods are Minorsky-type methods that relate the energy absorbed with the volume of the damaged material during a collision. These methods were intended to show that there is feasible to obtain a simple design method for the minor collision problem.

In the major collisions' field the methods, which are most known were developed by Minorsky (1959), NCRE (1967) and Akita et al. (1971, 1972). All the cited methods pertain to the global methods or simple design methods.

The pioneering method that was presented by Minorsky is based on data from twenty-six actual collision cases and predicts the absorbed energy for major collisions with a reasonable accuracy. The other two methods presented by NCRE and Akita et al., concluded to simple formulae based on experimental data.

The methods refer to the major collision problem will be further discussed in chapter 3 in confrontation with the proposed method developed by Hegazy (1980).

1.8 Aim of the Thesis

Ship to ship collisions is a very complicated phenomenon and the parameters involved are too many. There are several ways to study collisions. The ways are through experimental tests, finite element analysis, theoretical methods and the global methods (or simple design methods). The basic aim of all these methods are to provide guidelines and easy-to-use tools to enable designers to upgrade the crashworthiness of ship structures.

The experimental tests are a very useful help to the understanding of the collision mechanics. They are a great support to the theoretical studies but they can not be used as a design tool. The cost and the scaling difficulties are restrictive factors to the applicability of experiments.

Finite element analysis is a very powerful tool. However, it can not be used as a design tool because it is a time consuming procedure. Besides, the cost of FEA is so high that makes the method inhibitory for use in the preliminary design stage.

The approximate theoretical and the global methods are these, which are appropriate for the work of the designers. These methods provide a quick and low-cost approximation of the energy that will be absorbed during a collision from a particular ship structure.

In this thesis a method developed by Hegazy (1980) was used to appraise the energy absorption capacity of several ship structural designs during a side collision. The method was programmed in FORTRAN 90. The energy absorption capacity of different members of ship structure is plotted against the indentation and the volume of damaged material. The program runs for two different ship designs. The first ship design belongs to a small oil tanker with a structural configuration similar to the simplified one proposed by Hegazy.

Furthermore, the method is modified in terms of the strength calculation of decks. A new method calculating the ultimate buckling strength of plates is introduced in the Hegazy's method in order to achieve more accurate results. Results were produced and compared.

Moreover, the method is applied on a double hull design. Some modifications were made in order for the method to be applicable on a double hull design and work automatic for any indentation without interfering with the user. A single hull design was developed based on the principal dimensions of the double hull design. That was found to be a good way to compare the crashworthiness between single hull and double hull designs.

Finally, a parametric optimization was carried out. The method used gives the ability of assessing the energy absorbed from individual part of the structure. That's why, it is easy to see if a certain amount of extra material is given, where is the best part of the ship to be enforced in terms of the maximization of the energy absorbed by the structure.

It is believed that the work carried out in this project will provide useful data to the designers and the researchers. This thesis is hoped to be a step towards the better understanding of collision mechanics.

1.9 Layout of the Thesis

The second chapter contains a closer look to the internal mechanics of collisions. The mostly used assumptions are under discussion and an extensive description of the mathematical modeling is presented. Finally, the modes of Failure of the individual structural members are examined.

The third chapter begins with some discussion on the existing methods and their advantages and disadvantages. Further, the method that will be used for the calculations is cited and some remarks are made. The Fortran program algorithm is then presented. Concluding, some indicative results for a small oil tanker are derived and are estimated.

In the fourth chapter a method, developed by Pu and Das, is proposed for the calculation of the ultimate buckling strength of the decks. The method was incorporated in the program calculating the energy absorbed and some results were derived. The results from the modified program and the original one are compared.

In the fifth chapter the method is used to predict the energy absorption capacity of a double hull tanker. The assumptions that had to be made and the collapse mechanism and geometry are discussed. Finally, results are produced in terms of indentation and volume of the damaged material.

In the sixth chapter a single hull mid ship section is developed based on the principal dimensions of the double hull design. Furthermore, application of the method on the single hull design takes place. The results from the single hull are compared with those from the double hull design and some remarks are made.

In the seventh chapter a parametric optimization of the double hull design is conducted. The optimization is conducted in terms of most of the structural parameters affecting collision. An appraisal of the results takes place and conclusions are cited.

Concluding, the author makes proposals for future work to be carried out.

List of Figures

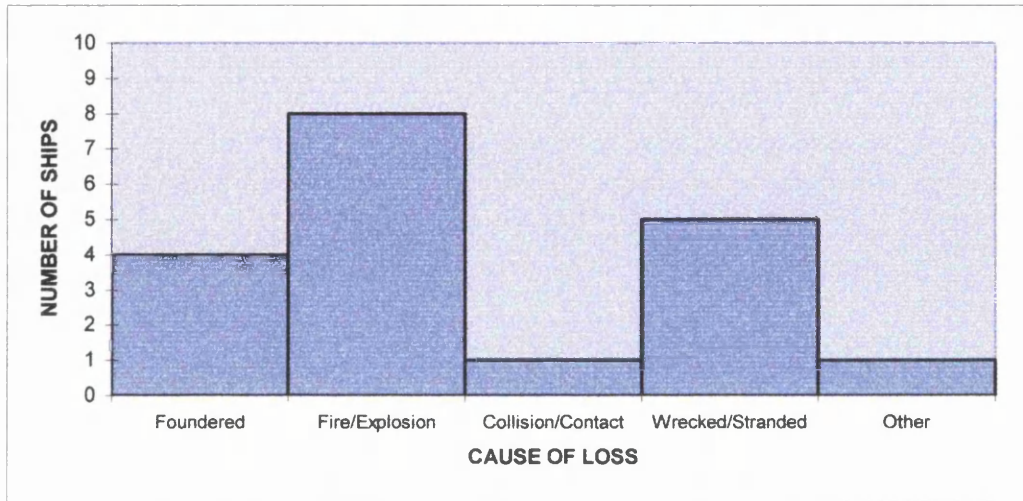


Figure 1.1: This figure illustrates the number of tankers, which were declared as total losses and the cause of the accident.

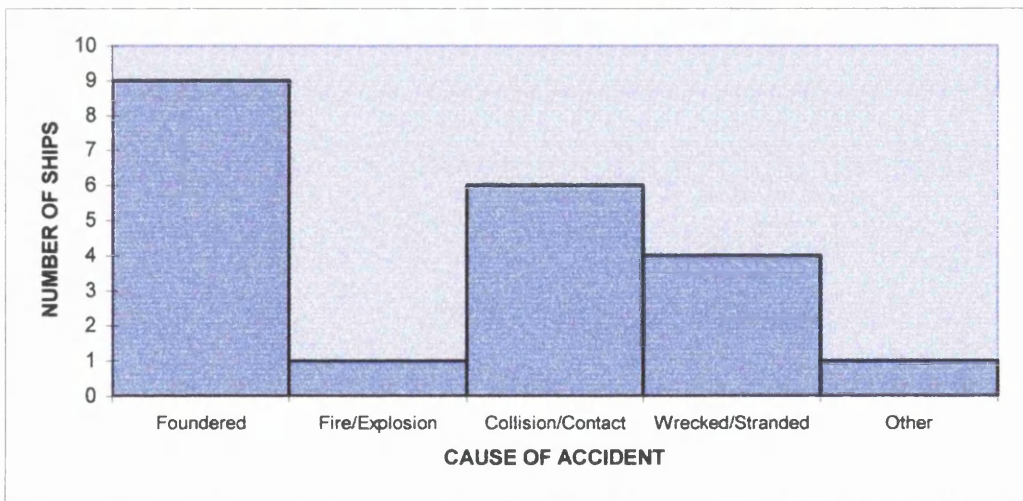


Figure 1.2: This figures illustrates the number of bulk carriers, which were declared as total losses and the cause of accident.

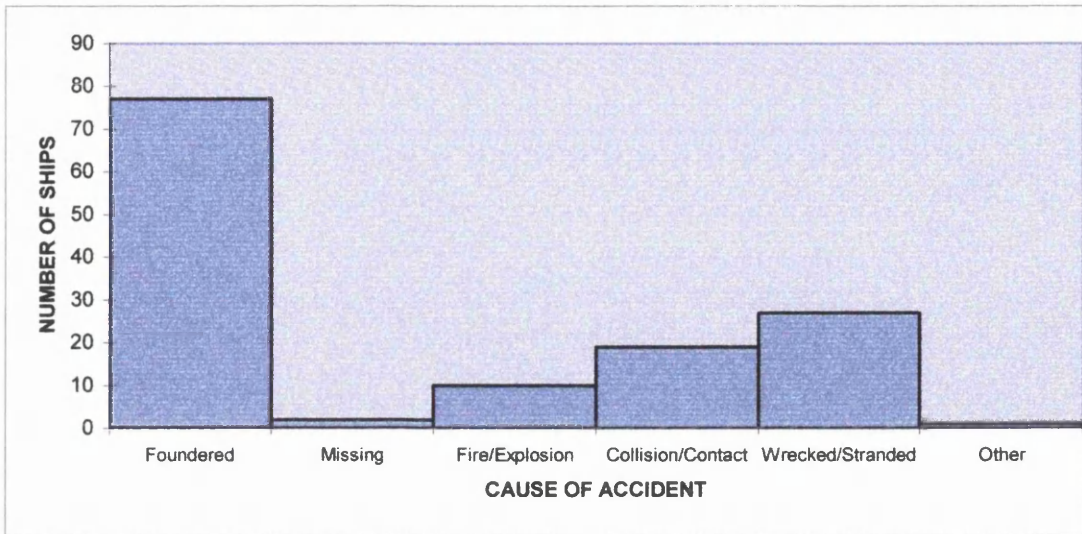


Figure 1.3: This figure illustrates the number of general cargo ships, which were declared as total losses and the cause of accident.

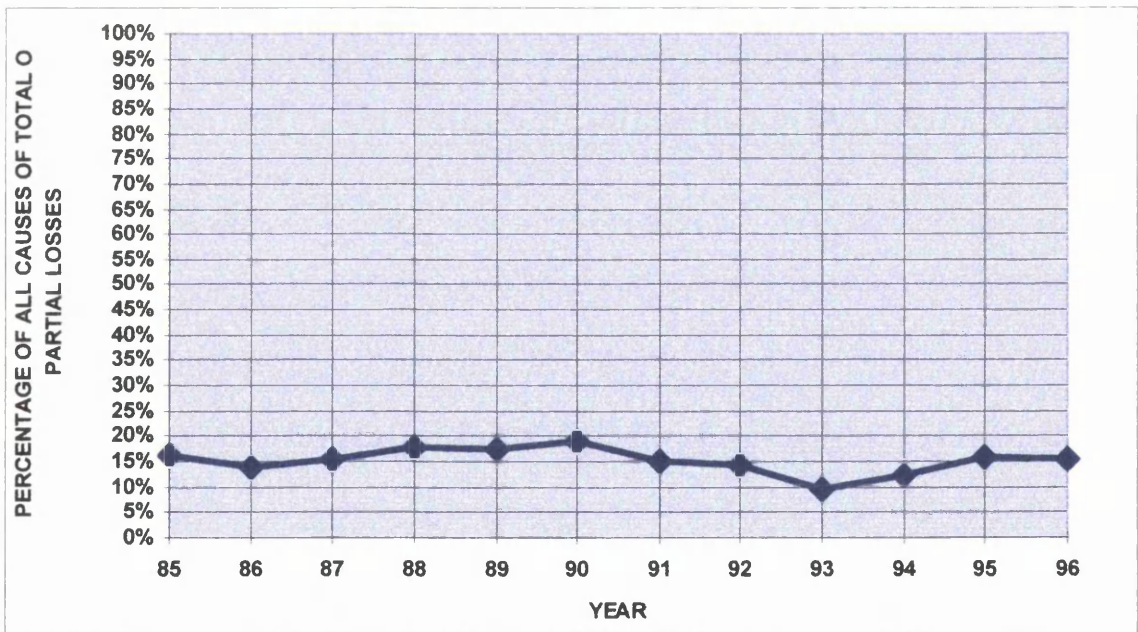


Figure 1.4: This figure shows the contribution of collisions in percentage among all accidents to the total and partial losses.

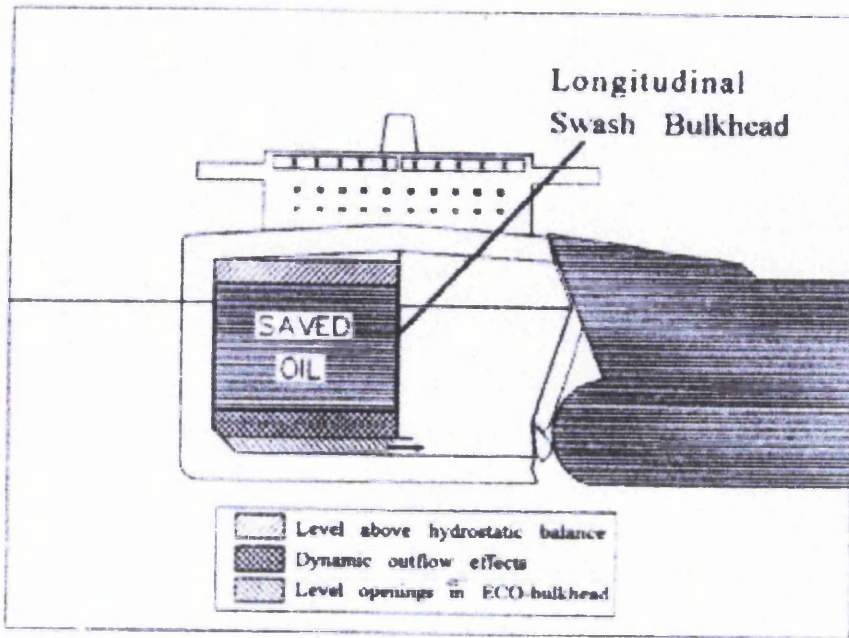


Figure 1.5: The figure illustrates a concept developed by Van der Laan, aimed to reduce replacement oil outflow.

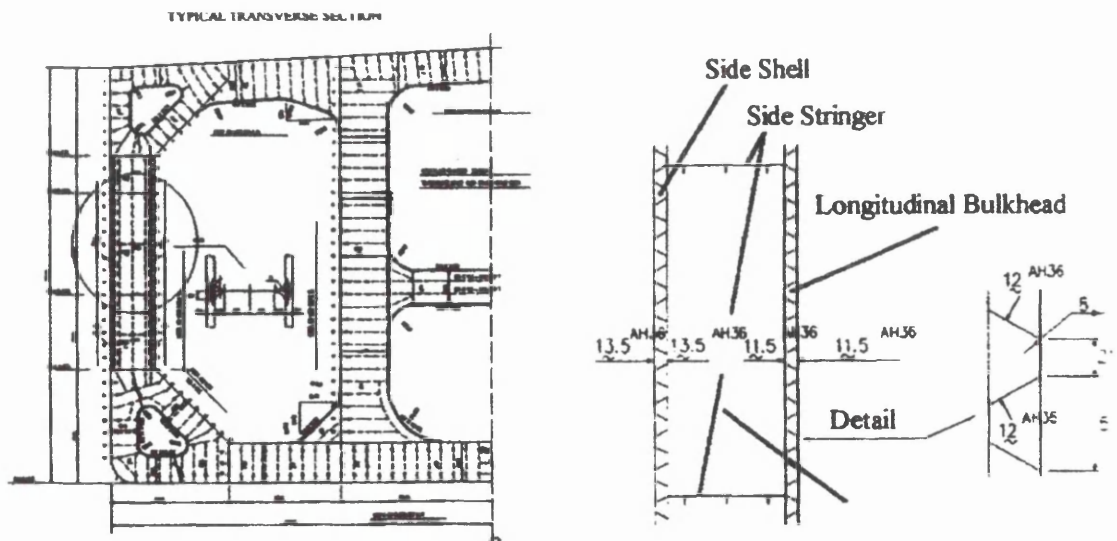


Figure 1.6: Kitamura proposed the above-illustrated design concept in which conventional longitudinally stiffened inner and outer shells are replaced by double skinned “Frame Panels”.

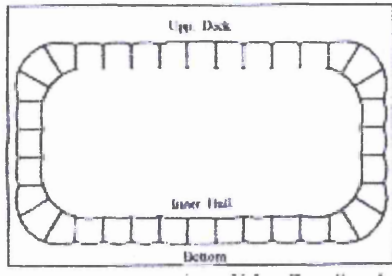


Figure 1.7.a: Mid-ship section of a design concept proposed by MarcGuardian.

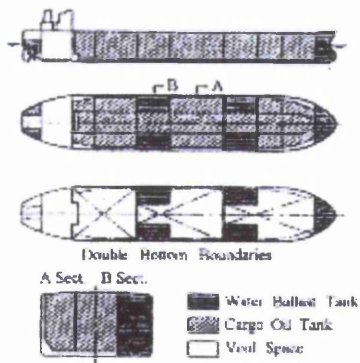


Figure 1.7.b: Void double hull space type VLCC.

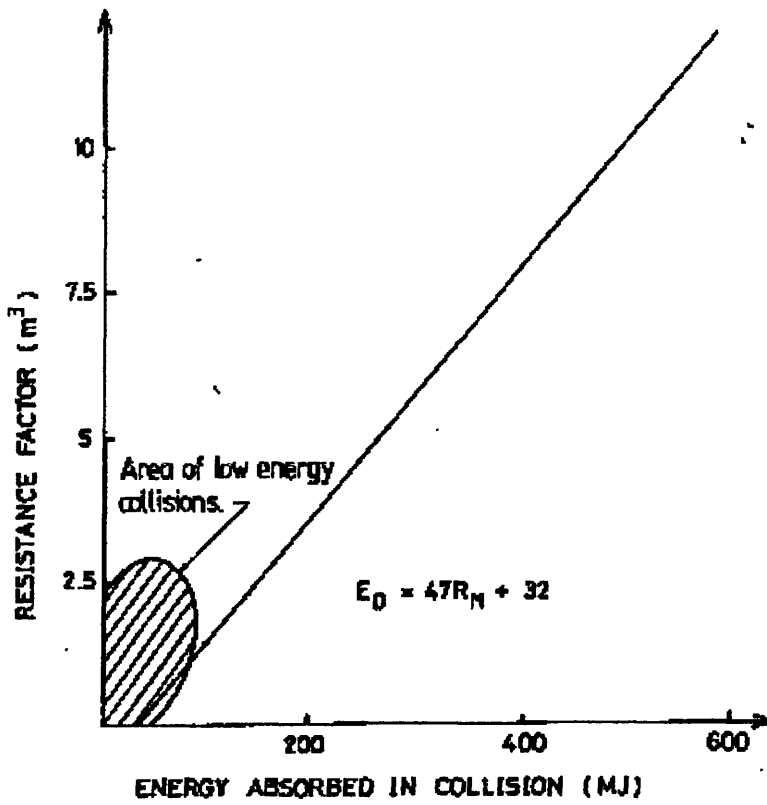


Figure 1.8: Empirical correlation between resistance to penetration and energy absorbed in collision. Minorsky (1959).

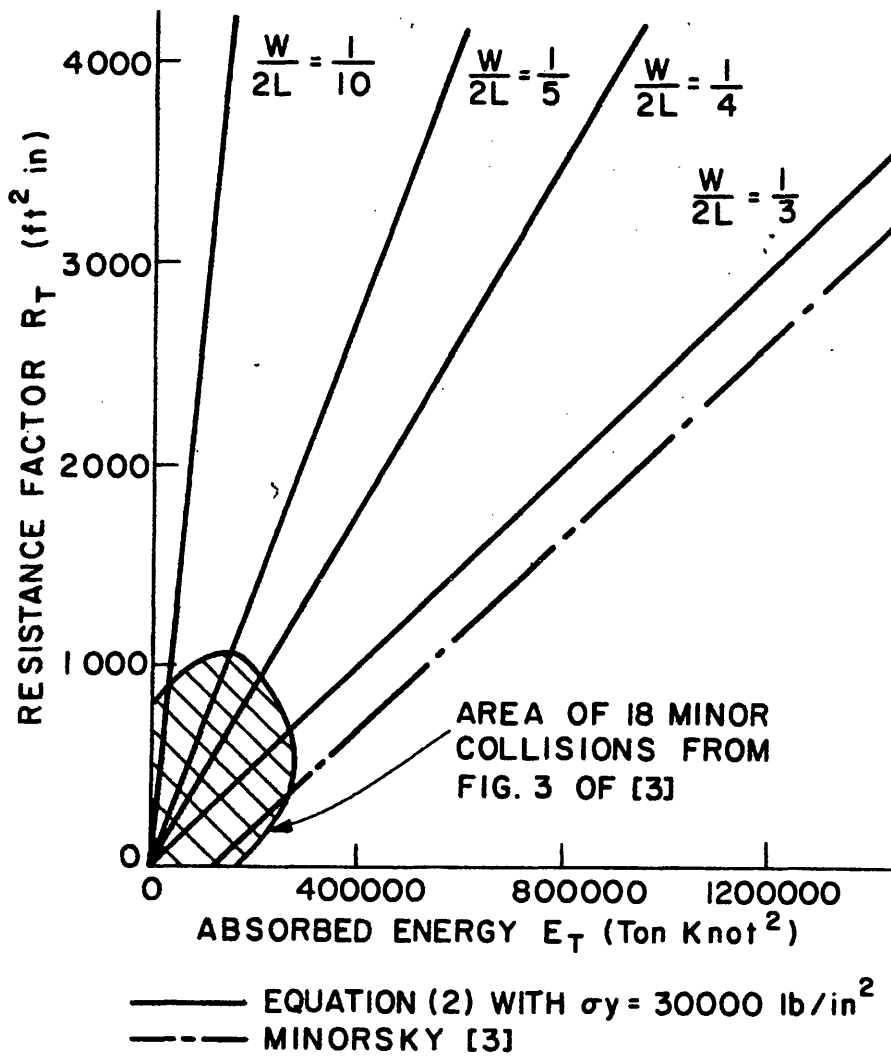


Figure 1.9: Jones formula plotted on a Minorsky graph.

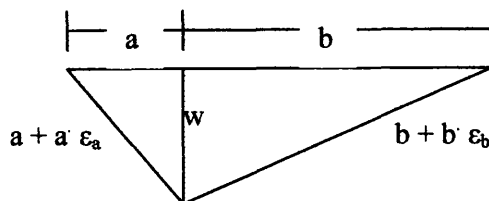
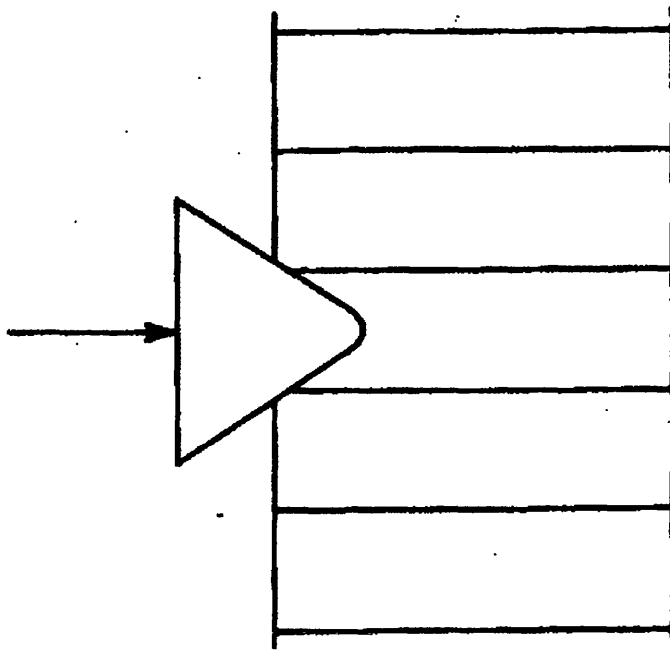
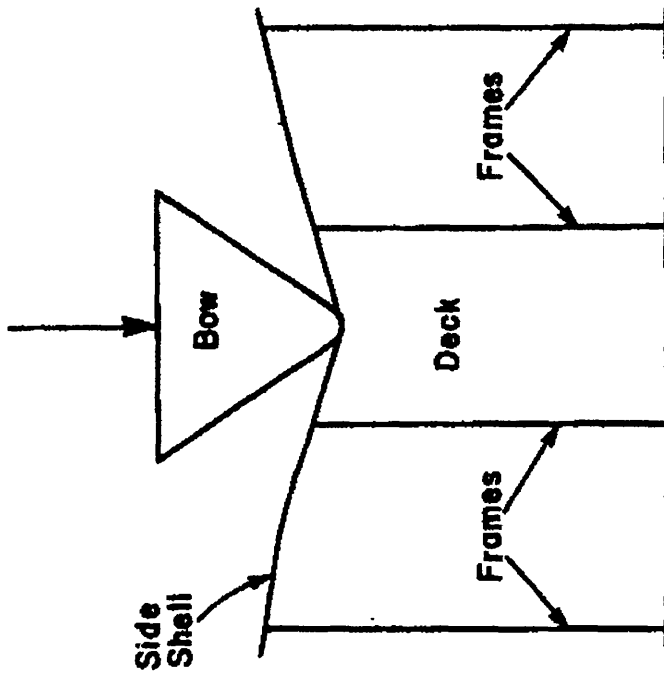


Figure 1.10: Van Mater's geometrical model.



(b) Crack or Encroaching Failure Mode in References [33] and [38]



(a) Deformation or Buckling Failure Mode in References [33] and [38]

Figure 1.11: Akita et al. (1967) observed that the two above – shown modes were responsible for the failure of the ship side models.

List of Tables

TANKERS	38%
BULK CARRIERS	10%
COMBINATION SHIPS	2%
CONTAINERS	2%
MISCELLANEOUS	20%
OFFSHORE VESSELS (Tugs, Supply vessels)	3%
PASSENGER	4%
REEFERS	2%
RO-RO	3%
GENERAL CARGO SHIPS	14%
UNKNOWN	2%
TOTAL	100%

Table 1.1: Ships, which caused oil-spills in 1994. Presented by Ventikos.

Fifty major oil spills from tankers and combined carriers

Rang/ Rating ^b	Name	Tanker Size		Spillage		Location	Cause						
		grt	dwt	Tons x10 ³ (metric)	Barrels x10 ³		Type	Co	Grm	F/e	S/h	N/k	
1	Atlantic Empress	128398	292666	257	1890	crude	x						
2	Castillo de Belver	138823	271540	239	1760	crude			x				
3	Amoco Cadiz	109700	237439	221	1628	crude				x			
4	Odyssey	65746	138392	132	925	crude					x		
5	Torrey Canyon	61263	121000	124	909	crude						x	
6	Sea Star	63989	120300	123	902	crude	x						
7	Hawaiian Patriot	45246	101038	101	742	crude							x
8	Independenta	88690	152408	95	696	crude	x						
9	Urquiola	59723	111125	91	670	crude						x	
10	Irenes Serenade	50903	105460	82	600	crude							
11	Khark 5	138394	284632	76	560	crude						x	
12	Nova	118654	239435	68	500	crude	x						
13	Wafra	36697	68600	62	480	crude							x
14	Epic Colocotronis	37469	64000	58	427	crude							x
15	Sinclair Petrolore	35744	56000	57	420	crude							x
16	Yuyo Maru No 10	43724	52836	42	375	wh prod							
17	Assimi	33847	59032	50	370	crude	x						x
18	Andros Patria	99460	122173	48	350	crude							x
19	World Glory	28323	45000	46	337	crude							

20	British Ambassador	27114	44929	46	337	crude	Japan				x
21	Metula	104379	206719	45	330	crude	Chile		x		
22	Pericles G.C.	38915	59096	44	324	crude	Qatar			x	
23	Mandoil II	25313	45000	41	300	crude	US West Coast	x			
24	Jacob Maersk	48252	88000	41	300	crude	Portugal		x		
25	Burmah Agate	32285	62663	41	300	crude	Us Gulf				
26	J. Antonio Lavalleya	68931	131663	38	280	crude	Algeria		x		
27	Napier	23690	38561	37	270	crude	Chile		x		
28	Exxon Valdez	94999	214861	36	267	crude	US, Alaska		x		
29	Corinthos	30705	56882	36	266	crude	US, Delaware	x			
30	Trader	21999	35000	36	263	fuel (cgo)	Greece				x
31	St Peter	20678	34730	33	246/700	crude	Ecuador			x	
32	Gino	26167	48760	32	240	carbon blk	France, Atlantic	x			
33	Golden Drake	16231	30004	32	238	crude	Bermuda			x	
34	Ioannis Angelicoussis	35269	68106	32	236	crude	Angola			x	
35	Chryssi	19183	29653	32 ^c	232	crude	Bermuda				x
36	Irenes Challenge	21090	34884	31	228	crude	Pacific Ocean				x
37	Argo Merchant	18743	28691	28	225	fuel (cgo)	US, East Coast		x		
38	Heimvrd	35335	55000	31	225	crude	Japan	x			
39	Pegasus	11089	-	25 ^c	225	wh prod	US, East Coast				
40	Pacoecean	17328	30016	31	225	crude	Northwest Pacific				x
41	Texaco Oklahoma	20084	35072	29	225	fuel (cgo)	South Africa				x
42	Scorpio	26031	42000	31	225	crude	Mexico, east		x		
43	Ellen Conway	27931	47566	31	225	crude	Algeria		x		

44	Caribbean Sea	18589	30661	30	225	crude	East Pacific Ocean			x	x
45	Cretan Star	19674	30372	27	218	crude	India, west				
46	Grand Zenith	18736	29930	26	213	fuel (cgo)	South Africa			x	
47	Athenian Venture	18251	31016	26	200	wh prod	Canada, Newfd		x		
48	Venoil	152328	330954	26	191	crude	South Africa				
49	Aragon	122583	238959	24	175	crude	Madeira			x	
50	Ocean Eagle	12065	18824	21	157	crude	Puerto Rico		x	13	12
					Total number of accidents :						
					Total tons(x10 ³) :						
					792						
					653						
					851						
					52						

^aCode: Co=collision; Grm=Grounding; F/e=Fire/Explosion; S/h=structurehull or machinery failure; Nk=Not known.

^bRanking is based in barrels spilled

^cSpillage data is in doubt.

Table 1.2: Daidola (1995) presented this table with fifty major oil spills from tankers and combined carriers.

Chapter 2

Internal Mechanics of Ship-Ship Collisions

Introduction

In the present chapter a more detailed look on the internal mechanics of ship to ship collisions is attempted. The field of the internal collision mechanics includes the evaluation of force-indentation response and of the damaged shape for the struck ship during collision. In side ship collisions, which comprises the aim of this study, the deformations of the structure can be quite large and as a result the structural members in the struck ship can experience failure modes such as yielding in buckling, crushing and rupture. Imperfections that would be considerably important to the usual design strength response will be of less importance to the response associated with ship collisions.

The structure of a struck ship will be deformed globally as well as locally. The coupling effects between local and global failure of the structure may be significant and their contribution to the resulted damage might have to be taken into account. Dynamic effects also, might be important and the demarcation line between the need of a static analysis and the need of a dynamic analysis has not been clearly determined yet.

The finite element analysis is a very powerful tool and it is able to carry out this kind of work by minimising the need of assumptions. However, the modelling and computing times required make FEA a not easy-to-use tool. Therefore, the efforts of researchers have

been focused on the development of an easy-to-use tool for the designing procedure of a ship.

The present study attempts to work with an approximate theoretical method. The restrictive assumptions of such methods affect the internal collision mechanics. The local and global deformations are assumed decoupled. Furthermore, static analysis of the collision is used. The effects of strain hardening and inertia of the ships are neglected.

2.1 Internal Mechanics of Ship to Ship Collision

The collision problem as it has been already mentioned, is divided in two phases the external collision mechanics and the internal collision mechanics. The definition of each one is shown below:

- External Mechanics: It is defined as motion of the ships during the collision
- Internal Mechanics: It is defined as the deformation and destruction of local ship structures.

The behaviour of two ships and their structural members following a collision involves the global dynamics of the ship structures in way of collision. External and internal mechanics are functions of the interaction forces between the ships, including the inertia forces of the ships and the hydrodynamic forces of the surrounding water. [Incecik and Samuelides, 1981].

The amount of energy released during collision is not fully dissipated in crushing the structures of the colliding ships. The energy is distributed to a number of phenomena associated with collision. The energy distribution is as follows:

1. Energy absorbed due to the rigid body motion of the colliding vessels (Fig. 2.9).
2. Energy absorbed due to the hydrodynamic resistance of the surrounding water.
3. Energy absorbed due to the overall elastic deformation of the struck and striking vessel. (see Figure 2.9).
4. Energy absorbed due to the elasto-plastic deformation of the structural members around the damaged area of the colliding vessels.
5. Energy absorbed during and after the rupture of the hull of the struck and/or striking ship.

The energy values associated with the internal collision mechanics are the fourth and the fifth cited energies. The elasto-plastic deformation of the structural members is assumed as only plastic deformation of the structural members. The effect of the energy absorbed during the elastic phase is assumed to be very small compared to the plastic energy. [McDermott et al. 1974].

2.2 Methods of Treatment

The bulk of methods that have been studying collisions are referred to the internal mechanics of collisions. Predicting the deformation and penetration that a ship will undergo during collision is of major importance. This can only be achieved through studying the internal mechanics of collisions.

The pioneering Minorsky method is one of the methods that takes into account the hydrodynamic energy involved in collision. This was not due to a theoretical analysis but due to the use of actual collision data. Minorsky (1959) used the added mass to calculate

the effect of the surrounding water. This added mass was taken to be 40% of the struck ship's mass.

On the other hand, most of the approximate theoretical methods ignore the effect of the surrounding water and the overall bending of the ship. McDermott et al. (1974) separated the elastic, plastic and hydrodynamic energy of collision. Through simplified approaches concluded that the elastic and hydrodynamic energies are small compared to the plastic energy available. Therefore, they can be neglected when estimating the energy absorbed in large indentations before the rupture of hull plating. Furthermore, it had been confirmed that the elastic energy involved in local elastic deformations and in the overall elastic vibratory response to the collision is negligible compared with plastic energy.

Almost all the approximate theoretical methods have adopted the above-cited conclusions. The deformation of the structural members is treated irrespectively of the rigid body motions of the colliding vessels.

2.3 Structural members involved in Collision

The models that are used to describe the structures of the colliding vessels are mostly simplified. The aim is to conclude in simple formulae for the energy absorption. Therefore, most of the methods are using models, which look like the one shown in Figure 2.1. This model is consisting from the decks (deck plating), the side shell plating, side transverses and deck transverses on the decks.

The usual assumption for the striking bow is that is considered to be infinitely stiff. This means that the collision energy is fully absorbed by the side structure of the struck ship.

The way of analysing the individual members of the structure of the struck ship is up to the researcher and the accuracy aimed. Most of the studies employ static analysis, and the strain hardening effect is being considered through an increase to the yield stress of the material.

2.4 Mathematical Modelling of the Internal Collision Mechanics

Bearing in mind, that the present study is dealing with oil tanker designs, the structural systems that will be reviewed will be tanker or tanker-like designs. In the following paragraphs an analysis is attempted of the behaviour of structural members of the struck structure during collision.

The U.S. Coast Guard in the early 1970's sponsored research to develop an analytical procedure to evaluate the structure of tankers from the viewpoint of the actual protection it affords the cargo during collision. McDermott et al. (1974) and Rosenblatt & Son (1975) developed the required method, which treats minor collision problems. It is a static analysis based on simplified models of various structural components in the struck ship. The energy absorbed by each component is computed and a summation of all components gives the total energy absorbed.

The failure mechanism is the point examined in this chapter. McDermott et al. (1974) uses the idealised collision model shown in Figure 2.3, which most of the researchers adopted in the study of collisions. Membrane tension in the side shell and stiffeners was identified to be the major mechanism absorbing energy in the collision.

The mathematical model assumed for analysing the structural behaviour of a struck ship involves three phenomena producing plastic deformations, longitudinal plastic bending of the stiffened hull plating and deck, plastic membrane tension in the stiffened hull plating and the deck, and yielding, buckling and/or shearing of the web frames. The flow diagrams of the possible structural response are shown in Figure 2.4 and 2.5 for a single hull tanker and a double hull respectively.

The collapse mechanism presented by McDermott and Rosenblatt is as follows. Initially, the stiffened hull plating will distort in a plastic bending phase, with plastic hinges forming in the vicinities of the strike and the web frames flanking the strike. During this phase, insignificant membrane tension will be developed. For a typical tanker with longitudinal angles stiffening the hull plating, the longitudinal angle-shaped stiffeners will then buckle in the vicinity of the flanking web frames, and possibly “trip” in the vicinity of the strike. Subsequently, the stiffened hull will unload momentarily as the strike continues, but will reload in a membrane tension phase. The hull will rupture at the end of this phase, with possibly the flanking web frames yielding or buckling before the hull ruptures. In such cases, the membrane tension phase will divide into the following two respective sub-phases: (1) there is no transverse movement of the web frames flanking the strike; and (2) the web frames flanking the strike move inward toward the ship’s centreline and the damage extends into the adjacent web frame spaces. During these phases, the deck is also distorting in membrane tension. However, the deck behaviour is presumed not to affect the sequences of the options listed in Figures 2.4 and 2.5.

As indicated in Figures 2.4 and 2.5, other sequence of phenomena are possible. In example, a hull with longitudinal stiffeners, such as rectangular bars that are not apt to buckle or trip, will tend to rupture before significant membrane tension has a chance to develop.

McDermott et al. (1974) assumed that once rupture has been initiated, it will propagate throughout the stiffened hull plating to the extent determined by the incursion of the striking ship with no further energy absorption by the stiffened hull plating.

This is a description of the sequence of phenomena occurring during collision. The above-cited mathematical model has been adopted by most of the researchers developing approximate theoretical methods.

2.5 Difficulties arising due to new structures

The above mentioned collapse mechanism is good and adequate enough, when it can be applied to a structure as mentioned before. The simplified model structure of the struck ship used is sometimes restricting the applicability of the sequence of phenomena proposed. This problem came up in the recent years with the diversification of structural concepts.

Before the OPA 90 regulations, most of the tank vessels were designed as single-skinned hulls. In the 1990 Oil Pollution Act, the U.S. Congress mandated the use of double-skin tanker designs. All of the new designs have been aimed to reduce oil outflow and maximise the energy absorption before rupture of the hull. Being this, the main objective of the designers, the structures that have been produced are very complicated and an application of the simplified model shown in Figure 2.1 is not feasible in most of these designs. The structural arrangements of the existing tankers offer an array of differing characteristics. The more new designs against potential pollution are proposed and adopted the more the structural characteristics will differ from one ship to another.

The differences in transverse sections between a conventional single-hull tanker and what might be considered a conventional double-hull tanker were presented by Daidola (1995) and are shown in Figure 2.6. In particular, the transverse structure in the wing or side tank region can be quite different. The transverse framing of a double hull vessel can be narrow and also the struts used to tie the frame together in a single hull vessel are either reduced or omitted.

Because of the difference in structural details, single hull and double hull vessels are not expected to respond in the same way during collisions. The energy absorption capacity will be a function of the width of the double skin, the arrangement of the longitudinal girders, the structural configuration, separation of bulkheads as well as material and scantlings. Daidola (1995) gave a list of which structural details are critical in the collision and grounding response of a single hull and two types of double hull tankers (Table 2.1). It is evident, that the structural details involved in collision are quite different for each ship.

It becomes clear that a simplified model as the one proposed by McDermott (1974) and Rosenblatt (1975) and further adopted by Hegazy (1980) and other researchers could not predict the energy absorbed of a complicated or a unidirectional double hull structure during collision without modification of the mathematical model used.

2.6 Analytical presentation of the failure modes of individual structural members and their role in collision

The conventional single and double hulls consist of certain characteristics, which can affect their energy absorption capacity. These characteristics are shown in Table 2.1 and will be further discussed here as well as their modes of failure.

Side stiffened plating: The membrane tension in the shell of a vessel has been identified as the most significant source of energy absorption during collision.

McDermott et al. (1974) considered the longitudinally stiffened side shell plating to be assemblies of independently acting “T-beams”, with each T-beam consisting of one longitudinal stiffener and the “effective width” of the plate with which are assumed to act as a structural unison. Generally, the effective width is assumed to be equal to the spacing between stiffeners and the dividing line between two adjacent T-beams is halfway between the stiffeners.

The collapse mechanism of this model is as follows. If the flange of the stiffener ruptures, the rupture is assumed to transmit to the stiffener and the attached plate. Subsequently the stiffener buckling (tripping) the side plating is assumed to immediately unload in bending and reload in membrane tension. At the end of the membrane tension phase the most strained T-beam ruptures and the rupture is assumed to propagate immediately to the whole damage height.

Hegazy (1980), in the method he developed for minor and major collisions, considers the side shell plating as a plate subjected to out-of-plane load. The effect of the stiffeners is introduced as an increase of the thickness of the shell plating (equivalent thickness

allowing for stiffeners). The side plate is modelled as a beam subjected to concentrated transverse load. With the transverse deformation increasing, the importance of bending moment and shearing force diminishes and the membrane force develops. At sufficiently large transverse displacement the membrane force dominates the behaviour. The formulae used for the energy absorbed during the membrane tension phase have been proposed by Jones (1973) and further confirmed by Wang and Ohtsubo (1997) (see Appendix B).

Wang and Ohtsubo (1997) presented three different mechanisms for the energy absorbed due to the plasticity of the side shell plating. Considering symmetric loading situations the models are shown in Figure 2.7. When the striking bow is very large, the struck side shell plating will stretch mainly in the longitudinal direction. In this case side plate can be modelled as a beam subjected to concentrated transverse load (Fig. 2.7(a)). On the other hand, when the striking bow is relatively small and sharp (for example the case of a VLCC struck by a small vessel), impact load is very local and concentrated. An appropriate model is a plate subjected to a point load (Fig. 2.7(c)). In between the two extremes there is another model, a plate subjected to a line load (Fig. 2.7(b)). The contact of the striking and struck ships is idealised as a line segment. The work of the authors concludes with the suggestion that the relative size of striking and struck vessels should be investigated in order to define realistic collision scenarios.

Web Frames: The structural damage stemming from collision is assumed to be confined between boundaries formed by adjacent heavy transverse members. Such members are the web frames along with the deck and bottom transverses. If these members collapse then the damage is extended to the area between the next pair of heavy transverse members (web frames).

McDermott et al. (1974) proposed the following assumptions for the behaviour of the web frames. The web frames are assumed to offer resistance to small movements of the stiffened hull plating in the longitudinal direction.

The collapse analysis of a web frame flanking the strike is concerned with evaluating the transverse forces, from the deformed T-beams units, that result in the incidence of yielding or buckling of the web frame. For the evaluation of the transverse force exerted on the web frame by the most highly strained T-beam when the web frame is failing is suggested an iterative solution. That is because there will be just one of the transverse forces exerted on the web frame.

Hegazy (1980) separates the structural parts of a heavy transverse member. The condition that have to be satisfied in order the damage to be extended in the adjacent bays, is to have collapse of the side transverse (web frame) and collapse of the deck transverses. As deck transverse can be identified as the heavy transverse member on the deck of the struck ship concurring with the side transverse (see Fig. 2.1).

The critical buckling load of the deck transverses is first to be calculated. If the reaction force exerted on the deck transverse reaches the collapse load of the deck transverse then the deck transverse collapses in buckling. The side transverse is assumed to be a beam subjected to a uniformly distributed load, which is the component of the membrane tension force in the side plating in the transverse direction. If this force overcomes the collapse load of the side transverse then the latter collapses.

Decks: The decks in the struck ship are structural members with major dimensions in the direction of collision. This characteristic enables them to play an important role in energy absorption during collision.

McDermott et al. (1974) proposed the following collapse mechanism of the decks. If the top of the striking bow is above the deck of the struck ship, the struck deck forms a series of low-pitch longitudinal folds (see Fig. 2.3) “gathered” at the location of maximum incursion and extending over a length equal to the damaged length of the hull. Any deck failure is by transverse rupturing resulting from longitudinal membrane tension.

The deck structure is analysed as being divided into elements originally longitudinal (each may conveniently be considered a deck stiffened-plate T-beam unit) which stretch horizontally in membrane tension over a length equal to the damaged length of the stiffened hull.

Hegazy (1980) proposed the analysis of the decks being subjected to a uniformly distributed load at the side of the collision. The decks assumed to absorb energy due to membrane tension developed and due to plastic buckling. The membrane tension force on the decks is calculated with simple procedures (Appendix C). The plastic buckling strength is also calculated through some simplifications (Appendix D). After the rupture of the hull commences another energy absorbing mechanism called wedge splitting of decks.

The method proposed by Hegazy (1980) accounts also for major collision problems. It is evident that after the rupture of the shell plating the only energy absorbing mechanism is the wedge splitting of decks. Hegazy, in order to calculate the force required for the wedge to penetrate to a certain depth in the decks, assumed that part of the force is required to tear the deck and another part is required to push aside the material to permit the entry of the wedge. Through these assumptions he came up with a simple formula similar to the one proposed by NCRE (1967).

Wang and Ohtsubo (1997) presented a mathematical model on calculating the energy absorption due to folding of the decks during collision and prior to rupture of the hull. The idealised model is shown in Fig. 2.8: a plate subjected to concentrated load at its edge. Under the indentation of a rigid object the plate buckles and deforms out of its original plane. A fold will occur, which shows that bending stress plays an important role in energy absorption. As the penetration increases a second and even a third fold may appear. The authors proposed that for calculating the energy absorption capacity the mean resistance during the forming of a fold is a reasonable representation of the deck's strength.

Jones (1987) presented a study on the plate tearing for ship collision and grounding damage. This situation arises after the rupture of the shell plating. Some experimental results were presented for the cutting of steel plates, which were struck on one edge by a rigid wedge. The work done by the striking web was analysed in cutting energy, distortional energy, elastic energy, and frictional contributions. The elastic energy was supposed to be zero since material plasticity dominated the response of the plate tests. There were identified five different deformation modes. Jones believed that more deformation modes could arise for other materials and test geometries. Finally, empirical formulae were developed for the cutting, bending, and friction energies absorbed in the steel plates, which appeared to agree reasonably well with the test results.

Transverse Bulkheads: The transverse bulkheads are very stiff transverse members, which do not buckle, yield or rupture in most of the cases.

McDermott et al. (1974) assumed that transverse bulkheads and the ship bottom do not distort in the transverse direction, although the hull longitudinal stiffeners may buckle in the vicinity of their connections to a transverse bulkhead. The longitudinal extent of

damage due to this assumption is restricted between to consecutive transverse bulkheads and above the bottom of the ship.

Most of the researchers have adopted the assumptions that transverse bulkheads are not deforming during collision. The stiffness of the transverse bulkheads will result in very little energy absorption, when the strike is near them.

2.7 Conclusions

The review on the internal mechanics of collision gives the opportunity to understand better the problems and the unclarity that there is in some of the subjects involving the theoretical analysis of collisions. The application of the theoretical methods and the finite elements analysis in some new double hull designs have provided us with some results and some intended ways of dealing with the problem.

McDermott et al. (1974) proposed the same mathematical model for the analysis of a double hull as the one for a single hull tanker. Of course some more assumptions and remarks were made for the inner hull engagement. The rupture of the outer hull was supposed not to affect the inner hull. The inner hull would rupture only when the striking ship was engaging it. The lateral movement of the web frames plays a very important role in the movement of the inner hull.

Hegazy (1980) has proposed a mathematical model for a double hull design. The major restriction of this model is that it assumes that the damage is confined between two adjacent web frames.

Daidola (1995) demonstrated the differences between the conventional double hull vessels and the unidirectional double hull vessels, which receive increased attention in recent years. The theoretical procedures could easily be applied to every structural design, when this is disassembled to its individual structural members. The problem is that the sequence of phenomena will be different and depended on the structural configuration of each design. Thus, it is difficult to be developed a theoretical method, which will be able to treat any design produced.

Furthermore, numerical simulations provided a number of results, which have to be appraised and incorporated or not to the mathematical modelling of double hull vessels collisions.

Paik and Pedersen (1996) presented some results through finite elements analysis of a side structure of a double hull vessel due to collision. The conclusions were that in a double-skinned structure, the inner platings would possibly deflect from the very beginning of the collision process. Rupture of the inner hull is very much dependent on the dimensions and arrangements of strength members. That is, the inner hull may not rupture even after the bow of the striking ship penetrates till the original position of the inner hull, or the inner hull may rupture even before the bow of the striking ship penetrates till the original position of the inner hull.

Kitamura and Kusuba (1997) carried out a series of numerical simulation of side damage due to collision adopting ASIS's methodology based on the explicit FEM

simulation system. The striking ship was assumed to be in the ballast condition. A Suez Max simplified rigid bow was impacting various double side Alternative Designs for VLCC in full load condition and a Standard VLCC design. The results showed that the difference in energy absorption capacity of Alternative Designs was not so remarkable in general, provided that the net steel weight of double side structure was limited to be equivalent to the Standard design.

The above mentioned remarks show that the field of the internal collision mechanics is not an easy one. A lot of simplifications have to be made each time and besides the sequence of phenomena occurring during collision could change from one ship to another.

In the present thesis is attempted an extension of the theoretical method proposed by Hegazy in order to treat double hull designs with lateral movement of the web frames. It was tried to keep the assumptions as general as possible in order for the method to be applicable in other double hull structures.

List of Figures

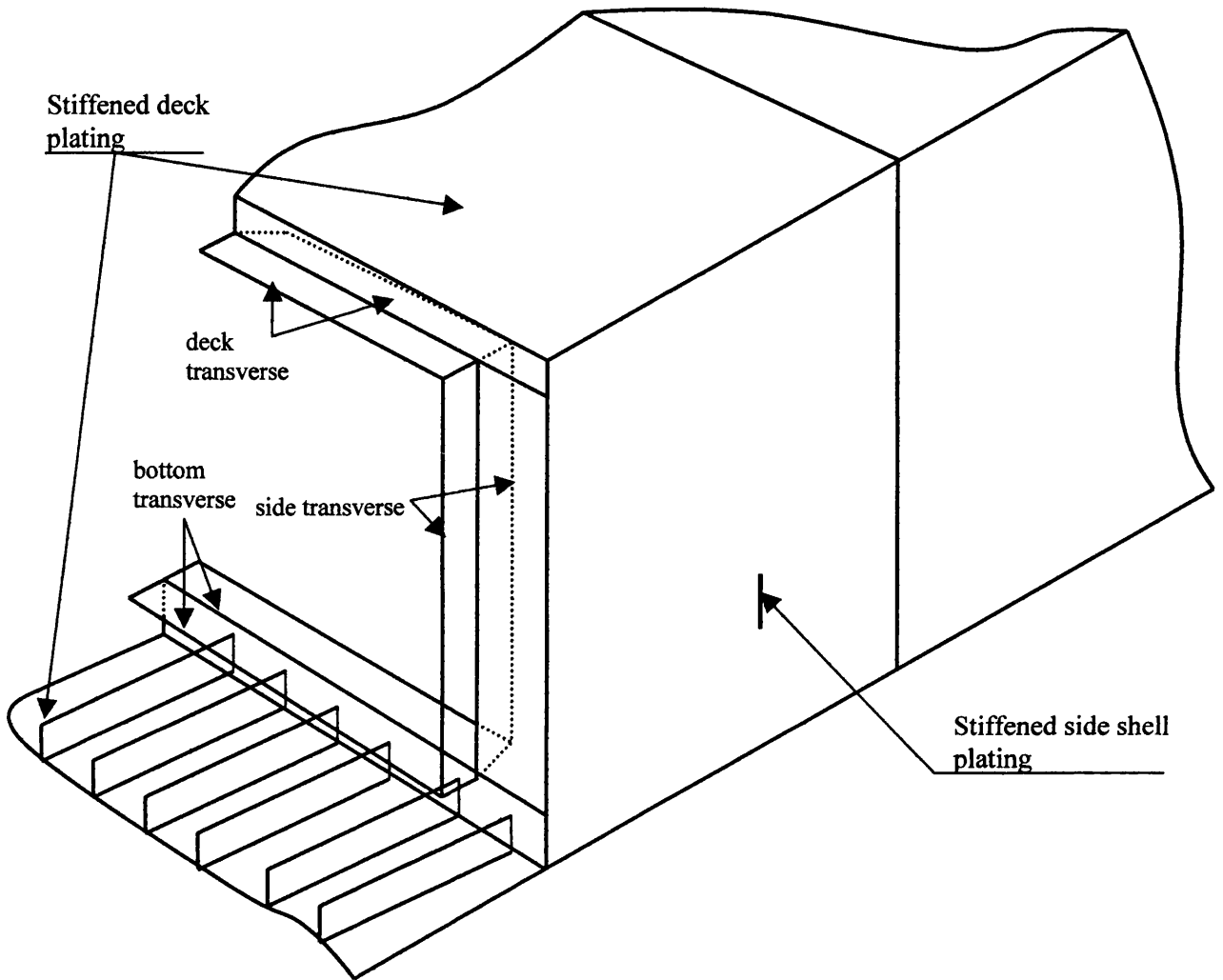


Figure 2.1: Simplified model of the side structure of the struck ship.

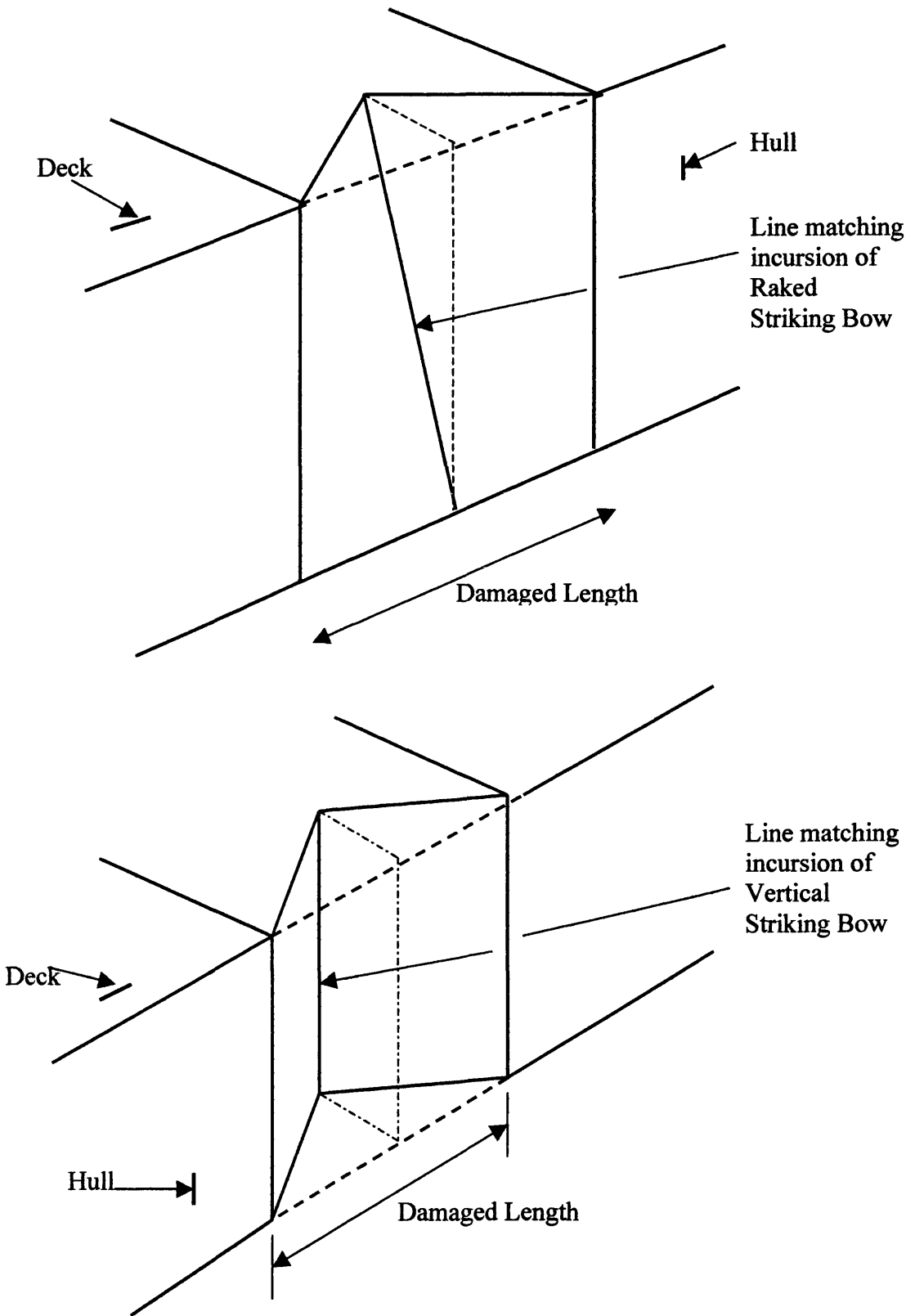


Figure 2.2: Assumed collision imprint in the struck ship used by Hegazy (1980).

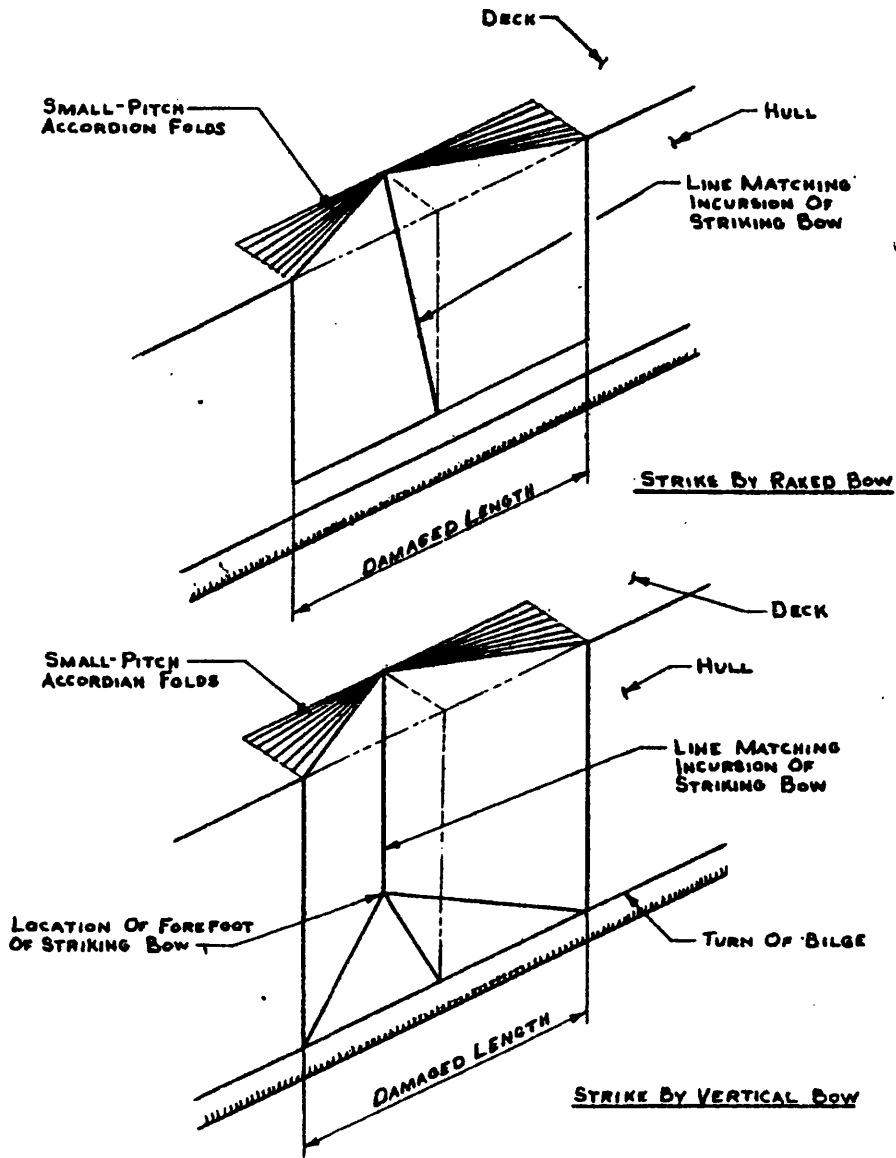


Figure 2.3: McDermott et al. (1974) assumed imprint in the struck ship.

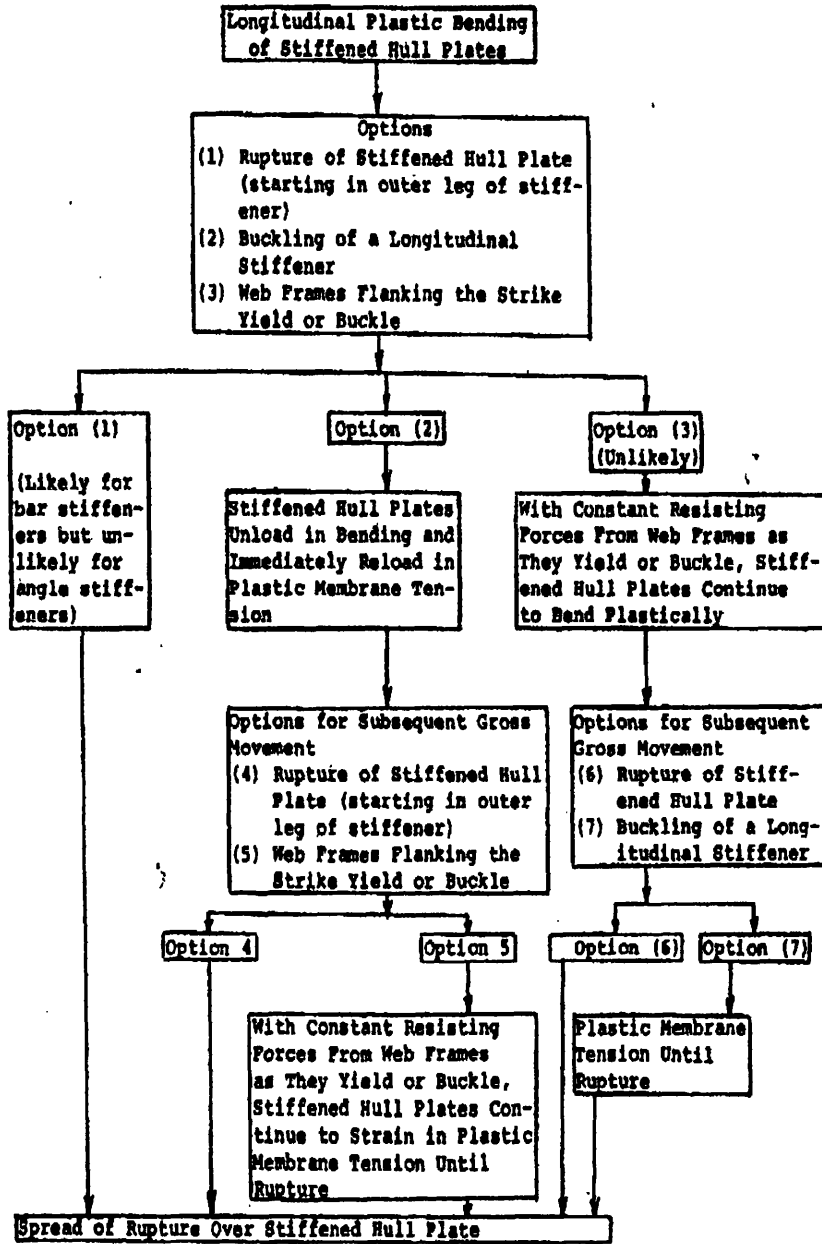


Figure 2.4: Macro flow diagram for side collision plastic-energy analysis of a single hull.

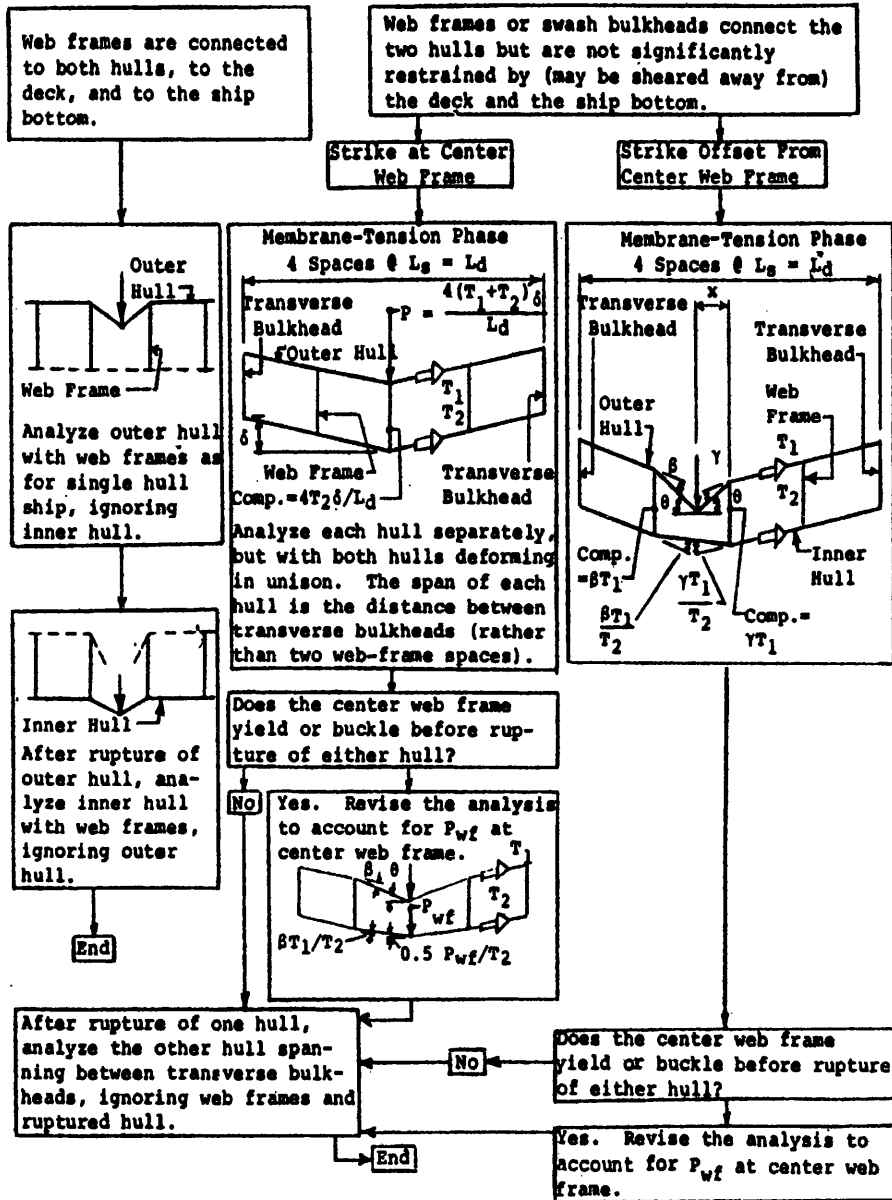


Figure 2.5: Macro flow diagram for side collision plastic-energy analysis of double hull.

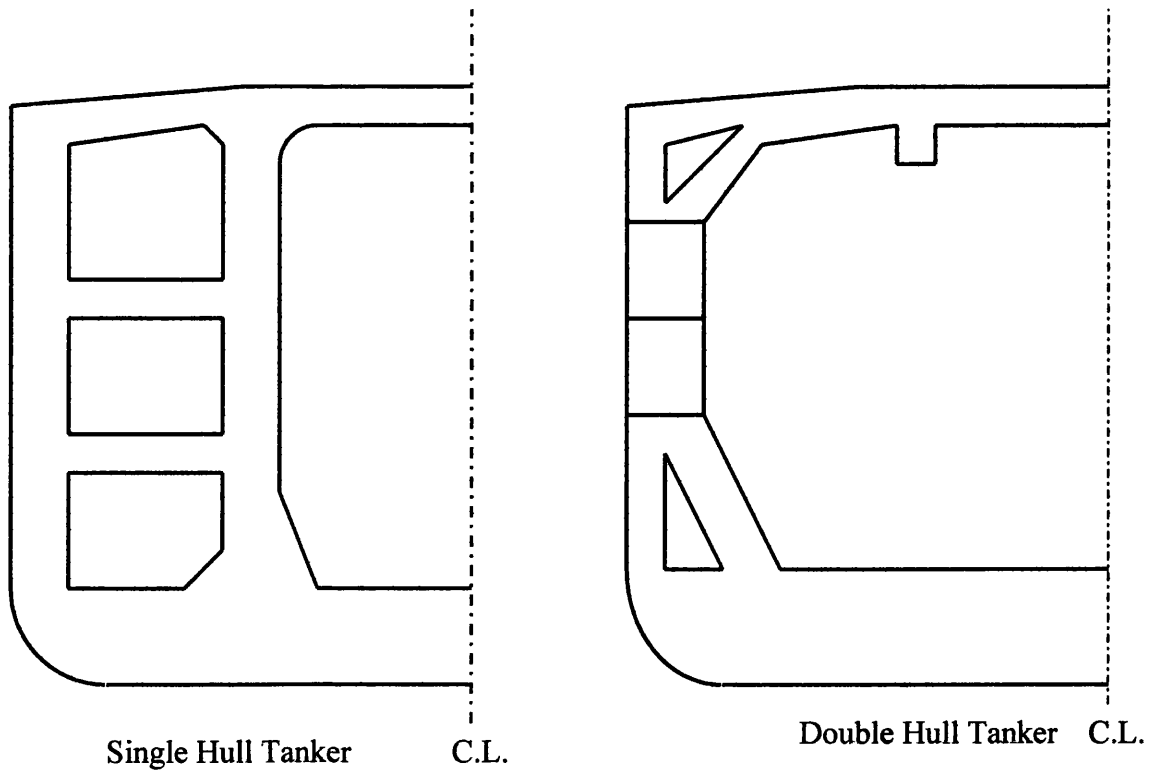
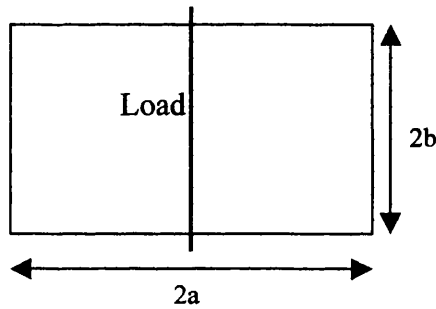
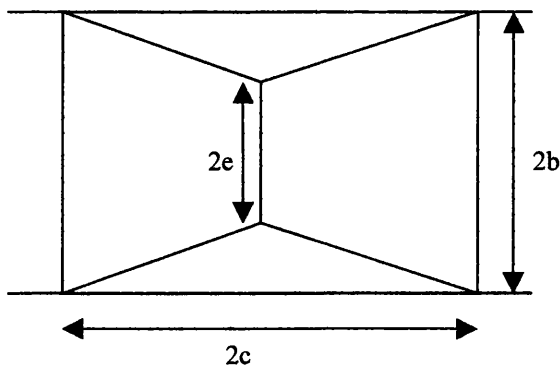


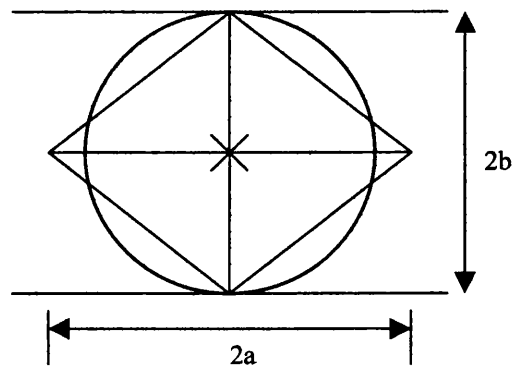
Figure 2.6: Comparison of Transverse sections of a single-hull and a double-hull tanker.



(a) Beam Model



(b) Plate Model: Line Load



(c) Plate Model: Point

Figure 2.7: Models presented by Wang and Ohtsubo for side ship plate subjected to very large out-of-plane load.

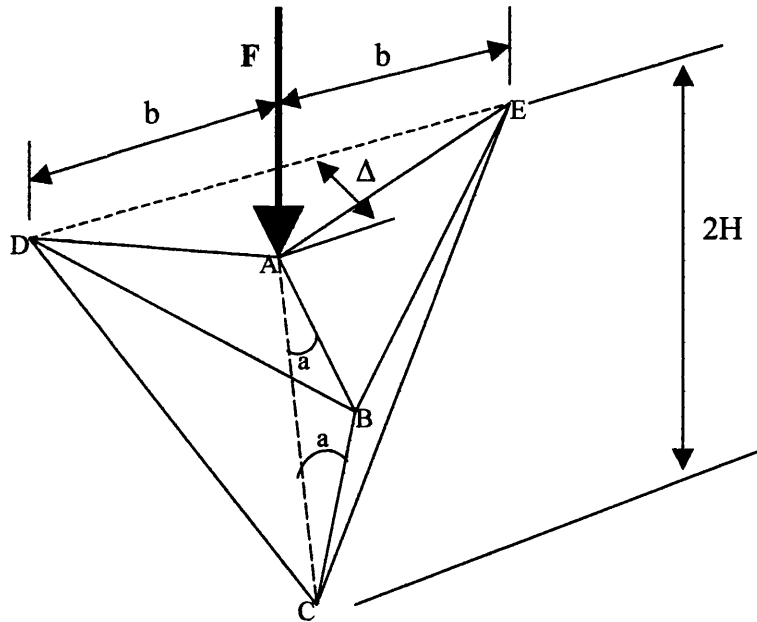


Figure 2.8: In-plane dented plate. Idealised model for the folding mechanism of the decks due to impact force. Presented by Wang and Ohtsubo (1997).

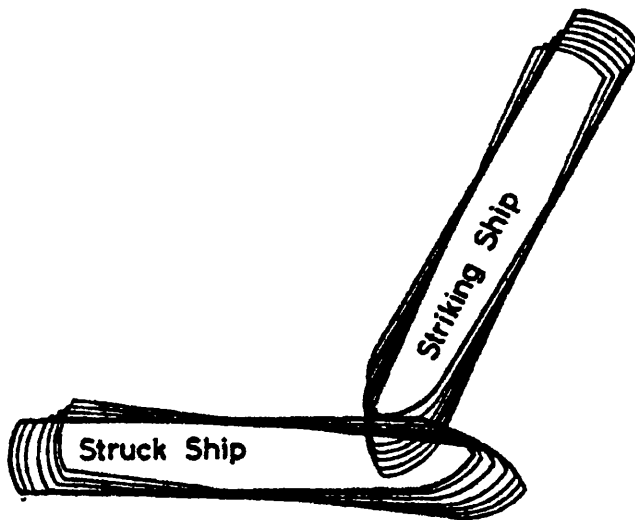


Figure 2.9: Simulation of an oblique collision between two similar ships showing the relative movement of the ships.

List of Tables

Table 2.1: Critical structural details for a conventional single hull vessel, a conventional double hull vessel and a unidirectional double hull vessel. Daidola (1995).

Table 2.1: Critical Structural Details
Conventional Single and Double Hulls
side and bottom stiffeners web frames brackets decks transverse bulkheads outboard bilge transverse floors material
Unidirectional Double Hull
longitudinal girders decks transverse bulkheads outboard bilge material

Chapter 3

Assessment of Collision Resistance of Ships

Introduction

Ship collision accidents often result in extensive damage to property and, less frequently, in loss of life. Although continuous efforts are being made to prevent their occurrence, it is likely that such accidents will continue to occur. Therefore, it is important to examine various methods of reducing the consequences of collision through improved vessel design.

Several methods are used for the assessment of collision resistance of ships. In most of the methods a large number of experimental data have been introduced in the theoretical analysis which might affect the validity of the method, when applied to different cases. Besides, the result of methods, which depend on model test data, might suffer from scaling effects when applied to full sized ships. Also, the pioneering Minorsky's method, which is based on actual collision cases between ships and presented in 1959, might be proved inaccurate due to the substantial changes in ship design and the world shipping fleet during the last 30 years.

The minor collisions were examined from McDermott et al. (1974), Jones (1979) and Van Mater (1979). Minorsky (1959), NCRE (1967) and Akita and Kitamura (1972) carried out research work in the area of the high-energy collisions. In all of the high-energy above

mentioned methods a number of experimental data have been introduced in the theoretical analysis, which might not remain valid in other cases.

In this chapter a method proposed by Hegazy (1980a and b) for estimating the energy absorbed by ships' structures during collision is presented. The formulae of this method were derived by using theoretical analysis of various structural failure modes of individual components suffering disruptive damage and by taking into account all necessary parameters resisting collision.

The method that was proposed by Hegazy in two reports (1980a and b), can treat both minor and major collision cases. This capability of the method along with the analysis of each individual member, which provides optimisation capability of each structural member, was the reason that this method was selected among others. Moreover, Hegazy (1980a) using the data of a series of test conducted by Akita et al. (1971,1972) and test values by Arita et al. (1977) verified the energies calculated by his method. The comparison between the theoretical results and test values revealed that the magnitude of the energy absorbed during collision can be reasonable predicted in the theoretical way proposed. The above mentioned advantages and the fact that a recently developed method is concerned gives hope for an easy and low cost designer tool to be produced.

Although the method agreed reasonably well with the experimental results, Hegazy (1980b) suggests that some experiments should be carried out to determine adequate corrections to the simple models of structural failure of the different parts of ships' structures used in the analysis. It would be also useful if the method could be applied to some practical cases or to full-scale collision tests.

3.1 Proposed Method – Hegazy (1980)

The method that will be presented in the following paragraphs was developed by Hegazy (1980). This method is then used for the calculations of particular ship designs in order to examine its applicability and feasibility when complicated structures are under consideration.

The need for the development of a new method by Hegazy came up through a review that he conducted, of the most cited works for analyzing the structural response of ships during collisions. The main disadvantages of the existing methods were detected and were reported in the paper along with the presentation of the proposed method. These remarks will be cited below.

The simple design procedures due to Akita and NCRE neglect the contribution of the shell plating to the energy absorption in the struck ship. On the other hand a comparison of the semi-empirical relationship of Minorsky and the actual collision cases shows a good correlation in the higher energy regions. Minorsky explained the poor correlation in the low energy regions by the relatively large errors in the calculated impact energies at low speeds resulting from small errors in the reported speeds of the striking ship. However these errors are probably not the only reason for the scatter in the low energy region. Minorsky's formula does not take into account all the relevant strength parameters, as for example, the effect of the side of the struck ship serving as a protection barrier. Considering two vessels of similar dimensions except for the thickness of the struck side plating the above mentioned methods would predict the same amount of energy to be absorbed by the vessels for similar penetration.

Another point that has to be made is that the above-cited methods do not give any information about the energy absorbed at the instant of rupture of the hull of the struck ship.

Furthermore, Minorsky's formula contains a constant value, which is independent of the resistance factor (this means constant for all collisions). This constant value has been interpreted by some writers as being the work that must be done before penetration occurs at all. If this is so, the value of such constant should be dependent on the struck ship and vary from one struck ship to another.

From the result of collision tests conducted by Akita and Kitamura (1972), it was observed that in a collision with a weak stem Minorsky's method tends to overestimate the absorbed energy of the side. In the contrary, in tests with very strong stem it tends to underestimate the absorbed energy of the side and overestimate that of the stem. In other words Minorsky's formula overestimates the absorbed energy of the stronger structure.

Concluding, the NCRE and Akita methods are based on experimental data and so might suffer from the scaling effect when applied to full sized ships. Meanwhile the substantial changes in ship design in the last forty years, since Minorsky developed his method, could affect the accuracy of the method, when applied to ship collisions now.

Hegazy (1980), through the critical review of the existing methods, believed that there was a need for the development of a more comprehensive study as a basis for developing practical procedures for prediction of the magnitude of the energy absorbed by the structures of colliding vessels with reasonable accuracy.

The method developed by Hegazy is a simple one, which evaluates the amount of the energy absorbed by different parts of ships' structures during a collision. The formulae were derived by using theoretical analysis of various structural failure modes of individual components suffering disruptive damage and by taking into account all necessary parameters resisting collision. Moreover, by following Minorsky's general idea, charts

relating the energy absorbed in collision to the volume of the damaged material in the colliding ships' structures were given for minor and major collisions.

At the end, the prediction by such a new method of the energy absorbed by the side structure of the struck ship and the striking bow during a collision was verified to be reasonable compared to a series of tests conducted in Japan.

3.2 Assumptions

For complicated problems, such as collisions between ships, some simplifying assumptions are necessary to make the problem solvable. Through an extensive review of the existing methods used to analyse the structural response of ships' structures during collisions, Hegazy found that the following assumptions were generally accepted and were used throughout the proposed method:

1. Collision between ships is an entirely inelastic process.
2. The structural response of ships' structures during collision can be estimated using static analysis. Any dynamic effects can be included as an increase in the value of the yield stress.
3. The failure criterion is based on the simple philosophy that rupture of plating occurs when the elongation of the hull plating between any of the side transverses (or transverse bulkheads) exceeds the stretching limit of steel. In other words, there is

no possibility of fracture of the plating prior to the attainment of the ductility limit of the material.

4. The variation of the deformation along the side of the struck ship is symmetrical about the incursion line.
5. The longitudinal extent of damage is the same for the deck, shell plating and all damaged longitudinals.
6. The longitudinal damage is likely to be restricted between the transverse bulkheads and/or strong side transverses.
7. The striking load is assumed to act along the incursion line only. For a raked striking bow a sloping incursion line is assumed, while for a vertical striking bow a vertical incursion line is assumed.
8. Straight lines can represent the deformation of the plating between adjacent side transverses (Figure 3.5 and 3.6).
9. During the membrane tension phase, the average longitudinal stress in plastically deformed portions of the plating is taken as the yield stress (σ_y). If the strain – hardening effect is to be taken into account then the value of this average stress (σ_m) is taken as the mean value of the ultimate stress (σ_u) and the yield stress. i.e.,

$$\sigma_m = \frac{\sigma_y + \sigma_u}{2}$$

10. The stiffened side plating and deck plating act as independent units, that is, there are no in – plane forces between them.
11. The energy absorbed during the plastic bending of shell plating is neglected due to its very small value in comparison with that due to membrane effects.

3.3 Theoretical Analysis of the Various Components of Energy Absorption

In the following subsections the various assumed structural failure mechanisms will be individually examined and analysed in order to evaluate the energy absorbed by different parts of ship structures during collision. The collapse mechanism of the side structure of the struck ship depends on whether the deck transverse (i.e. the heavy transverse members on deck) flanking the strike reaches or not its own collapse condition. Two cases now arise, the first when the damage is confined to one bay (area between the heavy transverse members) and the second when the damage is extended to more than one bays. The two collapse models are shown in Figures 3.1, 3.2.

In the below - cited paragraphs, the formulae for the absorbed energy by each structural member of the struck ship will be presented for a general case.

3.3.1 Determination of the Critical Indentation W_0

The collapse model of the side structure of the struck ship must be determined before the expressions for the absorbed energy are presented. The way that the side structure of the struck ship will respond to an impact load must be known, in order to be clear if the damage will be confined in one bay or if it will be extended to the adjacent bays. This is being achieved by calculating the value of the indentation ‘ W ’ at which the neighbouring deck transverses will collapse through buckling. This value is called “critical indentation W_0 ”.

Consider a strike at the mid – span between heavy transverse members. If for a certain indentation ‘ W ’ (at the strike location) stands that $0 < W < W_L$, where W_L is the limiting indentation beyond which rupture of the hull plating occurs, then the reaction force ‘ R ’ acting along the neighbouring deck transverses is less than the collapse load ‘ P_c ’ of the deck transverse, then there will not be any significant lateral deflection of the transverse frames flanking the strike. This is the case of the damage confined in one bay.

On the other hand, if $R \geq P_c$, then the flanking deck transverses will buckle and the collapse model will extend over two more deck transverses.

The value of the critical indentation W_0 can be calculated from the above – mentioned condition:

$$R = P_c \quad (3.3.1.1)$$

The reaction force (R) at the neighbouring deck transverses is (on the one side only):

$$R = \frac{F \cdot \sin \psi}{n} \quad (3.3.1.2)$$

where:

F = the sum of the membrane tension force in shell plating and deck platings as well as the buckling force in the latter, calculated for one side only of the incursion line

ψ = angle between the positions of side plating before and after collision:

$$\psi = \tan^{-1} \frac{W}{L}$$

n = number of decks in the struck ship involved in collision = the number of deck transverses on the one side only of the incursion line.

L = half distance between deck transverses.

As shown in Figure 3.4, the deck transverses are heavy transverse members on decks, comprising a frame and an effective part of deck plating associated with the frame as a «flange».

Strictly the collapse load of deck transverse (P_c) should be determined according to the ultimate capacity of a beam subjected to axial and bending stresses. To simplify the problem it is assumed that the collapse load of the deck transverse can be determined from the axial capacity of the effective part of the deck plating associated with the frame as a flange and the capacity of the frame alone, considering the jointed edges to be simply supported. The contribution of the frame alone is calculated from simple buckling formula. The resistance of the effective part of the deck plating is determined from the ultimate capacity of a postbuckled plate subjected to axial compression. Consequently, the final collapse load of the deck transverse will be:

$$P_c = 2 \cdot b_e \cdot t_d \cdot \sigma_y + \gamma \cdot \sigma_y \cdot A \quad (3.3.1.3)$$

where:

$$2b_e = \text{effective width of deck plating} = 2 \cdot C \cdot t_d \cdot \sqrt{\frac{E}{\sigma_y}}, \text{ by Timoshenko}$$

σ_y = yield stress of the material

E = modulus of elasticity

C = experimental constant varying with the proportions of the plate. $C \approx 1.0$.

$$\gamma = \sigma_{cr} / \sigma_y$$

t_d = thickness of deck plating.

σ_{cr} = buckling stress of the frame alone (for calculating σ_{cr} the span of deck transverse is taken as the distance between ship's side and the nearest heavy longitudinal girder).

A = cross sectional area of the frame alone.

Using equations (3.3.1.2) and (3.3.1.3) the critical indentation W_o , beyond which the collapse will extend beyond the adjacent deck transverses, can now be determined.

3.4 Energy Absorbed by Different Parts of Ships' Structures

3.4.1 Energy absorbed due to membrane tension in the stiffened side plating of the struck ship

The method used by McDermott et al. (1974), Jones (1978) and Van Mater (1978) for the structural analysis of minor collisions was considered to be suitable for the evaluation of the energy under consideration. Using the equation proposed from Jones (1973) for

rigid – plastic beams loaded transversely into the membrane range the following expression for the energy absorbed due to membrane tension in hull plating was obtained:

$$E_1 = \frac{1}{2} \cdot \sigma_y \cdot \left[\left(\frac{W - W_1}{L} \right)^2 \cdot R_{T_1}^{(1)} + \left(\frac{W_1}{2 \cdot L} \right)^2 \cdot R_{T_1}^{(2)} \right] \quad (3.4.1.1)$$

where, $R_{T_1}^{(1)}, R_{T_1}^{(2)}$ represent the volume of the deformed portion of shell plating for both sides of the incursion line in the region (1) and (2), (Figure 3.2) respectively, and they are given by:

$$\begin{aligned} R_{T_1}^{(1)} &= 2 \cdot L \cdot H \cdot t_s \\ R_{T_1}^{(2)} &= 4 \cdot L \cdot H \cdot t_s \end{aligned} \quad (3.4.1.2)$$

H= vertical depth of damage in the struck ship

W= indentation at the incursion line

W1= indentation at frame No. 1 (see figure 3.2)

σ_y = yield stress of the material

t_s = thickness of the side plating (equivalent thickness allowing for stiffeners)

It should be pointed out that the effect of in – plane displacement, which could arise due to horizontal bending of the struck ship or from local deformation of the supporting structure at the ends of the span, on the load carrying capacity of the beam is less important at larger lateral deflection, since all beams with the same axial restraint at the supports eventually reach the membrane or string state as demonstrated by Jones (1973).

Incidentally, Castagneto (1962) and Guido (1964) have proved that the effect of horizontal bending of the struck ship during collision is negligible.

In this paper, Hegazy has shown also that the value of the energy absorbed during the membrane tension phase of the hull plating, in the case of collision with a raked striking bow is always less than that for collision with a vertical bow and depends on bow angle and depth of penetration.

3.4.2 Energy absorbed due to membrane tension in the Decks of the struck ship

By assuming that for a particular indentation only the shaded area of the deck plating shown in Figure 3.7 is considered to be affected by the distortion, the following expression for the energy absorbed during the membrane tension phase of deck plating is obtained:

$$E_2 = \frac{1}{3} \cdot \sigma_y \cdot \left[\left(\frac{W - W_1}{L} \right)^2 \cdot R_{T_2}^{(1)} + \left(\frac{W_1}{2 \cdot L} \right)^2 \cdot R_{T_2}^{(2)} \right] \quad (3.4.2.1)$$

where, $R_{T_2}^{(1)}, R_{T_2}^{(2)}$ are the volumes of distorted portion of deck plating in the region (1) and (2), respectively.

$$\begin{aligned} R_{T_2}^{(1)} &= \sum_{i=1}^n (W - W_i) \cdot L \cdot t_{di} \\ R_{T_2}^{(2)} &= \sum_{i=1}^n 2 \cdot L \cdot t_{di} \cdot (W_1)_i \end{aligned} \quad (3.4.2.2)$$

t_d = thickness of deck plating (equivalent thickness allowing for stiffeners).

3.4.3 Energy absorbed due to buckling of decks of the struck ship

The plastic buckling problem of a stiffened deck is simplified by assuming that at failure the whole deck plating area between side transverses flanking the strike is subject to a uniform compressive stress of average value equal to “ $\Phi_d \sigma_y$ ”. The “ Φ_d ” is a factor depending on the scantlings of the deck structure and the system of framing used. The procedure for calculating the ultimate strength factor “ Φ ” is given in Appendix A.

The expression for the absorbed energy during the plastic buckling phase of deck structure was found to be:

$$E_3 = \frac{1}{2} \cdot \Phi_b \cdot \sigma_y \cdot \left[R_{T_3}^{(1)} + \left\{ 1 - \frac{1}{3} \cdot \left(\frac{W - W_1}{L} \right)^2 \right\} \cdot \bar{R}_{T_3}^{(1)} + \left\{ 1 - \frac{1}{3} \cdot \left(\frac{W_1}{2 \cdot L} \right)^2 \right\} \cdot R_{T_3}^{(2)} \right] \quad (3.4.3.1)$$

where, R_{T_3} is the volume of the displaced portion of deck plating due to buckling.

$$\begin{aligned} R_{T_3}^{(1)} &= \sum_{i=1}^n 2 \cdot L \cdot t_{di} \cdot (W_1)_i \\ \bar{R}_{T_3}^{(1)} &= \sum_{i=1}^n (W - W_1)_i \cdot L \cdot t_{di} \\ R_{T_3}^{(2)} &= \sum_{i=1}^n 2 \cdot L \cdot t_{di} \cdot (W_1)_i \end{aligned} \quad (3.4.3.2)$$

Φ_d = ultimate strength factor of deck plating = σ_m / σ_y

σ_m = average compressive stress at collapse (see Appendix A)

Equation (3.4.3.1) shows that the energy absorbed during the buckling phase decreases as the indentation W increases. This is because in this case the deck plating is subjected to axial and bending stresses and as indentation increases the plate elements deflect more and more. If the work done against the plastic hinges is neglected then the plastic buckling force must decrease and, consequently, the energy absorption also.

Hegazy recognizes that this model of failure may be an over – simplification and proposes more work to be done on this aspect.

3.4.4 Energy absorbed due to the buckling of deck transverses in the decks of the struck ship

If the reaction force overcomes the collapse load of the deck transverses flanking the strike then the latter collapse. The energy absorbed due to the collapse of all deck transverses is given by the following equation:

$$E_4 = 2 \cdot n \cdot \int_0^{w_1} P_C \cdot dW \quad (3.4.4.1)$$

Using the equation (3.3.1.3) for P_C , the above – cited formula reduces to:

$$E_4 = \sigma_y \cdot R_{T4} \quad (3.4.4.2)$$

where R_{T4} is the damaged volume of the deck transverses (on both sides of the incursion line) involved in a collision. R_{T4} is given by:

$$R_{T4} = 2 \cdot n \cdot W_1 \cdot (2 \cdot b_e \cdot t_d + \gamma \cdot A) \quad (3.4.4.3)$$

3.4.5 Energy absorbed due to the collapse of side transverses of the struck ship

The side transverse is considered to be an elastic – perfectly plastic beam with fully clamped ends and subjected to a uniformly distributed load q given by:

$$q = \sigma_y \cdot t_s \cdot (\sin \psi_1 - \sin \psi_2) \quad (3.4.5.1)$$

where,

$\sigma_y t_s$ = membrane tension force in side plating per unit height.

The uniformly distributed load for such a beam is given by Jones (1974) to be:

$$q_c = \frac{16 \cdot M_p}{S^2} \quad (3.4.5.2)$$

where,

M_p = the plastic collapse moment of the side transverse section,

S = the height of the side transverse (i.e. the distance between the decks or between deck and bottom) in the damaged panel.

Now if $q \geq q_c$ the side transverse fails and the plastic energy absorbed during collapse E_5 will be:

$$E_s = \frac{5 \cdot M_p \cdot S}{12 \cdot E \cdot I} \quad (3.4.5.3)$$

where,

I = second moment of area of the cross section of the side transverse about axis of bending.

It is obvious that if $q < q_c$ the side transverse does not fail and the energy E_s need not be calculated. It should be pointed out that the lateral movement of one or more of the supports at the end of a side transverse during the loading cannot effect the value of the collapse load as explained by Maier – Leibnitz, Neil (1965).

Equation (3.4.5.3) gives the amount of energy absorbed in the plastic hinges and is derived by assuming an ideal bending moment curvature relation, in which the yield moment (M_y) of the beam coincides with the fully plastic moment (M_p). Hegazy proposed this formula with some deliberation. He also proposed experiments to be carried out in order to be determined adequate correction to such a simple formula.

3.4.6 Rupture of hull and deck plating of the struck ship

The energy absorbed from the hull and deck plating is given by equation (3.4.1.1), (3.4.2.1), and (3.4.3.1). These equations remain valid until rupture of the hull occurs. The aim of this section is to obtain the value of the limiting indentation beyond which rupture of the hull occurs.

According to the failure criteria used (see assumption 3, section 3.5), when the strain due to stretching exceeds the ultimate strain (ductility) of the material (ϵ_u), rupture of hull and deck plating occurs. Consequently, the membrane tension forces in the hull and deck plating as well as the buckling force in decks no longer exist. A new failure mechanism, namely wedge splitting of decks, now occurs due to the penetration of the striking bow in the deck plating after the rupture of the latter.

The value of the limiting indentation, beyond which rupture of the hull occurs, was obtained by using small deflection geometry. Assuming that the deflection profile is a triangle and using small deflection geometry McDermott et al. (1974) gave an expression for indentation at rupture, when a mid – span strike is considered. The limiting indentation W_L is found to be:

$$(W_L - \overline{W}_1) = L \cdot \sqrt{2 \cdot \epsilon_u} \quad (3.4.6.1)$$

where,

W_L = limiting indentation at the incursion line, beyond which rupture of the hull and deck plating occurs.

\overline{W}_1 = indentation at deck transverse No. 1 at the instant of hull rupture.

ϵ_u = ultimate strain of the material.

The indentation \overline{W}_1 can be calculated by considering the equilibrium of forces at point 1 (see Figure 3.2). The equilibrium of forces in the transverse direction reveals (assuming a vertical striking bow and that P_c for all deck transverses in different decks is the same):

$$F_1 \cdot \sin \psi_1 - F_2 \cdot \sin \psi_2 = P_c \cdot n \quad (3.4.6.2)$$

The suffixes (1) and (2) denote which part of the distorted hull is being considered (see Figure 3.2).

The equilibrium of forces in the longitudinal direction gives:

$$F_2 = F_1 \cdot \frac{\cos \psi_1}{\cos \psi_2} \quad (3.4.6.3)$$

Substitution from (3.4.6.3) into (3.4.6.2) yields to:

$$\tan \psi_2 = \tan \psi_1 - \frac{P_c}{F_1} \cdot \frac{n}{\cos \psi_1} \quad (3.4.6.4)$$

From the geometry of the figure 3.2, $\tan \psi_1$, $\tan \psi_2$ and $\cos \psi_1$ can be expressed in terms of L , \overline{W}_1 and $(W_L - \overline{W}_1)$ and by using equation (3.4.6.1), equation (3.4.6.4) can be finally rewritten as:

$$\frac{\overline{W}_1}{2L} = \sqrt{2\varepsilon_u} - \frac{P_c \cdot n}{F_1} \cdot (1 + \varepsilon_u) \quad (3.4.6.5)$$

Knowing the values of ε_u , F_1 , P_c and n , \overline{W}_1 can be calculated and hence, using equation (3.4.6.1), the limiting indentation at the incursion line W_L can be calculated as:

$$W_L = L \cdot \sqrt{2 \cdot \varepsilon_u} + \overline{W}_1 \quad (3.4.6.6)$$

It should be pointed out that the amount of energy absorbed E_o by the struck ship just prior to the rupture of hull and deck plating is calculated as the sum of the expressions (3.4.1.1), (3.4.2.1), (3.4.3.1), (3.4.4.1) and (3.4.5.1) after replacing the values of W and W_1 by W_L and \overline{W}_1 , respectively. Hegazy has shown, as it is of course obvious from the formulae used, that the value of E_o depends on deck and shell plating thickness, system of framing, spacing between side transverses, scantlings of transverse frames and longitudinals, the vertical depth of damage and the mechanical properties of steel.

These factors are of great importance in the design of tanker vessel. This is one of the reasons that at chapter 7 a parametric optimization was carried out based on the above – mentioned factors. The aim is to find out where to put extra material in order to maximize the capacity of plastic energy absorption up to the rupture of the hull of a struck ship.

3.4.7 Energy absorbed due to wedge splitting of decks

Following the rupture of deck plating the bow of the striking ship will penetrate into the deck plating of the struck ship resulting in wedge splitting of these decks. The model for the deck and the penetrating bow is shown in figure 3.5. The stem half angle is θ , the indentation at which the deck plating is ruptured is W_L and the penetration is y .

In calculating the force required for the wedge to penetrate to a certain depth y it is assumed that part of the force is required to tear the deck plating and another part is to push aside the material to permit the entry of the wedge. These two forces are accounted for by the corresponding stresses σ and σ_o , respectively. Now since before wedge splitting the deck plating is ruptured, then $\sigma = 0$ and the force P required to push the wedge into

the deck plating is obtained by considering equilibrium of forces in the transverse direction.

$$P = 2 \cdot \sigma_o \cdot t_d \cdot y \cdot \tan\theta \quad (3.4.7.1)$$

The relation between the energy dissipated by penetration of the wedge into the deck plating is obtained as:

$$E_6 = \int_0^y P dy = \sigma_o \cdot t_d \cdot y^2 \cdot \tan\theta \quad (3.4.7.2)$$

The value of the crippling stress σ_o has been examined experimentally using small model tests by many investigators. In the NCRE method (1967) the value of σ_o was taken as $0.9\sigma_y$, while Akita et al. (1971) found it to be $0.8\sigma_y$.

Hegazy (1980) treated the problem theoretically. According to the plastic sector principle the stress along the wedge surface must be equal to the yield shearing stress which in turn, according to Mises' criteria, has the value of $0.5\sigma_y$. The relation between σ and σ_o can be written as:

$$\begin{aligned} \sigma &= u \cdot \sigma_o \\ \text{or} \quad \sigma_o &= \frac{\sigma}{u} = \frac{\sigma_y}{2 \cdot u} \end{aligned} \quad (3.4.7.3)$$

where,

u = coefficient of friction between striking bow and the deck plating of the struck ship

For mild steel on mild steel “u” is around 0.74. Substituting this value of “u” in (3.4.7.3) and then in (3.4.7.2) the final expression for the energy dissipated in wedge splitting of decks is becoming:

$$E_6 = 0.6 \cdot \sigma_y \cdot R_{T6} \quad (3.4.7.4)$$

where,

$$R_{T6} = \sum_{i=1}^n t_{di} \cdot y_i^2 \cdot \tan \theta \quad (3.4.7.5)$$

θ = stem half angle of striking bow

y = penetration into the deck of the struck ship

R_{T6} represents the volume of the damaged part of deck plating resulting from the penetration of the striking bow.

After describing the whole energy absorbing mechanism of the struck ship, it is evident that the total energy absorbed by the side structure of the struck ship can be expressed as:

$$E_s = E_o + 0.6 \cdot \sigma_y \cdot R_{T6} \quad (3.4.7.6)$$

This expression is consisting of two terms. The first term gives the energy absorbed by the struck ship just prior to the rupture of hull and deck plating. The second term gives the energy absorbed after the rupture of the hull and deck plating. It can be seen from this point that the method presented can treat minor and major collisions.

3.4.8 Energy dissipated in crushing the bow of the striking ship

The amount of energy absorbed by the striking bow may vary from 0 to 100% of the total impact energy depending on the ratio between the strength of the bow of the striking ship and the strength of the structure of the struck ship. In general, a stiff bow would absorb very little energy so that most of the kinetic energy lost during impact must be absorbed by the side of the struck ship. On the other hand, a weak bow may absorb most of the kinetic energy lost during a collision, leaving the side of the struck ship essentially undamaged. It should be pointed out that, while the damage suffered by the striking ship is such that the buoyancy of the vessel is seldom endangered, the damage to the struck ship may cause the vessel to sink, or, in case of a nuclear ship, may lead to a damage at the reactor containment vessel. Therefore, it is rational to believe that it is better that the bow of the striking ship should be capable of absorbing a certain amount of energy during collision, without, of course, jeopardising the strength characteristics required for normal operation at sea. This will, probably, result to a smaller penetration of the struck ship.

The main mechanism of damage is assumed to be crumbling of the bow. Although a certain amount of tearing may occur, most of the energy absorbed by the striking bow in a collision goes into pushing the leading material back into the ship.

The model used for the bow structure is an idealized wedge – type model with transverse or longitudinal system of framing. It is assumed that at failure the side and deck platings are subject to a uniform compressive stress of average value equal to $\Phi_b \sigma_y$. Φ_b is the ultimate strength factor of the bow structure. The resultant in the direction of the strike, of the forces acting on the overall frame cross – section in the bow structure at failure is given by:

$$P_b = \Phi_b \cdot \sigma_y \cdot A_s \cdot \cos\theta + \Phi_b \cdot \sigma_y \cdot (2 \cdot x \cdot \tan\theta \cdot t_d) \quad (3.4.8.1)$$

where,

A_s = the cross sectional area of the stiffened side plating in the striking bow.

The energy required for crushing the bow is given by the following expression:

$$E_b = \Phi_b \cdot \sigma_y \cdot R_{Tb} \quad (3.4.8.2)$$

where, R_{Tb} approximately represents the volume of the crushed material in the striking bow and is given by the formula below:

$$R_{Tb} = \left(A_s \cdot \cos\theta + \frac{1}{2} \cdot A_d \right) \cdot z \quad (3.4.8.3)$$

where,

z = the horizontal damage in the striking bow

A_d = the cross sectional area of the stiffened plating of decks in the bow structure involved in collision taken at the end of the damage length.

3.5 Minor and Major Collisions

There appears to be no universal agreement as to how collisions could be classified. What is important for a ship might not be important for the other. Let's assume a tanker and a nuclear vessel. For the tanker, are of great importance the tanks to remain intact. For the nuclear vessel, it is important that the damage do not affect the reactor containment vessel. Nevertheless, Hegazy has used the following commonly used definitions in his report.

As it has been already mentioned in the introduction, a minor collision is a collision, in which the shell plating of a ship could be badly dented but, if fracture did not occur in the outer plating of a single hull ship or in the inner plating of a double hull ship, then it would be classified as a minor collision.

On the other hand, the term "major collision" is used to describe a collision, which causes large inelastic strains and fracture of the shell plating.

3.5.1 Minor Collisions

According to the formulae presented in Hegazy's report a minor collision may be also defined as one in which the indentation W in the hull of the struck ship is less than or equal to the limiting indentation W_L (as given by equation (3.4.6.6)):

$$W \leq W_L \quad (3.5.1.1)$$

In this case the kinetic energy E_T lost during collision is accommodated by plastic material response of the struck ship without rupturing as well as the striking bow:

$$E_T = E_1 + E_2 + E_3 + E_4 + E_5 + E_b \quad (3.5.1.2)$$

Where E_1 , E_2 , E_3 , E_4 , E_5 and E_b are given by the equations proposed in the previous subsections.

When $W = W_L$ equation (3.5.1.2) becomes:

$$E_T = E_o + E_b \quad (3.5.1.3)$$

Where E_o is the energy absorbed by the struck ship just prior to the rupture of hull and deck plating.

3.5.2 Major Collisions

When $W > W_L$, rupture of the hull and deck plating occurs and the striking bow starts to penetrate the decks of the struck ship. The total absorbed energy in this case is given by:

$$E_T = E_o + E_6 + E_b$$

(3.5.2.1)

Substituting for E_6 and E_b from equations (3.4.7.4) and (3.4.8.2), respectively, equation (3.4.2.1) becomes:

$$E_T = E_o + 0.6 \cdot \sigma_y \cdot R_{T6} + \Phi_b \cdot \sigma_y \cdot R_{Tb} \quad (3.5.2.2)$$

For an infinitely rigid bow, the value of R_{Tb} is zero. Also if the strain – hardening effect has to be taken into account, then σ_y in the calculation of the equations (3.4.1.1) and (3.4.2.1) must be replaced by $\frac{\sigma_y + \sigma_u}{2}$, as proposed in assumption 9.

3.6 Conclusions

Hegazy (1980) in this study proposed a collapse model, which takes into account every structural member of the struck ship involved in collision. The basic advantages of this method are:

- The method is applicable for analysing structural ships' resistance for both minor and major collisions.
- The collapse model proposed is dependent on the struck ships' structure. Values, which are individual for each ship, are calculated by the method and these are what define the shape of the deformed form of the struck ships' side structure at the end of the collision.

The Hegazy's method was used to calculate the energy absorbed by the struck ship during collision with an infinitely rigid bow. The results were compared with the test values given by Akita et al. (1977). The comparison of the calculated and recorded energies revealed that the theoretical values obtained by using the proposed method agreed reasonably well with the measured energies in most of the tests. Compared to the results

from the methods by Minorsky, NCRE, Akita, Hegazy's method approached much more close to the experimental results. It must be pointed out that the three above mentioned methods predicted the same amount of energy to be absorbed by all side models, in spite of the fact that the models have different thickness of side plating ranging from 1.2mm to 6.0mm. This occurred because these methods neglect totally the influence of shell plating in the struck ship, which must absorb some energy during a collision.

Due to these remarks, Hegazy's method was used in the present work for analysing the side structures of a struck ship during collision. It was found to be a good idea to check how the method works on real ship structures, which do not have the design simplicity of the assumed idealised models.

3.7 Development of Fortran code based on Hegazy's Method

The basic thought was that the proposed method could serve as an easy-to-use designing tool. The aim was to develop a program based on this method, which could be used easily and give results in short time. A major difficulty was to construct a program that it would be able to apply in different structures.

The simplified Hegazy's model of the side structure considering decks having similar deck transverses is not applicable in an actual ship collision, when the deck transverses have different collapse loads. When the penetration is small and the damage is confined in one bay (damage confined between two adjacent web frames), the geometrical model is easy and the calculation of the energy absorbed is straightway. As the penetration increases the weaker deck transverse will collapse at a certain indentation at which the other deck transverses will remain intact. Thus, the geometrical model is changing and the damage is

extended in an unpredictable way (see Fig. 3.9). A new model is needed in order to define the indentations at the web frames flanking the strike, which will alter with the damage height, and the definition of the damaged region.

The programming was commenced with the simplest case. The first program developed was just producing the energy absorbed by a simplified structure with indicative scantlings. A number of subprograms were developed calculating the strength of different parts of the structure of the struck ship. The following strength calculations had to be conducted:

- critical buckling stress of deck transverses
- critical/ultimate buckling stress of deck plate
- plastic collapse moment of the side transverse
- critical buckling stress of side transverse (double hull designs)

Furthermore, some indentations at which the collapse model was going to transform had to be calculated. These indentations are:

- critical indentation W_0 . Indentation at which the deck transverses flanking the strike collapse.
- limiting indentation W_L . Indentation beyond which rupture of the side shell plating occurs.
- \overline{W}_1 : Indentation at the deck transverses flanking the strike at the instant of hull rupture.

The aim was to make the program automatic to predict the absorbed energy for a random indentation rather than calculating the energy, when the form of the damaged structure is known. The calculation of the above-mentioned values of the penetration is of

major importance. During the iterative procedure the program uses these values to define the shape of the damaged structure for various values of penetration.

In order the program to be applicable on a double hull design further assumptions had to be made. The program's flow diagram for the simplified model is shown at the end of this chapter. The modified program flow diagrams are not presented in the following chapters but the sequence of phenomena occurring as well as a discussion for the changes required in its case are further cited

3.8 Application on a small Oil Tanker design

The small oil tanker design presented herein was found to be the closest one to the proposed simplified model (Hegazy 1980). The vessel is a small single skinned oil tanker with a mid-ship form shown in Figure 3.10. The scantlings of the structure required to conduct the calculations are shown in the Table 3.1, pg. 113.

In order to produce results, some collision scenarios had to be assumed. The striking bow was assumed to be vertical, infinitely rigid and impacting the struck ship in right angles at the mid-span between two adjacent web frames. Because of the structure's magnitude (Depth moulded = 4.822m) and assuming that the striking ship will at least be of equal size with the struck ship, only two different scenarios were proposed and presented in Fig. 3.11. The first case occurs when the struck ship is in Full Load Condition and the striking ship in Ballast Condition (Fig. 3.11(a)). The second case occurs irrespectively of the striking ship's load condition and assuming that the struck ship is in Full Load Condition (Fig. 3.11(b)).

As far as the former case is concerned, the structural members of the struck ship that are involved in collision are:

- main deck plating
- deck transverse
- side transverse
- side shell plating

For this case the appraisal of the absorbed energy is straightway using the simplified model proposed by Hegazy. The results produced by the program's run are shown in Fig. 3.12 – 3.19.

The structural members of the struck ship involved in collision for the second proposed case are:

- main deck plating
- side shell plating
- bottom plating
- main deck transverse
- bottom transverse
- side transverse

A slight modification on the program is needed in order to cope with this case. The difference between this case and the previous one is that there are two deck and bottom transverses with two different collapse loads. This means that at a certain penetration depth the weaker deck transverses will collapse and the stronger bottom transverses will remain intact. This progress will result in the extension of the damage to the adjacent bay initially for the upper part of the side structure and later on for the lower part. Therefore, some assumptions have to be made to deal with the alteration of the geometry (Fig. 3.9) and the definition of the damage height to the adjacent bays.

The results consist of graphs plotting the total energy absorbed by the side structure of the ship, and the energy absorbed by individual structural members against the penetration depth. Furthermore, the collision force is plotted against the penetration. Finally, the total energy absorbed by the side structure is plotted against the volume of the damaged material. In figures 3.13, 3.21 the volume of the damaged side shell plating material has been excluded in the calculations. This is, in order this graph to be straight comparable with graphs from the global methods (Minorsky, Akita, NCRE, e.g.), which neglect the effect of the side shell plating.

3.9 Results and Conclusions

First Collision Scenario

The first assumed collision scenario is considered. The striking ship (ballast condition) impacts the struck ship (full load condition). The damage height is 3.000m. The structural members of the struck ship, which are subjected to the impact load are referred in the subsection 3.8.

A brief description of the way that the structure deforms is given. As the penetration increases the side shell plating and the main deck are loaded in membrane tension and the main deck also in buckling. At the penetration value $W_{\text{odt}} = 0.395\text{m}$ the deck transverses flanking the strike collapse and the damage is extended to the adjacent bays. The decks and the side shell plating of the adjacent bays are now receiving the impact load also. Before the collapse of two more deck transverses, the side shell plating ruptures at an indentation $W = 2.020\text{m}$. Subsequently, the rigid vertical bow starts to tear the main deck plating of the struck ship. The energy absorbing mechanism is now the wedge splitting of

the main deck plating. All of these can be shown graphically in Figures 3.16 to 3.23 as well as the impact force plotted against the penetration depth.

Second Collision Scenario

In the second collision scenario the whole side structure of the small oil tanker is impacted from the rigid striking bow. The structural elements involved in collision are cited in subsection 3.8.

The collapse model is a little more complicated than in the first collision scenario. The transverses on the main deck and on the bottom deck have different collapse loads. The structure has been divided in two structures consisting of the half depth of the side shell plating and the main deck or the bottom deck respectively. The energy absorbed from each part is being added at each penetration depth.

The weaker deck transverses collapse at the penetration value $W_{ot} = 0.355\text{m}$ and the damage is extended to the adjacent bays for the upper part of the structure. The stronger bottom transverses collapse at the penetration value $W_{ot} = 0.527\text{m}$ and the damage is extended to the adjacent bays for the lower part of the structure. Due to the strongest bottom transverses the rupture of the side shell plating occurs for a smaller penetration depth at the lower part of the structure. As McDermott et al. (1974) proposed, once the rupture is initiated is assumed to extend throughout the whole side shell plating. Thus, even if the upper part of the structure can absorb more energy before rupture of the hull, it ruptures due to the initiation of the rupture to the lower part of the structure. The penetration value at which rupture occurs is $W_L = 1.714\text{m}$. The figures illustrating the behaviour of the side structure of the small oil tanker for the second collision scenario are Figures 3.20 to 3.27.

Concluding, it is evident that when the first collision scenario is considered, the total energy absorbed is lower but due to the weakness of the deck transverses the penetration

depth, at which rupture of the hull occurs, is larger than in the second collision scenario. On the other hand, considering the whole structure under impact loading the total energy absorbed is higher but the penetration depth, at which rupture of the hull occurs, is smaller. The rupture in this case is induced from the lower part of the structure, where there are the stronger bottom transverses.

List of Figures

PART ONE: Hegazy's method – Figures illustrating the collapse mechanism

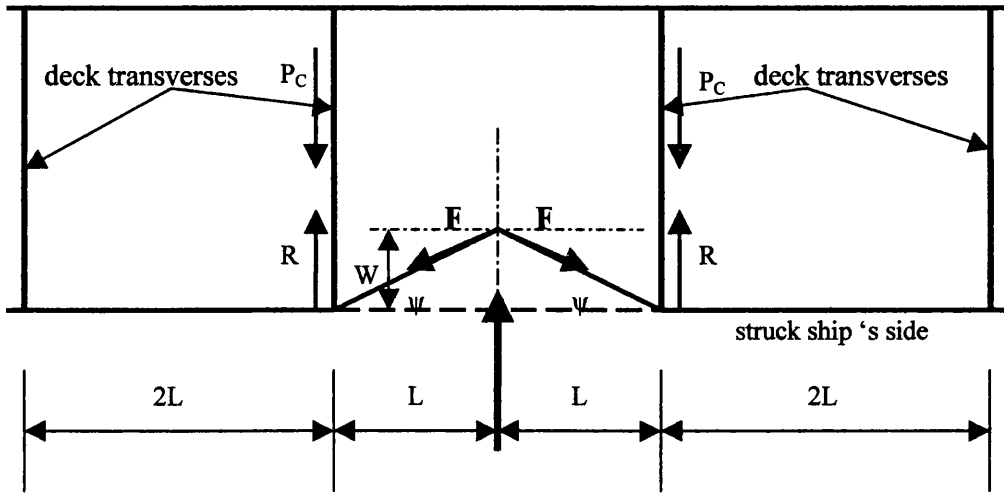


Figure 3.1: Collapse model with no lateral movement of the flanking main transverse frame.

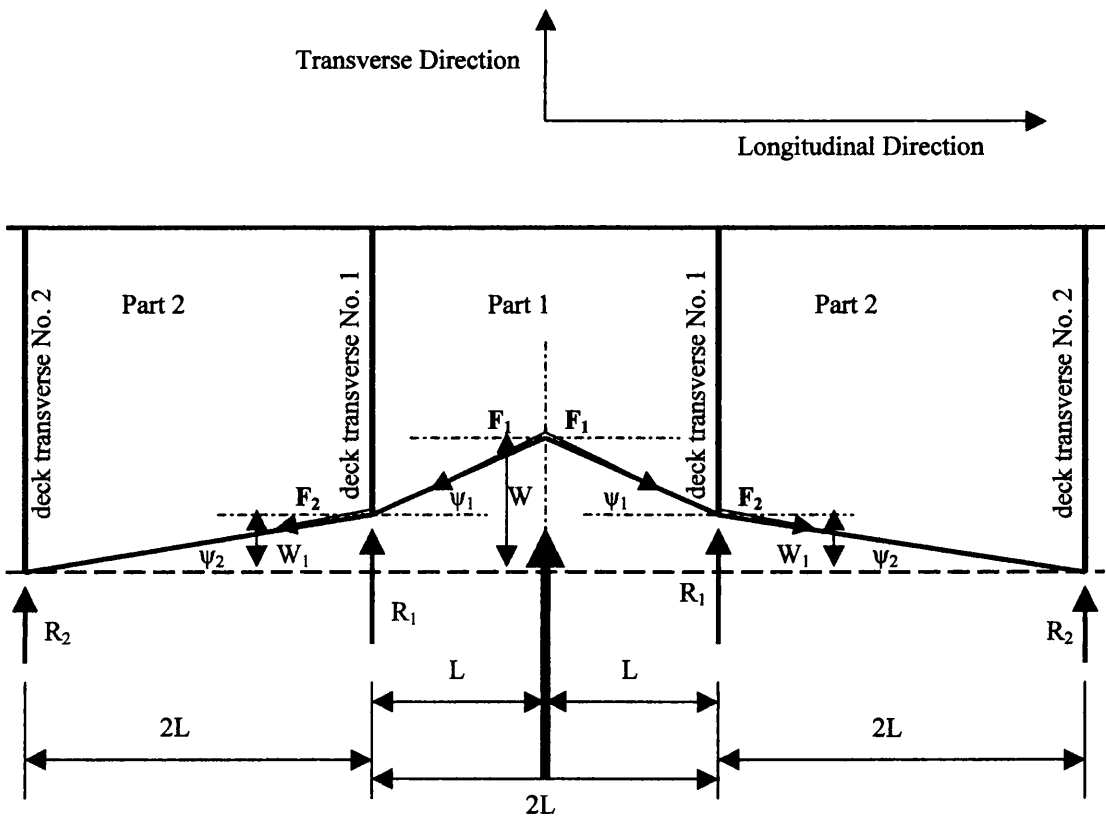


Figure 3.2: Collapse model with lateral movement of the flanking main transverse frames.

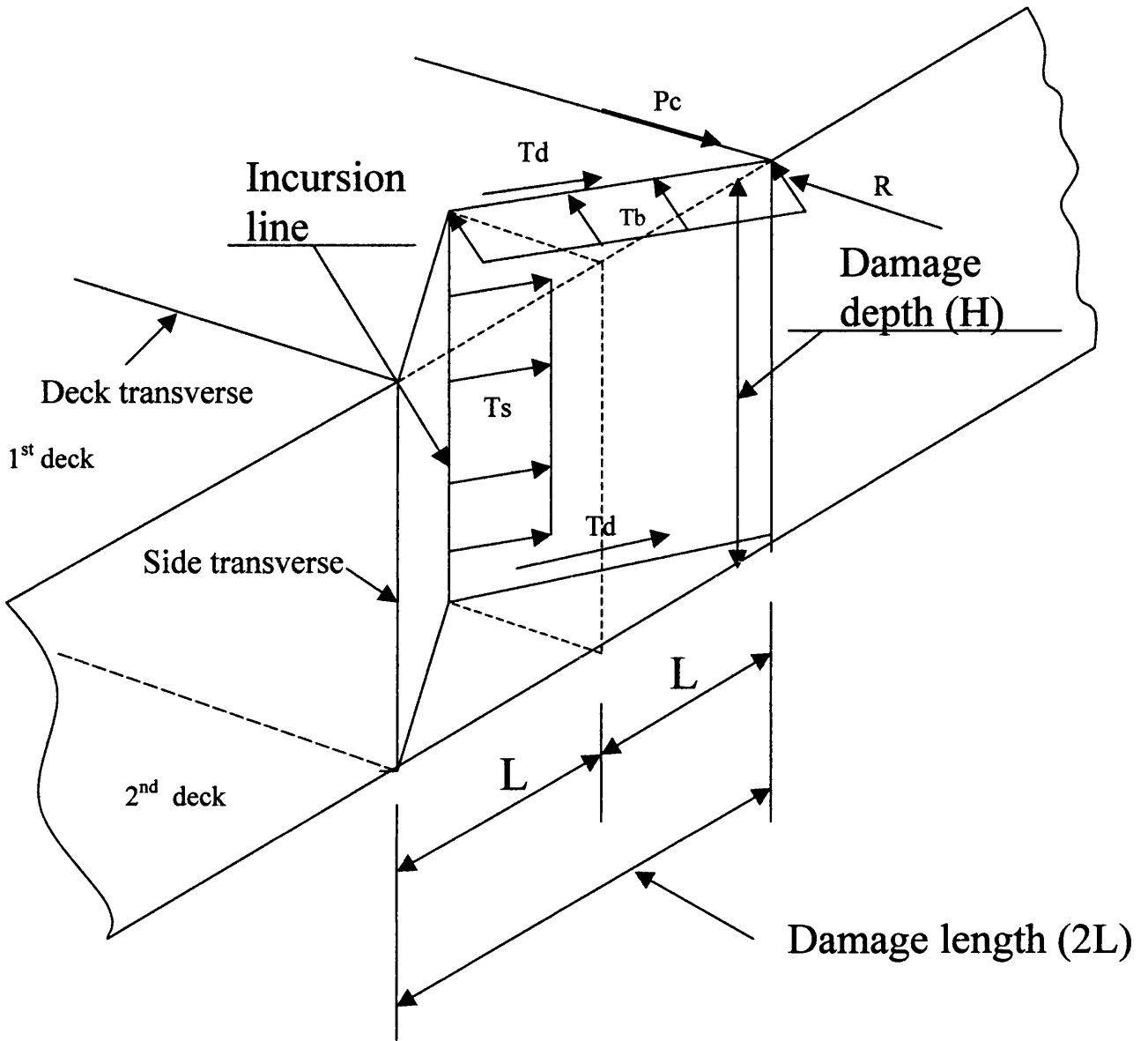


Figure 3.3: Collision case involving two decks.

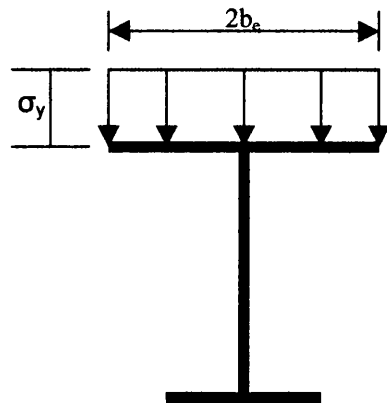


Figure 3.4: Collapse of deck transverse.

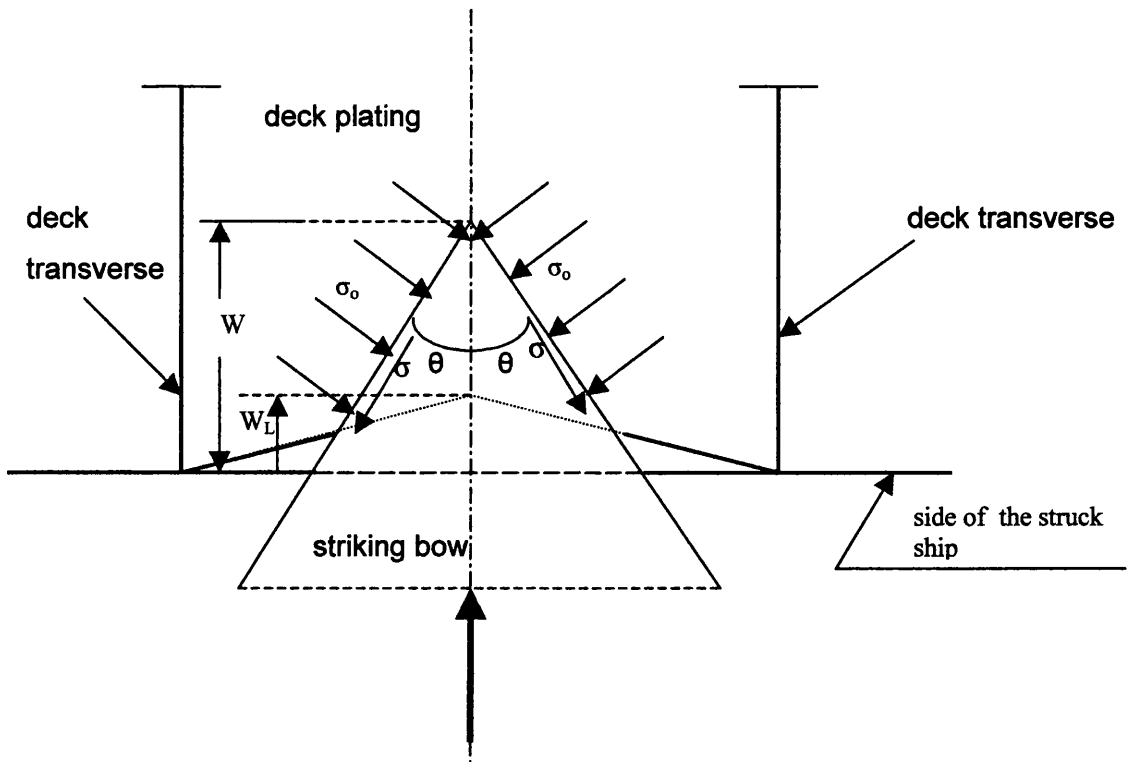


Figure 3.5: Wedge splitting of decks.

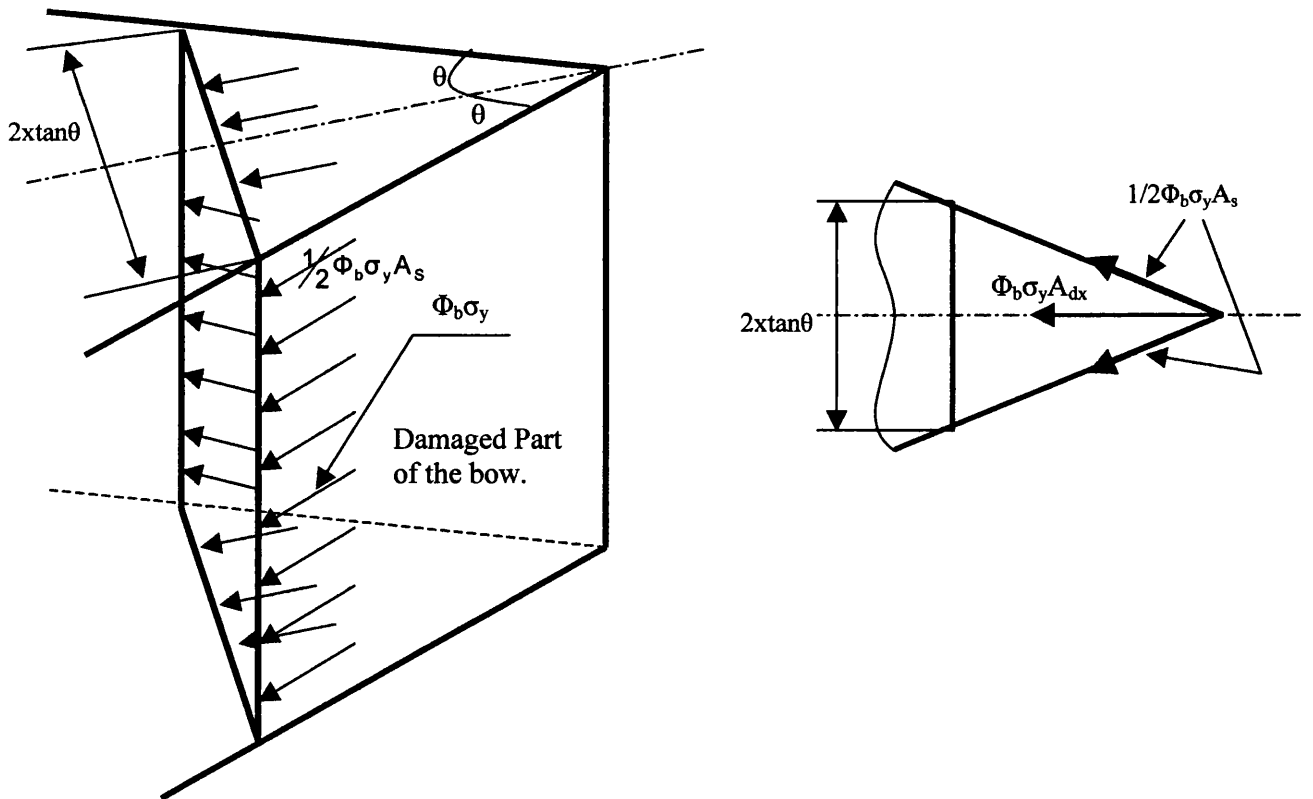


Figure 3.6: Analysis of striking bow damage.

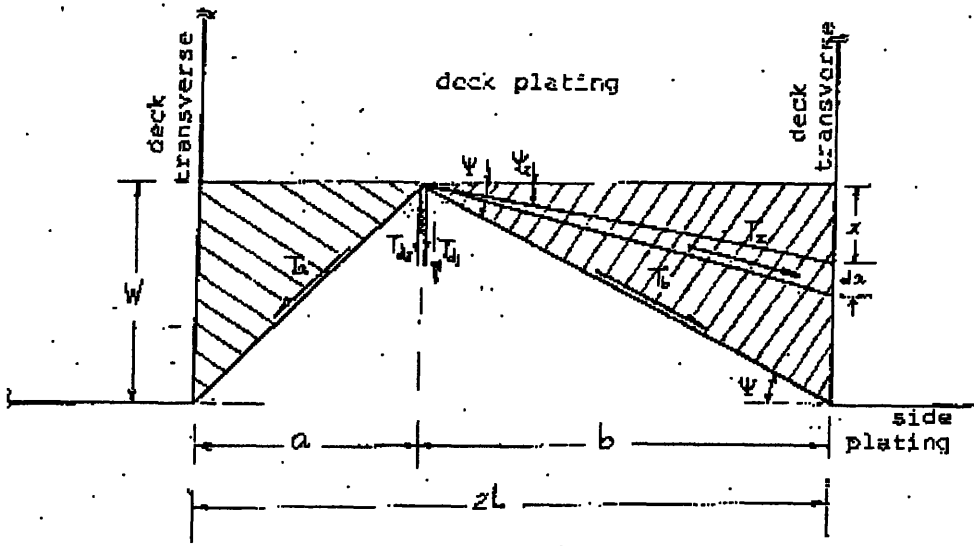


Figure 3.7: Membrane tension force in the deck.

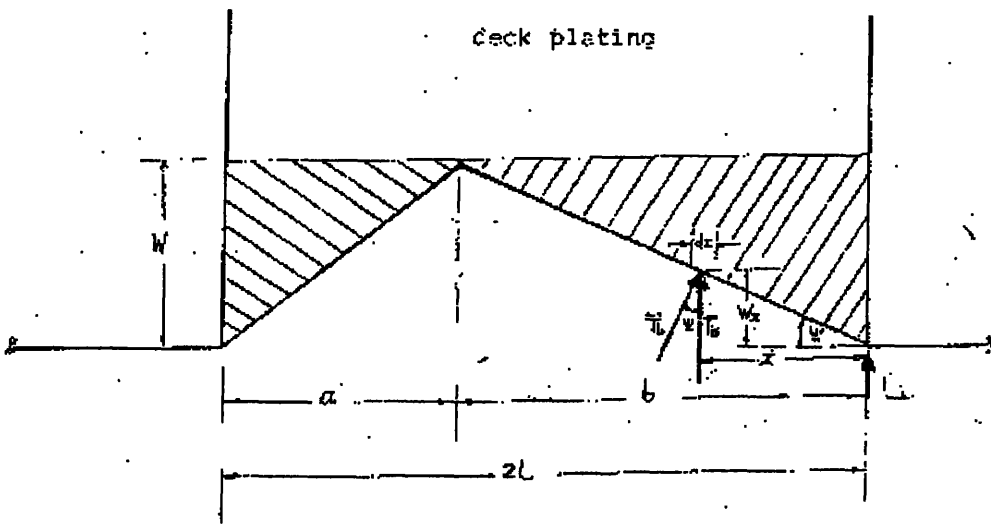


Figure 3.8: Buckling of deck plating.

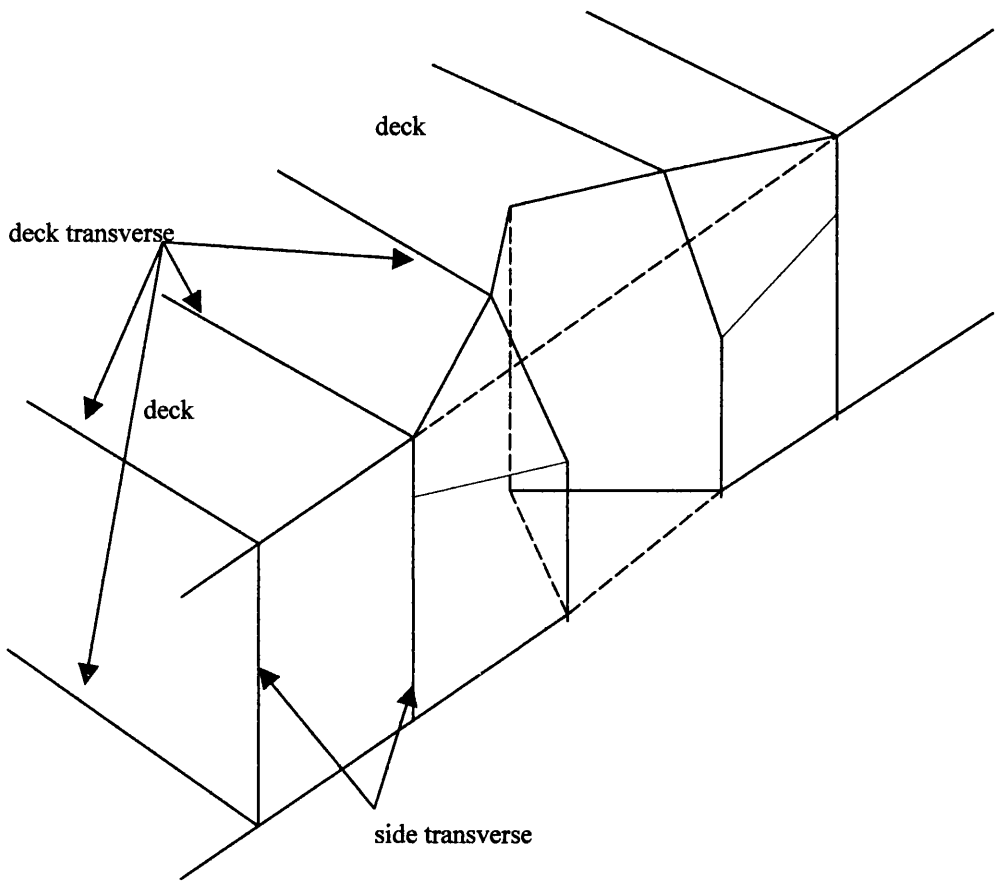


Figure 3.9: Damage profile, when the weaker deck transverses on one of the decks collapse.

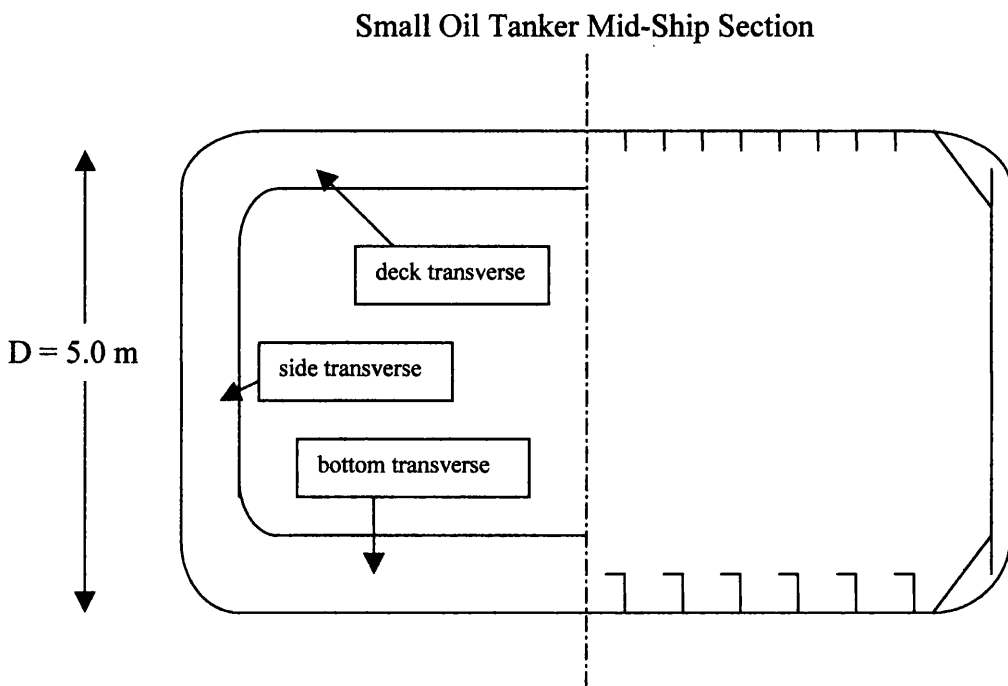
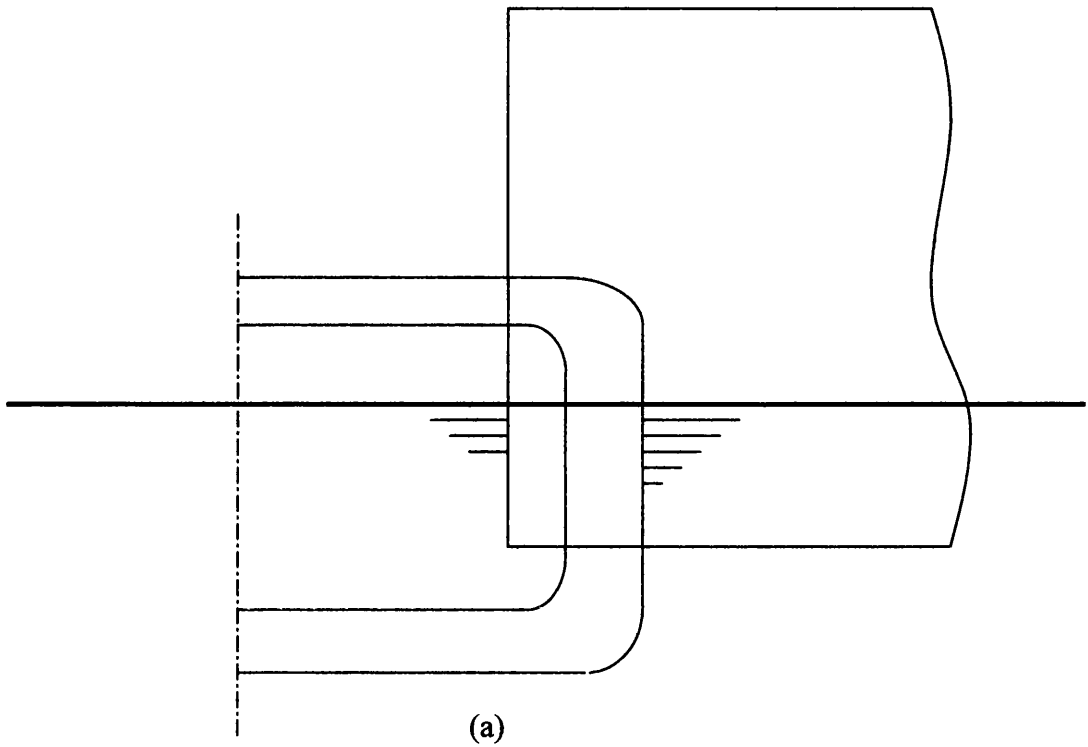


Figure 3.10: Mid-ship section of the Small Oil tanker “Esso Caernarvon”.

First assumed Collision Scenario



Second assumed Collision Scenario

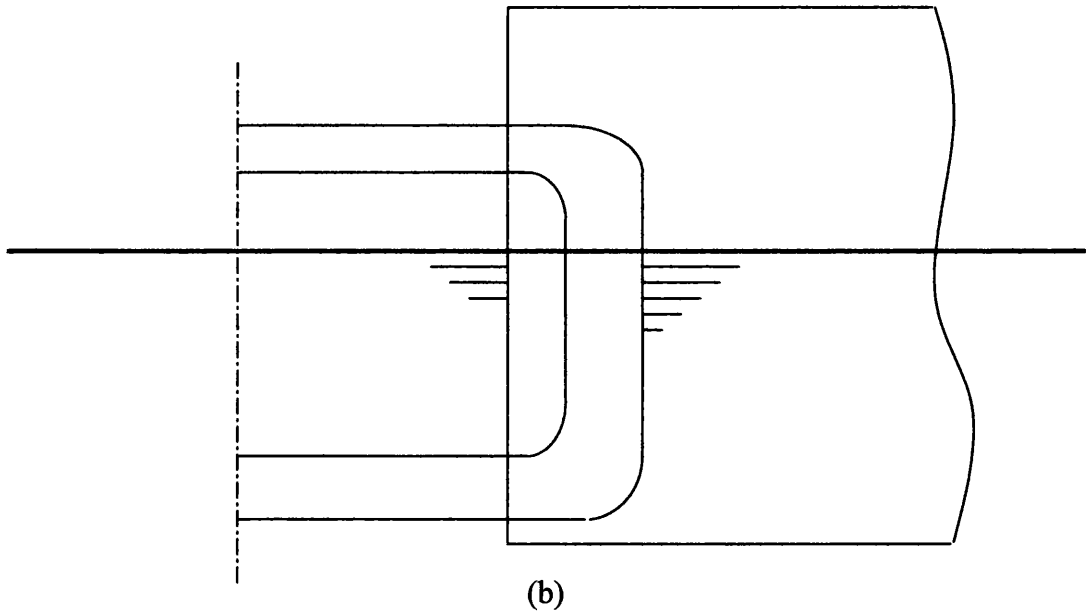


Figure 3.11: The two assumed collision scenarios are illustrated in this figure. (a) The small oil tanker impacted by a vertical and infinitely rigid bow in the ballast condition. (b) The small oil tanker impacted by a vertical and infinitely rigid bow in the full load condition.

PART TWO: Small Oil Tanker – Results for the first Collision Scenario

Total Energy Absorbed by the Side structure

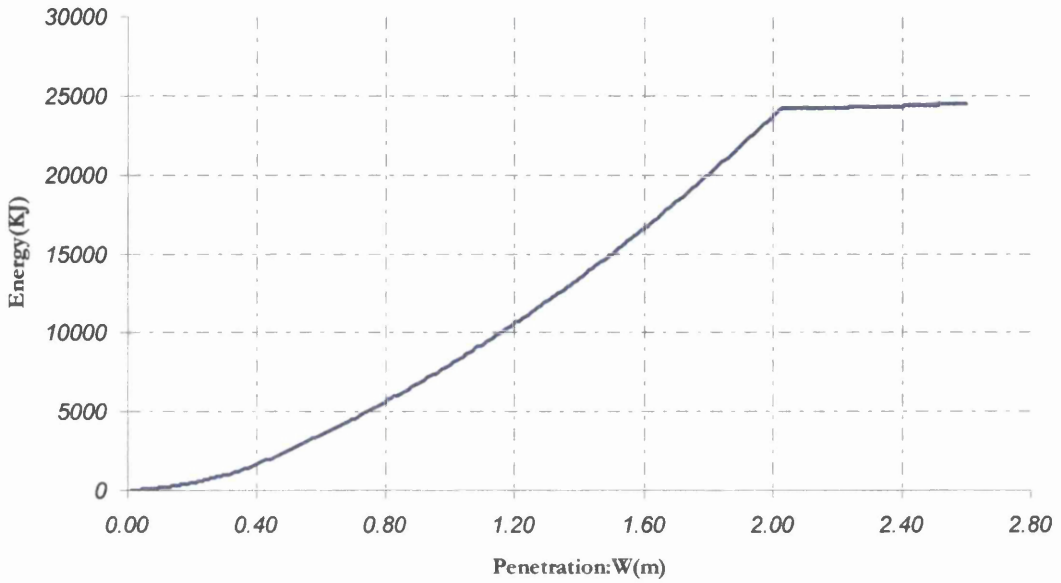


Figure 3.12: Total energy absorbed from the side structure regarding the first collision scenario.

Total Energy Absorbed against the Volume of the Distorted Material

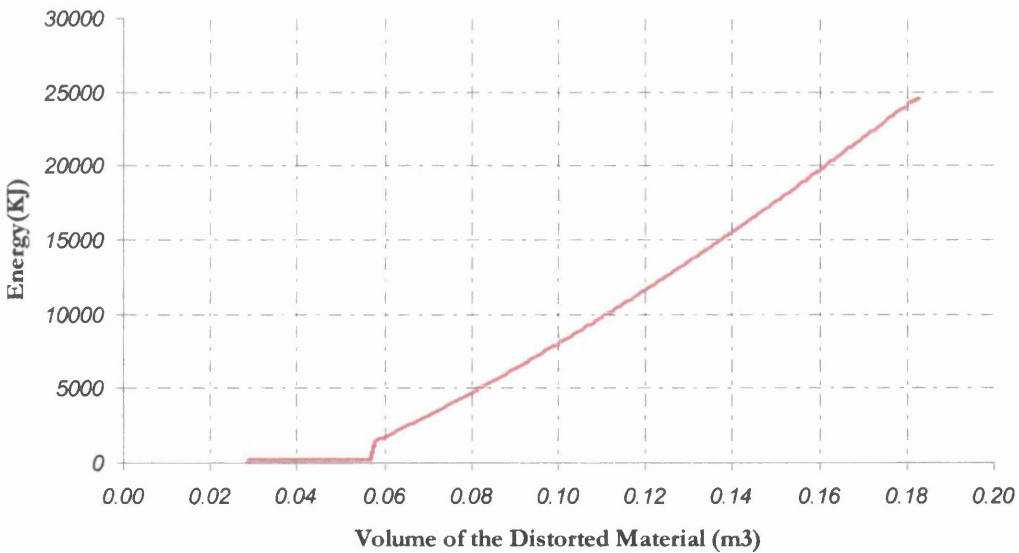


Figure 3.13: Total energy absorbed plotted against the volume of the damaged material. From the calculations of the damaged material volume has been excluded the volume of the damaged side shell plating, in order the calculations to be comparable with the global methods.(Minorsky, Akita e.t.c.).

Energy Absorbed due to membrane tension on the Side Shell plating

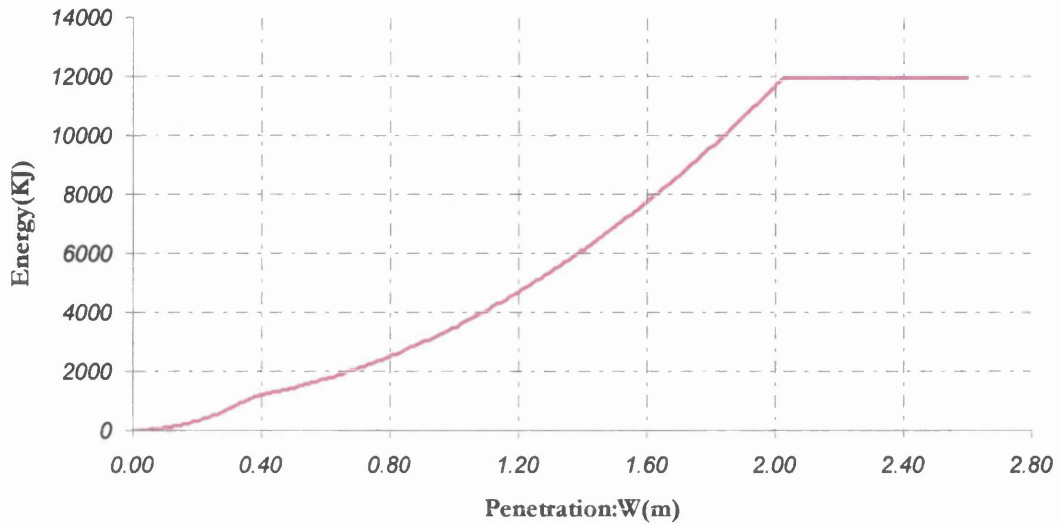


Figure 3.14: Energy absorbed due to membrane tension in the stiffened side shell plating.

Energy Absorbed due to membrane tension on the Main Deck Plating

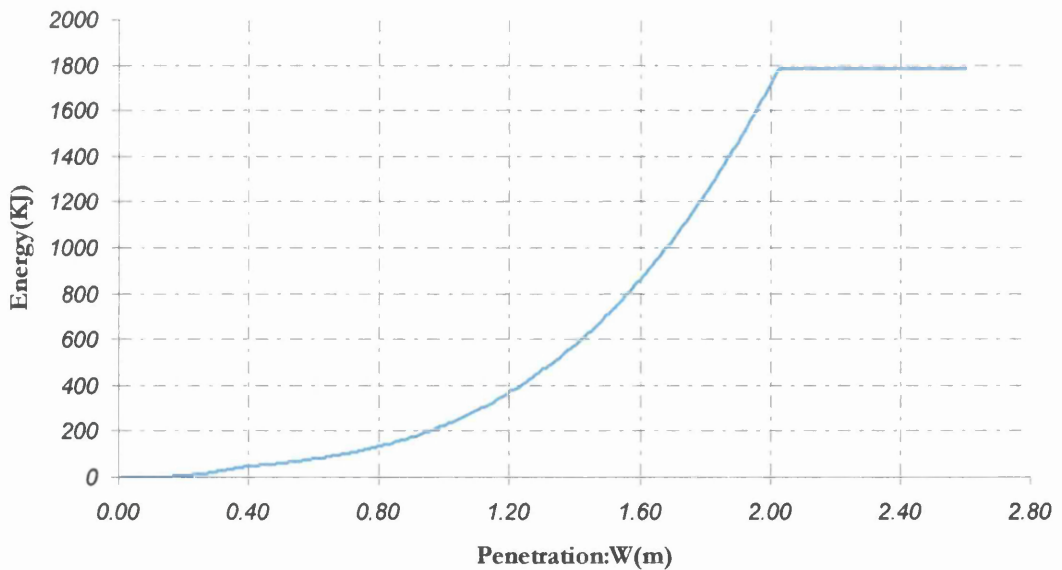


Figure 3.15: Energy absorbed due to membrane tension on the main deck of the struck ship.

Energy Absorbed due to Buckling of the Main Deck plating

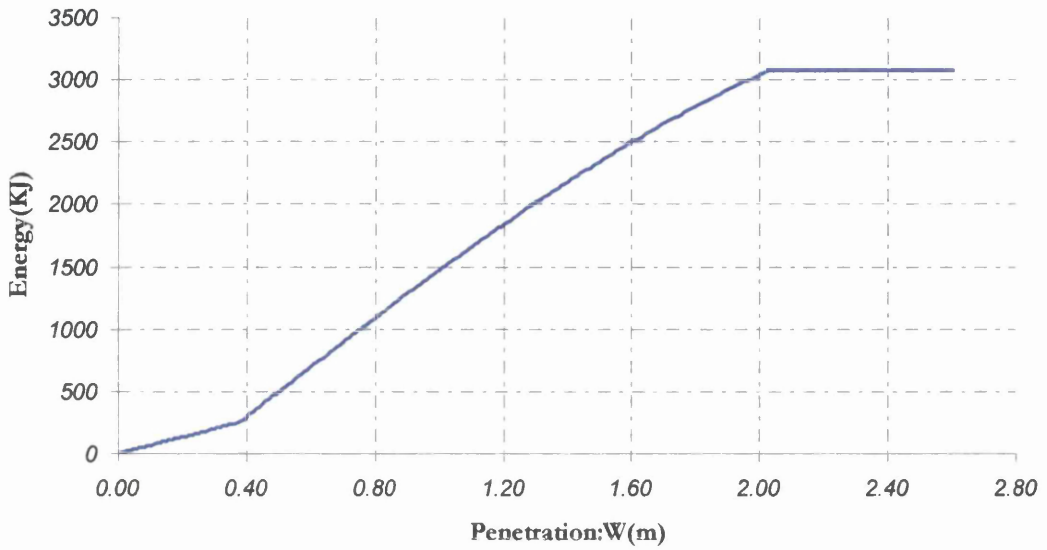


Figure 3.16: Energy absorbed due to buckling of the main deck plating.

Energy Absorbed due to the collapse of the Main deck's transverses flanking the strike

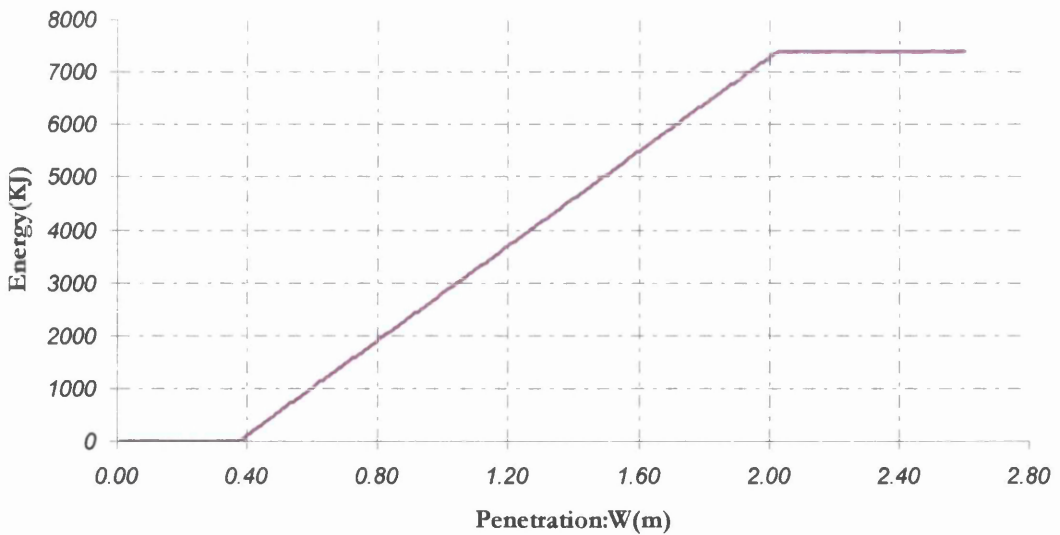


Figure 3.17: Energy absorbed due to the collapse of the main deck transverses flanking the strike.

Energy Absorbed due to Wedge Splitting of Main Deck

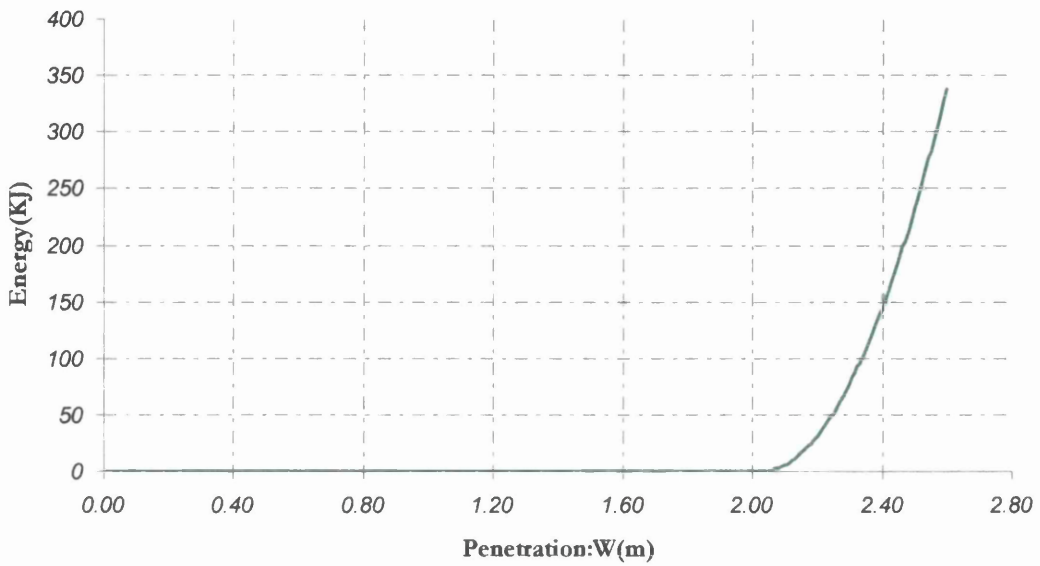


Figure 3.18: Energy absorbed subsequently after the rupture of the side shell plating of the struck ship. The collapse mechanism is the wedge splitting of the main deck plating.

Impact Force history: First Collision Scenario

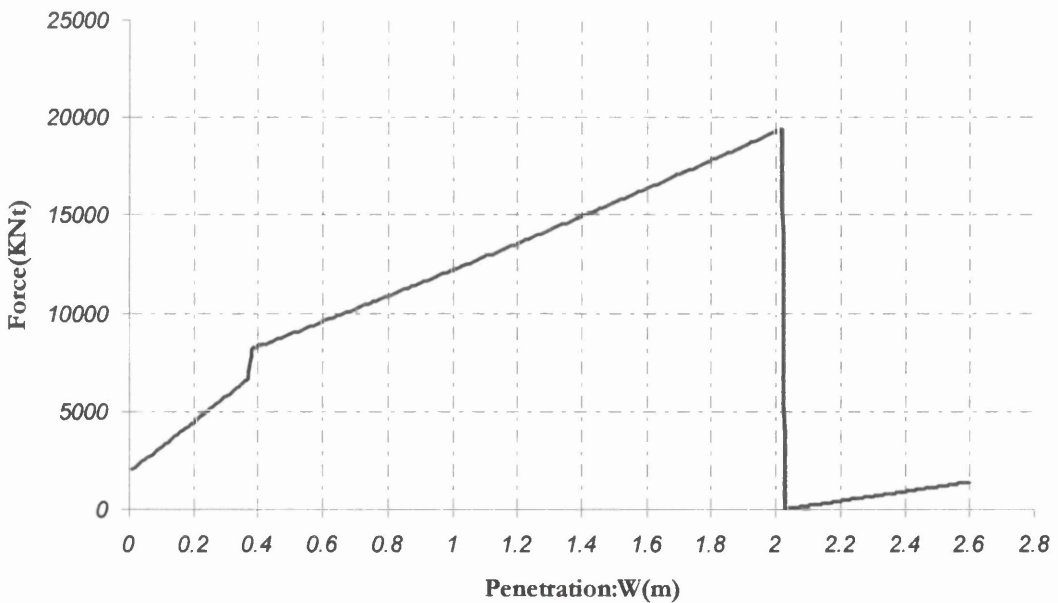


Figure 3.19: In this figure the history of the impact force is shown. The step for the penetration 0.377m is due to the involvement of the adjacent bays.

PART THREE: Small Oil Tanker – Results for the second Collision Scenario

Total Energy Absorbed from the side structure

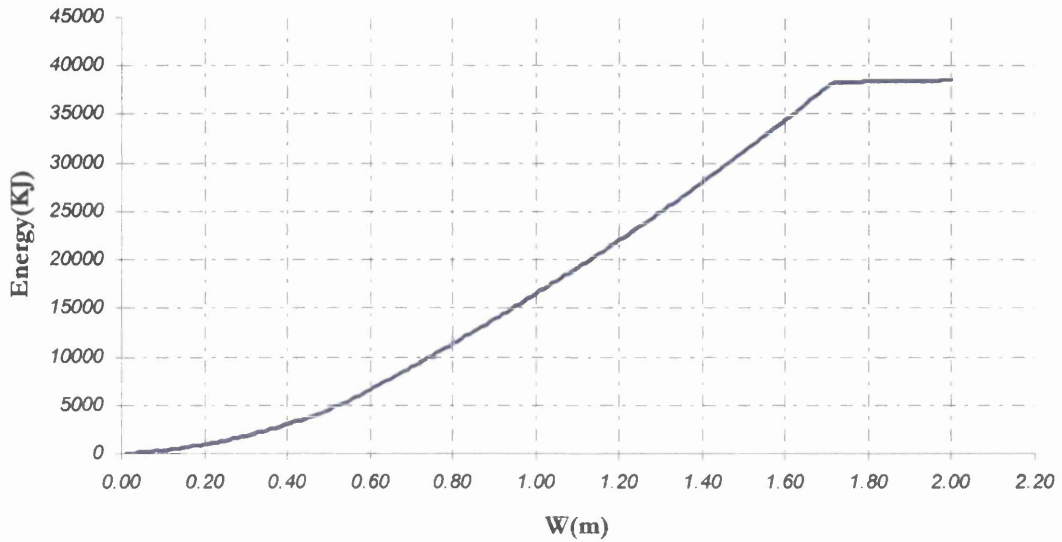


Figure 3.20: Total energy absorbed from the side structure of the struck ship regarding the second collision scenario.

Total Energy Absorbed from the Side Structure



Figure 3.21: The total energy absorbed is plotted against the volume of the damaged material. The volume of the damaged side shell plating has not been included in the calculations.

Energy Absorbed due to membrane tension on the stiffened side shell plating

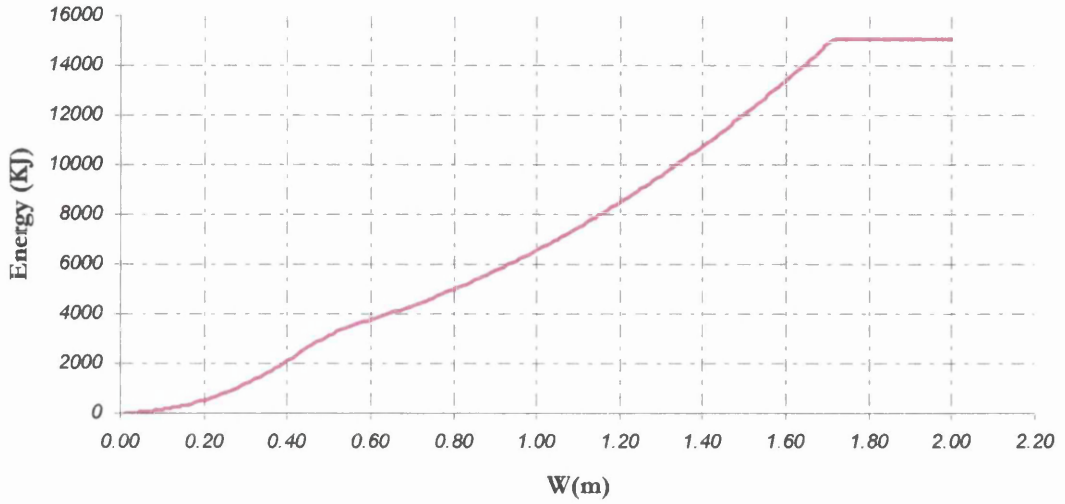


Figure 3.22: Energy absorbed due to membrane tension in the stiffened side shell plating.

Energy Absorbed due to membrane tension on the deck plating

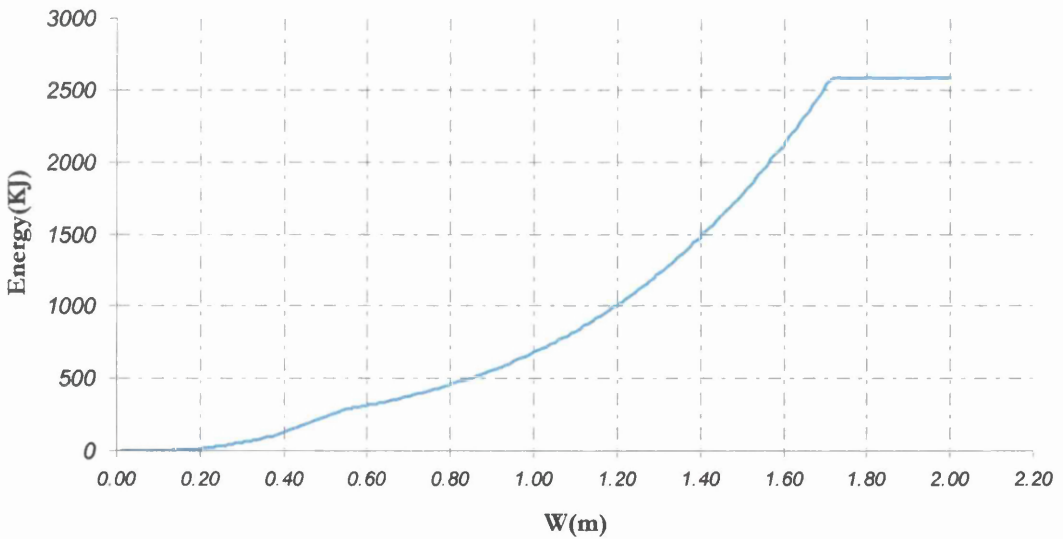


Figure 3.23: Energy absorbed due to membrane tension on the main deck and bottom plating.

Energy Absorbed due to the buckling of the decks

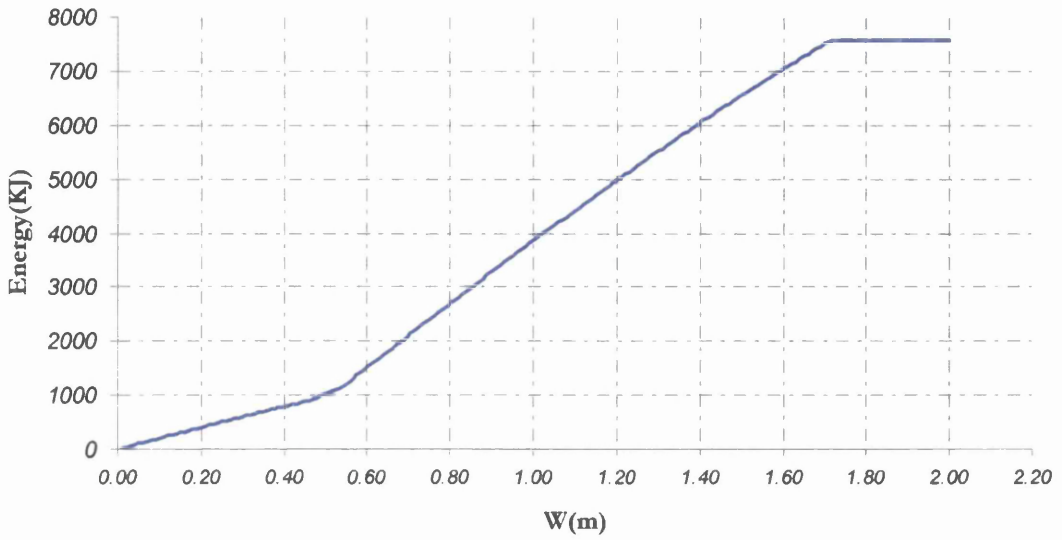


Figure 3.24: Energy absorbed due to buckling of the main deck and bottom plating.

Energy Absorbed due to the collapse of the deck and bottom transverses

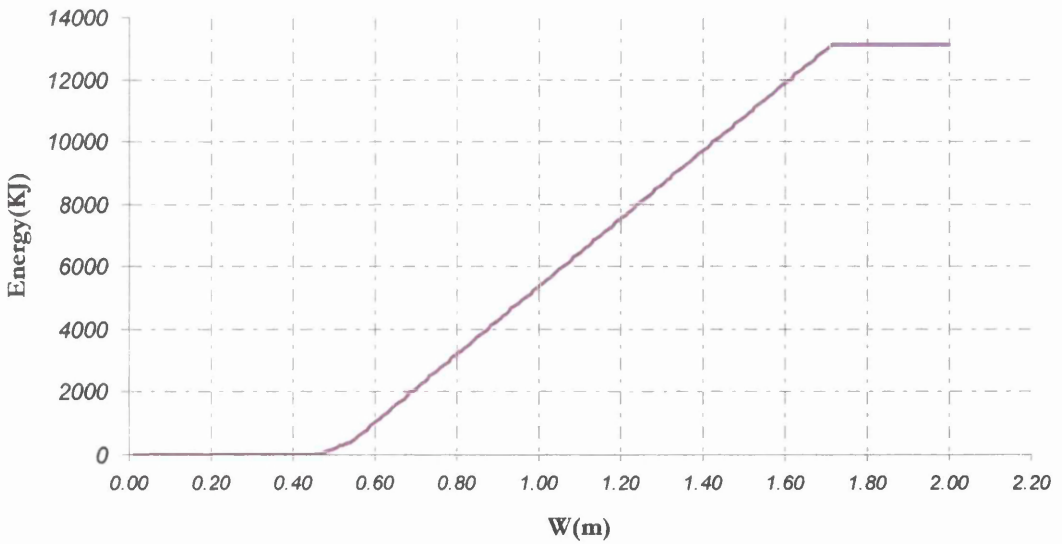


Figure 3.25: Energy absorbed due to the collapse of the main deck transverses and the bottom transverses.

Energy Absorbed due to wedge splitting of decks

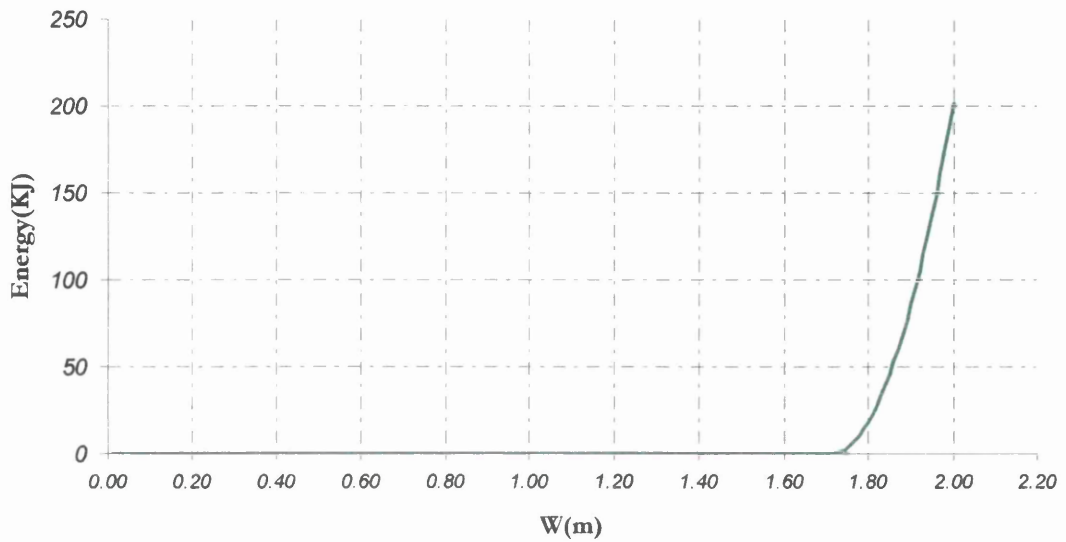


Figure 3.26: Energy absorbed after the rupture of the side shell plating. The collapse mechanism is the wedge splitting of the main deck and bottom plating.

Impact Force history: Second Collision Scenario

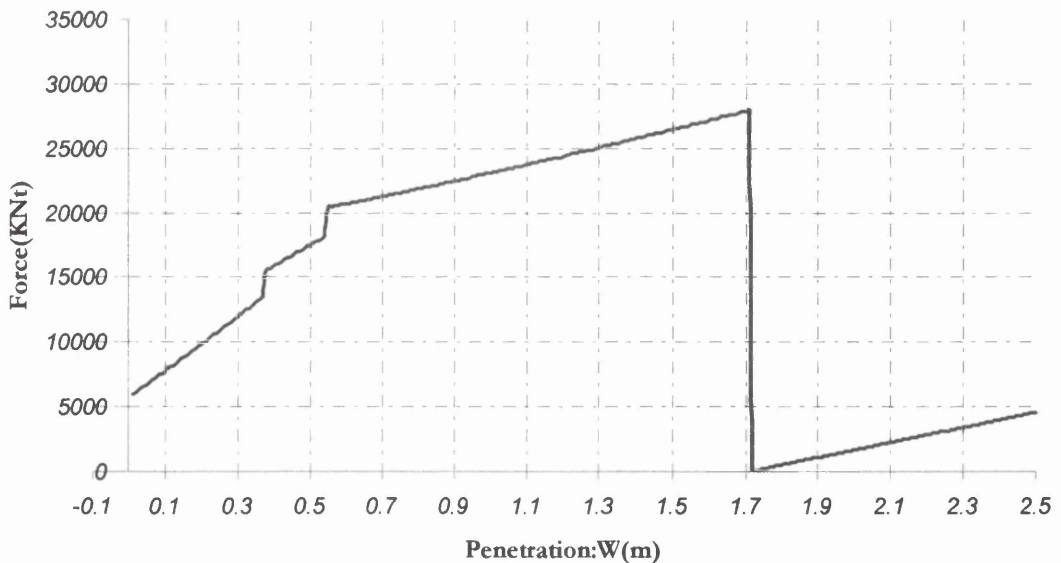


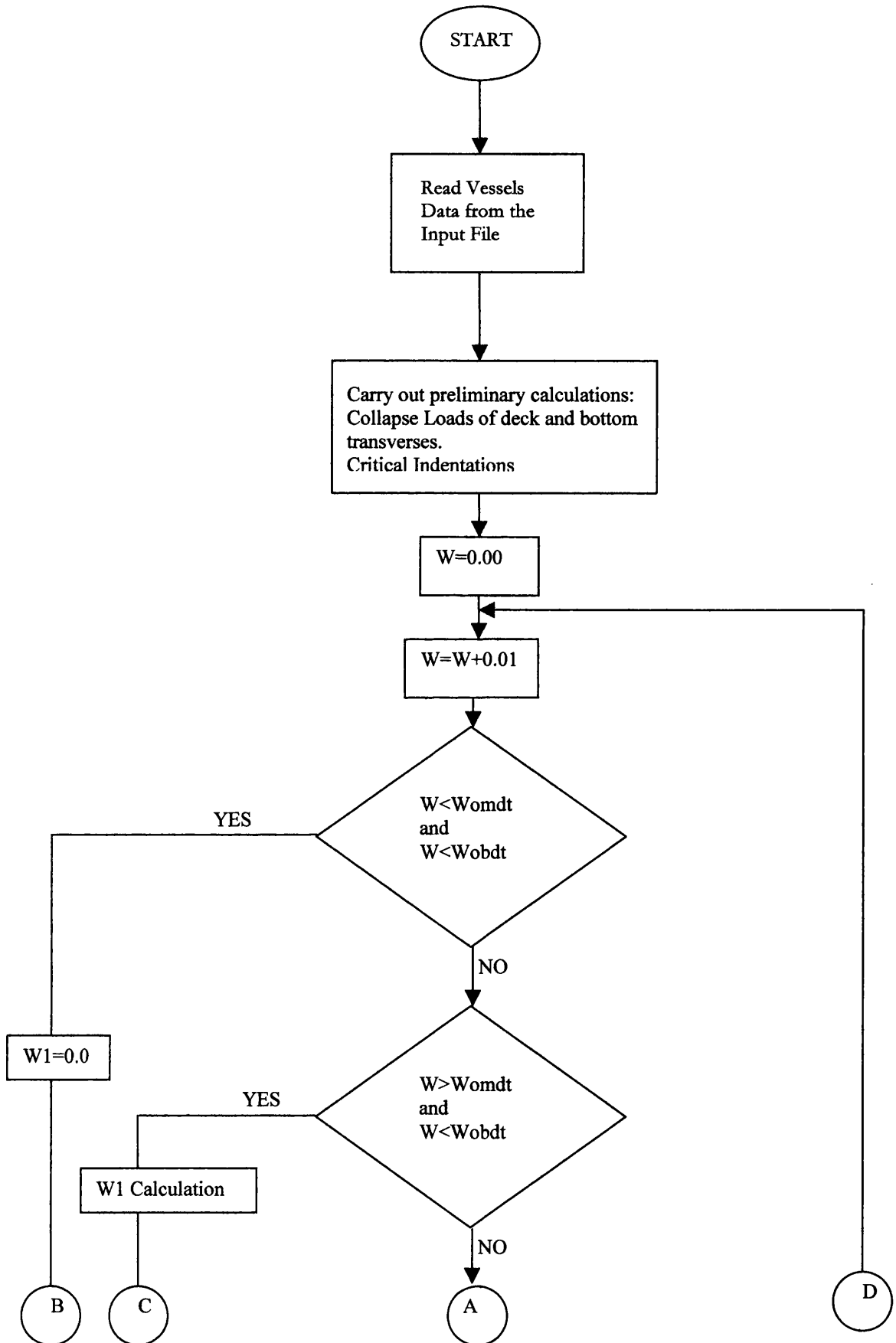
Figure 3.27: This figure illustrates the history of the impact force. The two steps at the penetration values 0.355m and 0.527m are due to the collapse of the main deck transverses and the bottom transverses, respectively.

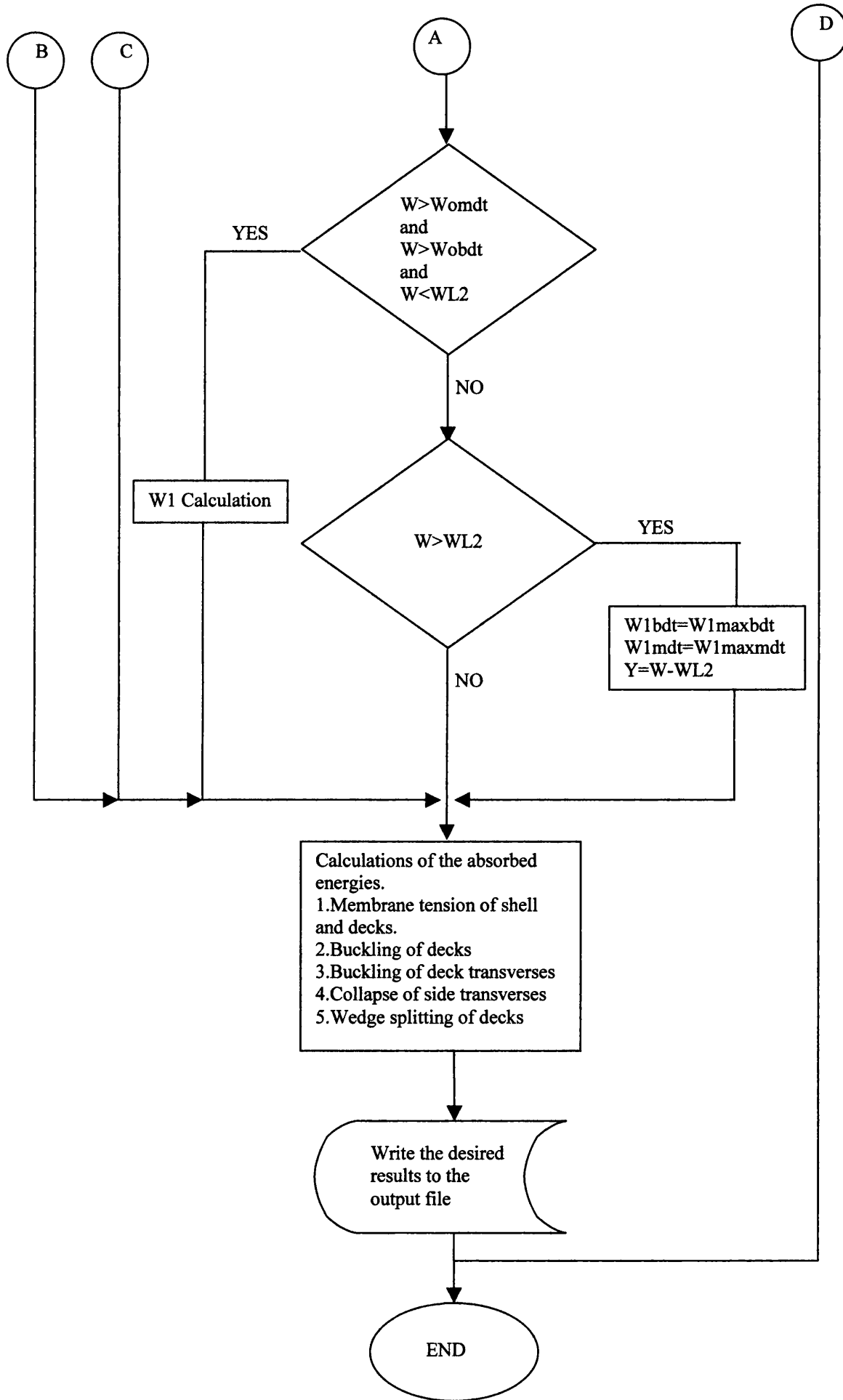
List of Tables

STRUCTURAL DETAILS OF THE OIL TANKER	
Length B.P. =	66.380m
Breadth =	10.575m
Depth moulded =	4.822m
Design Draft =	4.335m
Main deck plating thickness: t_d =	0.0085 m
Bottom Plating thickness: t_b =	0.012 m
Side Shell plating thickness: t_s =	0.0102 m
Spacing of Main deck's stiffeners: s_d =	0.660 m
Spacing of bottom stiffeners: s_b =	0.660 m
Spacing of Side shell stiffeners: s_s =	0.660 m
Dimensions of Main deck stiffeners:	0.155 x 0.077 x 0.0102
Dimensions of bottom stiffeners:	0.280 x 0.077 x 0.012
Dimensions of side shell stiffeners:	0.150 x 0.065 x 0.0102
Dimensions of Main deck transverse:	0.713 x 0.203 x 0.012
Dimensions of Bottom transverse:	0.865 x 0.203 x 0.012
Dimensions of Side transverse:	0.254 x 0.130 x 0.010
Spacing of Web Frames:	1.200 m
Distance between side shell plating and the next heavy longitudinal member:	5.350 m

Table 3.1: Structural details of the small oil tanker design.

Fortran Algorithm





The above shown flow diagram is an oversimplification of the complicated existing program code. The volume of the program made its presentation for each case described in the present thesis inevitable. The above flowchart describes the code used for the calculation of single-skinned vessels. The notation used is shown below:

W: penetration depth

W_{omdt}: critical indentation beyond which the main deck's transverse starts to buckle.

W_{obdt}: critical indentation beyond which the bottom deck's transverse starts to buckle.

W₁: Indentation at the web frames flanking the strike (see Fig.3.2).

W_{1maxmdt}: Maximum indentation at the web frames at the instant of rupture of the hull at the main deck height.

W_{1maxbdt}: Maximum indentation at the web frames at the instant of rupture of the hull at the bottom deck height.

Chapter 4

Buckling Strength of the Decks

Introduction

Buckling of stiffened plates is a field, which has attracted much attention. The elastic theory, which deals with small deflection buckling of plates loaded up to the elastic critical buckling stress σ_{cr} , is basically used in the design procedure. However, the elastic critical buckling stress does not represent the actual capacity of the plate to carry loads. It is evident that the plate will continue to carry load beyond the elastic critical load up to the point of the plastic yield of the material. This point is characterized by the ultimate buckling stress σ_u .

The type of analysis required is depended on the cause that the plate serves. Unserviceability is treated through critical elastic stress, while “ultimate strength” is treated through ultimate stress.

However, the ultimate strength of a plate is not always greater than the elastic critical buckling strength. For sturdy plates it is possible for yielding to occur before buckling. This case is known as plastic (or inelastic) buckling.

In the study of ship collisions the plasticity dominates the behaviour of the plates. The theory around such phenomena is called elasto-plastic large deflection analysis. In collisions, the interest is concentrated on the plates of the decks and the side shell, which

are subjected to large compressive loads. A good evaluation of the limit load, beyond which the plate yields, lead to a better evaluation of the energy absorbed by the decks.

Elasto-plastic large-deflection theory is quite complicated because there are three separate sources of nonlinearity:

- Yielding
- Large deflections
- Restraints from edge pull-in, which appears and becomes significant for really large deflections.

Because of the complexity that this field exhibits, there is no analytical method, which will give results for every different case. Adequate results can usually be obtained through numerical computer base techniques (finite element analysis). In the theoretical study of collisions some simplified formulae are employed to deal with this kind of problem.

In the present chapter a method by Pu and Das (1994) calculating the “ultimate strength” of stiffened plates will be presented. Furthermore, this method was incorporated in the Hegazy’s method for calculating the ultimate strength of the decks of the struck ship. Hegazy (1980) proposed the orthotropic plate theory for the calculation of the critical buckling strength of the deck plating. He also proposed that more investigation of plate and deck buckling strength under such conditions was needed.

The effect of the buckling strength’s calculation depends very much on the dimensions of the plate and the orientation of the load. The deck plating is considered clamped at the edges between two consecutive web frames. The one dimension of the plate is always defined as the spacing between web frames. If the plate of the deck under consideration is restricted in the transverse direction from a longitudinal bulkhead, which is closer to the side shell than the spacing between web frames, then the case is a plate compressed on the long edges (Fig. 4.1). Usually in this case, the ultimate strength and the elastic buckling strength have no significant difference. On the other hand, if there is no

longitudinal bulkhead and the length of the plate is larger in the transverse direction of the ship than in the longitudinal, then the case is a long thin plate compressed on its short edges (Fig. 4.2). In this case the plate may have a significant post-buckling reserve of strength beyond the critical elastic buckling stress.

4.1 Orthotropic and Discrete Beam methods

The failure of a stiffened plate can occur through several different ways. The failure modes are:

- plate failure (local failure of plate between the stiffeners)
- stiffener-plate column failure, which is further divided in two modes:
 1. plate induced failure
 2. stiffener induced failure
- torsional failure of the stiffener
- overall grillage buckling

The plate will fail when any of the above-mentioned failure mode occur first. In shipbuilding care is taken to avoid the overall buckling of a plate and the torsional failure of stiffener, because these modes do not give the opportunity of using the post-buckling strength. That is, after this kind of failure occurs, the plate collapses with a small additional load. It is evident that the orthotropic method does not take into account local buckling as well as stiffener related failure modes.

The orthotropic method is based in the simple assumption that the stiffened plate will respond as an unstiffened one with two different values of flexural rigidity in the two orthogonal dimensions. Hence, the accuracy obtained with this approach depends entirely

on the degree to which the stiffened plate resembles a uniform orthotropic plate. This method obtains quite good accuracy when applied to double wall cross-stiffened panels such as a double bottom.

On the other hand, the discrete beam approach is more accurate than the orthotropic plate approach for all singly plated stiffened panels, that is, for all types of loads and for unidirectional and cross-stiffening. For doubly plated panels the two methods have approximately the same accuracy. The discrete beam method's accuracy is rational because it takes into account a number of parameters that have been proved to affect the strength of a stiffened plate.

The orthotropic method proposed by Hegazy is illustrated in Appendix D, along with the whole method for calculating the ultimate strength factor of the deck plating.

The method presented in the following subsections is a discrete beam method, which obtains the critical elastic load of a plate as well as its ultimate strength.

4.2 Parameters affecting stiffened plating strength

The strength of a stiffened plate is strongly affected by the behaviour of the plating. Because overall buckling of the plate is avoided by design the local buckling of the plating and the column (an effective width of plate associated with a stiffener) failure are the usual failure modes. It is clear that the prediction of plate strength plays a very important role.

The parameters affecting the plate's strength are:

- plate slenderness
- residual stress
- initial distortion
- boundary condition
- plate aspect ratio
- load type

Aside from the above-mentioned parameters some more are to be considered when a stiffened plate is to be calculated.

- stiffener slenderness
- ratio of stiffener to cross sectional area
- ratio of top flange to web area (stiffener)
- cross-sectional area of the stiffener
- initial stiffener deflection
- relative stiffener deflection
- axial welding stresses in the stiffener

The below-cited method accounts for all of the parameters affecting the strength of a stiffened plate through the calculations of the “effective width” of plate associated with the stiffener.

4.3 Proposed Method

Pu and Das (1994) through a study on the existing formulae for the calculation of the ultimate strength of stiffened plates, remarked that Guedes Soares' formulae give the best ultimate strength prediction of plate panels. The method that was then proposed adapted these formulae to Faulkner's formulation. All the formulae are presented below:

Pu and Das's Method

The ultimate strength of stiffened plate is expressed as:

$$\phi = \frac{\sigma_u}{\sigma_o} = \frac{\sigma_e}{\sigma_o} \cdot \left[\frac{A_s + b_e \times t}{A_s + b \times t} \right]$$

(4.3.1)

where,

$$\frac{\sigma_e}{\sigma_o} = 1 - \frac{1}{4} \frac{\sigma_o}{\sigma_E} \quad \text{for} \quad \sigma_E \geq 0.5\sigma_o$$

(4.3.2.a)

$$\frac{\sigma_e}{\sigma_o} = \frac{\sigma_E}{\sigma_o} \quad \text{for} \quad \sigma_E < 0.5\sigma_o \quad (4.3.2.b)$$

where,

$$\sigma_E = \frac{\pi^2 \cdot E \cdot r_{ce}^2}{\alpha^2} \quad (4.3.3)$$

$$r_{ce}^2 = \frac{I'_e}{A_s + b_e \cdot t}$$

where, EI'_e is the buckling flexural rigidity of the stiffener. The tangent effective width of the plate (b'_e) is given by:

$$\frac{b'_e}{b} = \begin{cases} \frac{1}{\beta_e} \cdot R_n \cdot R_\delta \cdot R_{n\delta} & \beta_e \geq 1 \\ R_n \cdot R_\delta \cdot R_{n\delta} & 0 \leq \beta_e \leq 1 \end{cases} \quad (4.3.4)$$

The effective width of the plate is related to the slenderness as follows:

$$\frac{b_e}{b} = \begin{cases} 1.08 \cdot \phi_b \cdot R_n \cdot R_\delta \cdot R_{n\delta} & \beta_e \geq 1 \\ 1.08 \cdot R_n \cdot R_\delta \cdot R_{n\delta} & 0 \leq \beta_e \leq 1 \end{cases} \quad (4.3.5)$$

where,

$$\beta_e = \frac{b}{t} \sqrt{\frac{\sigma_e}{E}} \quad (4.3.6)$$

$$\phi_b = \frac{2}{\beta_e} - \frac{1}{\beta_e^2} \quad (4.3.7)$$

$$R_n = \left(1 - \frac{\Delta\phi_b}{1.08 \cdot \phi_b} \right) \cdot (1 + 0.0078n) \quad (4.3.8)$$

$$R_\delta = 1 - (0.626 - 0.121\beta_e) \frac{\delta_o}{t} \quad (4.3.9)$$

$$R_{n\delta} = 0.665 + 0.006n + 0.36 \frac{\delta_o}{t} + 0.14\beta_e \quad (4.3.10)$$

where,

$$\Delta\phi_b = \frac{\sigma_r}{\sigma_o} \frac{E_t}{E} \quad (4.3.11)$$

The residual stress σ_r can be obtained from the equation:

$$\frac{\sigma_r}{\sigma_o} = \frac{2n}{\left(\frac{b}{t}\right) - 2n} \quad (4.3.12)$$

$$\frac{E_t}{E} = \left(\frac{\alpha_3 \cdot \beta^2}{\alpha_4 + p_r \cdot (1 - p_r) \beta^4} \right)^2 \quad \text{for } 0 \leq \beta \leq \frac{1.9}{\sqrt{p_r}} \quad (4.3.13.a)$$

$$\frac{E_t}{E} = 1.0 \quad \text{for } \beta \geq \frac{1.9}{\sqrt{p_r}} \quad (4.3.13.b)$$

at which:

$$p_r = \frac{\sigma_p - \sigma_r}{\sigma_o} \quad (4.3.14)$$

where σ_p is the proportional limit of the material.

Faulkner suggested that p_r for marine structures could be taken 0.5.

The constants α_3 and α_4 depend on the boundary conditions and their values are:

$$\alpha_3 = 3.62 \quad \alpha_4 = 13.1 \quad \text{for simply supported plates}$$

$$\alpha_3 = 6.31 \quad \alpha_4 = 39.8 \quad \text{for clamped plates}$$

Through a large number of experiments in frigates, Faulkner suggested that the mean value of plate central deflection can be calculated by:

$$\frac{\delta_o}{t} = 0.12\beta^2 \left(\frac{t_w}{t} \right) \quad \text{for } t_w \leq t, \beta \leq 3 \quad (4.3.15)$$

$$\frac{\delta_o}{t} = 0.15\beta^2 \left(\frac{t_w}{t} \right) \quad \text{for } t_w \leq t, \beta > 3 \quad (4.3.16)$$

$$\frac{\delta_o}{t} = K\beta^2 \left(\frac{t_w}{t} \right) \quad \text{for } t_w > t \quad (4.3.17)$$

where $K = 0.12$ for frigates and 0.15 for merchant ships.

Carlsen pointed out that the initial deflection in most cases meets:

$$\frac{\delta_o}{t} \leq \frac{1}{200} \frac{b}{t} \quad (4.3.18)$$

It is obvious that the foregoing sequence of calculations must be performed iteratively.

The above-cited method is used to calculate the ultimate strength of transversely stiffened decks subjected to impact load as it is shown in figure 4.1 and 4.2, and can not be used to calculate the ultimate stress of longitudinally stiffened decks under the same loading.

For the longitudinally stiffened decks another formula is used to calculate the ultimate strength of the plates between the stiffeners (local buckling) since overall buckling in such plates is very unlikely and usually is avoided by design.

The formula has been proposed by Faulkner et al. (1973) and gives the ultimate strength of wide plates:

$$\frac{\sigma_{yu}}{\sigma_Y} = \frac{0.9}{\beta^2} + \frac{1.9}{\alpha \cdot \beta} \cdot \left(1 - \frac{0.9}{\beta^2}\right) \quad (4.3.19)$$

When the decks are longitudinally stiffened then the equation (4.3.19) is used for the calculation of the strength factor of the decks.

4.4 Incorporation of the proposed method to the program

Due to the iterative nature of the proposed ultimate strength method it can be easily incorporated in a computer program. The Pu and Das method was used from the program to calculate the strength of the decks (σ_u) of the struck ship when its decks are transversely stiffened.

Hegazy (1980) had proposed that the value $\frac{\sigma_u + \sigma_y}{2}$ could be used for the calculations of the energy absorbed in order to account for the strain rate sensitivity of the material. In the results produced in this thesis the yield stress (σ_y) has been used in the energy absorption formulae and only the ultimate strength factor (Φ_d) of decks has been edited. Φ_d is now calculated with the ultimate strength of the decks and not with the critical elastic buckling stress (σ_{cr}).

For the needs of the project a subprogram was developed for the above-cited method and was incorporated in the main program calculating the energy absorbed due to collision. In this chapter results have been obtained for the small oil tanker that was

presented in the previous chapter, using the modified method. Detailed experimental data was not feasible to be found so the comments on the results are purely theoretical.

4.5 Comparison of the results and Conclusions

Results have been produced for two different cases. The small oil tanker was assumed to have transversely stiffened decks in the first case. In the second case the tanker was assumed to be as in the original design with longitudinally stiffened decks. Only the second scenario proposed in chapter three has been considered herein. This means that the whole side structure of the ship is under the impact load.

The details that alter due to the usage of the ultimate strength of the decks are:

- The indentation W_o , at which the deck transverses flanking the strike collapse.
- The indentation \overline{W}_1 at the deck transverses flanking the strike at the instant of rupture.
- The energy absorbed from the decks due to plastic buckling.

Figures 4.8 to 4.16 corresponding to transversely framed decks, plot the values obtained using the ultimate strength of the decks along with values obtained using the orthotropic theory for the critical elastic buckling stress.

Figures 4.16 to 4.24 are being referred to longitudinally framed decks and plot the values obtained using ultimate strength of the decks along with the values obtained with critical elastic buckling of decks.

The differences can be clearly seen. The decks of the struck vessel can absorb more energy than with the previous method due to the reserve of strength in the post-elastic region.

The lack of experimental data does not give us the opportunity to evaluate this modification of the method. Considering the graphs proposed by Hegazy, where the experimental values were in most of the cases higher than the estimated ones, it is believed that this modification gives an even better correlation between the estimated values and the experimental tests.

List of Figures

PART ONE: Stiffened deck Plating Strength

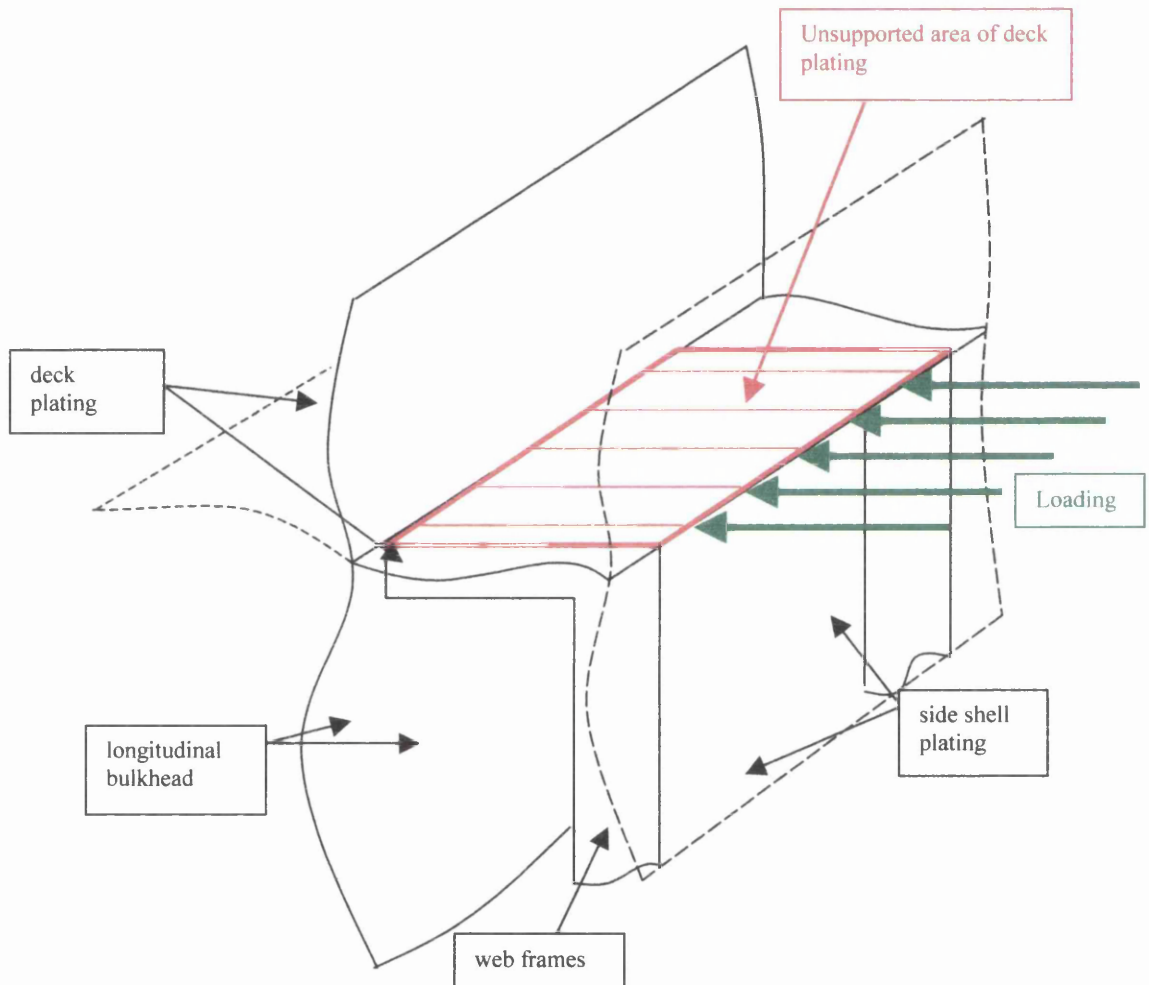


Figure 4.1: Transversely stiffened deck plating loaded on its long edges.

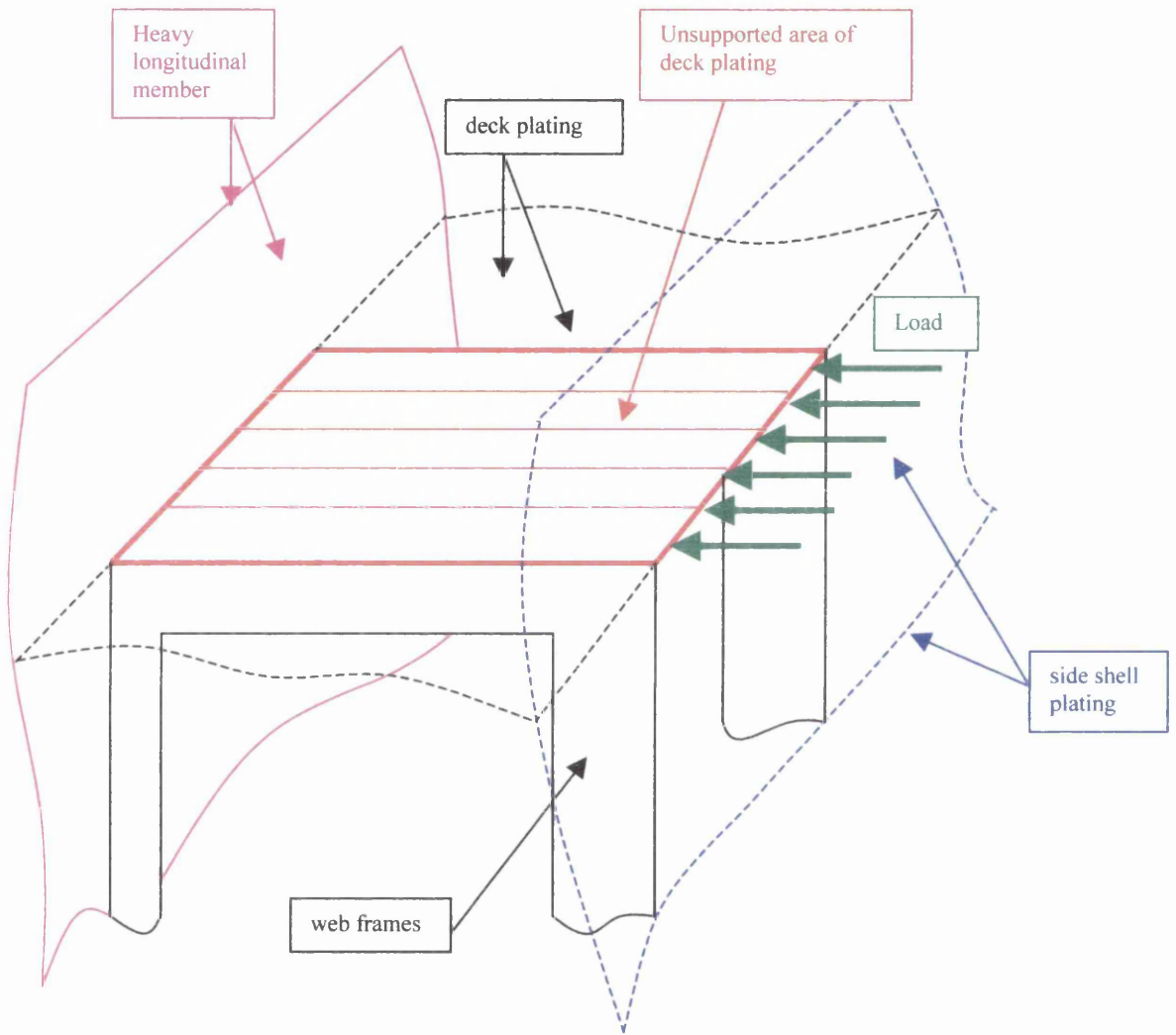


Figure 4.2: Transversely stiffened deck plating loaded on its short edges.

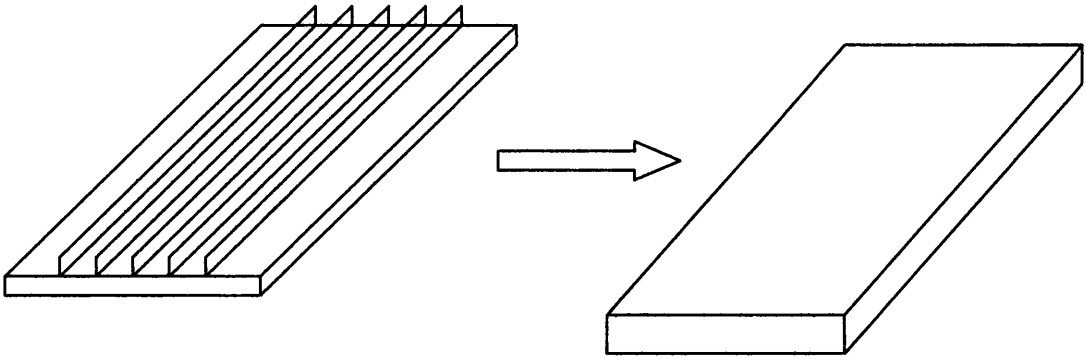


Figure 4.3: Orthotropic method: From a stiffened plate to a plate with different flexural rigidities in the two orthogonal directions.

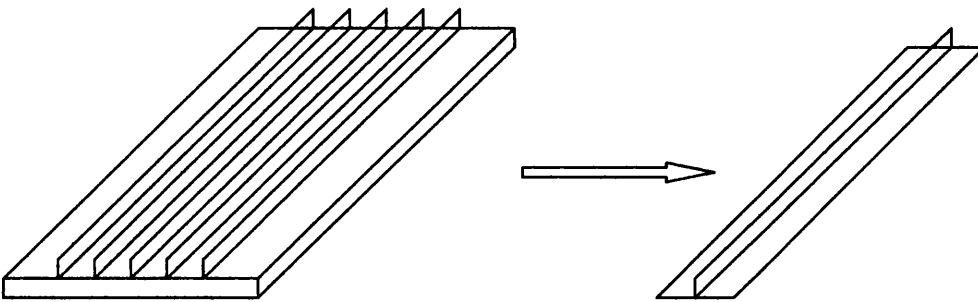
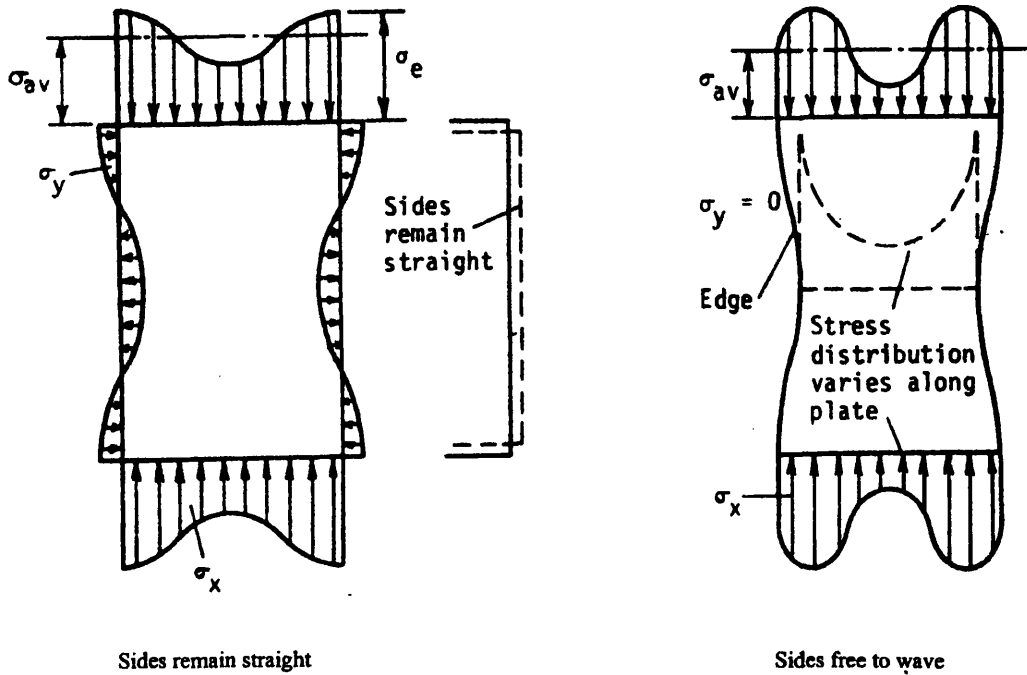


Figure 4.4: Discrete beam method: From a stiffened plate to a stiffener associated with a plate having an effective width provided by the method.



Sides remain straight

Sides free to wave

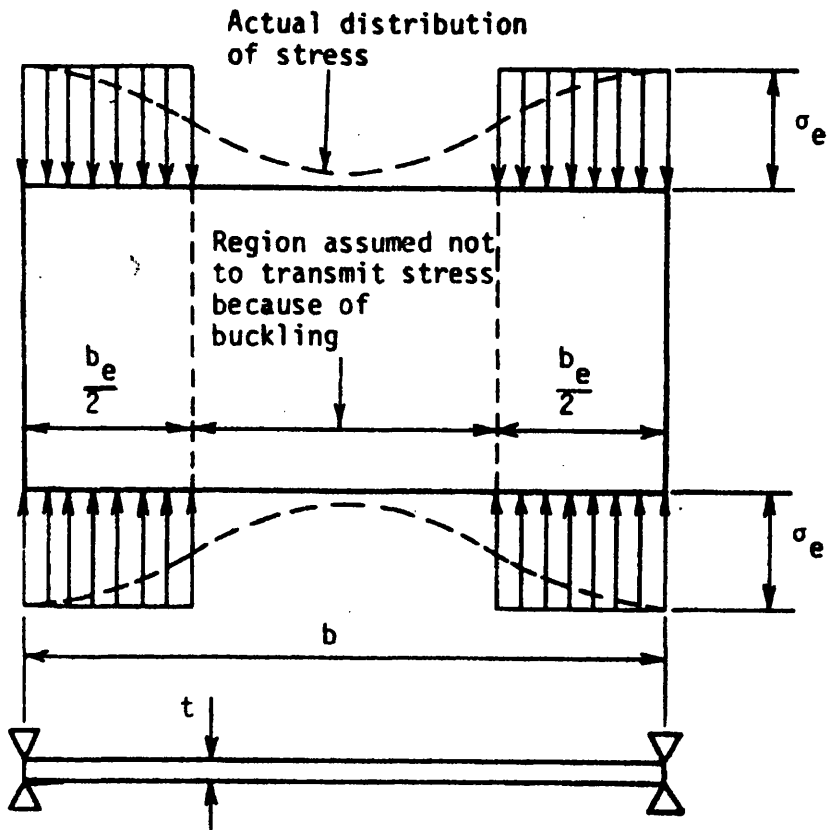


Figure 4.5: Stress distribution on a Post- buckled unstiffened plate.

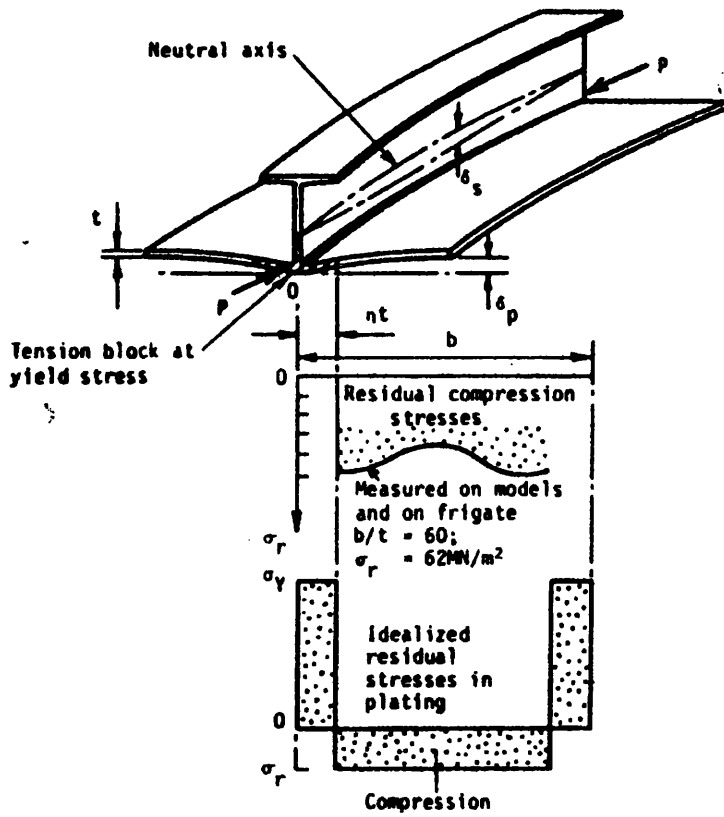


Figure 4.6: Weld shrinkage actions on a flat plate.

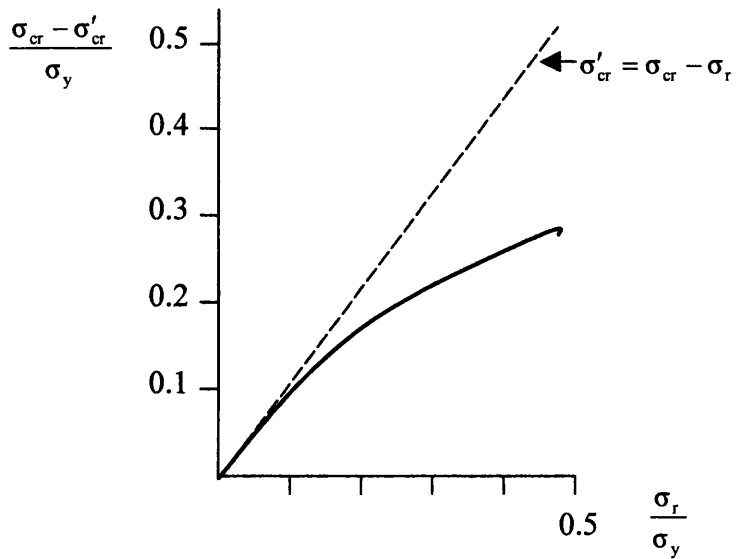


Figure 4.7: Effect of residual compressive stress on theoretical critical stress.

PART TWO: Application of the modified method on an assumed Transversely stiffened Small Oil Tanker Design.

Total Energy Absorbed from the side structure

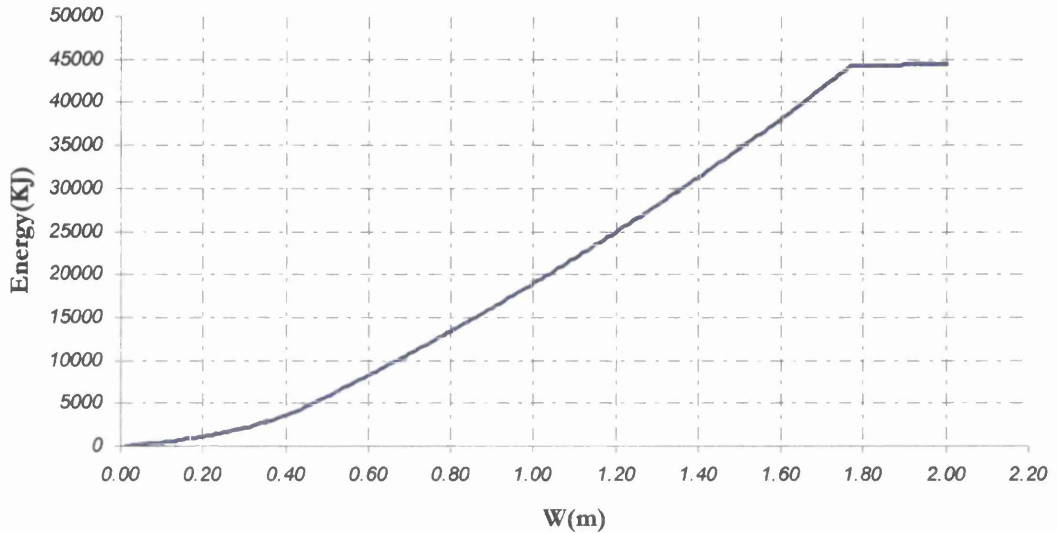


Figure 4.8: Total energy absorbed from the side structure of a transversely framed small oil tanker. The ultimate load of the deck has been calculated with a discrete beam method.

Total Energy Absorbed from the Side Structure



Figure 4.9: Total energy absorbed plotted against the volume of the damaged material. The volume of the damaged side shell plating has not been included in the calculations.

Energy Absorbed due to membrane tension on the stiffened side shell plating

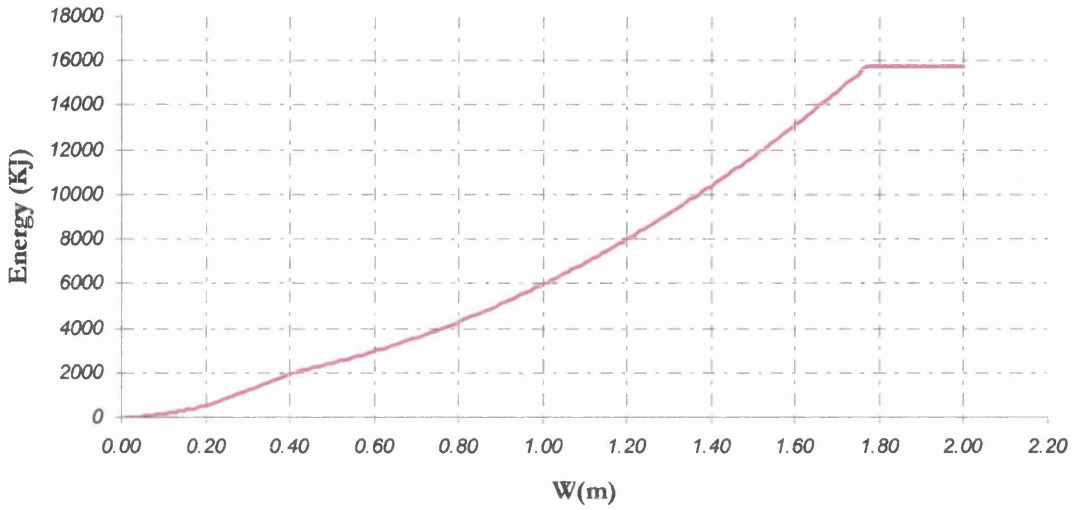


Figure 4.10: Energy absorbed due to membrane tension in the stiffened side shell plating.

Energy Absorbed due to membrane tension on the deck plating

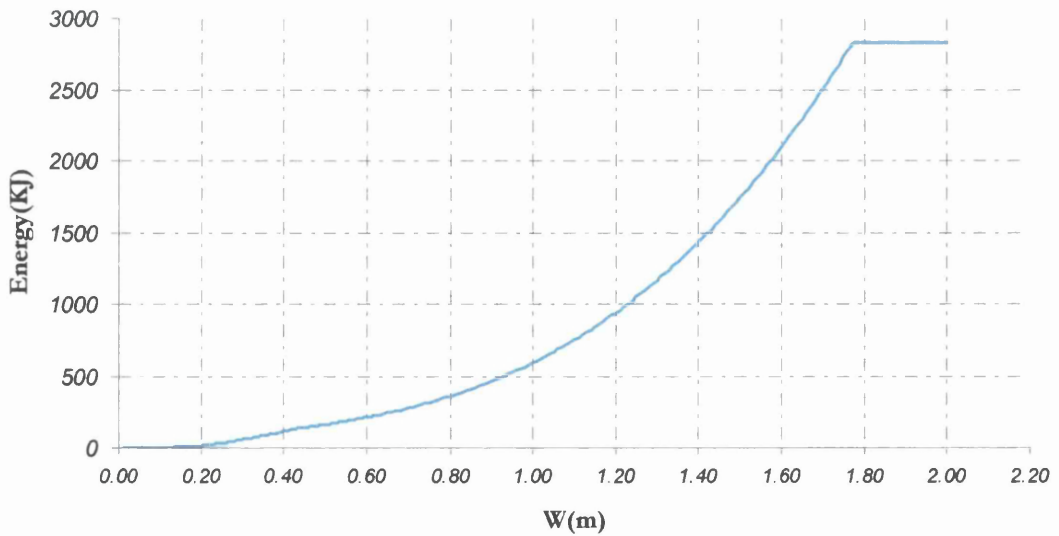


Figure 4.11: Energy absorbed due to membrane tension on the main and bottom deck plating.

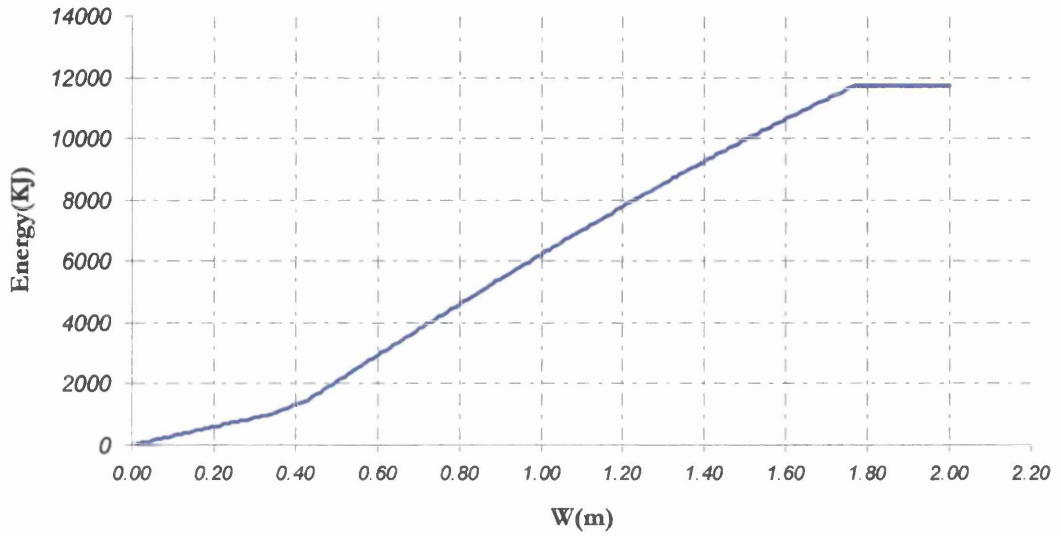
Energy Absorbed due to the buckling of the decks

Figure 4.12: Energy absorbed due to the buckling of the main and bottom deck plating.

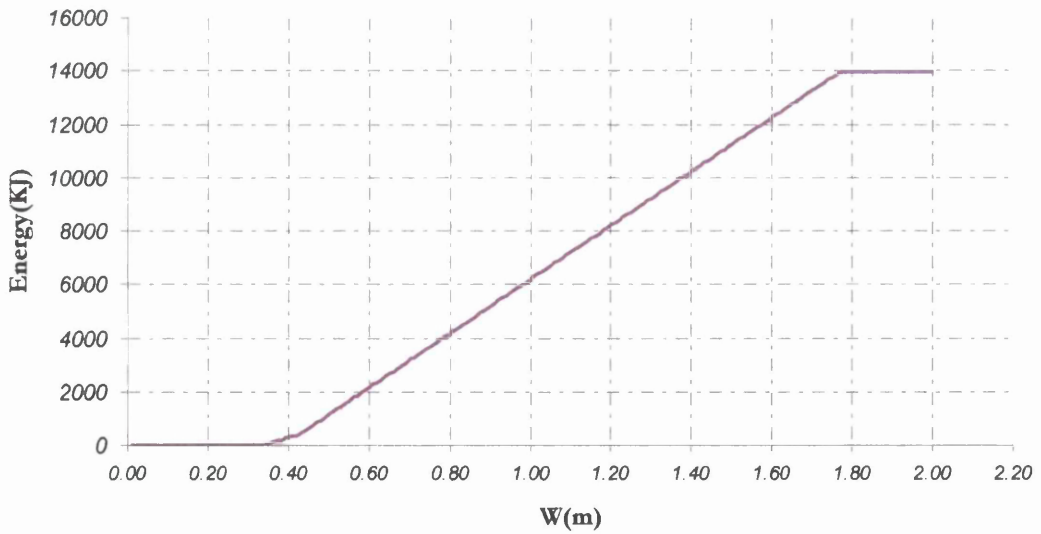
Energy Absorbed due to the collapse of the deck and bottom transverses

Figure 4.13: Energy absorbed due to the collapse of the main deck and bottom transverses.

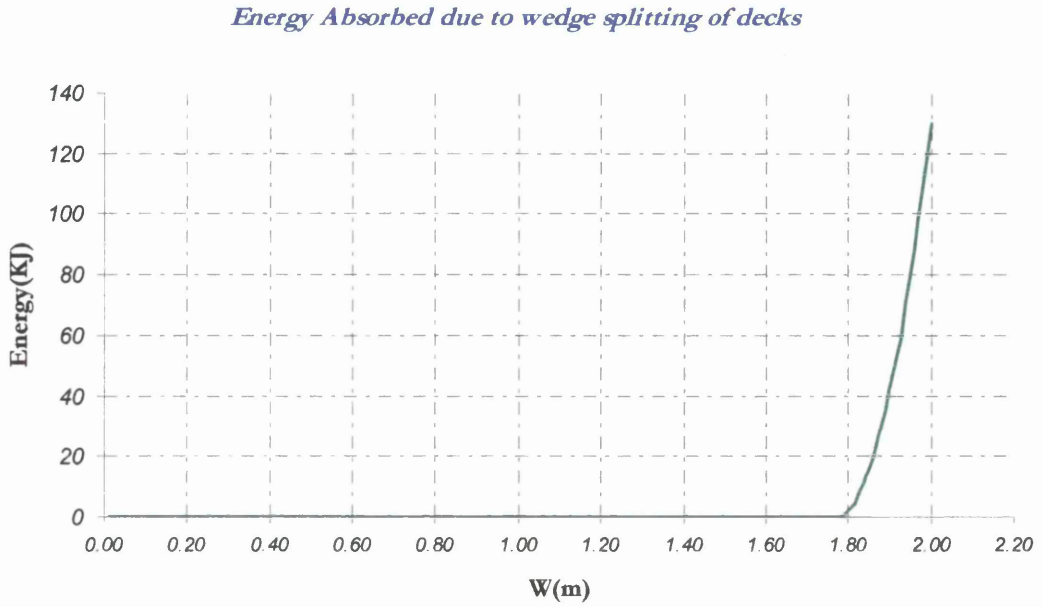


Figure 4.14: Energy absorbed due to the wedge splitting of decks subsequently after rupture of the hull occurs.

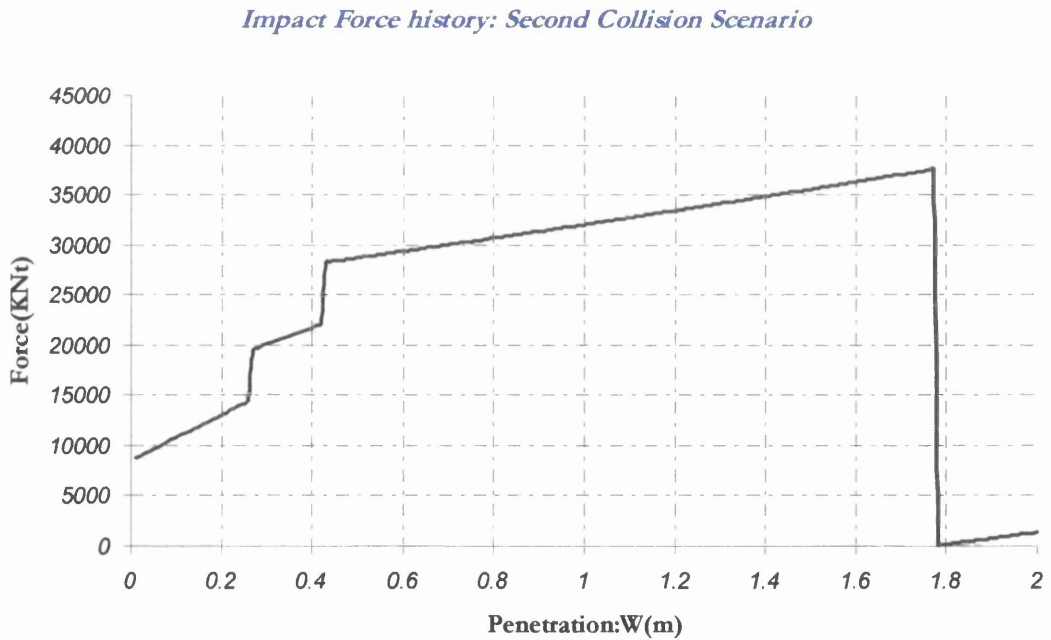


Figure 4.15: This figure illustrates the history of the impact force for the case of a transversely framed structure. The steps at the indentations 0.275m and 0.423m are showing the extension of the damage to the adjacent bays, first in the upper side structure and then in the lower side structure.

PART THREE: Application of the modified method on the existing longitudinally stiffened small oil tanker design.

Total Energy Absorbed from the side structure

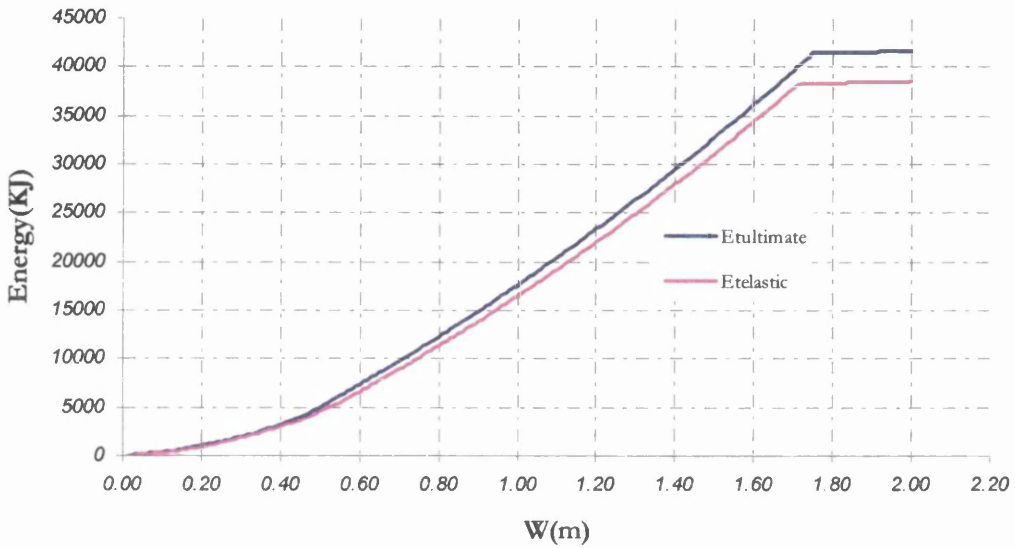


Figure 4.16: Total energy absorbed from the side structure of the longitudinally framed oil tanker. The difference due to the calculation of the ultimate strength of the decks instead of the critical elastic buckling stress is clearly shown.

Total Energy Absorbed from the Side Structure

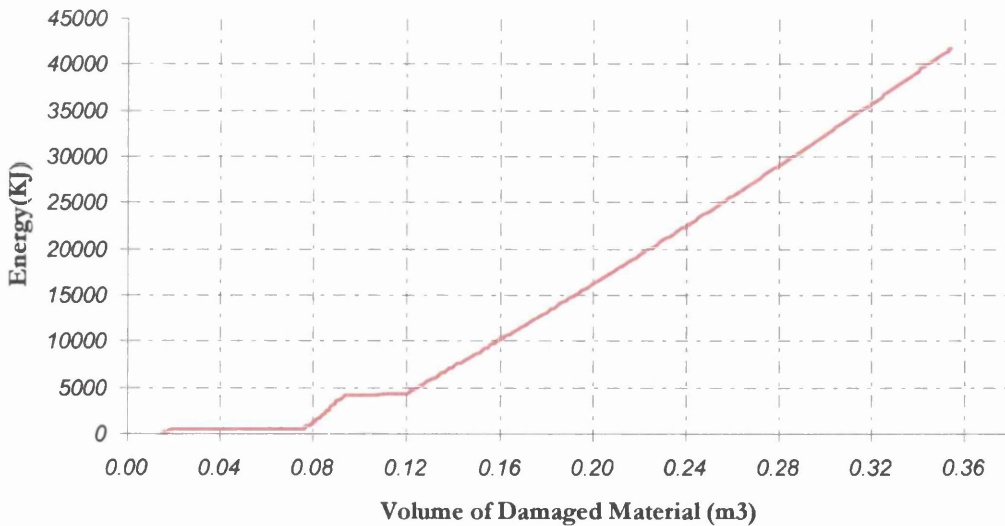


Figure 4.17: Total energy absorbed plotted against the volume of the damaged material. As previously the side shell plating material is not taken into account in the calculations.

*Energy Absorbed due to membrane tension on the stiffened side shell
plating*

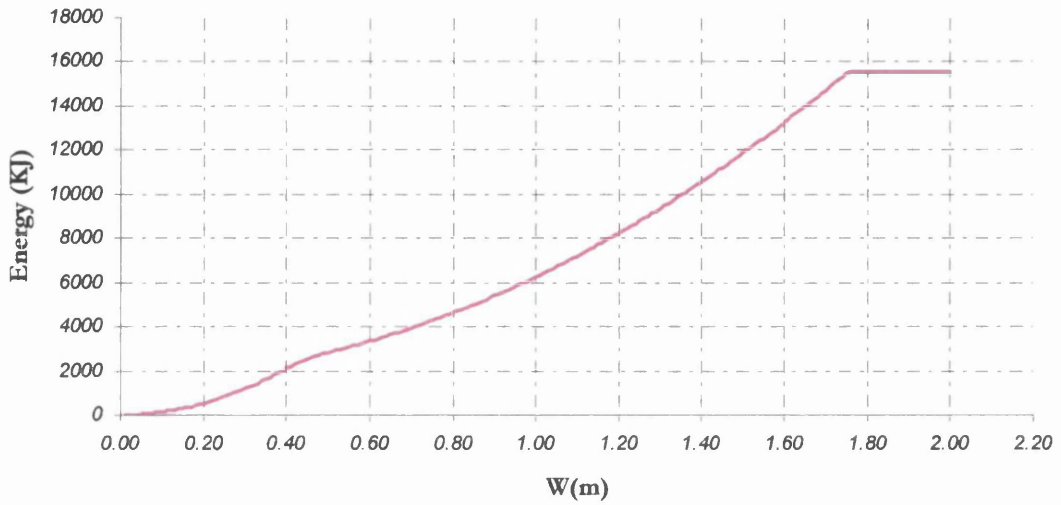


Figure 4.18: Energy absorbed due to membrane tension on the stiffened side shell plating.

Energy Absorbed due to membrane tension on the deck plating

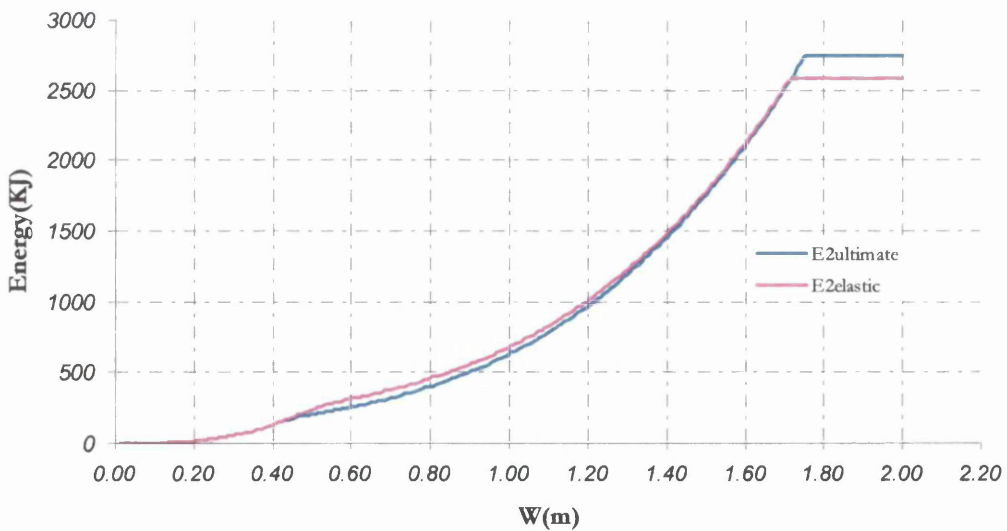


Figure 4.19: Energy absorbed due to membrane tension on the main deck plating and the bottom plating by using the ultimate and the critical elastic buckling stress.

Energy Absorbed due to the buckling of the decks

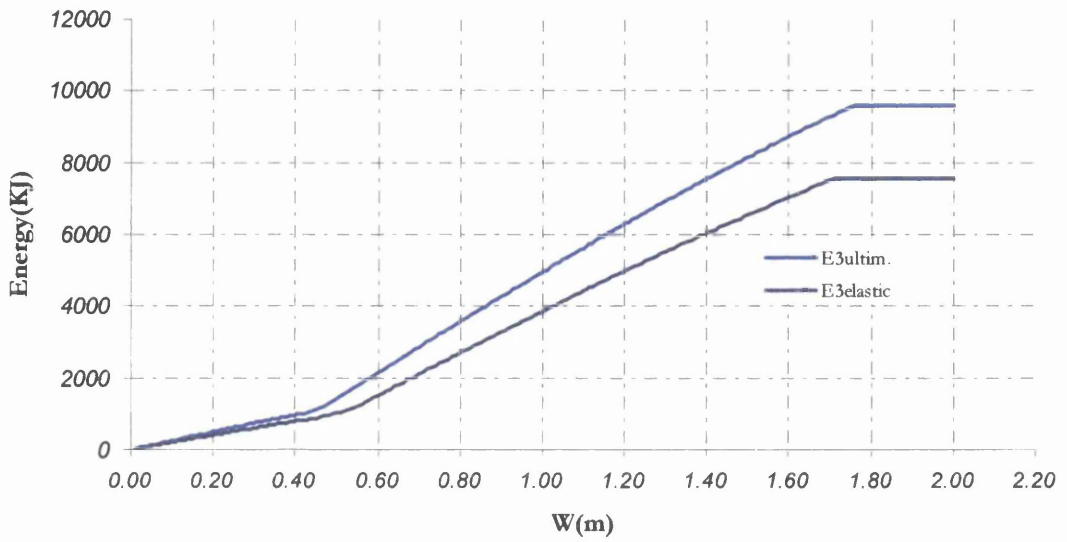


Figure 4.20: Energy absorbed due to buckling of the main and bottom deck plating. The difference in the energy absorption, when the ultimate stress is considered instead of the critical elastic buckling stress, is shown.

Energy Absorbed due to the collapse of the deck and bottom transverses

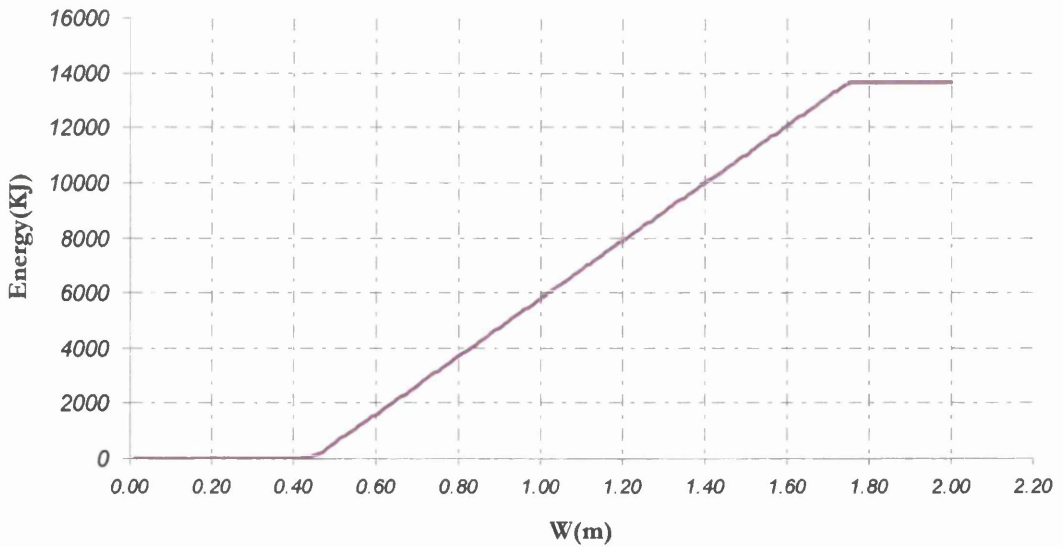


Figure 4.21: Energy absorbed due to the collapse of the main deck's and bottom deck's transverses.

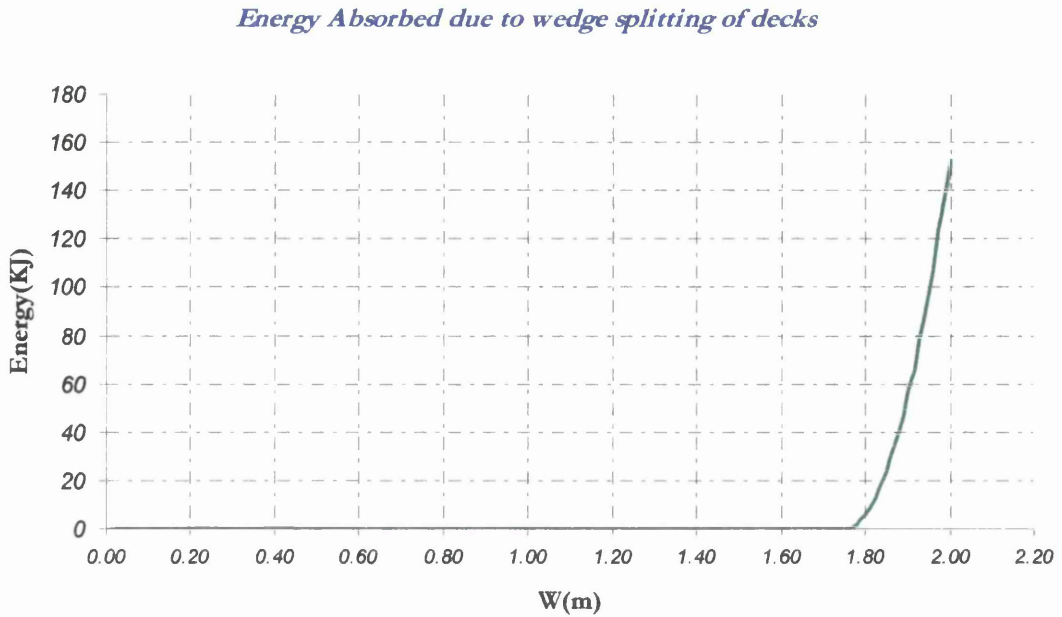


Figure 4.22: Energy absorbed due to the wedge splitting of decks following the rupture of the hull.

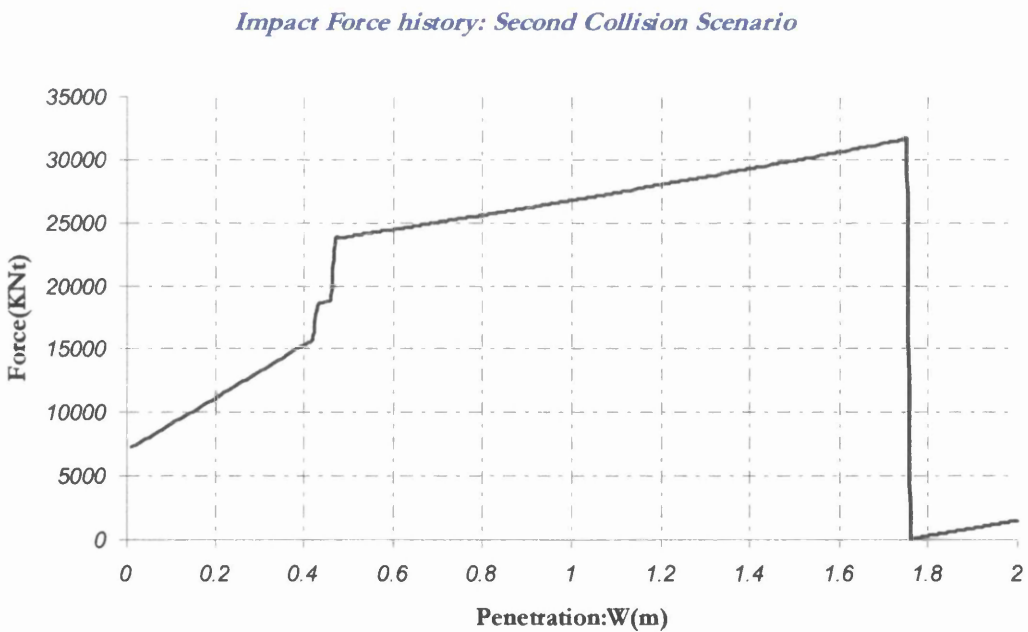


Figure 4.23: The impact force is illustrated against the penetration depth. The critical indentations for the collapse of the deck transverses are changing, when the ultimate stress of the decks is used. The critical indentation for the deck transverse is now $W_{odt} = 0.422\text{m}$ instead of $W_{odt} = 0.355\text{m}$ obtained by the unmodified method. The critical indentation for the bottom transverse is $W_{obt} = 0.466\text{m}$ instead of $W_{obt} = 0.527\text{m}$.

Chapter 5

Estimation of the Crashworthiness of a Double-Hull vessel

Introduction

In this chapter is under inspection the collapse mechanism of the double hull tanker. The difficulties arising in such an analysis have been generally discussed in chapter 2. Theoretical methods as the one used, have to be modified in order to be applied on double-hull structures. Some assumptions were made and will be discussed here in order to define their necessity and their soundness. Basically, these assumptions refer to the sequence of phenomena occurring during impact and their employment was inevitable.

Hereinafter, the collapse mechanism of the structure is described. The modes of failure of the individual structural members and the effect of each member to the resulting damage are discussed.

The vessel in consideration is a large shuttle tanker. The principal dimensions as well as the structural details required are shown in Figure 5.1. It was assumed that due to the large moulded depth and the non-symmetrical form of the mid-ship section around the horizontal axis more than one collision scenarios should be considered. Thus, results have been derived for four different collision scenarios (see subsection 5.4).

5.1 Introduction of the method to a Double Hull design

In chapter 3, where Hegazy's method was presented, it became clear that the method can be easily used for the analysis of a single hull design and even for the analysis of a double hull, when the damage is confined between two adjacent web frames. Through the theoretical analysis of different designs was discovered that in the absolute majority of the cases the web frames flanking the strike collapse before the rupture of the hull.

The differences between the single-skin vessels and the double-skin ones consist basically in the unlike sequence of phenomena occurring during the penetration of the striking ship into their side structure. Particularly, the vessel considered in this chapter exhibits further difficulty due to its complicated side structure (see Figure 5.1). That is due to the presence of topside tanks and other sloped structural members.

Moreover, the damage height and location in the particular vessel play an important role in the capacity of the energy absorption before the rupture of the hull. When the depth of the striking ship is small and the hit is between the topside tank and the double bottom structure of the double-skin struck vessel then the value of the energy absorbed before rupture of the side shell plating will be obviously small. If the topside tank or the double bottom structures are involved in collision the amount of the damaged material increases and so does the value of the energy absorbed.

In the following subsection the assumed occurring sequence of phenomena during impact will be discussed.

5.2 Mathematical model for the double-hull tanker

A rigid vertical bow is assumed to strike the double-skin vessel at the mid-span between web frames. The angle of encounter is right angled. The damage height is dependent on the depth of the striking vessel as well as the relative position of both vessels. The side structure of the double hull is shown in Figure 5.2. There are three different colors defining three different areas. The definition is as follows:

- Red color: Upper area; from the main deck plating to the bottom of the topside tank
- Blue color: Middle area; from the bottom of the topside tank to the inner bottom plating
- Green color: Lower area; from the inner bottom plating to the bottom plating (double bottom structure).

The side structure has been presented like this in order the definition of the damage to be easy and to be easily detected every time, which structural members are involved.

In order to get a general idea of the phenomena occurring during collision at the side structure of the struck ship under consideration, a striking bow with depth larger than the depth of the struck ship will be theoretically considered. This means that the main deck of the bow is assumed to be above the main deck of the struck ship and the bottom of the bow is assumed to be below the bottom of the struck ship. The whole depth of the side structure will then be deformed (red, blue and green areas, Figure 5.2).

The plastic energy absorbed in a double-skin struck ship before rupture of the hull, includes the plastic energy of each hull at the time of its rupture, the plastic energy of the

decks when the second hull ruptures (membrane and buckling components), and any plastic energy absorbed by the web frames up to the instant that the second hull ruptures. When longitudinal decks between the double hull exist then there is additional energy absorption due to the wedge splitting of these decks before the striking ship engages the inner hull.

The wedge splitting mechanism starts in the main deck plating, the inner bottom plating and the bottom plating, immediately after the rupture of the outer hull. So the relating energies have to be considered also.

In a more analytical way the sequence of phenomena for the particular double-skinned design are as follows:

1. The striking ship engages the outer hull of the struck ship. The outer side shell plating deforms and loads in membrane tension. The energy absorbed is due to membrane tension.
2. The main deck plating, the inner bottom plating, the bottom plating and the decks between the two hulls absorb energy due to membrane tension and plastic buckling.
3. The penetration reaches the critical value, at which the weaker main deck's transverse collapses and the damage in the upper area extends in the adjacent bays.
4. The penetration reaches the critical value, at which the stronger bottom's transverse collapses and the damage in the lower area extends in the adjacent bays.
5. The side transverses collapse. Energy absorbed through bending of the side transverses as beams associated with the plating of the inner and outer hull.
6. The outer hull ruptures and the decks are being torn from the striking bow. Energy absorbed due to wedge splitting of decks.

7. The inner hull is impacted by the striking bow. Energy absorbed due to membrane tension. At the end of this phase the inner hull ruptures and the only energy absorbing mechanism is the wedge splitting of the main deck plating, the inner bottom plating and the bottom plating.

A program has been developed in Fortran 90 to conduct the calculations of the energy absorbed from the shuttle tanker. A worksheet in Microsoft Excel was also created for the same reason in order to check the results of the program.

The inputs in the program are all the structural details describing the decks, side shell plating, and material properties as well as the range of the penetration for which the calculations will be conducted. As the penetration increases in every iteration the program carries out the following checks:

- If the penetration (W) is less than the critical indentation (W_c) and also less than the limited indentation for the first bay (W_{L1}) then the energy absorbed is:
 1. Energy absorbed due to membrane tension in the side shell plating
 2. Energy absorbed due to membrane tension in the decks.
 3. Energy absorbed due to buckling of the decks.

- If the penetration (W) is greater than the critical indentation (W_c) and less than the limited indentation of the three bays collapse model (W_{L2}) then the deck transverses flanking the strike have collapsed and the damage is extended to the adjacent bays. The energy absorbed is:
 1. Energy absorbed due to membrane tension in the side shell plating
 2. Energy absorbed due to membrane tension in the decks
 3. Energy absorbed due to buckling of the decks
 4. Energy absorbed due to the collapse of the deck transverse

The above-cited energies are calculated for the extent in the three bays collapse model.

- If the penetration (W) is greater than the limiting indentation (W_{L2}) then the outer hull ruptures and the energy absorbed is:
 1. Energy absorbed due to membrane tension of the side shell at the instant of rupture
 2. Energy absorbed due to membrane tension in the decks at the instant of rupture of the outer hull.
 3. Energy absorbed due to buckling of decks at the instant of rupture of outer hull.
 4. Energy absorbed due to the collapse of the deck transverse at the instant of rupture of the outer hull.
 5. Energy absorbed due to the wedge splitting of decks.

- If the penetration (W) overcomes the value required to reach the inner hull, which will be the distance between the two hulls plus the distance that the inner hull moved due to the movement of the web frames, then the energy absorbed is:
 1. The summation of the energies calculated in the previous case.
 2. Energy absorbed due to membrane tension in the inner hull

When the inner hull is engaged by the striking bow then the analysis is the same as the one for the outer hull.

It must be remarked that in the above-cited mathematical model the critical indentation (W_o) at which the deck transverses collapse is less than the limiting indentation (W_{L1}) beyond which rupture of the side shell plating occurs. This means that there will not be rupture of the hull before the collapse of the deck transverses flanking the strike.

These two values are characteristic values of each structure and give us the opportunity to know the collapse model of the structure in advance. If a side structure consists of very strong web frames then (W_o) will be greater than (W_{L1}) and the damage will be confined in one bay (speaking for a mid-span right angle strike).

Finally, an output file is produced with the energies absorbed from the individual structural members of the struck ship as well as the impact force and the volume of the material damaged at each value of the penetration.

5.3 Assumptions

Due to the complexity of the particular double-skin structure some assumptions had to be made and are presented through a discussion on the collapse model.

Stiffened Outer Hull: The stiffened outer hull is the first part of the struck ship that is subjected to the impact load. As the outer hull is displaced towards the ship interior membrane tension forces are present in the stiffened outer hull's plating. The energy absorbed from this member of the ship is due to these membrane forces.

Decks between the Double Hull: The decks between the two hulls are the very next structural members that are subjected to the impact load. The decks are absorbing energy due to membrane tension forces and due to buckling.

Stiffened Inner Hull: The stiffened inner hull is the third member that concludes the structural members that exist between two adjacent web frames and between deck and bottom structures. The stiffened inner hull will be deformed after the collapse of the decks between double hull. That will happen if no heavy transverse member collapses before the striking bow reaches the inner hull. If collapse of the heavy deck and bottom transverses occur before the indentation reaches the value of the double hull breadth then the damage extends to the adjacent bays before any damage to the inner hull is made.

Main Deck Transverse: The structure below the deck of this ship design is somehow complicated because the particular ship has a topside tank. The deck transverse in the region of the topside tank is triangular and stronger than the rest of the deck transverse. The triangular member will not be taken into account when the critical indentation beyond which collapse of the member occurs will be calculated. That is due to the strength of the triangular member which makes it to stand the force when the rest of the deck transverse collapses.

Bottom Transverse: The bottom transverse is subjected to a reaction force, which consists of the membrane tension forces coming from the outer and inner hull and the membrane and buckling forces coming from the decks between double hull. The share of the reaction force acting on the deck and bottom transverse is assumed to be:

Deck transverse: All the membrane and buckling forces for damage height the height of the topside tank measured at the side of the vessel.

Bottom transverse: All the membrane and buckling forces for damage height the height of the double bottom structure.

The length of the bottom transverse for the strength calculations is taken to be the unsupported length between two adjacent girders. In any case the damage is assumed to confine in one or three bays maximum. This means that the transverses flanking the strike might collapse and the damage might extend in the adjacent bays but no further transverses will collapse. Thus, the damage is confined in three bays. If the transverses are very strong the damage will be confined in one bay.

Side Transverse Lower and Upper Part: The side transverse is the heavy vertical member that joins the deck and bottom transverse. The side transverse in this ship consists of two parts with different unsupported length. This is the reason that the side transverse will be treated as two clamped beams. With this assumption we get different collapse values for the side transverse and a more complicated model. Therefore, when the damage extends to the adjacent bays due to the different collapse values of the deck, bottom and side transverses sloped indentation lines had to be assumed at the web frames.

Collapse Mechanism for the Complete Structure: Because of the complications that are presented in this particular structure, it is very difficult to define in advance the way that the structure will deform under an impact load. A good way to conduct this kind of work is with critical indentations for each member as was shown previously.

If we know the critical indentations for every structural member then it is easy to see which members will collapse first and which later. This work is needed when the prediction of the behavior of the side ship structure in various penetrations is important.

On the other hand for a given deformed struck ship, it is easy to calculate the absorbed energy by simply applying the theoretical plastic analysis formulae on each individual member.

5.4 Collision Scenarios

Collision scenarios play a very important role in the amount of energy absorbed from the struck ship structure. There are a lot of parameters involved in the definition of a collision scenario. In the present study the striking ship impacts the struck ship at right angles and at the mid-span between web frames.

The collision scenarios assumed herein were proposed from the Germanischer Lloyd in order to estimate the crashworthiness of a ship. The scenarios are depending on the load conditions of the vessels involved. Four different cases were examined:

1. Struck ship in ballast condition. Striking ship in the full load condition.
2. Struck ship in ballast condition. Striking ship in ballast condition.
3. Struck ship in full load condition. Striking ship in full load condition.
4. Struck ship in full load condition. Striking ship in ballast condition.

The scenarios are illustrated in Figures 5.3 to 5.6. The striking ship was assumed to have a depth of $D = 15.000\text{m}$. The selection of the depth was based on a statistical search from actual ship to ship collisions. Most of the collided vessels were found to have a depth around fifteen meters. Also this depth was convenient for showing the irregularities that arise during collision. In figures 5.3 to 5.6 can also be seen the structural members of the struck ship that will suffer damage, involved in each case.

5.4.1 Estimation of the Drafts

The designs of the shuttle tanker, which were provided are:

- Midship Section
- General Arrangement Plan
- Longitudinal BHD at C.L.
- Tanktop and Hopper
- Maindeck and Bottom
- Shell Expansion

Stability Booklet for the ship has not been provided to us. Thus, an evaluation for the Ballast Condition Draft has to be done. From the General Arrangement Plan, the diameter of the propeller of the ship and the height of the propeller's shaft can be measured. The diameter is $D = 6.20$ m and the height of the shaft from the keel is $H_s = 4.20$ m.

The regulations require that in ballast condition a tanker's propeller must be 300mm below water. So the aft draft of the ship must be:

$$T_{\text{AFT}} = (H_s - D/2) + D + 0.3 = 7.10 \text{ m}$$

The regulations require that in ballast condition a tanker's trim must not be greater than 300mm. So we assume that the forward draft is:

$$T_{\text{FRW}} = T_{\text{AFT}} - 0.3 = 6.80 \text{ m}$$

The above made calculations give us a mean draft in Ballast Condition:

$$T_{\text{MBALLAST}} = 6.95 \text{ m}$$

For the Full Load Condition we have the Design Draft:

$$T_D = 15.950 \text{ m}$$

Therefore, in the estimation of the relative position of the colliding vessels these drafts are used. For the striking bow the required drafts were assumed to be those of an existing tanker vessel having depth $D = 15.000\text{m}$. The drafts are shown below:

- $T_D = 9.900 \text{ m}$
- $T_B = 4.300 \text{ m}$

Results have been derived for all of the above-cited scenarios and are discussed along with the occasionally made assumptions, in the following subsection.

5.4 Results and Conclusions

The results have been produced for four different collision scenarios. It is very interesting to see the difference in the total energy absorbed by the side structure, when the damage area is changing. Each scenario is separately discussed and assessed.

First Collision Scenario:

The struck vessel is in ballast condition and the striking vessel is in full load condition. The damage height is 12.050 m, measured from keel. The structural members involved in collision are:

- bottom plating

- bottom transverse
- inner bottom plating
- outer hull
- lower side transverse
- inner hull
- two decks between the two hulls

As the striking bow penetrates towards the centerline of the struck ship the sequence of phenomena occurring is the following.

1. The outer hull is loaded in membrane tension. The decks between the two hulls load in membrane tension and in buckling as well as the bottom and the inner bottom deck plating.
2. As the penetration depth increases the bottom transverses and the side transverses flanking the strike collapse and the damage is extended in the adjacent bays.
3. Rupture of the outer hull occurs at the end of this phase and the rigid bow starts to tear the decks plating.
4. The striking bow engages the inner hull. Energy is absorbed due to membrane tension in the inner hull plating. The bottom and the inner bottom plating load in membrane tension and buckling.
5. The inner hull ruptures and the energy absorbing mechanism is the wedge splitting of bottom and inner bottom deck plating.

The results are shown in Figures 5.7 to 5.18. The energy absorbed up to the rupture of the inner hull is $E_{\text{minor}} = 423187$ KJ. The maximum penetration before the rupture of the inner hull is $W_{\text{LMAX}} = 5.630$ m.

Second Collision Scenario:

The struck vessel is in ballast condition and the striking vessel in ballast condition. The damage height is 15.000 m. The damaged area is from 0.450 meters above the inner bottom plating to 0.950 meters above the third deck between the two hulls (counting from the bottom). The structural members that are absorbing energy are:

- three decks between the two hulls
- outer shell plating
- lower and upper part of the side transverse
- inner shell plating

As it can be seen no deck transverses are involved in the calculations. The side transverses do not buckle or yield before the rupture of the hulls and the damage is confined in one bay.

The sequence of phenomena is as follows:

1. The outer hull is loaded in membrane tension. The decks between the two hulls are loaded in membrane tension and in buckling.
2. At the end of this phase rupture of the outer hull occurs. The mechanism that absorbs energy now is due to the wedge splitting of the decks between the two hulls.
3. The striking bow engages the inner hull, which loads in membrane tension.
4. The inner hull ruptures and the striking bow penetrates into the cargo tank without any further resistance.

The results for this scenario are shown in Figures 5.19 to 5.25. The total energy absorbed just prior to the rupture of the inner hull is $E_{\text{minor}} = 172740 \text{ KJ}$. The maximum penetration at the instant of the inner hull's rupture is $W_{\text{LMAX}} = 3.166 \text{ m}$.

Third Collision Scenario:

The struck vessel is in full load condition and the striking vessel in full load condition. The damage height is 15.000 m. The damaged area is from 0.100 m above the first deck between the two hulls to 0.800 m below the main deck plating. The structural members suffering damage are:

- two decks between the two hulls
- outer shell plating
- topside tank's bottom plating
- inner shell plating
- lower and upper part of the side transverses

The damage is confined in one bay as previously and the sequence of phenomena is as follows:

1. The outer hull loads in membrane tension. The decks between the two hulls load in membrane tension and in buckling.
2. The outer hull ruptures and the decks between the two hulls are being torn from the striking bow.
3. The bow engages the inner hull, which loads in membrane tension. The topside tank's bottom loads in membrane tension and buckles.
4. The inner hull ruptures and the only energy absorbing mechanism is the wedge splitting of the topside tank's bottom plating.

The results for the third scenario are presented in Figures 5.26 to 5.36. The total energy absorbed up to the rupture of the inner hull is $E_{\text{minor}} = 171822$ KJ. The maximum penetration just prior to the rupture of the inner hull is $W_{\text{LMAX}} = 3.166$ m.

Fourth Collision Scenario:

The struck vessel is in full load condition and the striking vessel is in ballast condition. The damage height is 9.450 m. The damaged area is from 1.150 meters above the second deck between the two hulls to the main deck (main deck included). The structural members involved in the damage are:

- main deck plating
- main deck's transverses
- topside tank's bottom plating
- upper part of side transverses

The sequence of phenomena is as follows:

1. The outer hull loads in membrane tension. The main deck and the deck between the double hull load in membrane tension and in buckling.
2. The deck transverses flanking the strike collapse and the damage is extended to the adjacent bays.
3. The outer hull ruptures and the striking bow tears the deck between the two hulls as well as the main deck.
4. The bow engages the inner hull, which loads in membrane tension.
5. Finally, the inner hull ruptures and the remaining absorbing mechanism is the wedge splitting of the main deck and topside tank's bottom plating.

The results for the third scenario are presented in Figures 5.37 to 5.46. The total energy absorbed from the side structure up to the rupture of the inner hull is $E_{\text{minor}} = 208238$ KJ. The maximum penetration just prior to the rupture of the inner hull is $W_{\text{LMAX}} = 4.780$ m.

The maximum energies absorbed up to the rupture of the inner hull along with the maximum penetrations at the instant of the inner hull rupture are presented conclusively in the next table:

	Total Energy Absorbed prior to the rupture of the inner hull, E_{minor}	Penetration depth at the instant of inner hull's rupture, W_{LMAX}
First Collision Scenario	423187 KJ	5.630 m
Second Collision Scenario	172740 KJ	3.166 m
Third Collision Scenario	171822 KJ	3.166 m
Fourth Collision Scenario	208238 KJ	4.780 m

	First Collision Scenario	Second Collision Scenario	Third Collision Scenario	Fourth Collision Scenario
Volume of Damaged Material (including inner and outer shell)	10.374 m ³	2.727 m ³	2.644 m ³	3.994 m ³

It can be seen that in the second and third scenario, where no deck transverses are involved, rupture of the inner hull occurs for identical penetration depths. The damage in these two cases is confined between two consecutive web frames and the value of the penetration is calculated as the limiting value of the inner hull displacement before rupture occurs plus the width of the span between the two hulls.

In the first and fourth cases, where the deck/bottom transverses flanking the strike collapse, the maximum penetration depth is dependent on the lateral movement of the transverses. The greater strength of the bottom transverse - in the first scenario – provides great resistance to penetration and so the energy absorbed is the larger from all the

scenarios. This is also due to the strong bottom and inner bottom plating. The weaker deck transverse – fourth collision scenario - moves towards the centerline of the vessel more easily and that is the reason for the penetration value of 4.780 m. On the other hand, the energy required for this penetration depth to be reached is very much smaller than the first scenario.

The damaged material in each scenario is shown in the presented table and justifies the differences in the energy absorption capacity.

From the obtained results, it becomes evident that the right selection of the structural scantlings is not an easy thing. That is why an optimization procedure is required when a ship is designed and an easy-to-use prediction method is the way this aim is achieved.

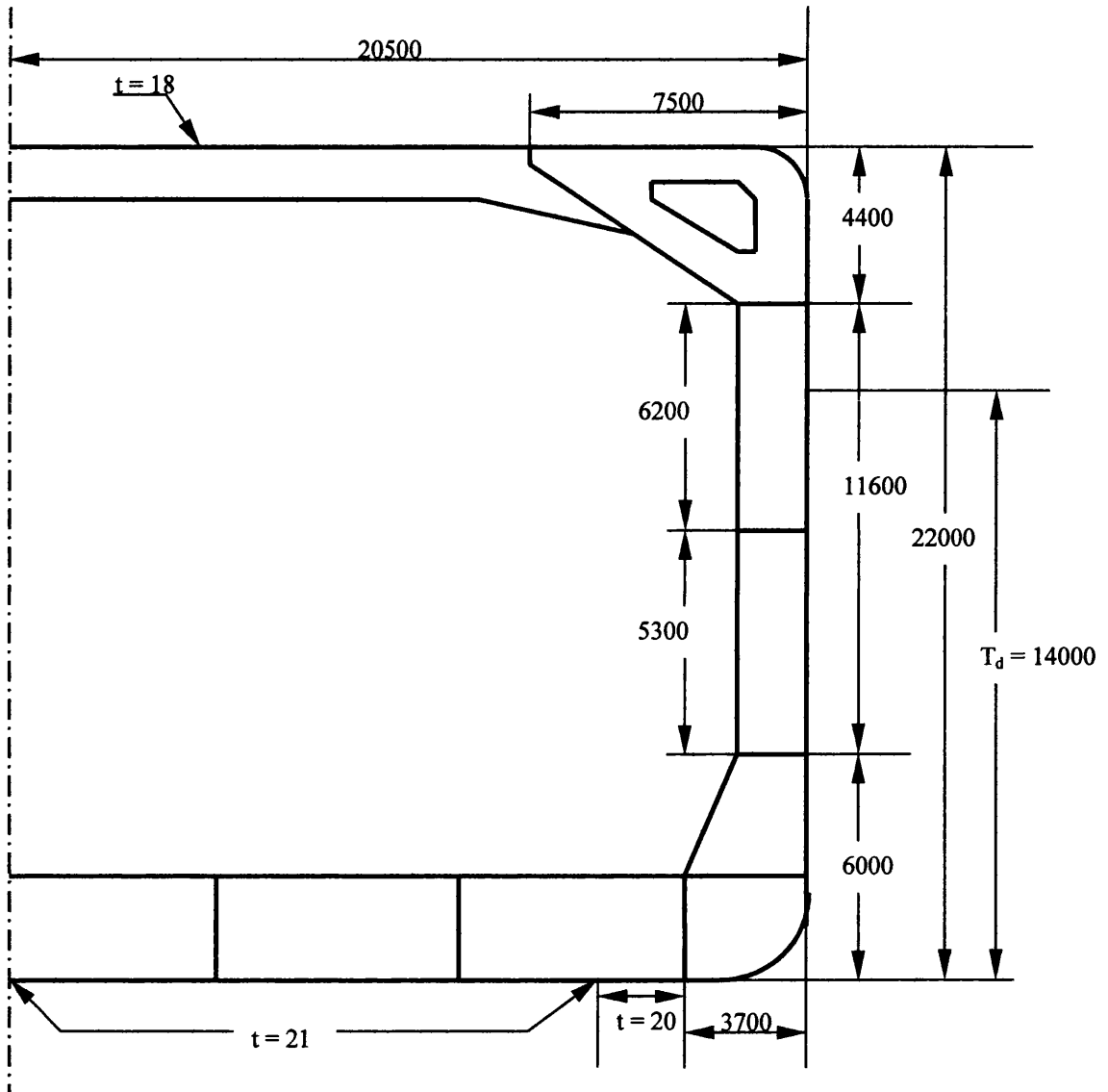
List of Figures***PART ONE: Double Hull design – Damage profiles – Collision Scenarios.***

Figure 5.1: Mid-ship section of the shuttle tanker provided by Lloyd's Register.

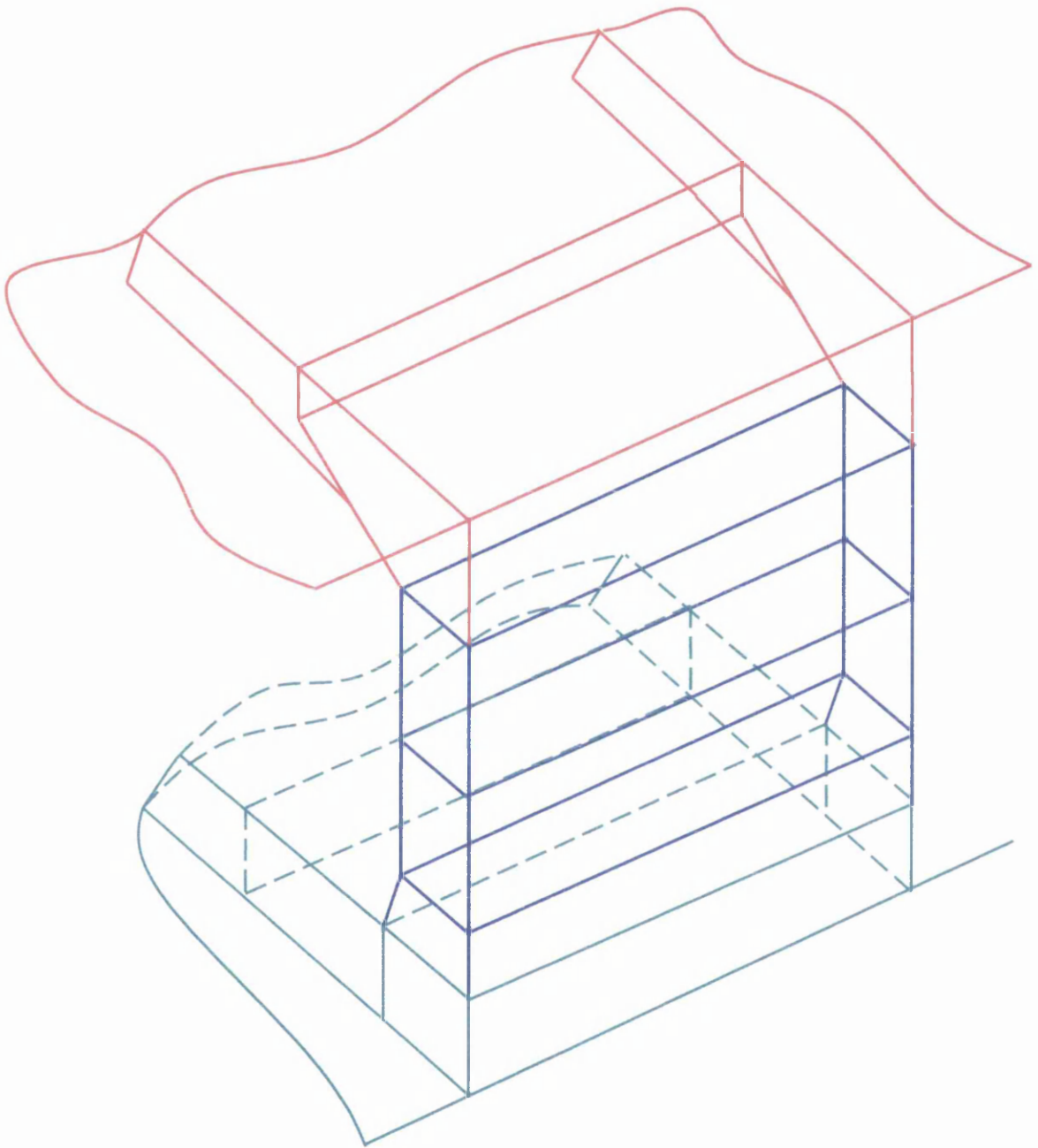


Figure 5.2: Three-dimensional model of the double hull tanker. The three different colors define the areas of the topside tank, the double shell, and the double bottom structures.

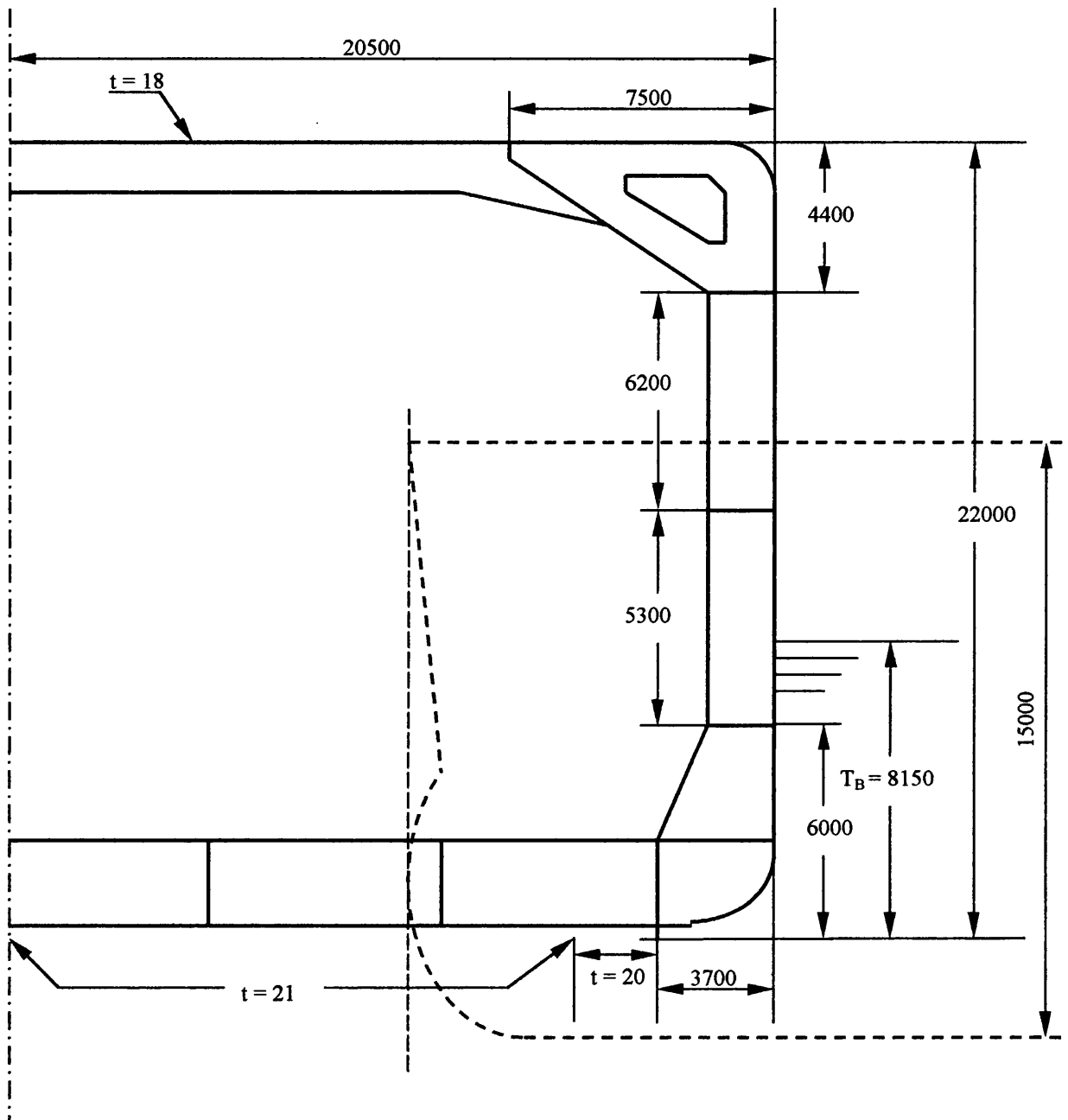


Figure 5.3: Assuming the struck ship in the Ballast Condition and a striking ship with Depth=15000mm in the Full Load Condition.

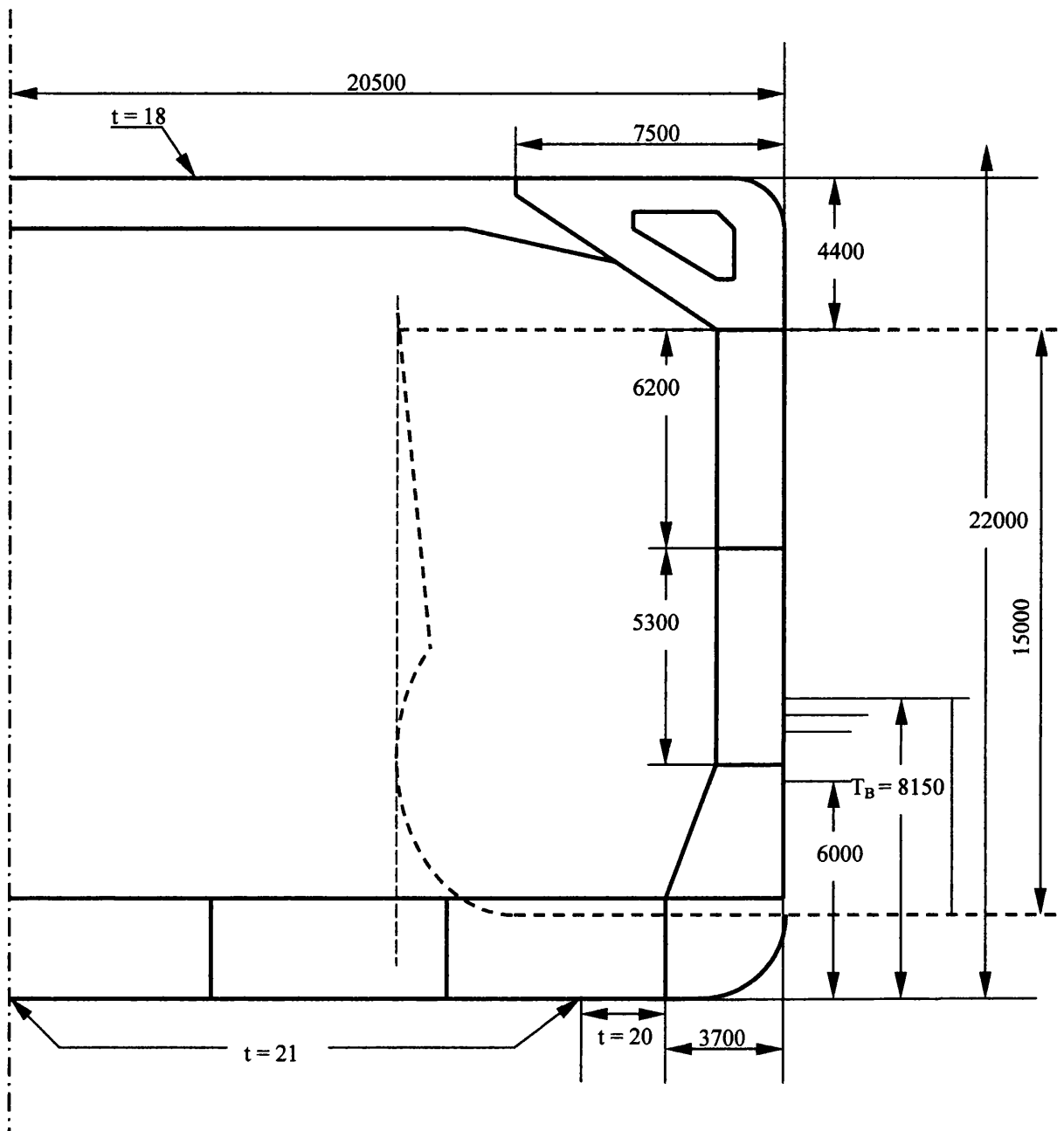


Figure 5.4: Assuming the struck ship in the Ballast Condition and a striking ship with Depth = 15000mm in the Ballast Condition.

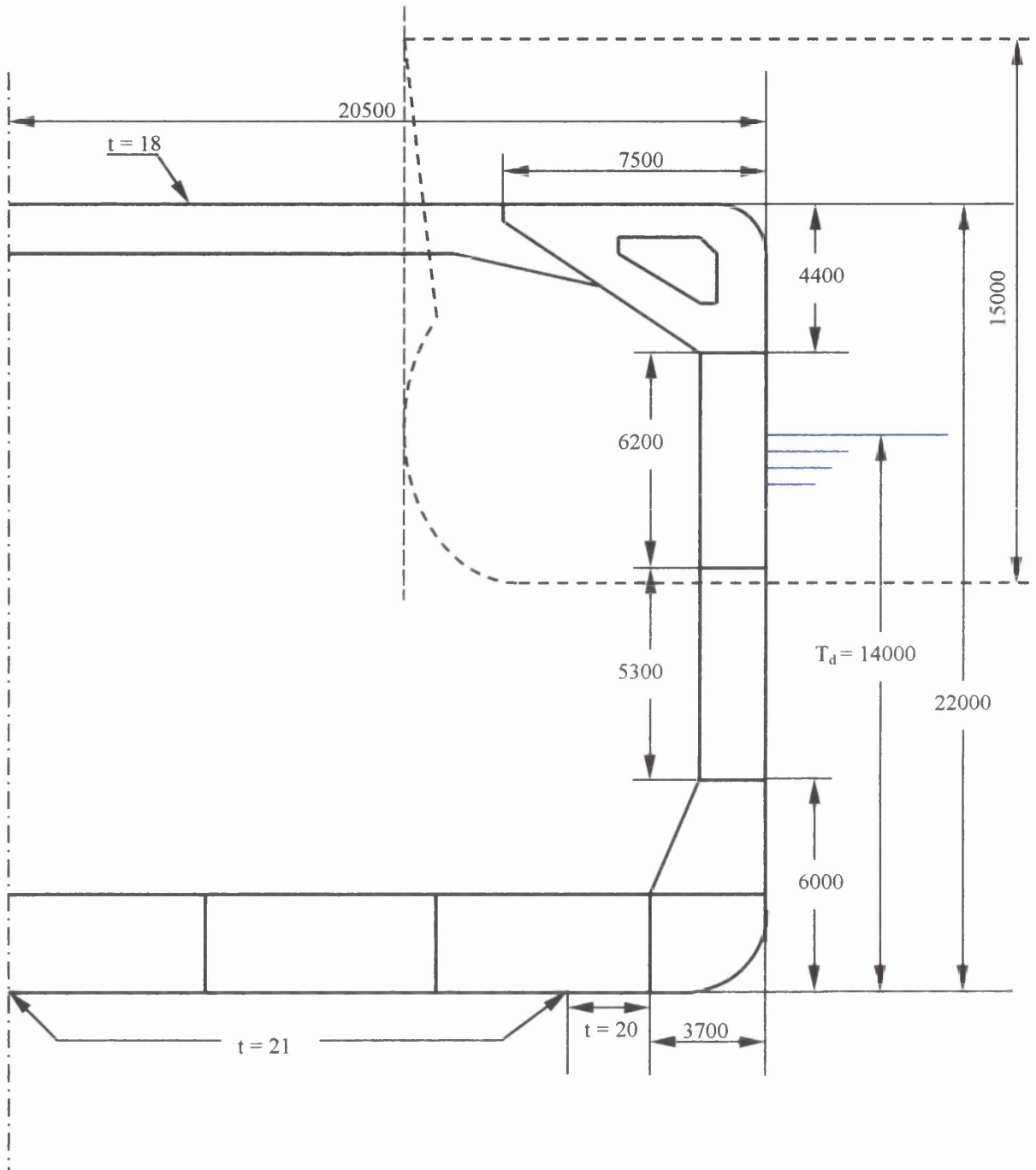


Figure 5.6: The struck ship is assumed to be in the Full Load Condition and a striking ship with Depth=15000mm in the Ballast Condition.

PART TWO: Double-skin tanker - Results for the First Collision Scenario

Total Energy Absorbed - First Collision Scenario

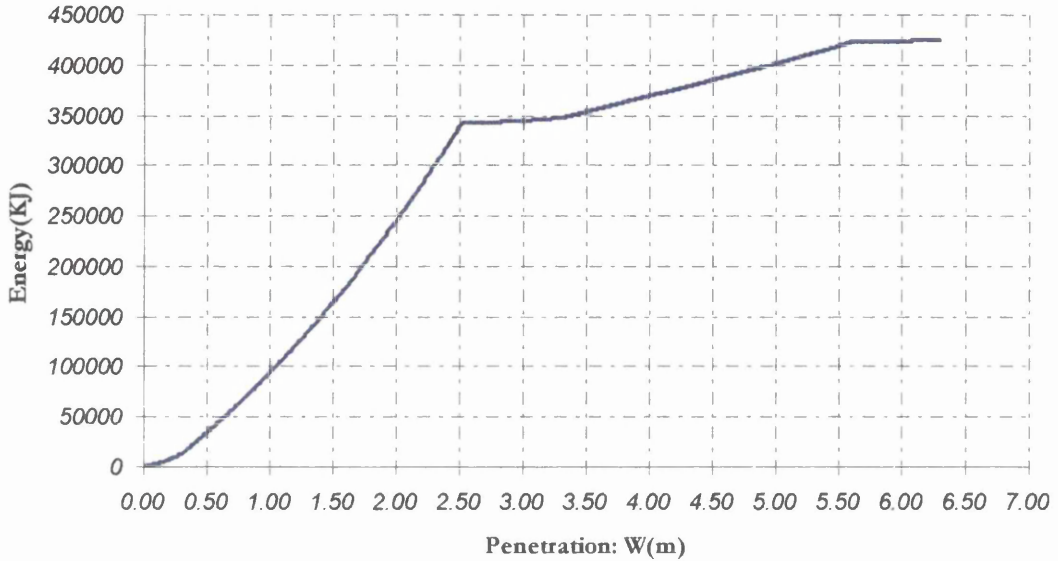


Figure 5.7: Total energy absorbed by the side structure of the double-skin tanker regarding the first collision scenario.

Total Energy Absorbed - Volume of Damaged Material

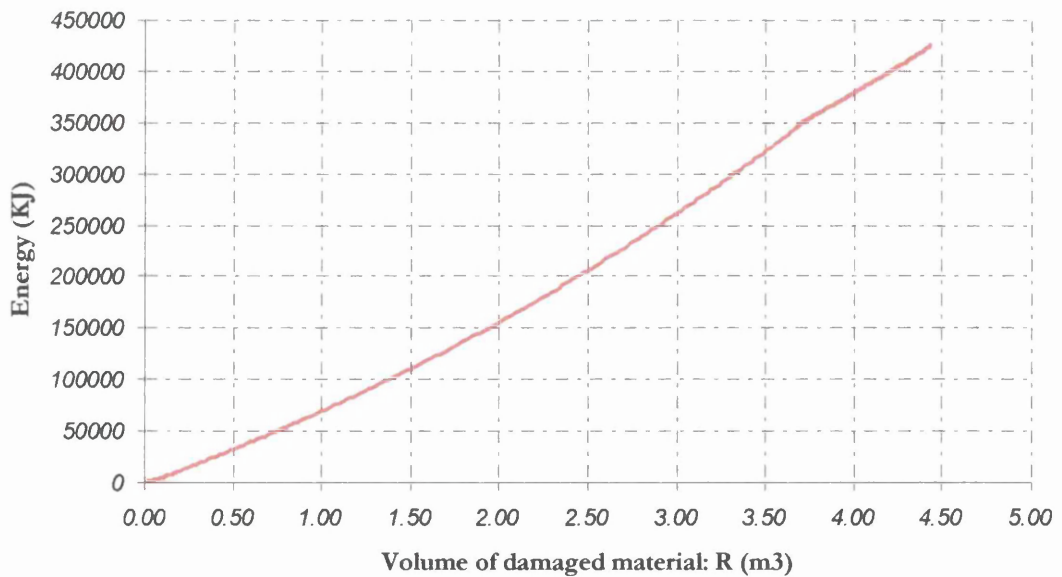


Figure 5.8: Total energy absorbed plotted against the volume of the damaged material. The outer and inner shell volume of damaged material has not been included in the calculations.

Energy Absorbed due to membrane tension on the outer side shell plating

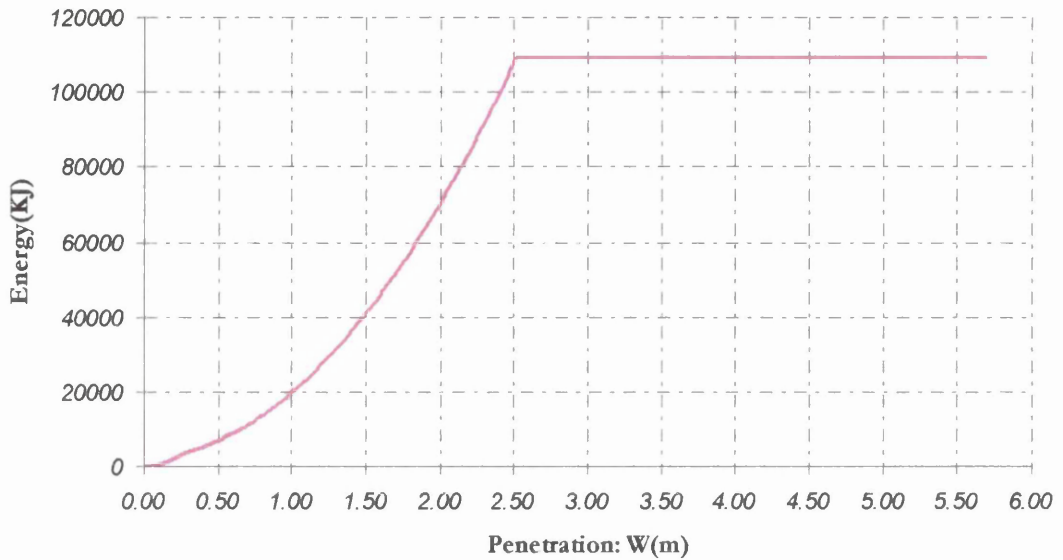


Figure 5.9: Energy absorbed due to membrane tension in the stiffened outer hull of the struck vessel.

Energy Absorbed due to membrane tension on the decks between the two hulls

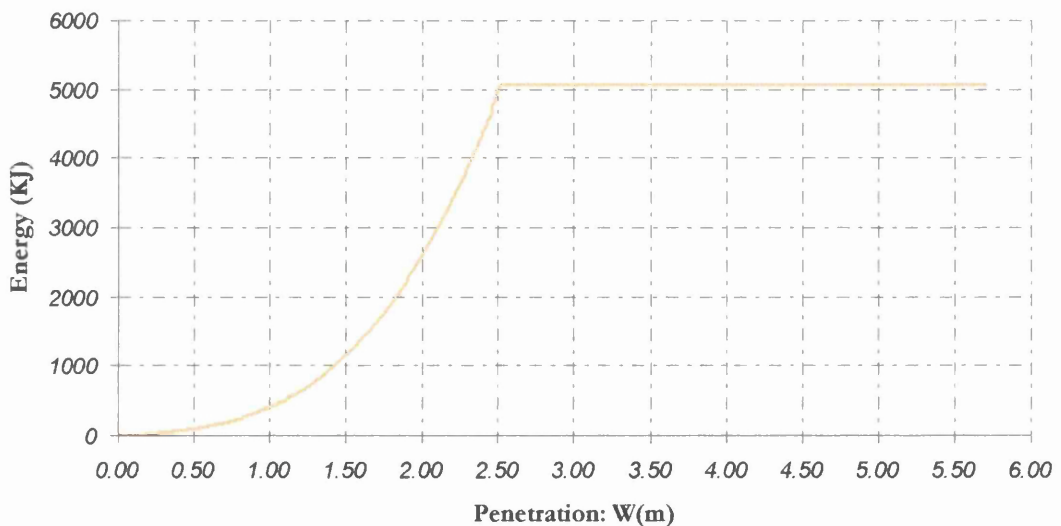


Figure 5.10: Energy absorbed due to membrane tension in the decks between the two hulls of the struck vessel.

Energy Absorbed due to buckling of the decks between the two hulls

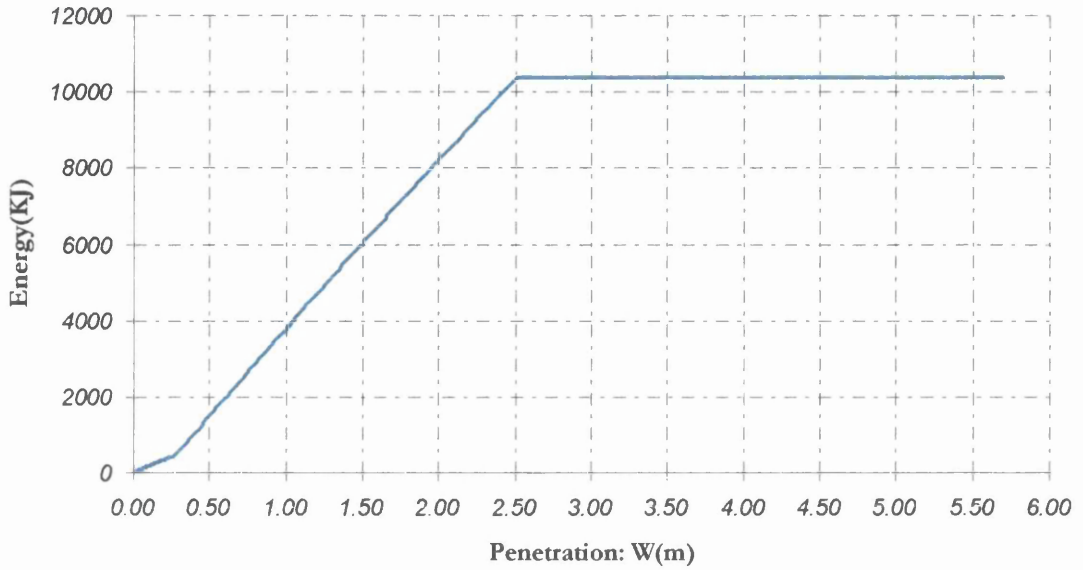


Figure 5.11: Energy absorbed due to the buckling of decks between the two hulls of the struck vessel.

Energy absorbed due to membrane tension on the bottom deck plating

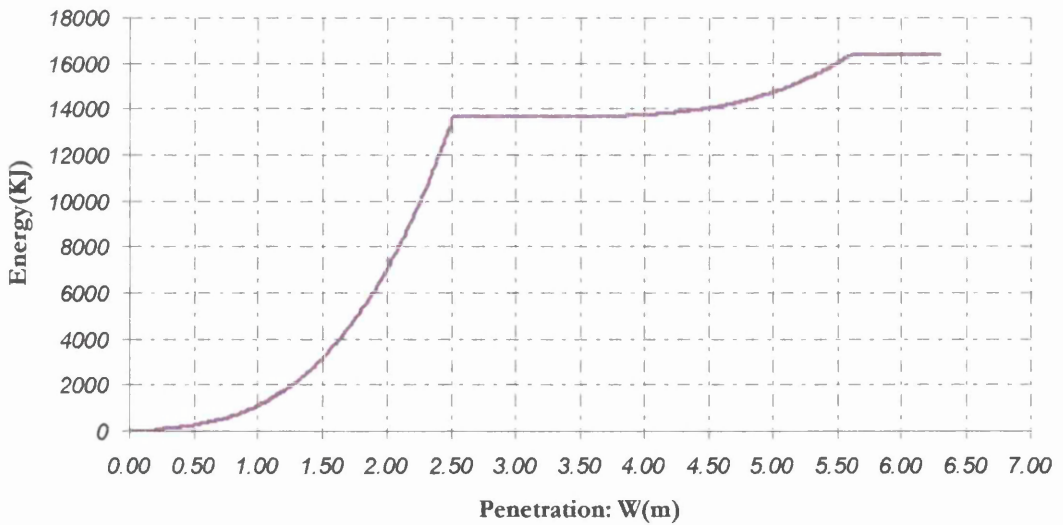


Figure 5.12: Energy absorbed due to membrane tension in the bottom plating of the struck vessel.

Energy Absorbed due to buckling of the bottom deck plating

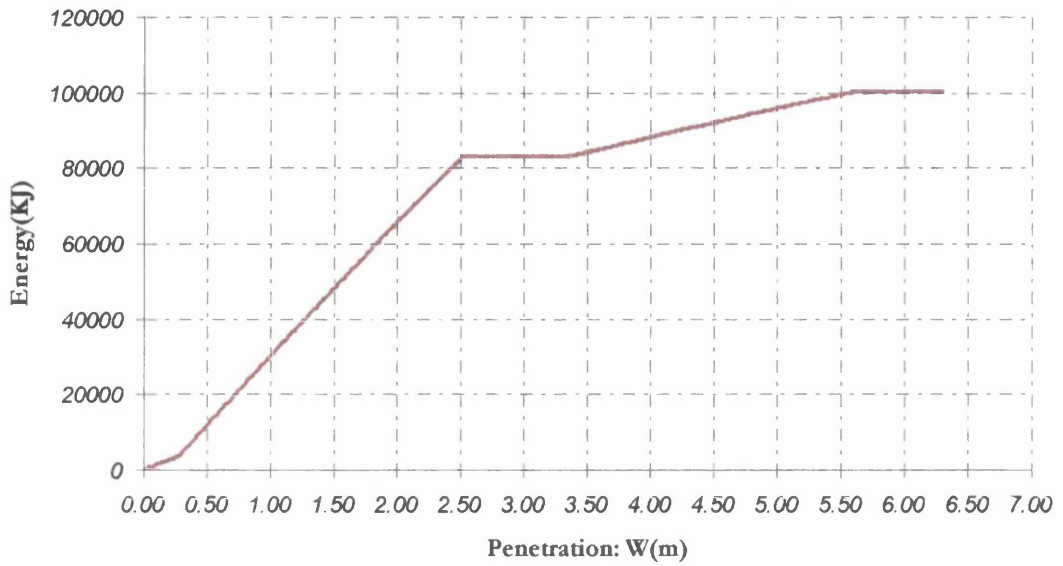


Figure 5.13: Energy absorbed due to buckling of the bottom plating of the struck vessel.

Energy Absorbed due to membrane tension on the inner bottom plating

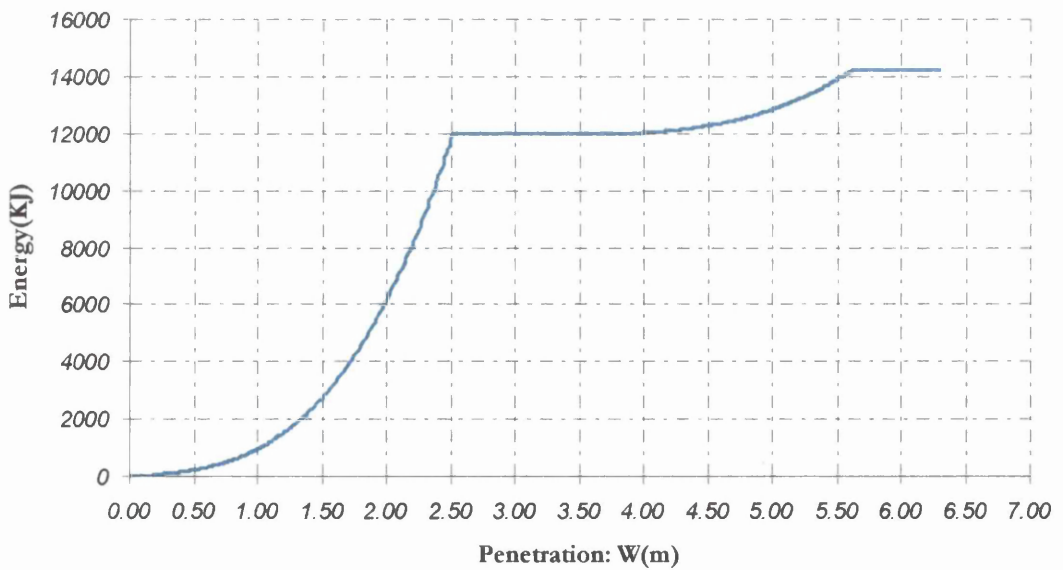


Figure 5.14: Energy absorbed due to the membrane tension on the inner bottom plating.

Energy Absorbed due to buckling of the inner bottom plating

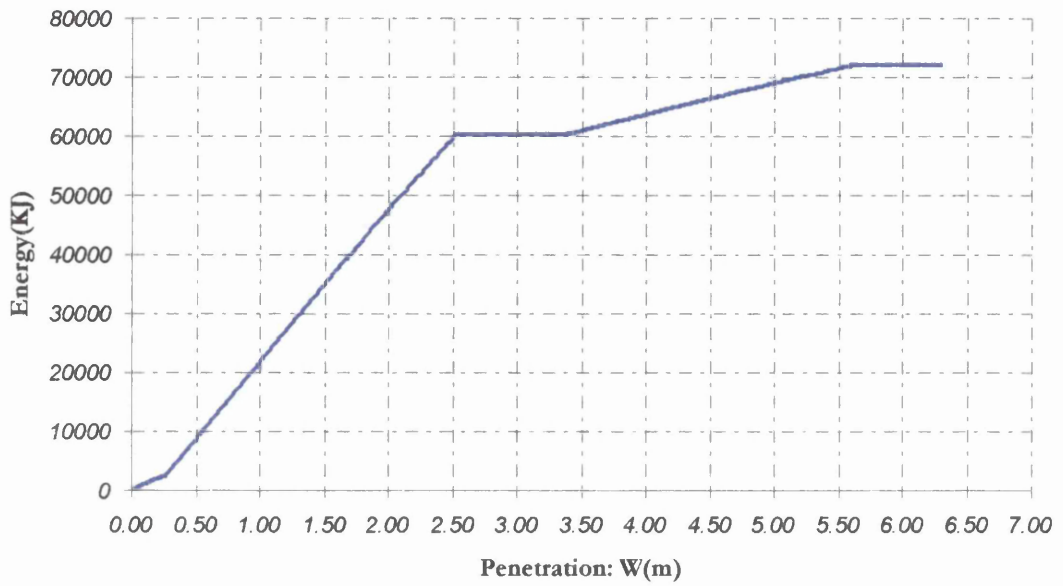


Figure 5.15: Energy absorbed due to buckling of the inner bottom plating of the struck vessel.

Energy Absorbed due to the Collapse of the bottom transverse

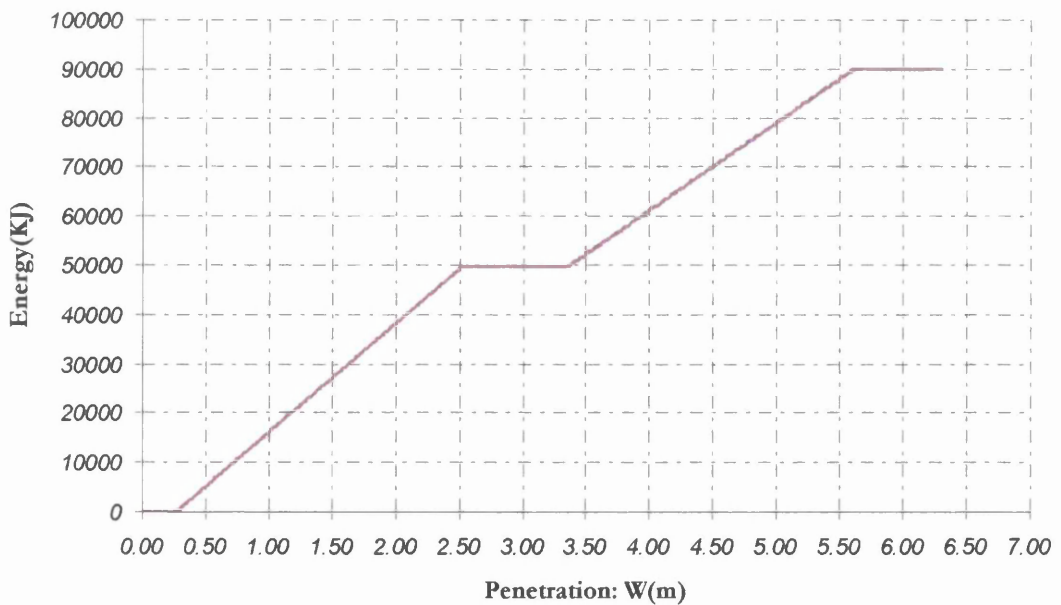


Figure 5.16: Energy absorbed due to the collapse of the bottom transverses flanking the strike.

Energy Absorbed due to membrane tension on the inner hull plating

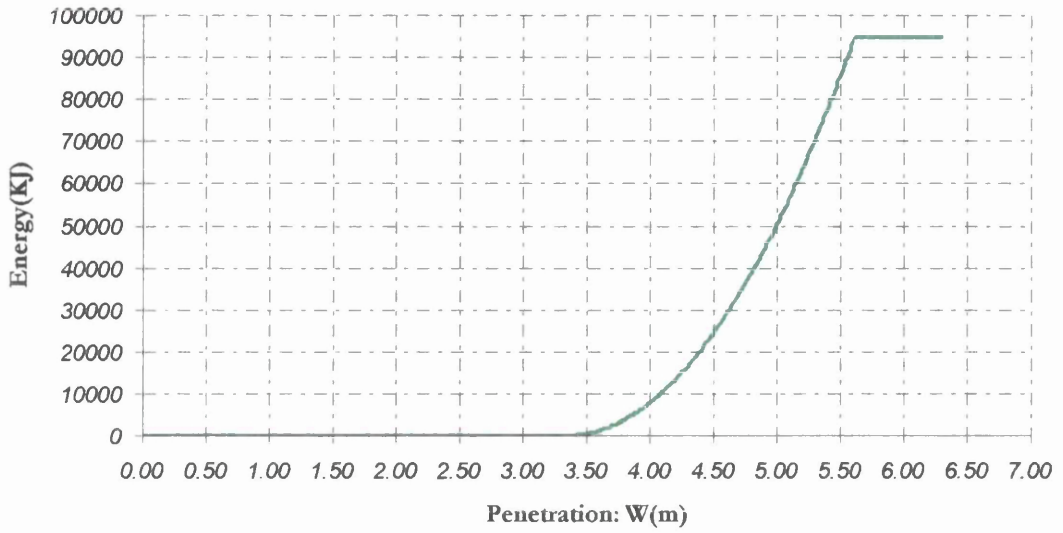


Figure 5.17: Energy absorbed due to membrane tension in the inner hull plating.

Energy Absorbed due to the wedge splitting of Decks

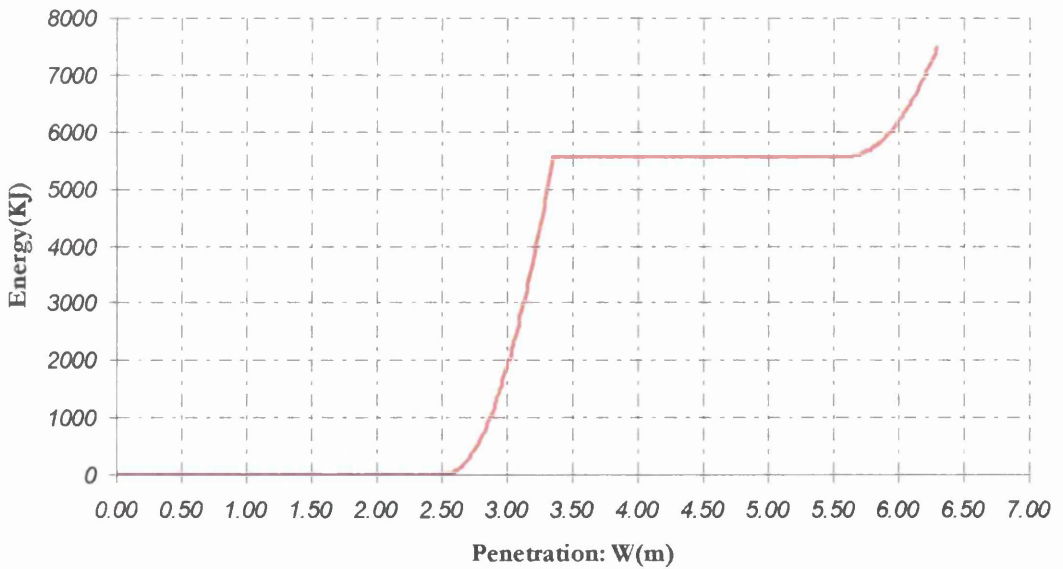


Figure 5.18: Energy absorbed due to the wedge splitting of decks (bottom and inner bottom plating as well as the two decks between double hull involved).

PART THREE: Double-skin tanker – Results for the Second Collision Scenario

Total Energy Absorbed - Second Collision Scenario

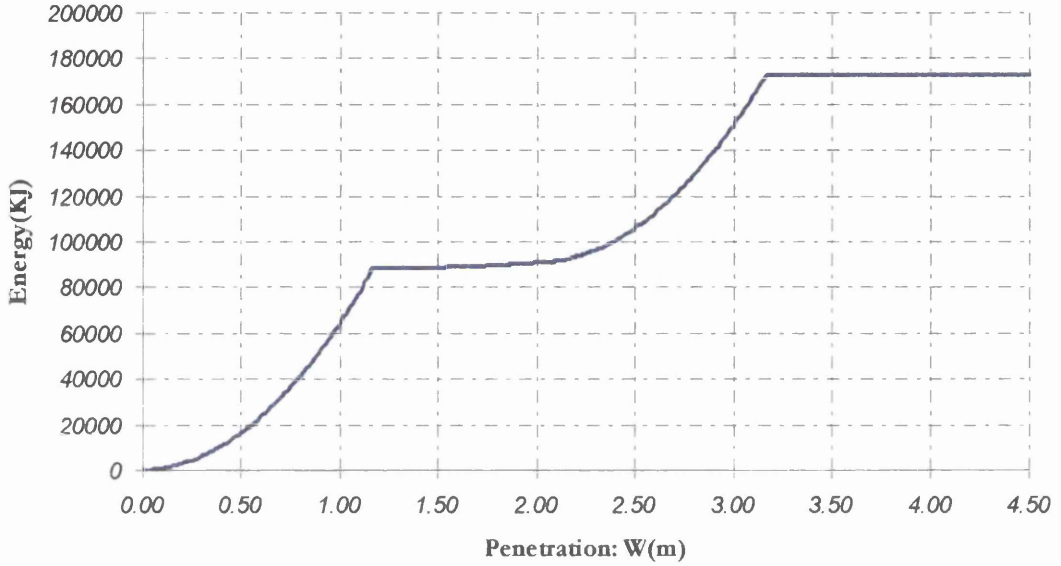


Figure 5.19: Total energy absorbed by the side structure of the double hull vessel plotted against the penetration depth.

Total Energy Absorbed - Volume of Damaged Material

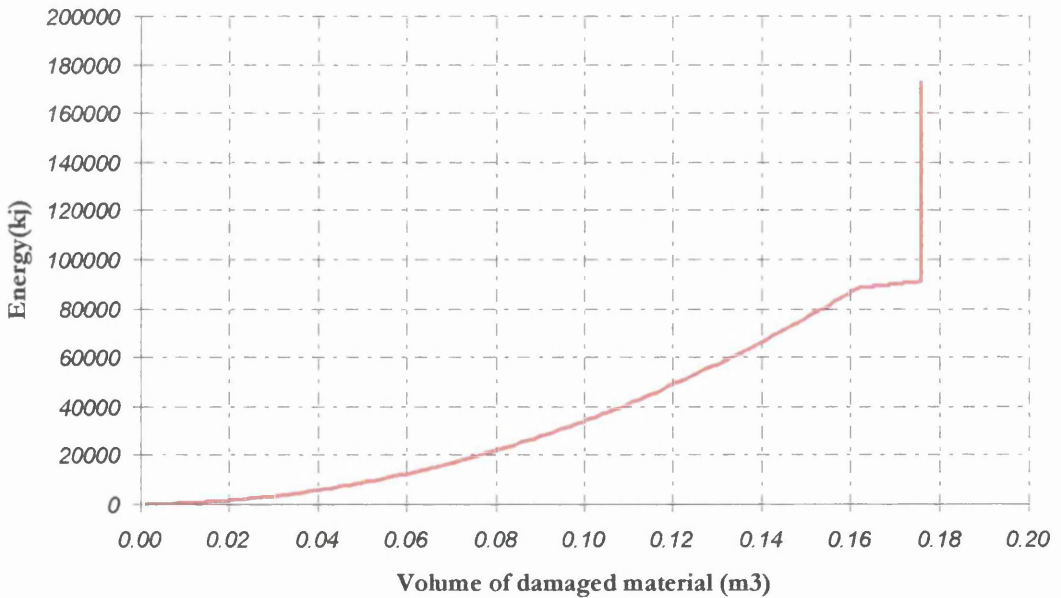


Figure 5.20: Total energy absorbed plotted against the volume of the damaged material. The volume of the inner and outer hull damaged material has been excluded the calculations, that is why for a constant amount of material energy is being further absorbed.

Energy Absorbed due to membrane tension on the outer side shell plating

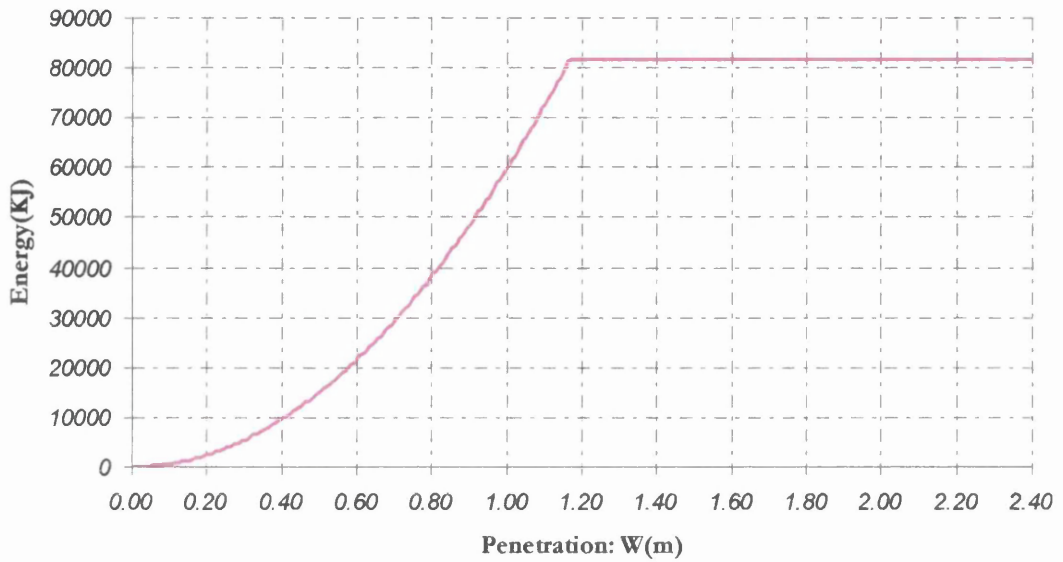


Figure 5.21: Energy absorbed due to membrane tension on the outer side shell plating.

Energy Absorbed due to membrane tension on the decks between the two hulls

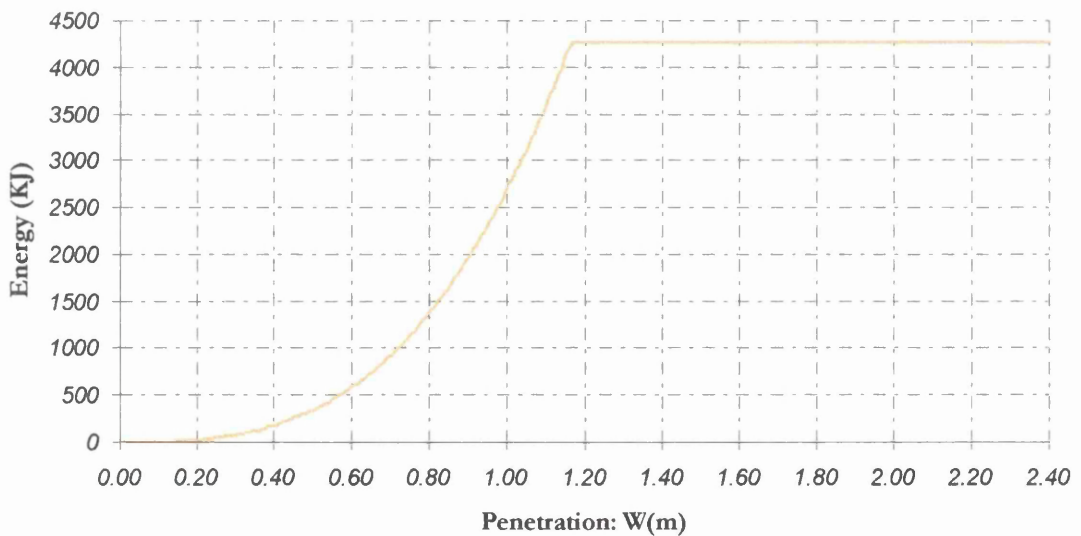


Figure 5.22: Energy absorbed due tot membrane tension on the decks between the two hulls.

Energy Absorbed due to buckling of the decks between the two hulls

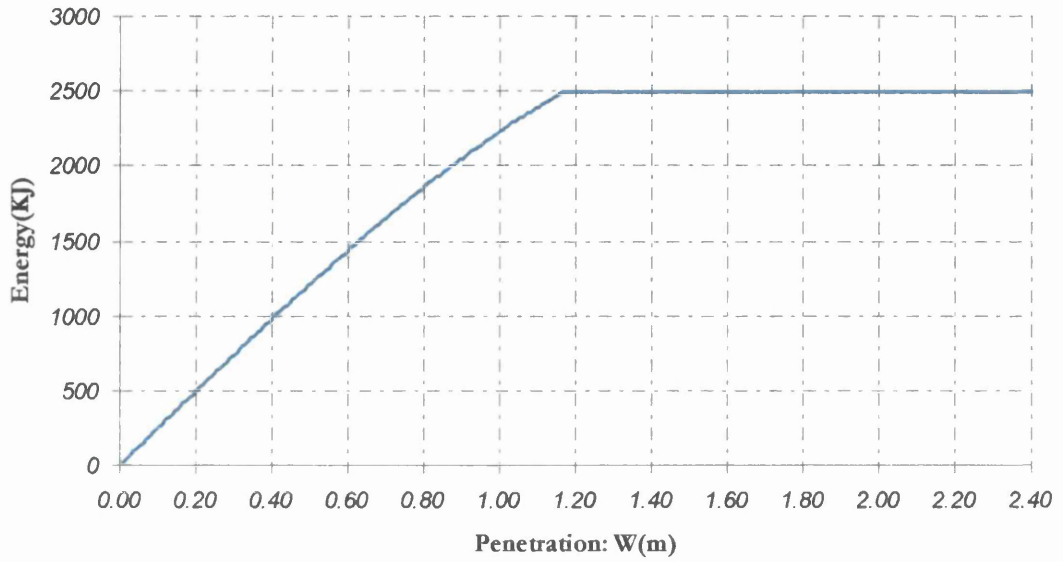


Figure 5.23: Energy absorbed due to the buckling of the decks between the two hulls.

Energy Absorbed due to membrane tension on the inner hull plating

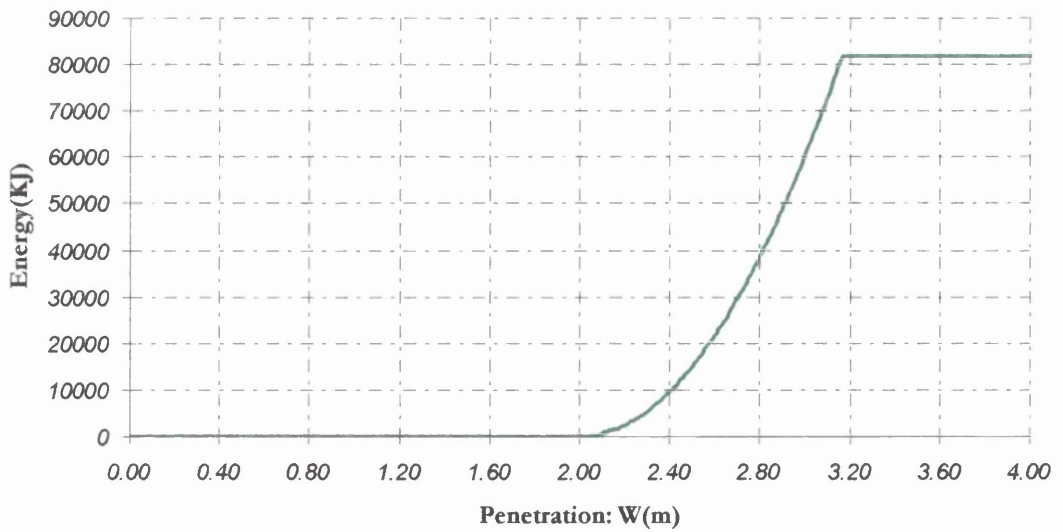


Figure 5.24: Energy absorbed due to membrane tension on the inner side shell plating.

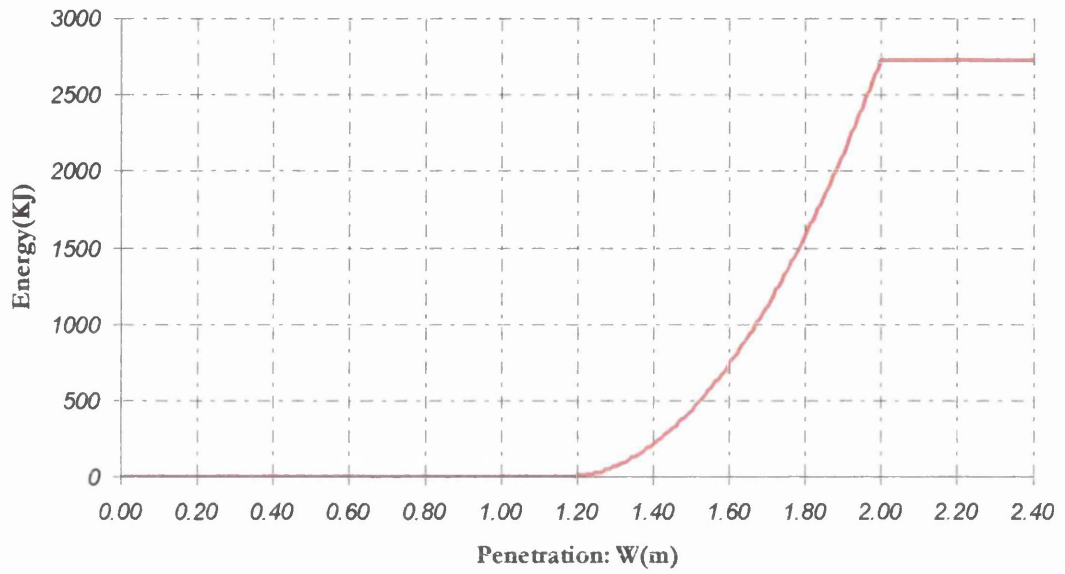
Energy Absorbed due to the wedge splitting of Decks

Figure 5.25: Energy absorbed due to wedge splitting of the decks between the two hulls.

PART FOUR: Double-skin tanker – Results for the Third Collision Scenario

Total Energy Absorbed - First Collision Scenario

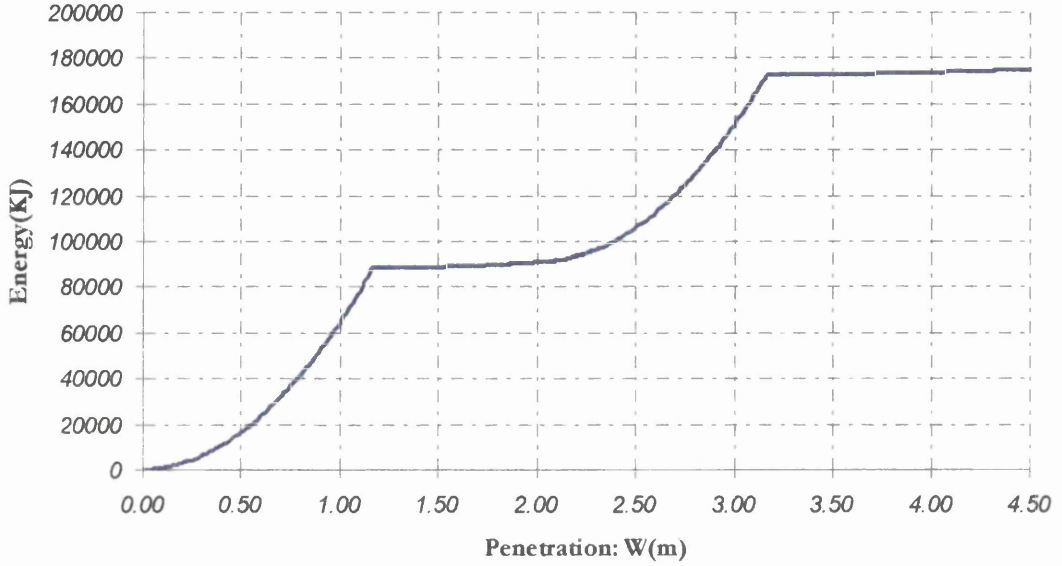


Figure 5.26: Total energy absorbed from the side structure of the struck vessel plotted against the penetration depth.

Total Energy Absorbed to the Volume of the Damaged Material

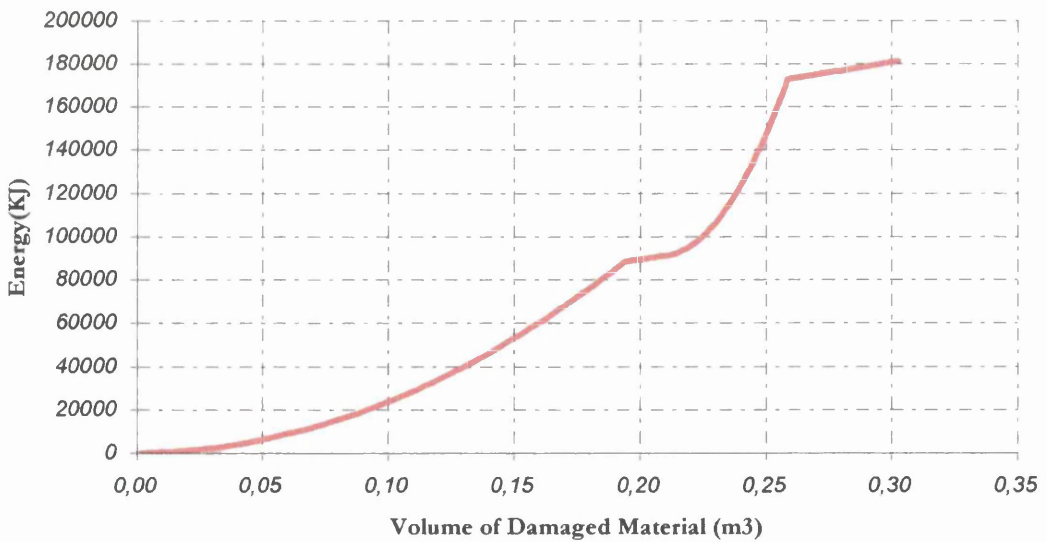


Figure 5.27: Energy absorbed plotted against the volume of the damaged material. Outer and inner shell material has been excluded in the calculation.

Energy Absorbed due to membrane tension on the outer side shell plating

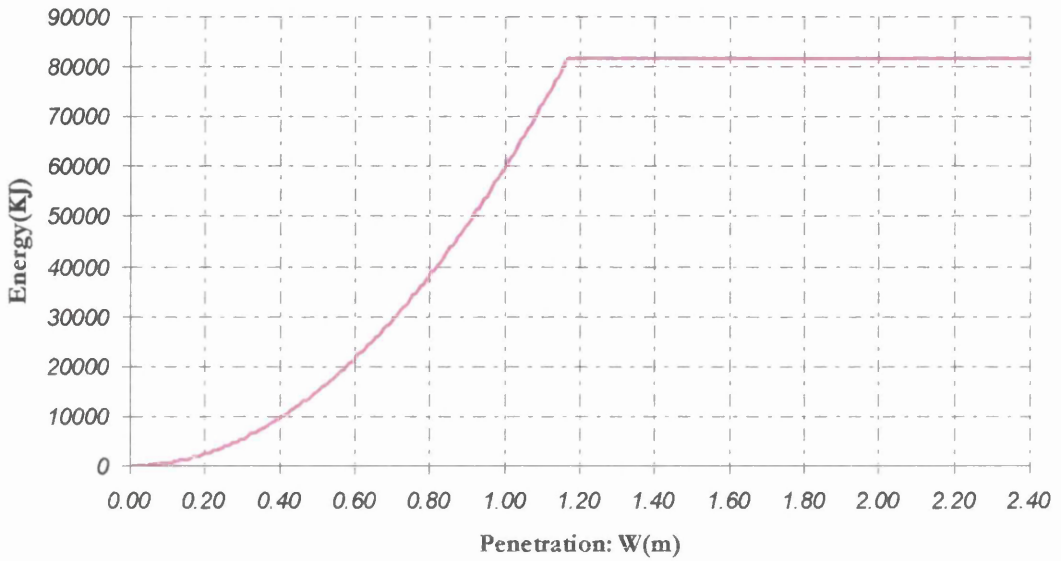


Figure 5.30: Energy absorbed due to membrane tension on the outer side shell plating.

Energy Absorbed due to membrane tension on the decks between the two hulls

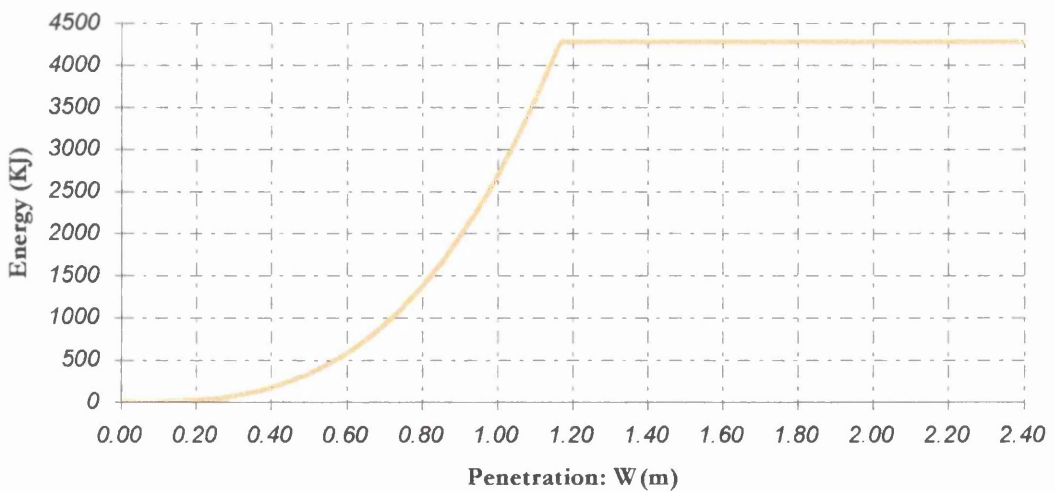


Figure 5.31: Energy absorbed due to membrane tension on the decks between the two hulls.

Energy Absorbed due to buckling of the decks between the two hulls

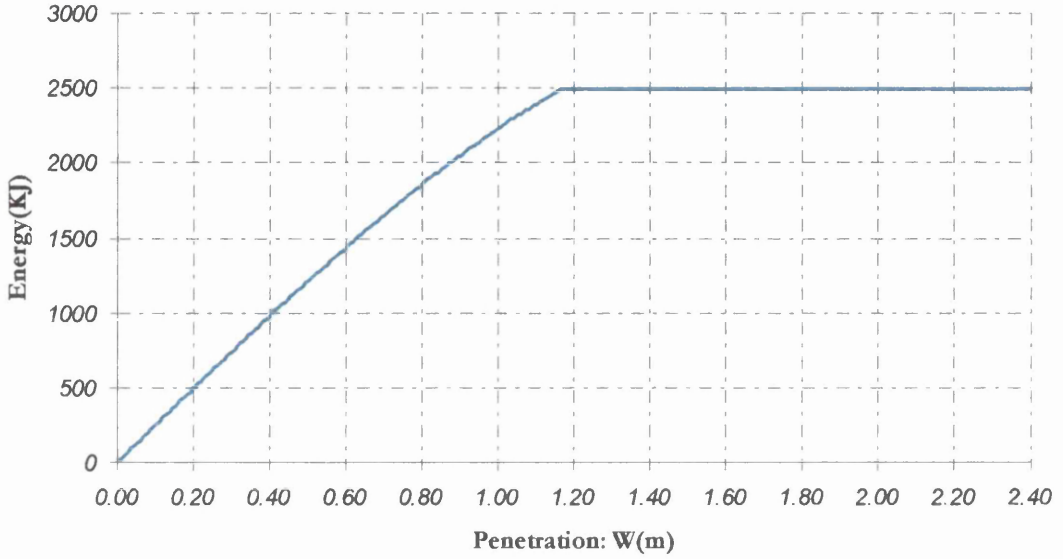


Figure 5.32: Energy absorbed due to buckling of the decks between the two hulls.

Energy absorbed due to membrane tension on the topside tank's bottom deck plating

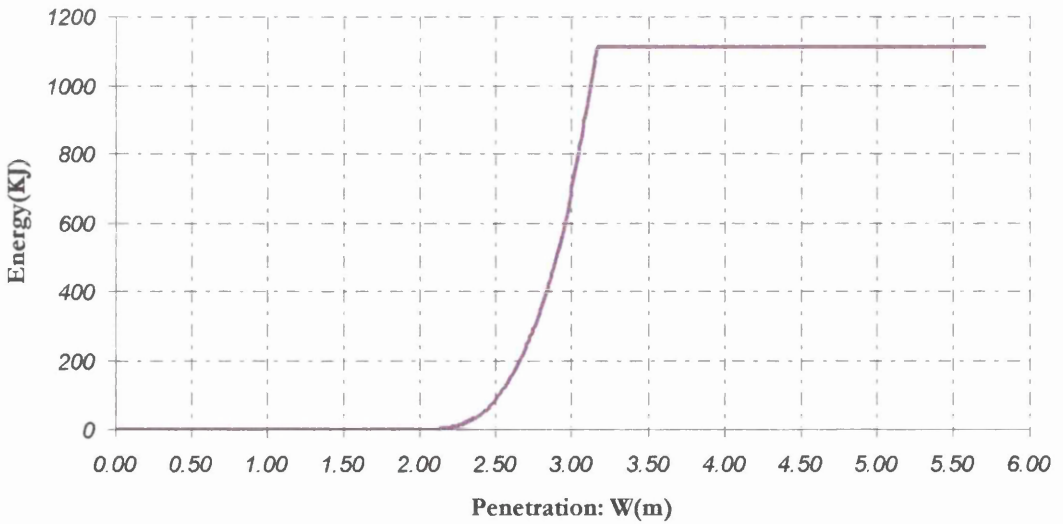


Figure 5.33: Energy absorbed due to membrane tension on the topside tank's bottom plating.

Energy Absorbed due to buckling of the topside tank's bottom deck plating

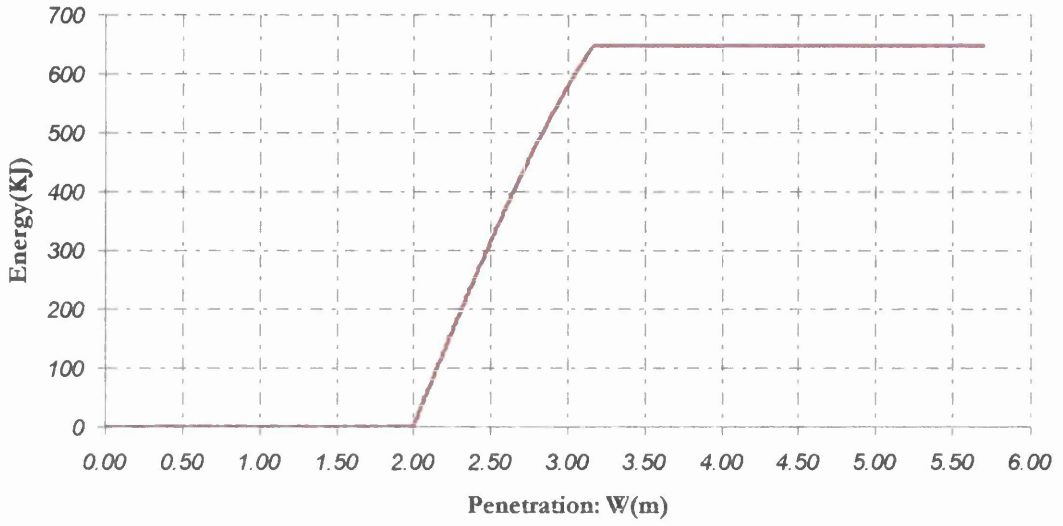


Figure 5.34: Energy absorbed due to the buckling of the topside tank's bottom plating.

Energy Absorbed due to membrane tension on the inner side shell plating

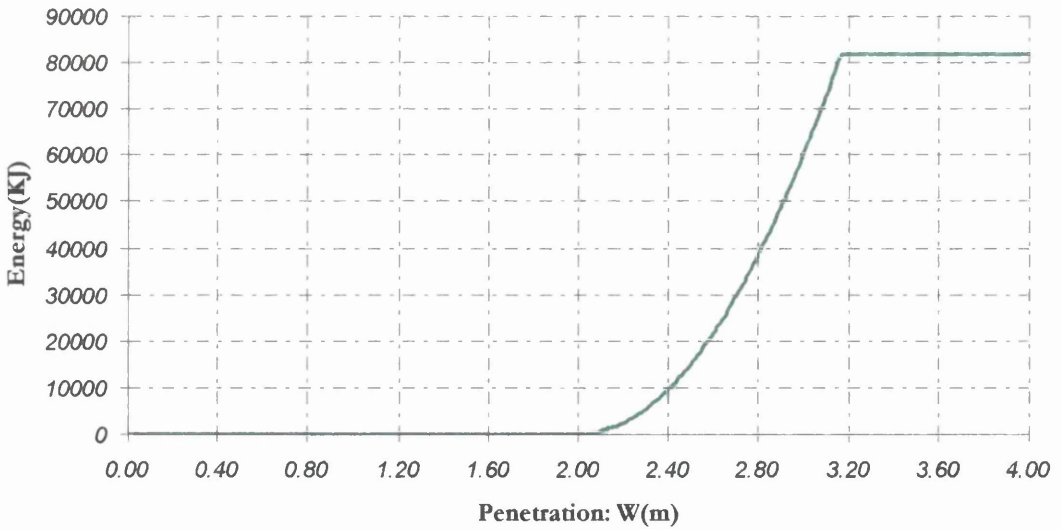


Figure 5.35: Energy absorbed due to membrane tension on the inner shell plating.

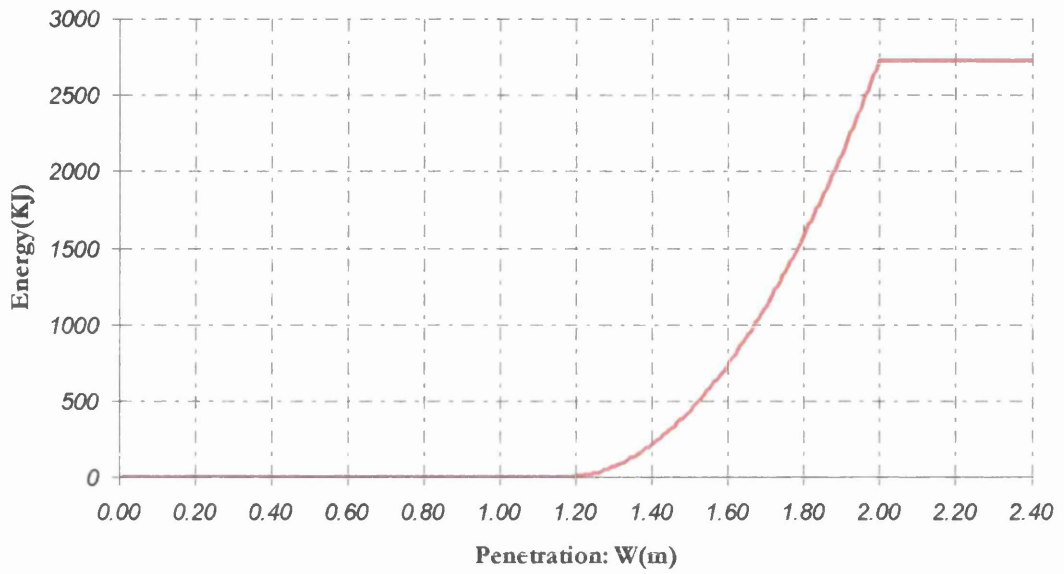
Energy Absorbed due to the wedge splitting of Decks

Figure 5.36 : Energy absorbed due to the wedge splitting of the decks between the two hulls as well as the topside tank's bottom plating.

PART FIVE: Double-skin tanker – Results for the Fourth Collision Scenario

Total Energy Absorbed - Fourth Collision Scenario

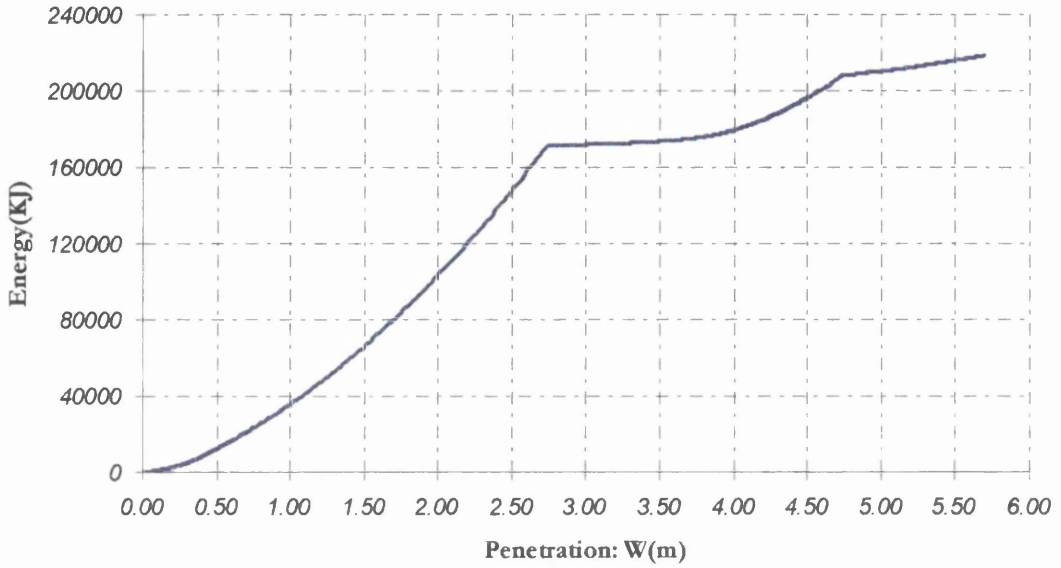


Figure 5.37: Total energy absorbed from the side structure of the struck vessel plotted against the penetration depth.

Total Energy Absorbed - Volume of Damaged Material

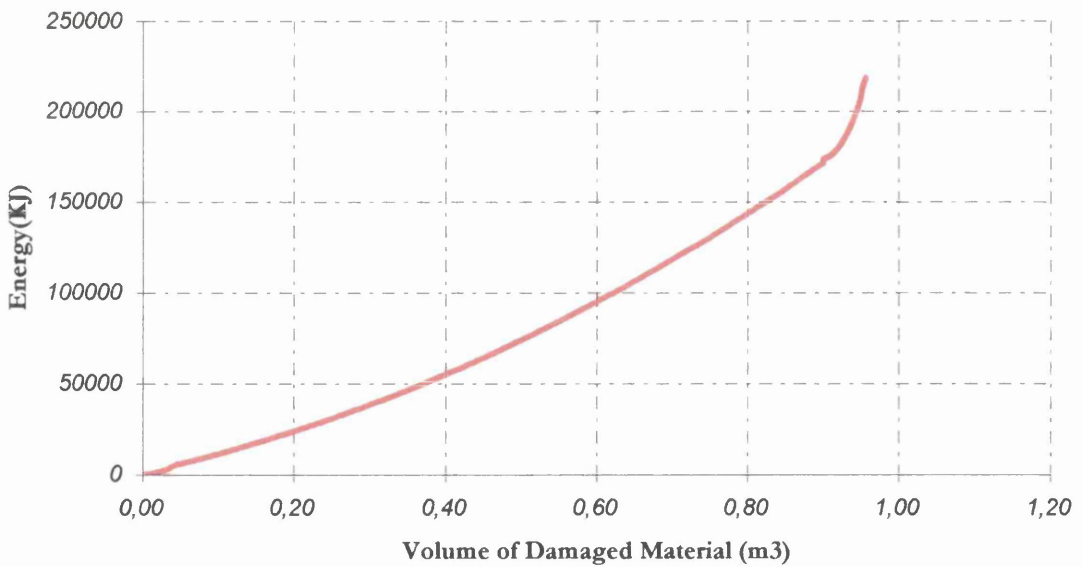


Figure 5.38: Total energy absorbed plotted against the volume of the damaged material. The outer and inner shell volumes of damaged material have not been taken into account.

Energy Absorbed due to membrane tension on the outer side shell plating

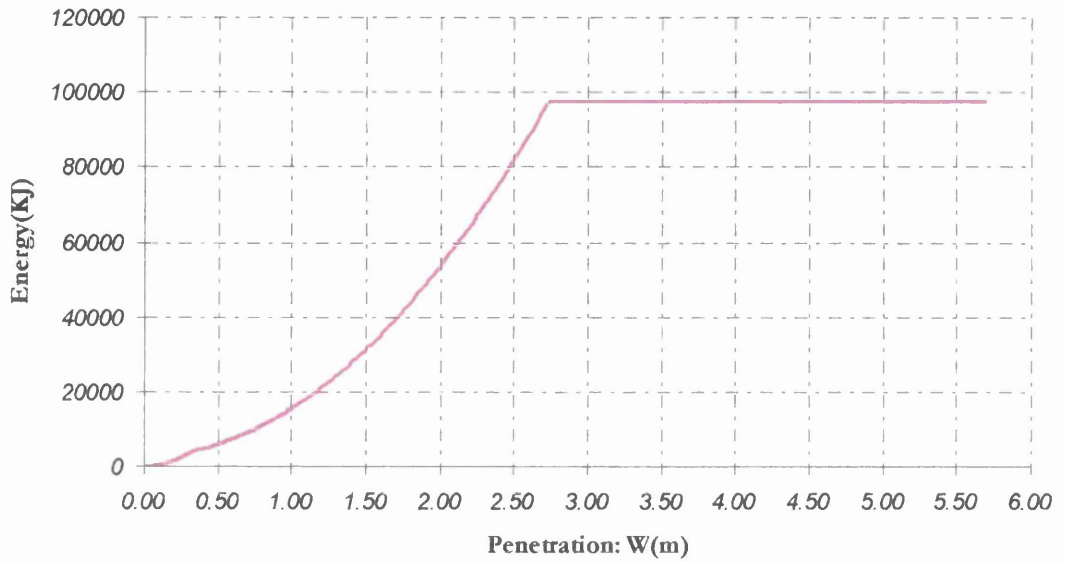


Figure 5.39: Energy absorbed due to membrane tension on the outer shell plating.

Energy Absorbed due to membrane tension on the deck between the two hulls

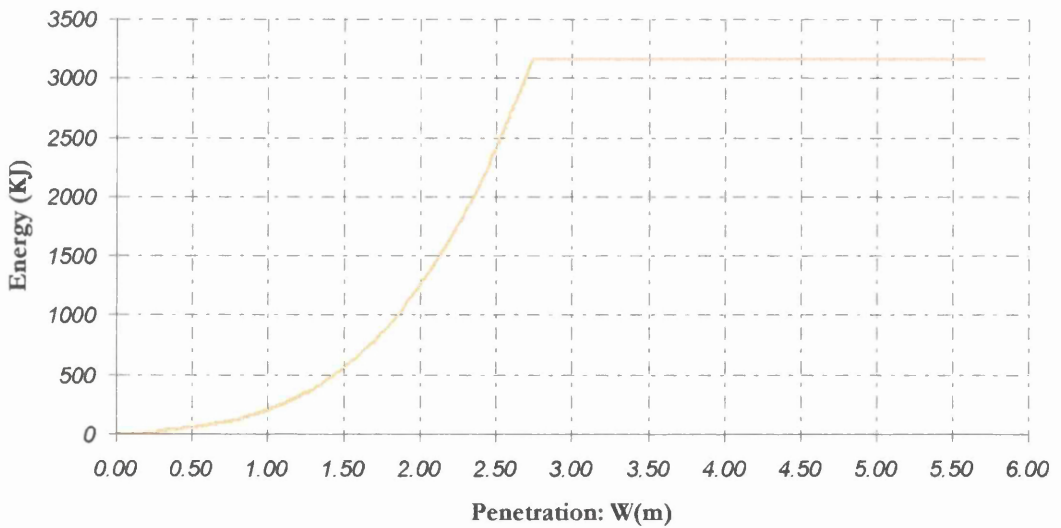


Figure 5.40: Energy absorbed due to membrane tension on the deck between the two hulls.

Energy Absorbed due to buckling of the deck between the two hulls

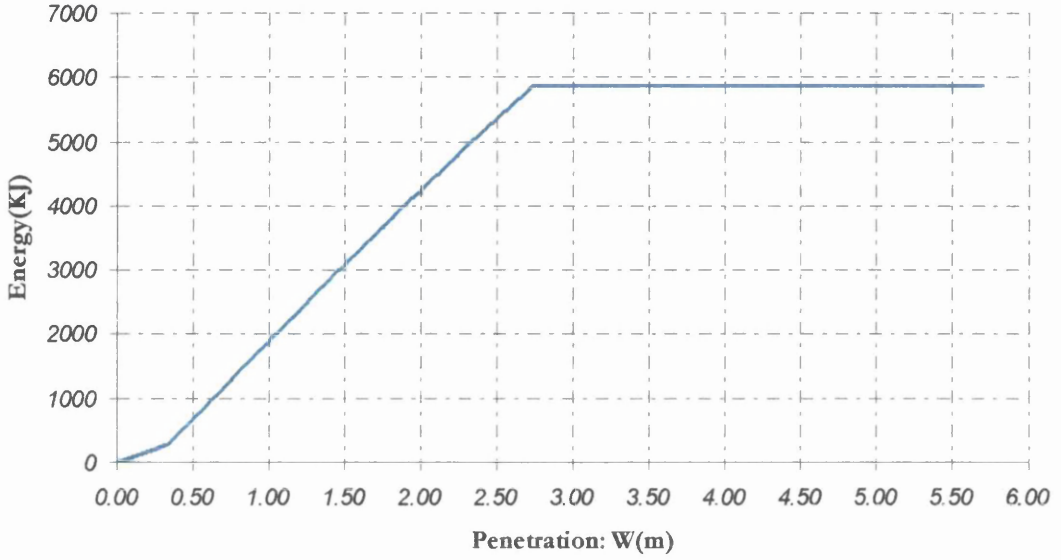


Figure 5.41: Energy absorbed due to buckling of the deck between the two hulls.

Energy absorbed due to membrane tension on the main deck plating

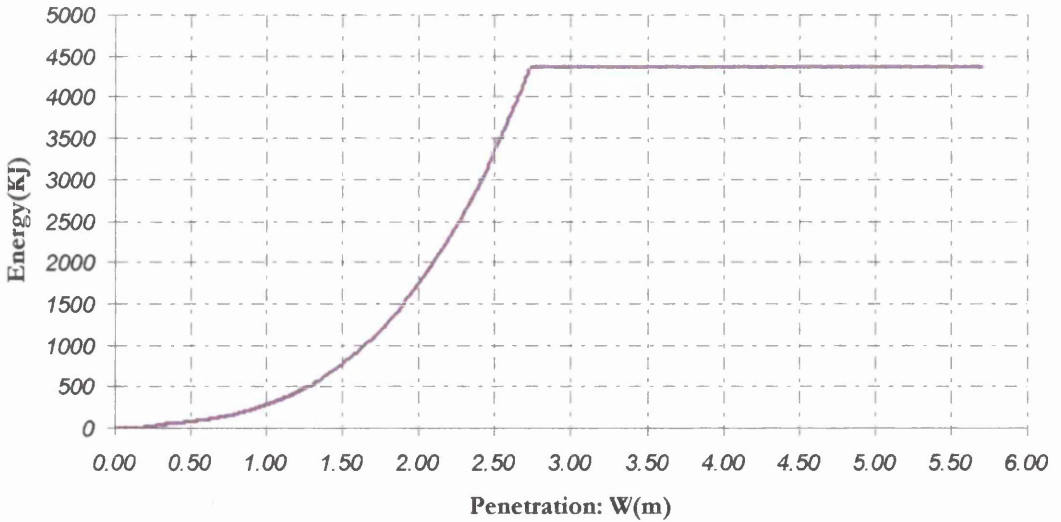


Figure 5.42: Energy absorbed due to membrane tension on the main deck plating.

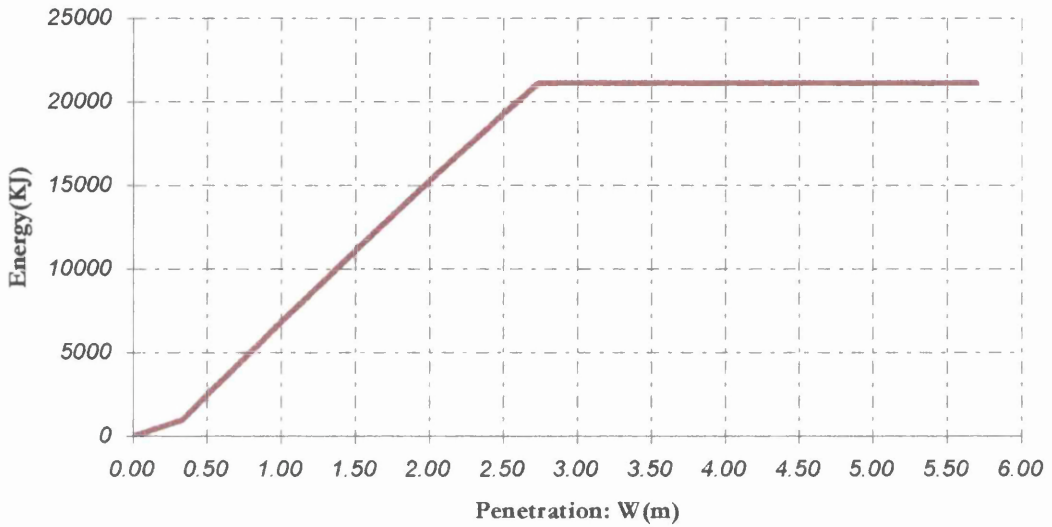
Energy Absorbed due to buckling of the main deck plating

Figure 5.43: Energy absorbed due to buckling of the main deck plating.

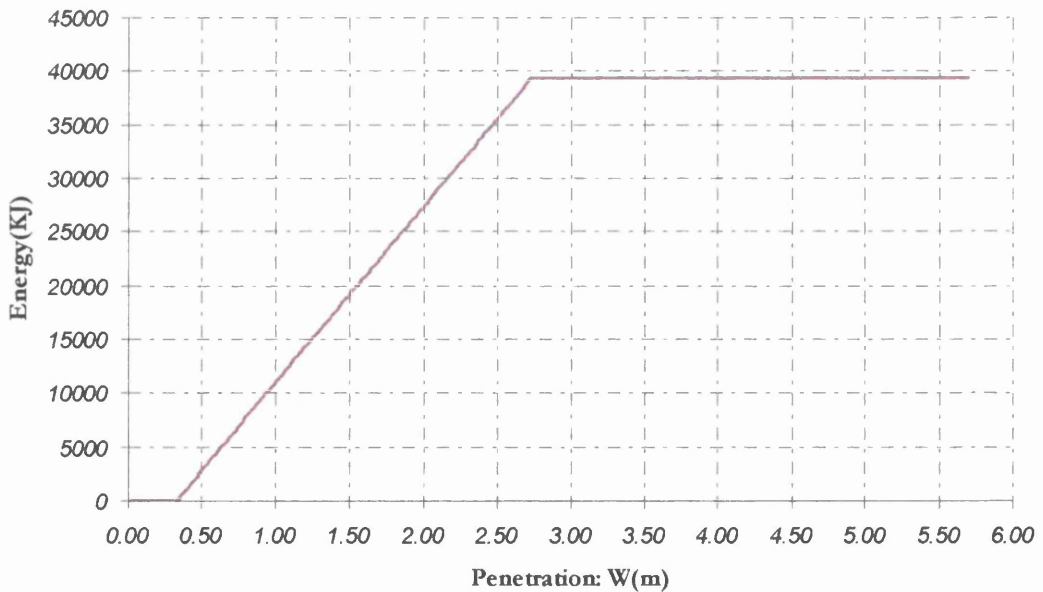
Energy Absorbed due to the Collapse of the main deck transverse

Figure 5.44: Energy absorbed due to the collapse of the main deck's transverses.

Energy Absorbed due to membrane tension on the inner hull plating

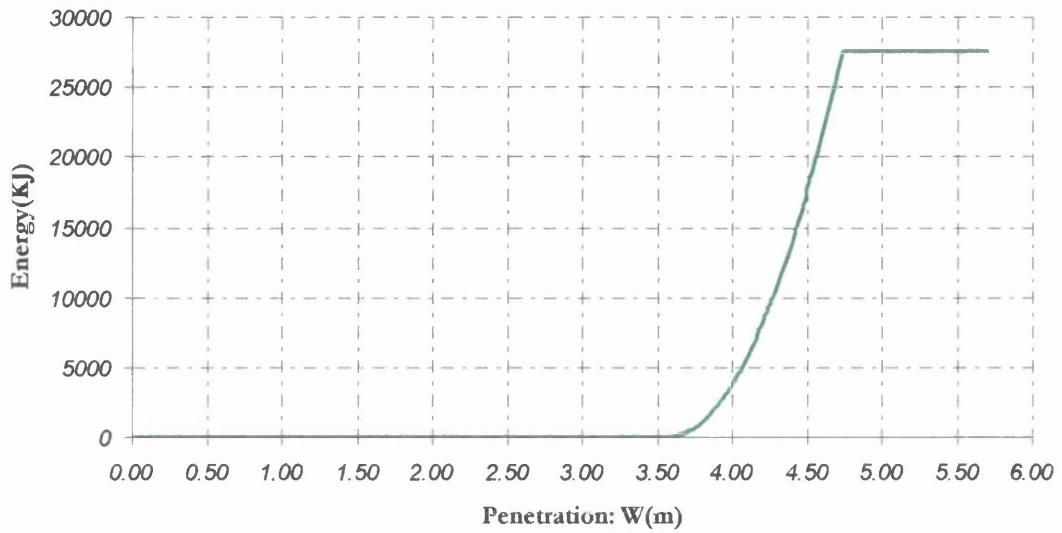


Figure 5.45: Energy absorbed due to membrane tension on the inner hull plating.

Energy Absorbed due to the wedge splitting of Decks

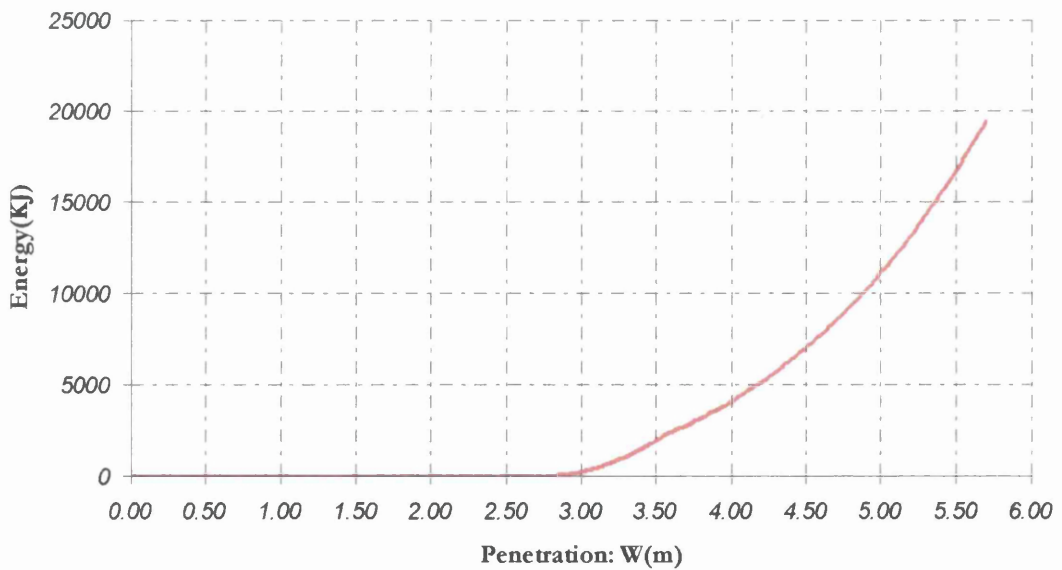


Figure 5.46: Energy absorbed due to the wedge splitting of main deck plating, deck between the two hulls and topside tank's bottom plating.

Chapter 6

Estimation of the Crashworthiness of a Single Hull Tanker

Introduction

The estimation of the energy absorbed from a double-skinned tanker was the subject of the previous chapter. Results were produced and discussed from the view of internal collision mechanics.

The double-hull tankers have been questioned regarding their structural integrity. Cracks have been developing and propagating specially in the double bottoms of these structures from the early stages of their service life. A good question then would be, how are they doing with energy absorption during collision? Thus, it was found a good idea to compare a double-hull vessel with a single-hull vessel having the same principal dimensions. It was not feasible to run a search for an existing single hull tanker, so it was decided to derive the single-hull vessel through preliminary design methods. The principal dimensions of the shuttle tanker were used to calculate the mid-ship section of the single hull one. The calculations of the bending moments and shear forces were conducted using ABS and Lloyd's formulae. The thickness and scantlings of stiffeners calculations were carried out using ABS equations, because a later edition of these rules was available. Further, the mid-ship section was accomplished and calculation of its properties (neutral axis, section modulus) took place.

Finally, the method by Hegazy was applied on the single-skinned tanker to calculate the energy absorption capacity of the vessel. Results are compared and discussed, with those derived for the double-skin tanker, at the end of this chapter.

6.1 Single-skin tanker

The form of the mid-ship section of the single hull design was assumed similar with two other conventional tanker designs that we had in hand. The shape proposed is shown in Figure 6.1. As it can be seen it is a single shell and single bottom design. The characteristics of the vessel that were calculated are the following:

- Required Section Modulus
- Frame Spacing
- Web Frame Spacing

The structural members, of which the scantlings were calculated, are the following:

- Bottom Shell Plating
- Keel Plating
- Side Shell Plating
- Shearstrake
- Deck Plating
- Center Girder
- Side Girders
- Bottom Plating Stiffeners
- Deck Plating Stiffeners
- Side Shell Stiffeners

- Transverse Frames
- Web frames
- Deck Transverse
- Bottom Transverse

The calculations of the scantlings, the choices of the stiffeners, and the calculation of the properties of the mid-ship section are shown in Appendix A.

6.2 Application of the proposed method

The method proposed by Hegazy can be easily applied to a design like the developed single-skin tanker. The configuration of this design fits quite good the simplified model presented in the method. The only difficulty is the difference between the collapse load of the main deck's and bottom's transverses.

Four collision scenarios were assumed as in the previous chapter. The scenarios along with the damage height at each case are shown in Figures 6.2 to 6.5.

Graphs have been produced plotting the total energy absorbed by the side structures as well as the energy absorbed from each individual structural member against the penetration.

6.3 Results and Conclusions

First Collision Scenario:

The struck vessel is in ballast condition and the striking vessel in full load condition. The damage height is 12.050 m, measured from the keel. The structural members involved in the damage are:

- bottom plating
- bottom transverse
- side transverse

The sequence of phenomena occurring after the engagement of the side shell plating by the striking bow is:

1. The outer hull loads in membrane tension. The bottom plating loads in membrane tension and in buckling.
2. The side transverses flanking the strike collapse.
3. Rupture of the hull occurs and the striking bow tears the bottom plating.

The bottom transverses flanking the strike do not collapse before the rupture of the hull. This fact yields to the following assumption: The damage is confined in one bay, because the deck and bottom transverses, which remain intact, provide a strong boundary to the side shell plating. The yield of the side transverses results in an increase of the energy absorbed.

The results for this scenario are presented in Figures 6.6 to 6.13. The total energy absorbed up to the rupture of the side shell plating is $E_{\text{minor}} = 291425$ KJ. The maximum penetration at the instant of the hull rupture is $W_{\text{LMAX}} = 3.280$ m.

Second and Third Collision Scenario:

Second Scenario: The struck vessel is in ballast condition and the struck vessel in ballast condition. The damage height is 15.000 m. The damaged area is from 2.650 meters above keel to 17.650 m above keel. The structural members suffering damage are:

- side transverses
- side shell plating

The sequence of phenomena occurring is very simple:

1. The side shell plating loads in membrane tension.
2. The side transverses flanking the strike collapse.
3. The side shell plating ruptures and the striking bow enters the cargo tank with no further resistance.

The third scenario for this vessel is exactly the same as the second one. The damage height is 15.000 m. The damaged area begins at 6.050 m above keel to 0.800 m below the main deck plating. The structural members involved are the same as in the second scenario and so is the sequence of phenomena.

The results are presented in Figures 6.11 to 6.15. The total energy absorbed up to the rupture of the side shell plating is $E_{\text{minor}} = 120117$ KJ. The maximum penetration just prior to the rupture of the hull is $W_{\text{LMAX}} = 1.394$ m.

Fourth Collision Scenario:

The struck vessel is in full load condition and the striking vessel in ballast condition. The damage height is 9.450 m. The damaged area is from 11.650 meters above keel to the main deck (main deck included). The structural members involved in the damage are:

- main deck plating

- side shell plating
- deck transverses
- side transverses

The deck transverses flanking the strike do not collapse. The damage is confined in one bay. The sequence of phenomena is as the first collision scenario if the bottom plating is substituted with the main deck plating.

The results for this case are shown in Figures 6.16 to 6.20. The total energy absorbed up to the rupture of the hull is $E_{\text{minor}} = 83765$ KJ. The maximum penetration at the instant of hull rupture is $W_{\text{LMAX}} = 1.394$ m.

The results are presented in the table below. The larger amount of energy was absorbed when the damage height was the greater one. This means that the membrane tension in the side shell plating plays a dominant role in the energy absorption capacity. In none of the scenarios the deck transverses flanking the strike collapsed. This fact kept the limiting penetration, beyond which rupture of the hull occurs, constant throughout the four cases.

	Total Energy Absorbed just prior to the rupture of the hull, E_{minor}	Penetration depth at the instant of the hull rupture, W_{LMAX}
First Collision Scenario	291425 KJ	3.280 m
Second and Third Collision Scenario	120117 KJ	1.394 m
Fourth Collision Scenario	255683 KJ	3.310 m

	First Collision Scenario	Second and Third Collision Scenario	Fourth Collision Scenario
Volume of Damaged Material (m ³)	5.645 m ³	2.351 m ³	5.045 m ³

6.4 Comparison of the Crashworthiness of the double and single – skin tankers

The table below gives the values of the energy absorbed and maximum penetration up to the rupture of the hull obtained for the two tankers. The principal dimensions of the two vessels are the same as it has been already mentioned.

		Energy absorbed prior to the rupture of the hull, E_{minor}	Penetration depth at the instant of hull rupture, W_{LMAX}
First Collision Scenario	Double-Skin	423187 KJ	5.630 m
	Single-Skin	291425 KJ	3.280 m
Second Collision Scenario	Double-Skin	172740 KJ	3.166 m
	Single-Skin	120117 KJ	1.394 m
Third Collision Scenario	Double-Skin	171822 KJ	3.166 m
	Single-Skin	120117 KJ	1.394 m
Fourth Collision Scenario	Double-Skin	208238 KJ	4.780 m
	Single-Skin	255683 KJ	3.310 m

The double hull design in three of the cases absorbs quite larger amounts of energy before the rupture of its inner hull. The single hull tanker absorbs quite large amounts of energy in most of the cases and in the fourth collision scenario it overcomes the energy absorbed by the double-hull. This is due to the strong main deck transverse that exist in the single hull structure and the increased thickness of the main deck plating, which are required for the integrity of the structure. The double-skin tanker has a very strong double-bottom structure, which provides a huge resistance to the penetrating bow.

It can be seen that if the fourth collision scenario would occur, the single-skin tanker would require more energy from the striking bow up to the rupture of its hull. On the other hand, in all the other scenarios the double-skin tanker has undoubtedly an advantage against the single-skin tanker.

List of Figures

PART ONE: Single Hull Tanker development

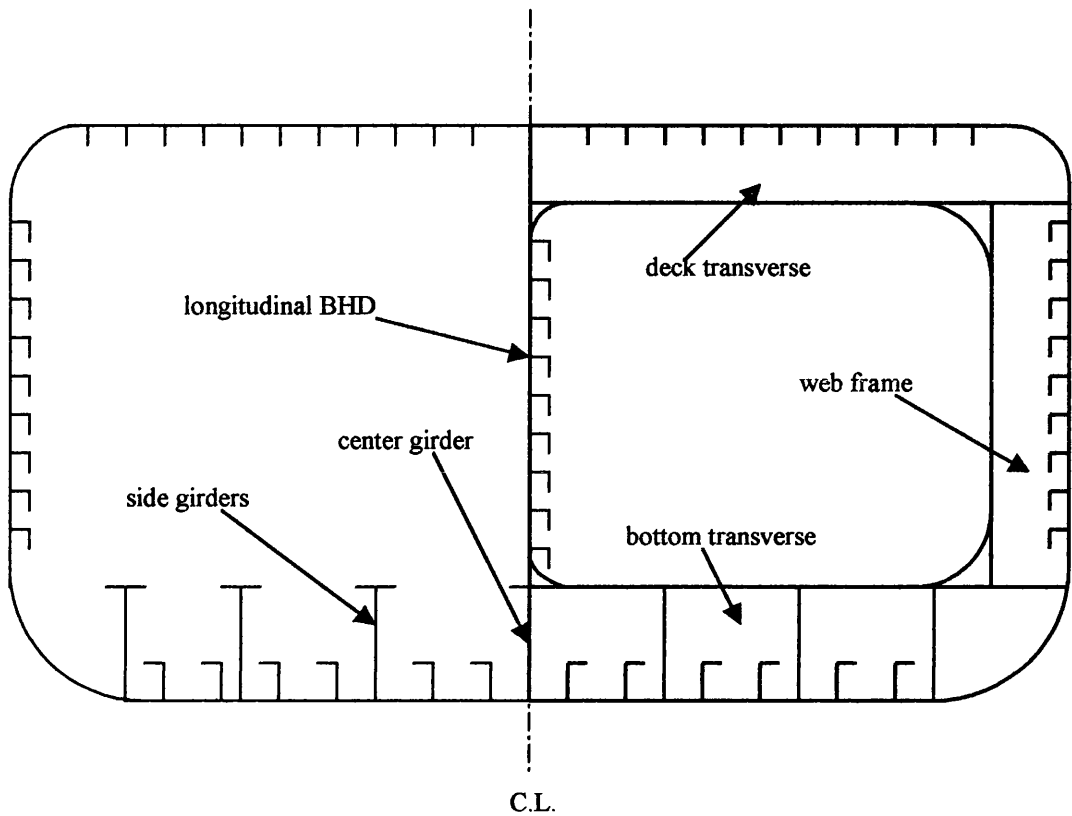


Figure 6.1: This figure illustrates the mid-ship section of the developed single hull tanker along with definitions of some of the crucial structural members in terms of collision damage.

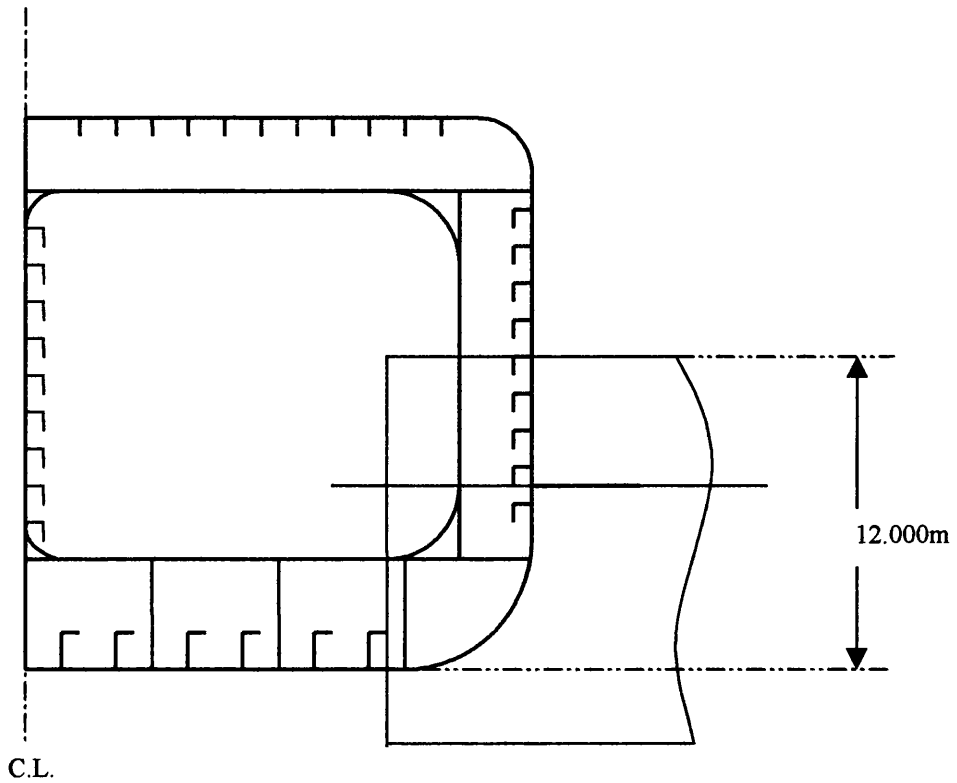


Figure 6.2: First assumed collision scenario: Struck vessel in Ballast Condition. Striking Vessel in Full Load Condition. The damage height is also shown.

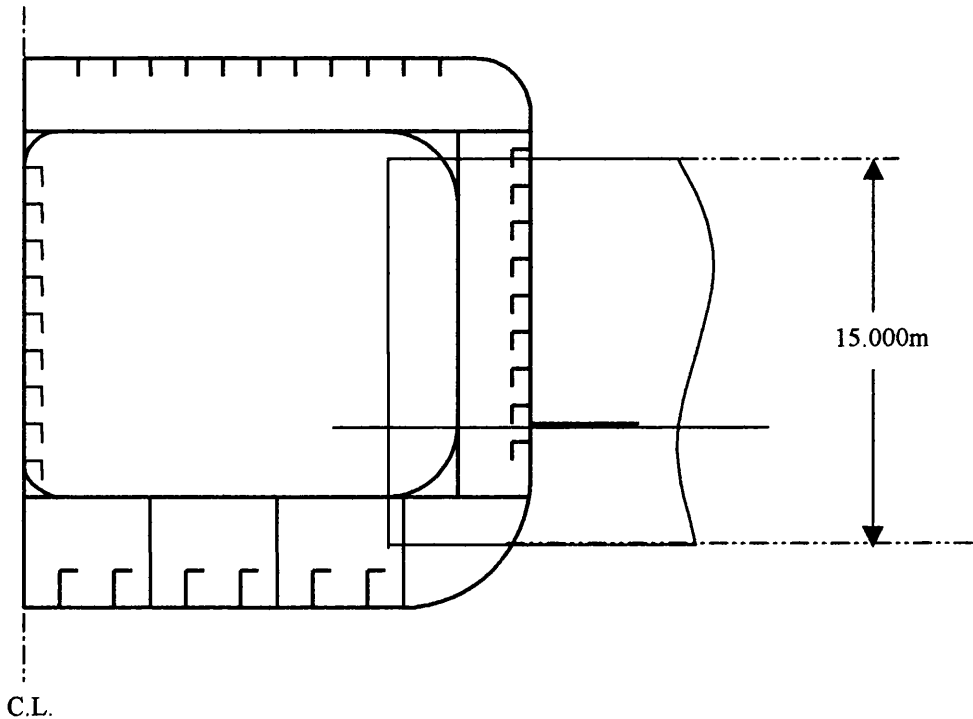


Figure 6.3: Second assumed collision scenario: Struck vessel in Ballast Condition. Striking vessel in Ballast Condition. The damage height equals the depth of the striking ship.

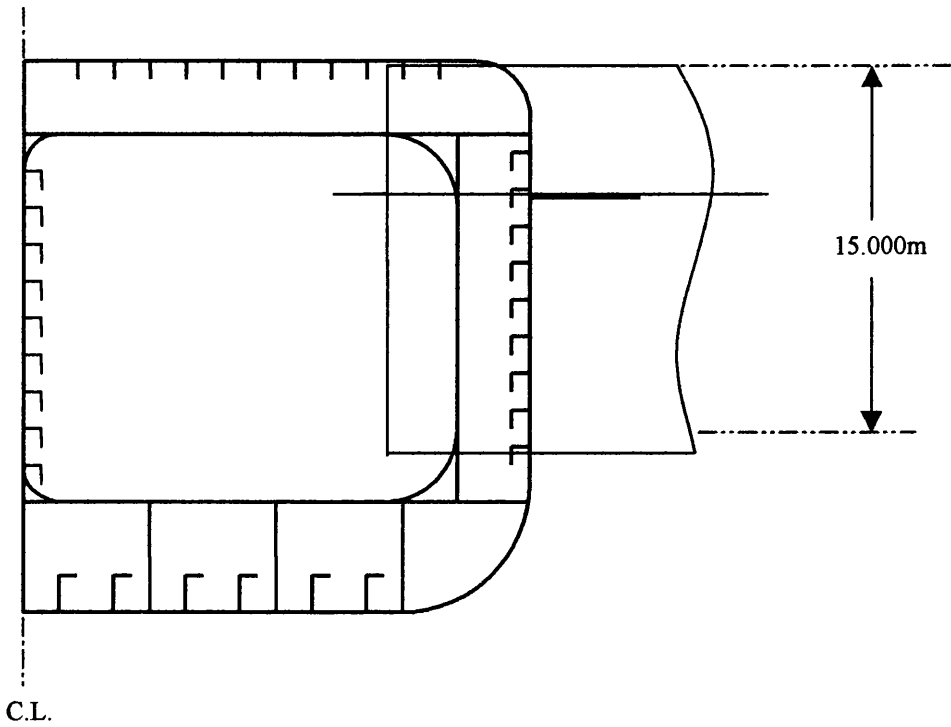


Figure 6.4: Third assumed collision scenario: Struck vessel in Full Load Condition. Striking vessel in Full Load Condition. The damage height equals the depth of the striking ship.

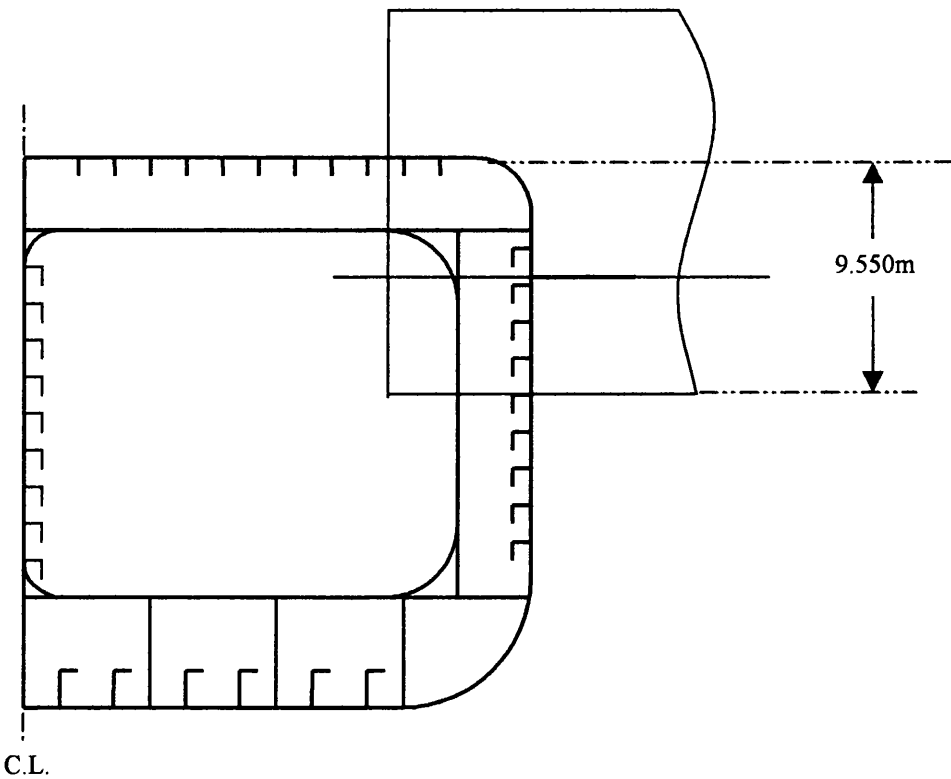


Figure 6.5: Fourth assumed collision scenario: Struck vessel in Full Load Condition. Striking vessel in Ballast condition. The damage height is also shown.

PART TWO: Results derived for the single hull tanker – First Collision Scenario

Total Energy Absorbed by the Side structure - First Collision Scenario

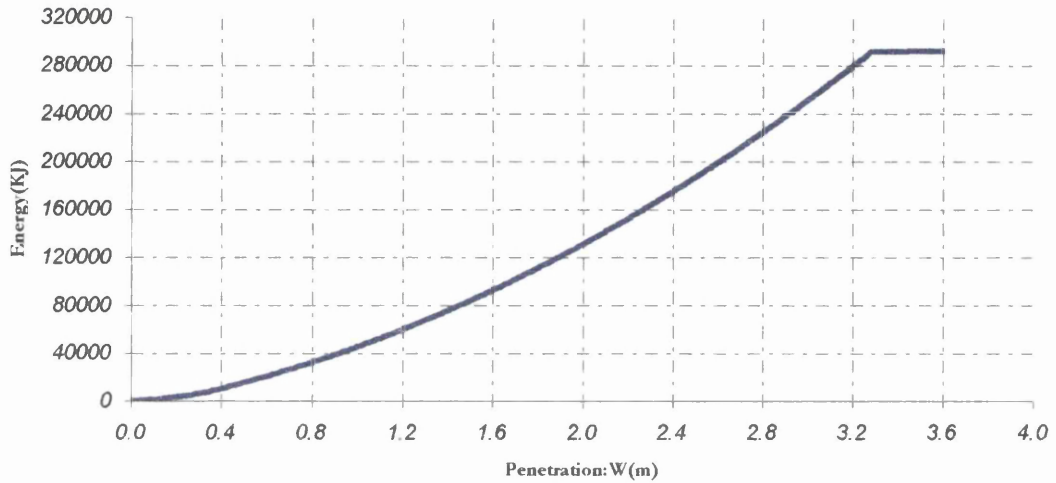


Figure 6.6: Total energy absorbed by the side structure of the single-skin tanker plotted against the penetration depth.

Total Energy Absorbed against the Volume of the Distorted Material

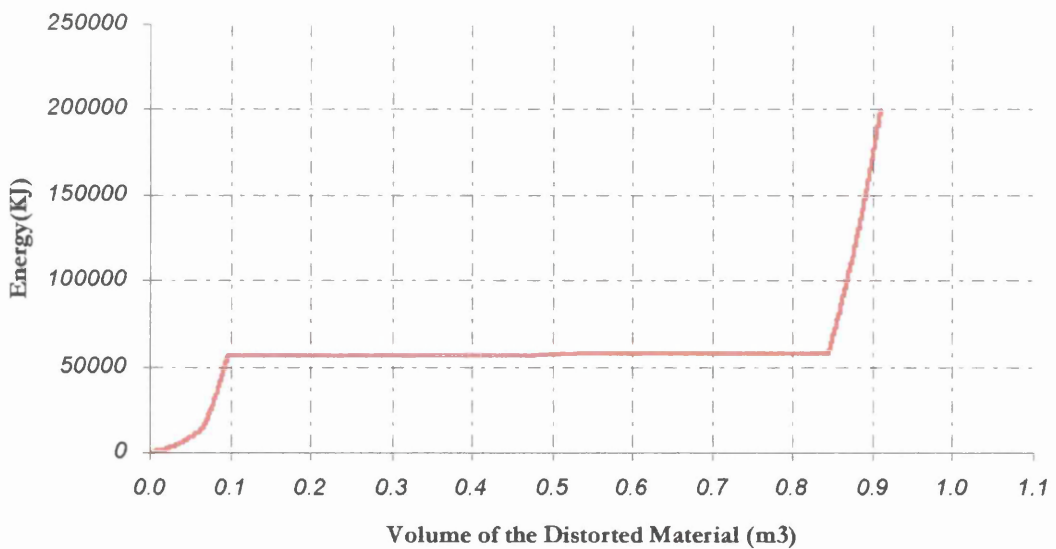


Figure 6.7: Total energy absorbed plotted as a function of the volume of the damaged material. The volume of the side shell plating material has not been included in the calculations.

Energy Absorbed due to membrane tension on the Side Shell plating

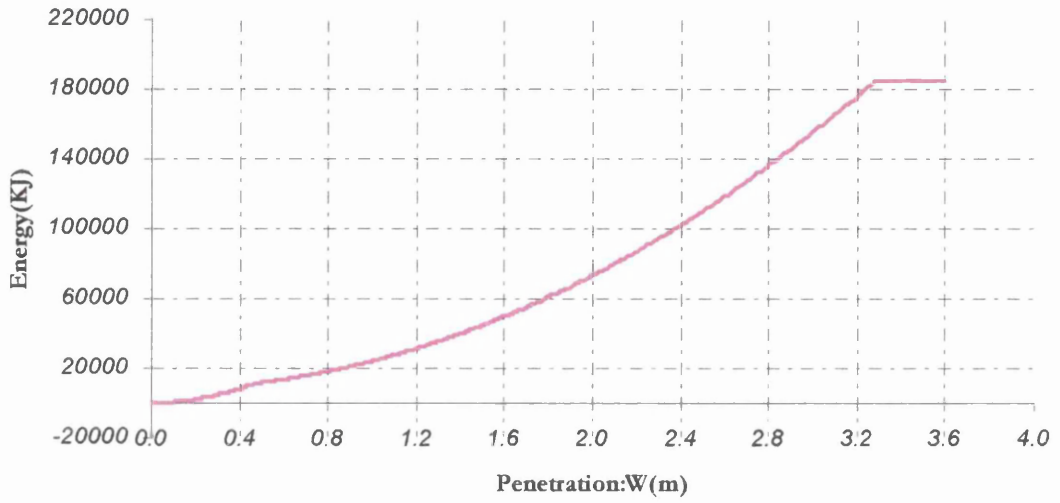


Figure 6.8: Energy absorbed due to membrane tension on the side shell plating.

Energy Absorbed due to membrane tension on the Bottom Deck Plating

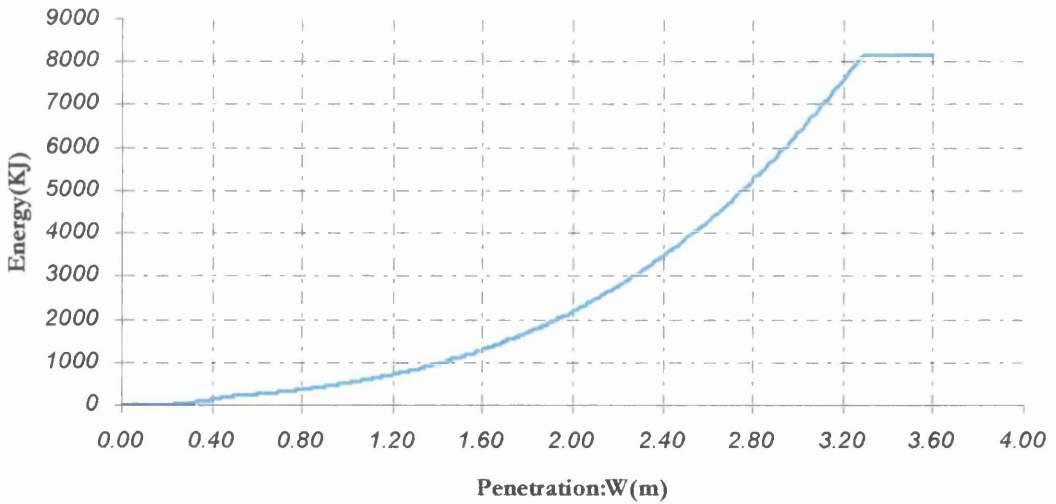


Figure 6.9: Energy absorbed due to membrane tension on the bottom deck plating.

Energy Absorbed due to Buckling of the Bottom Deck plating

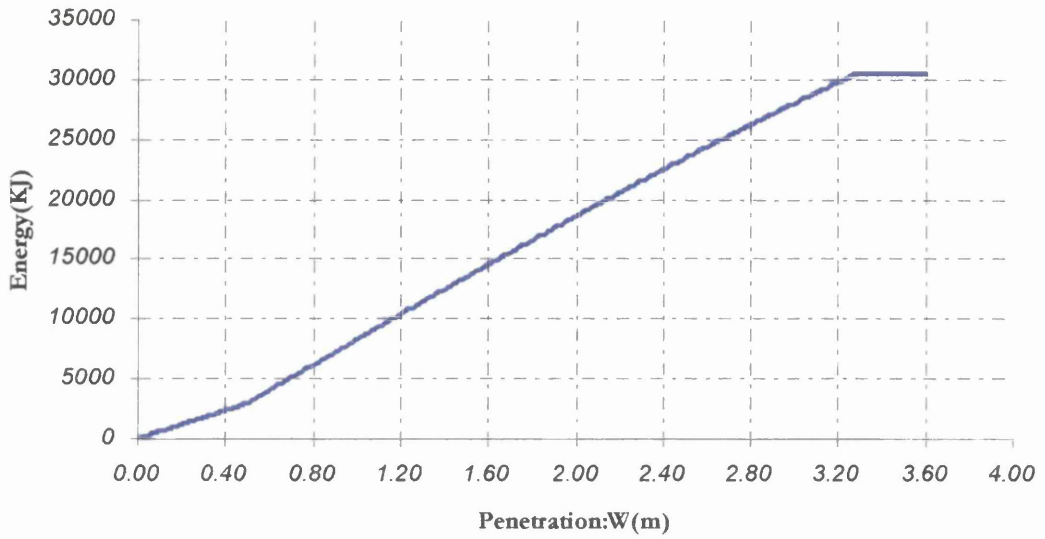


Figure 6.10: Energy absorbed due to the buckling of the bottom plating.

Energy Absorbed due to the collapse of the Bottom deck's transverses flanking the strike

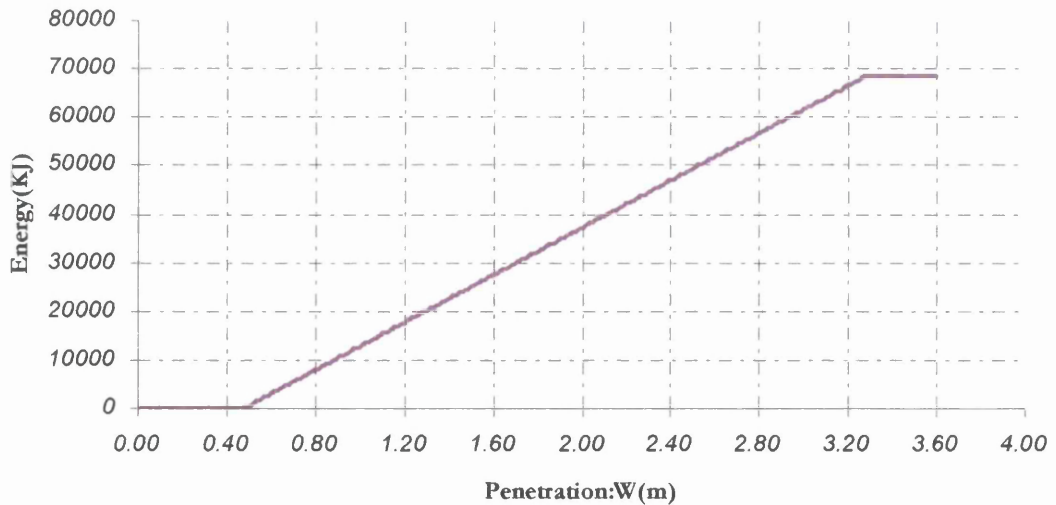


Figure 6.11: Energy absorbed due to the collapse of the bottom transverses flanking the strike.

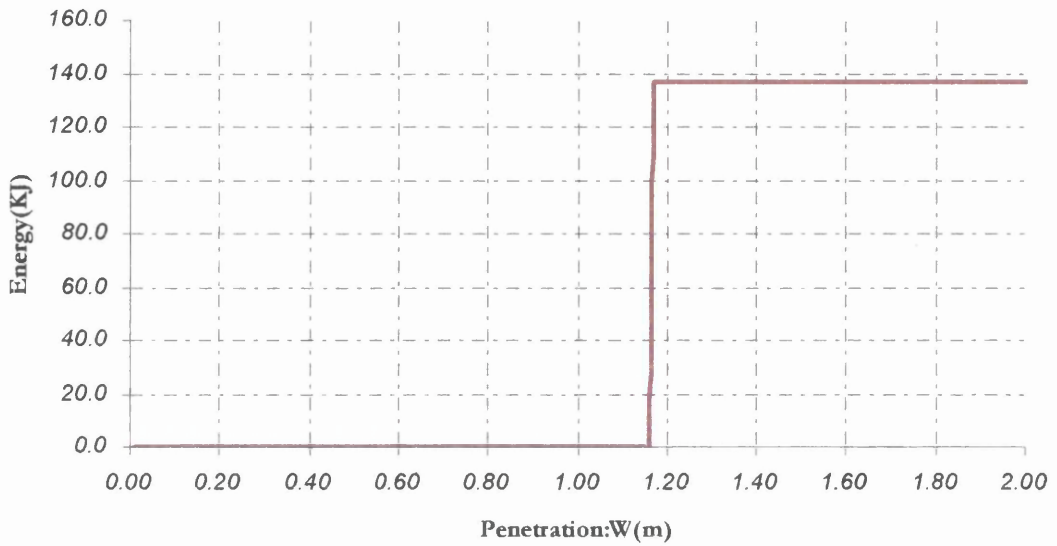
Energy Absorbed due to the collapse of the Side transverses

Figure 6.12: Energy absorbed due to the collapse of the side transverses flanking the strike.

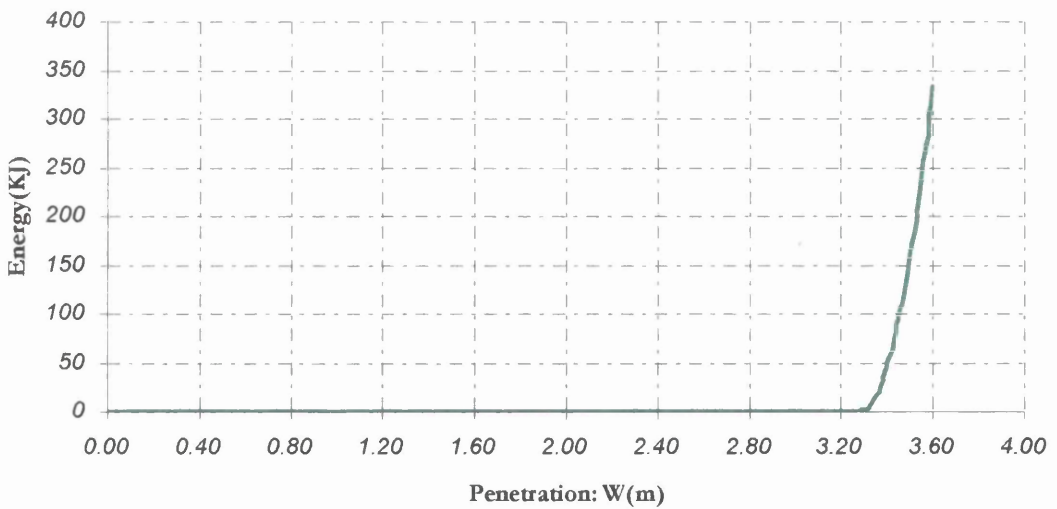
Energy Absorbed due to wedge splitting of the bottom deck plating

Figure 6.13: Energy absorbed due to wedge splitting of the bottom plating, following the rupture of the side shell plating.

PART THREE: Results derived for the single hull tanker – Second and Third Collision Scenario

Total Energy Absorbed by the Side structure - Second and Third Collision Scenarios

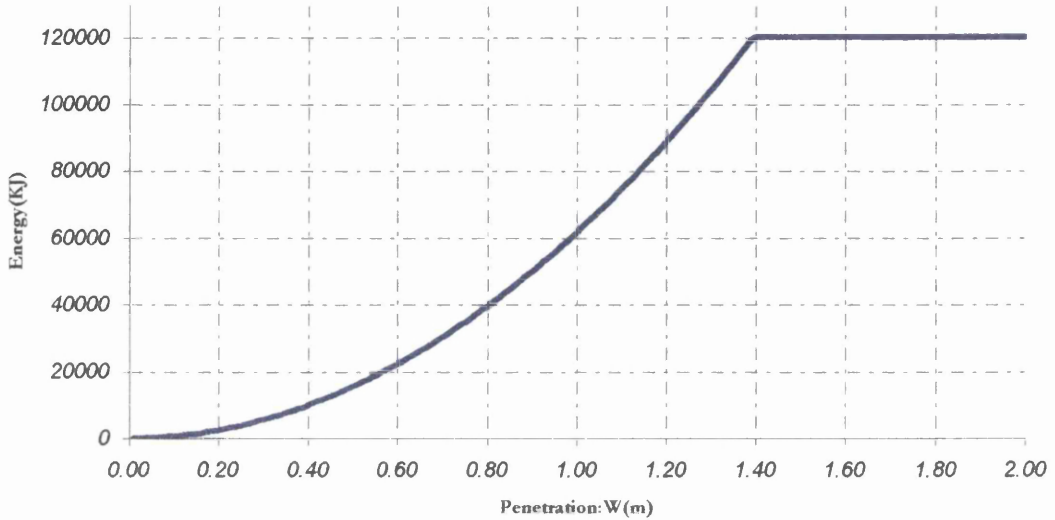


Figure 6.14: Total energy absorbed from the side structure of the struck vessel plotted against the penetration depth.

Total Energy Absorbed against the Volume of the Distorted Material

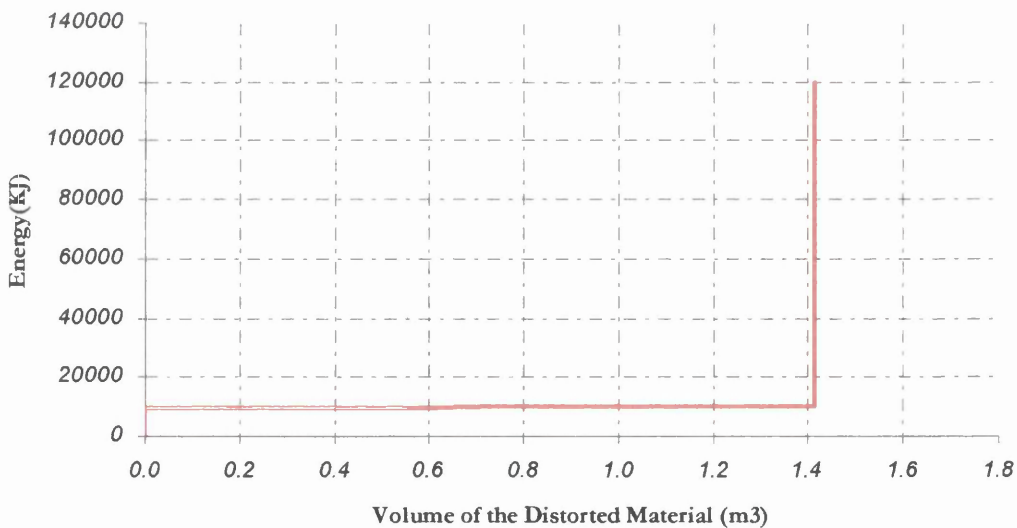


Figure 6.15: Total energy absorbed plotted as a function of the volume of damaged material. The side shell plating material has not been included to the calculations. The second and the third collision scenario involve purely the side shell plating of the struck vessel. That is why the shape of the graph look likes that.

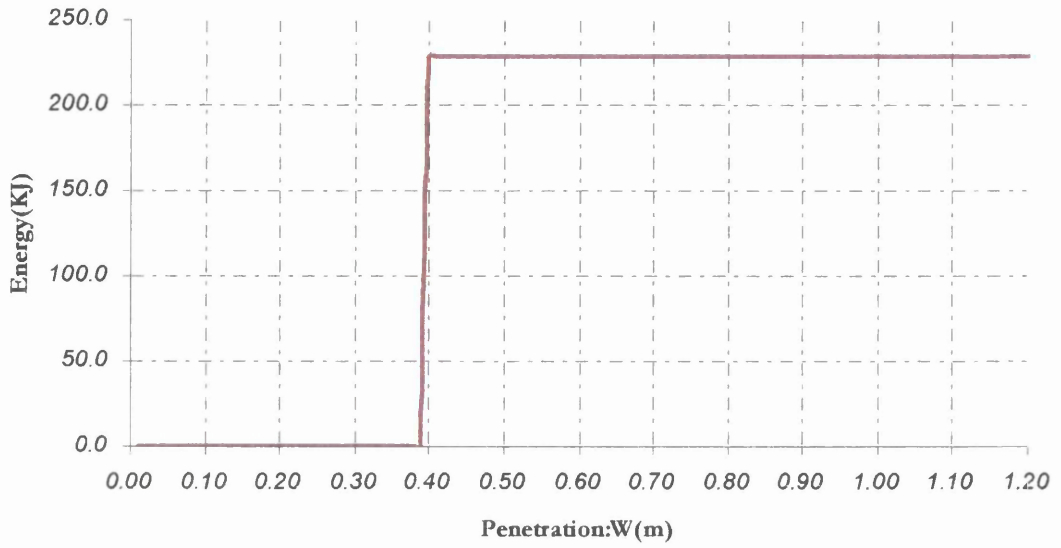
Energy Absorbed due to the collapse of the Side transverses

Figure 6.16: Energy absorbed due to the collapse of the side transverses flanking the strike.

PART FOUR: Results derived for the single hull tanker –Fourth Collision Scenario

Total Energy Absorbed by the Side structure - Fourth Collision Scenario

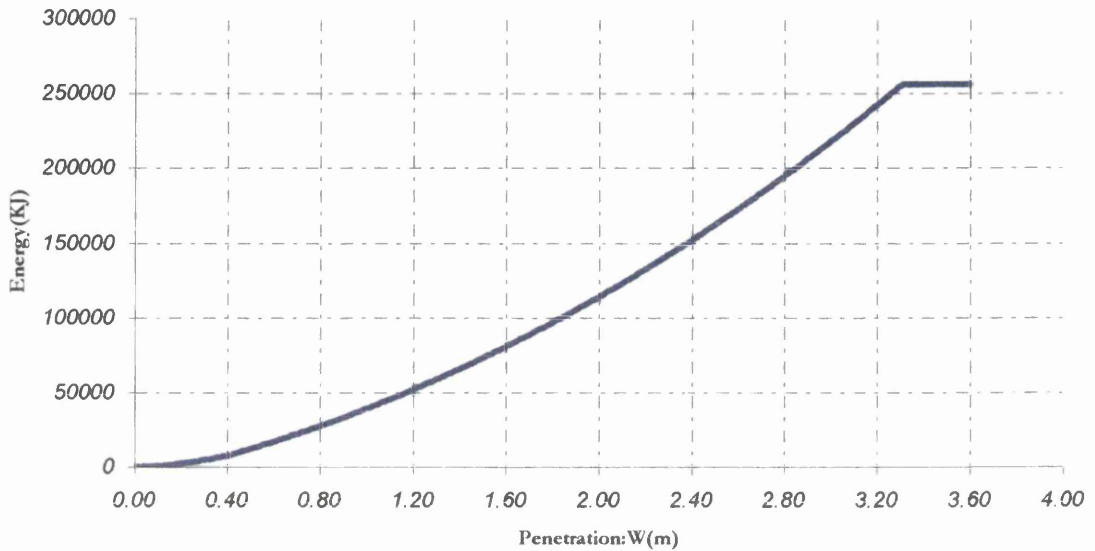


Figure 6.17: Total energy absorbed from the side structure of the struck vessel plotted against the penetration depth.

Total Energy Absorbed against the Volume of the Distorted Material

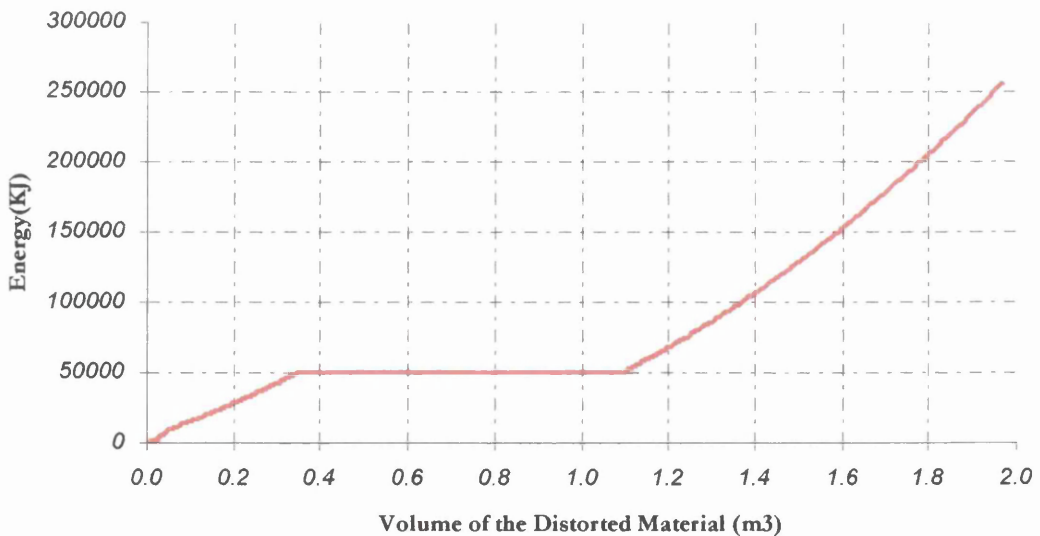


Figure 6.18: Total energy absorbed as a function of the volume of the damaged material. The side shell plating material has been excluded from the calculations. The straight line is due to the collapse of the side transverses flanking the strike.

Energy Absorbed due to membrane tension on the Side Shell plating

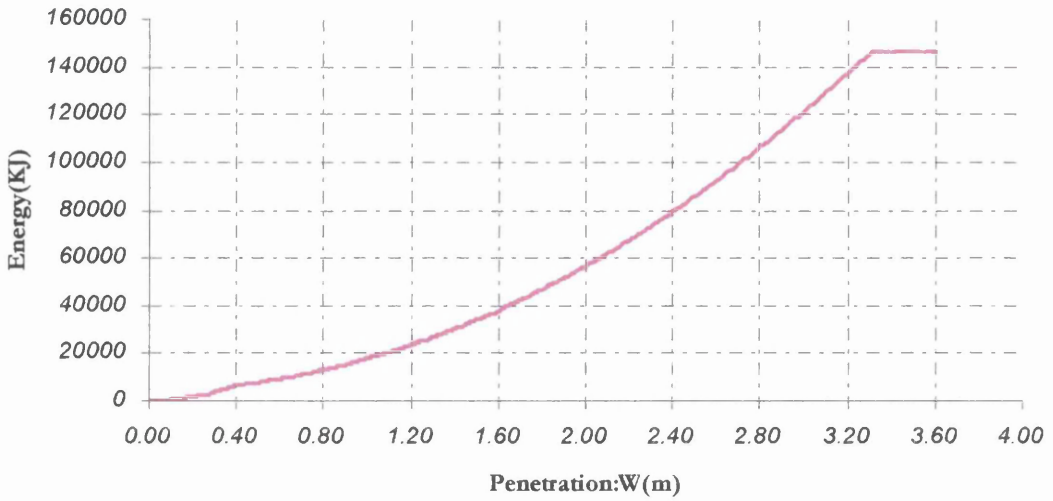


Figure 6.19: Energy absorbed due to membrane tension on the side shell plating of the struck vessel.

Energy Absorbed due to membrane tension on the Main Deck Plating

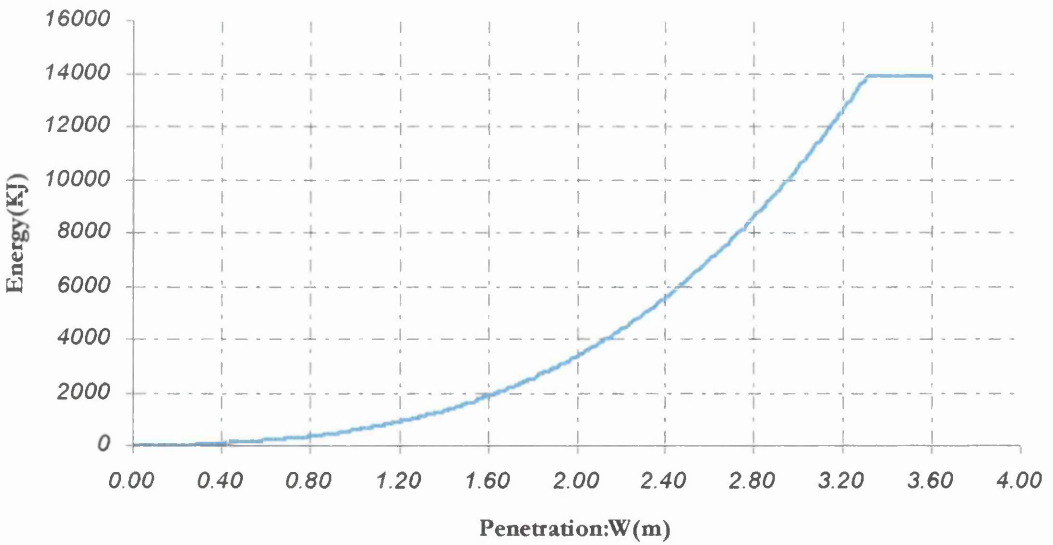


Figure 6.20: Energy absorbed due to membrane tension on the main deck plating.

Energy Absorbed due to Buckling of the Main Deck plating

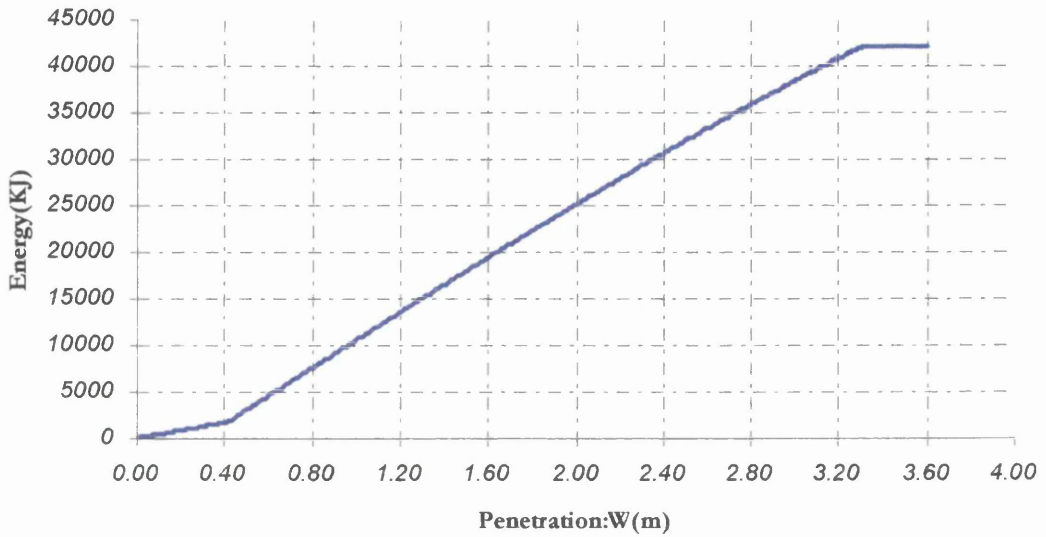


Figure 6.21: Energy absorbed due to the buckling of the main deck plating of the struck vessel.

Energy Absorbed due to the collapse of the Main deck's transverses flanking the strike

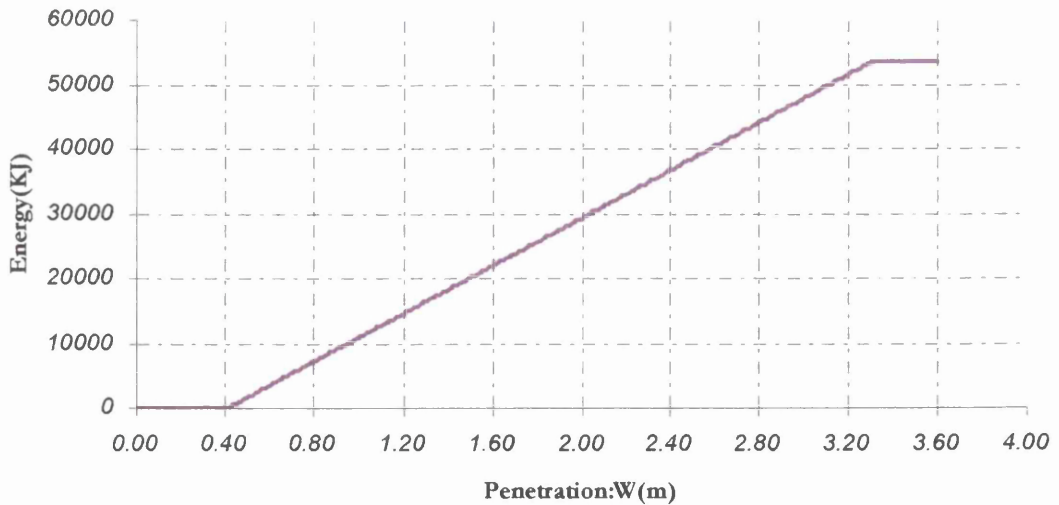


Figure 6.22: Energy absorbed due to the collapse of the main deck's transverses flanking the strike.

Energy Absorbed due to the collapse of the Side transverses

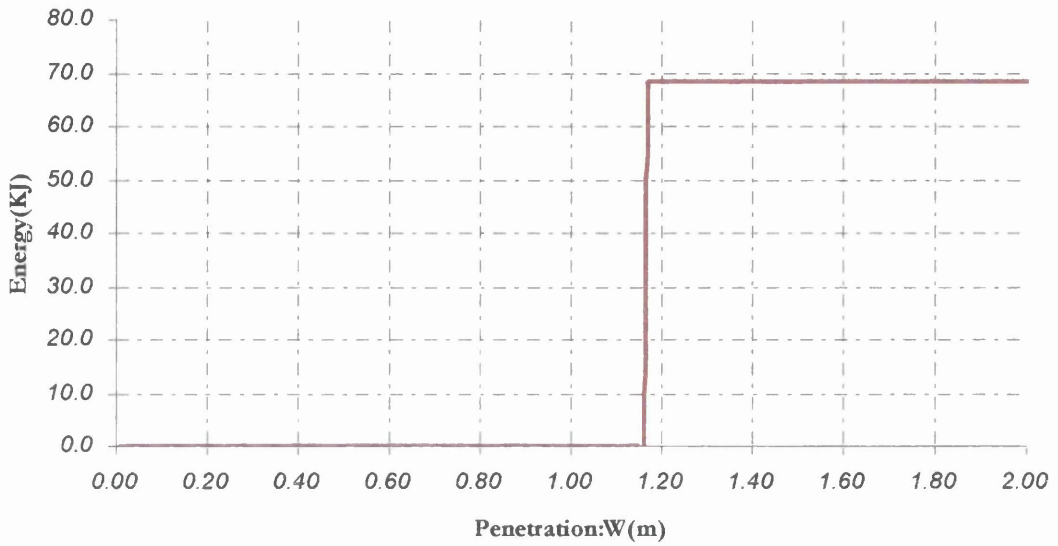


Figure 6.23: Energy absorbed due to the collapse of the side transverses flanking the strike.

Energy Absorbed due to wedge splitting of the main deck plating

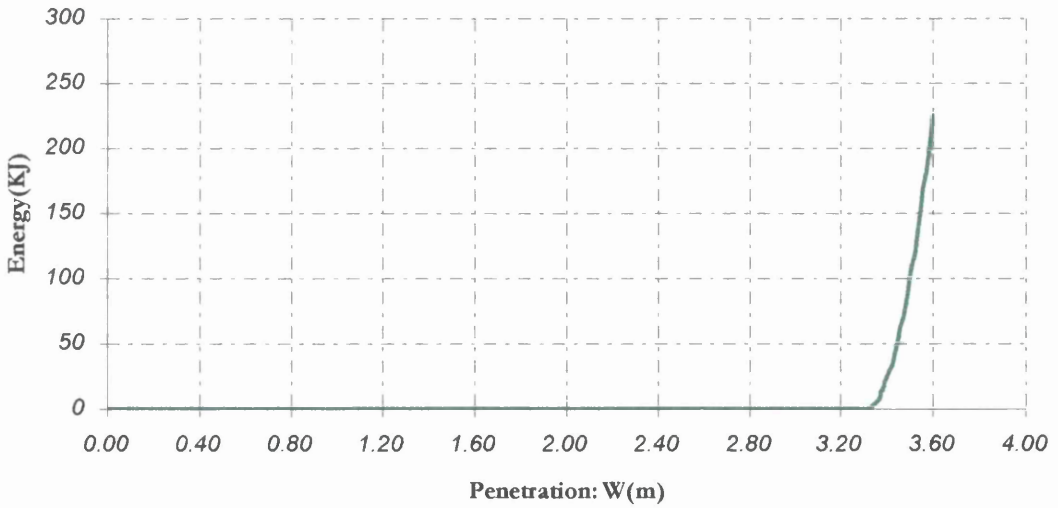


Figure 6.24: Energy absorbed due to the wedge splitting of the main deck plating following the rupture of the hull.

Chapter 7

Parametric Optimisation of the Double Hull Tanker

Introduction

The final work carried out in the present thesis is optimisation of the structural parameters of the struck ship. The structure was optimised in terms of the energy absorption capacity of a vessel in collision. Parameters such as cost and weight of the added material was not taken into account.

The existing methods by Minorsky (1959), Akita (1972), NCRE (1967) are simplified formulae, which do not give the ability of an optimisation procedure to be applied in every component of a side structure. Moreover, these formulae disregard the effect of the side shell plating in the energy absorption capacity. Minorsky only includes a constant energy component in his formula, which has been characterised, from many researchers, to be the energy dissipated before the rupture of the hull. Akita and NCRE methods are exclusively based on the mechanism of wedge splitting of decks and so the volume of the damaged material is considered to be only the one on the torn decks.

These disadvantages of the global methods make them ineligible to be used for the optimisation of a vessel structure. For example, if the above-mentioned methods were applied to a vessel with side shell thickness 0.01m and then reapplied to that vessel but

considering side shell thickness 0.03m then they would predict the same amount of energy absorbed for a constant penetration even if the thickness of the side shell was different in each case. Further, these formulae do not take account of the lateral movement of the web frames. It is evident that when very strong web frames exist in the struck ship's structure then the damage is confined between these web frames. On the other hand, when the web frames are weak the damage is extended to the adjacent bays (area between two consecutive web frames) and the capacity of the energy absorption increases due to the larger volume of the damaged material. Because of the capability to account for each individual member, the method proposed by Hegazy was found convenient for an optimisation procedure.

The Hegazy's method will be used herein for parametric optimisation of the double-skin vessel. This is, for basic parameters affecting the energy absorption capacity of the struck vessel graphs have been derived plotting the variation of energy adsorbed to the variation of each parameter.

Furthermore, a constant amount of material (20 m^3) is distributed to one structural member each time and the energy absorption capacity of the modified structure is calculated. This scenario came up considering the work of a designer. Let's assume that an extra amount of material is available to be placed on a vessel during the design procedure. What will be the best place to put the material regarding the energy absorption capacity of the vessel?

For this purpose the whole amount of the material is placed on one structural member each time (let's say: enforcement of side shell plating) and when all the structural members have been considered, the results are being compared.

For the optimisation procedure, a new collision scenario has been assumed. The striking vessel is assumed to have depth greater than the struck vessel. The whole side

structure of the double-skin vessel, introduced in chapter 5, is now subjected to the impact load (see Figure 7.1).

7.1 Web Frame Spacing

The spacing of the web frames plays a very important role in the value of the limited indentation beyond which rupture of the hull occurs, (W_L). The larger the spacing is the larger the value of the limited indentation becomes. This affects the energy absorption capacity because the membrane tension on the side shell and the decks as well as the buckling force on the decks are acting as an energy absorbing mechanism for a larger penetration. Although the energy absorbed before the rupture of the hull increases with the increase of the spacing between web frames, the classification society's rules restrict its value.

In Figure 7.2 is illustrated the energy absorbed by the double hull vessel's side structure up to the rupture of the inner hull against several values of the half-spacing between web frames. It is evident that the energy absorption increases about 15% for an increase of 20cm in the spacing between web frames.

7.2 Distance between the outer and inner hull.

The width of the double hull is another important factor affecting collision. It is understood that a larger distance between the hulls increases the penetration depth needed from the striking bow to engage the inner hull. Also the energy absorption increases due to the existence of decks connecting the two hulls, which resist the penetration.

The energy absorbed up to the rupture of the inner hull is plotted against the width of the double-hull. The increase in the energy absorption capacity is 1 to 1.5% for an increase of 10 cm in the width of the double-hull (see Figure 7.3). The increase is not so impressive as in the increase of the web frames' spacing but 1.5% in this case corresponds to 10000 KJ.

7.3 Double bottom height

The double bottom height does not seem to affect the energy absorption capacity of the particular vessel. The decrement in the energy absorption is almost negligible for an increase to the double bottom height up to 0.800 m (see Figure 7.4).

The only role that the double bottom structure plays in the energy absorption capacity is seems to be the provision of extra strength to the bottom transverse. Thus, as soon as the area of the bottom transverse remains constant the height of the double bottom can not affect the capacity of the energy absorption of the structure.

7.4 Addition of Material to the Structure

Since a parametric optimisation without any design and strength constraints was considered to be useless, another scenario seemed to be a good idea. By assuming that a constant extra amount of material is available, where is the best area to be placed?

Through the designs provided for the double-skin vessel, a rough estimation of the volume of material was made. The procedure is as follows: The web frame spacing is 3.80m and the length of the ship between perpendiculars 228.0m. The number of web

frames of the vessel's structure was assumed to be (length/spacing) 60. Besides, the cross sectional area of the deck transverses, bottom transverses, main deck plating, bottom and inner bottom plating, side shell and inner shell plating were calculated. For the deck and bottom transverses by multiplying with the number of web frames the volume of the material of each individual member obtained. The same was done for the plating areas (multiplying with the length of the ship).

Judging from the magnitude of the individual volumes obtained, the constant amount to be available for addition to the structure was assumed to be twenty cubic meters (20 m^3). The total volume of the material of the ship was approximately calculated to be 1300 m^3 . Thus 20 m^3 is 1.5% of the total volume, which will probably not increase the cost of the structure too much.

Afterwards, the reverse procedure than the one described above the material was distributed to each individual member. For example, the 20 m^3 were added to the bottom deck transverse and the thickness of the web became 0.016 instead of 0.012 that it was in the original design.

The structural members, which were enforced sequentially, are the following:

- main deck transverse
- bottom transverse
- main deck plating
- bottom plating
- decks between double hull
- side shell plating
- inner shell plating

The results obtained for each case are shown in Figures 7.5 to 7.11. The total energy absorbed by the side structure is not affected as differently as it was expected. The added material increases of course the energy absorption capacity of the side structure but the structural member that it is being placed does not seem to play an important role.

The following table shows the results obtained for each case as well as the energy absorbed from the original structure just prior to the rupture of the hull

Enforced Structural Member	Energy absorbed by the side structure up to the rupture of the inner shell plating, E_{minor}	Penetration depth at the instant of inner hull's rupture, W_{LMAX}
None	973025 KJ	6.20 m
Main deck Transverses	991810 KJ	6.20 m
Bottom Transverses	924153 KJ	6.10 m
Main Deck Plating	1040729 KJ	6.22 m
Bottom Plating	1026697 KJ	6.04 m
Decks between Double Hull	1026017 KJ	6.22 m
Side Shell Plating	1026156 KJ	6.25 m
Inner Shell Plating	993558 KJ	6.21 m

7.5 Conclusions

From the above-cited results is obvious that the increase in the energy absorbed by the side structure is not increasing much. Although, the increase is not seemed to be much in figures is as follows: For 1.5% increase on the material of the structure the increase in the absorbed energy varies from 2% to 7%.

The only case that the crashworthiness of the vessel is decreased is when the bottom transverses are being enforced. It is evident that when the transverses in the decks of the struck vessel are very strong the damage can not extend in the adjacent bays and the energy absorbed as well as the penetration beyond which rupture of the hull occurs, can not reach large values due to the restricted amount of the material between the two consecutive web frames. Even if a strong deck transverse collapses, its movement towards the centreline of the struck ship is being restricted by its strength. On the other hand, very weak deck transverses collapse early and do not leave chances for the best operation of the structure in terms of energy absorption capacity. This is the case for the main deck transverse, which following the addition of the material, provided better energy absorption characteristics to the structure.

The addition of the extra material to the bottom plating, the decks between double-hull and the side shell plating yielded similar results. Although, the values of the critical indentations were different in each of the above-mentioned cases the results are the same.

The addition of material to the bottom plating results in increased energy absorption due to membrane tension and buckling and also decreases the critical indentation of the bottom transverse by exercising a larger force on it.

The addition of material to the decks between the two hulls increases the total energy through the energy absorbed in their wedge splitting.

The effect of the enforced side shell plating and inner shell plating is apparently the increased energy absorbed due to membrane tension.

Finally, the main deck plating proved to be the place to put the extra material. The percentage obtained (7% increase in the total energy) is believed to be a satisfactory one for the 1.5% material added.

This optimisation procedure made clear that there is no specific formula for optimising in general types of ships. Every vessel requires to be analysed singularly and no general directions (except the basics) are feasible.

List of Figures

PART ONE: Parametric Optimization

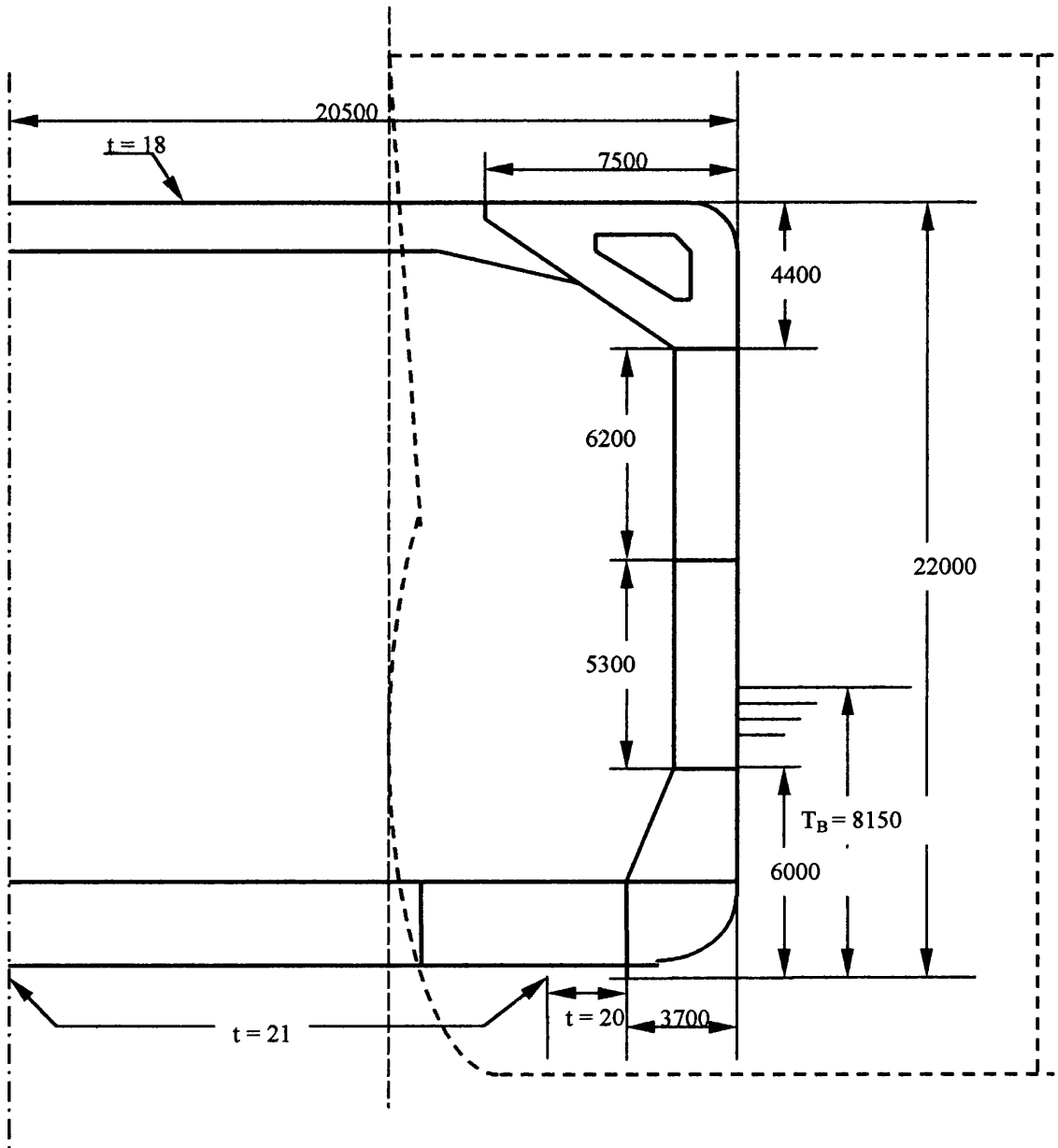


Figure 7.1: Assumed Collision Scenario for the Optimization Procedure.

Total Energy Absorbed up to the rupture of the Inner hull

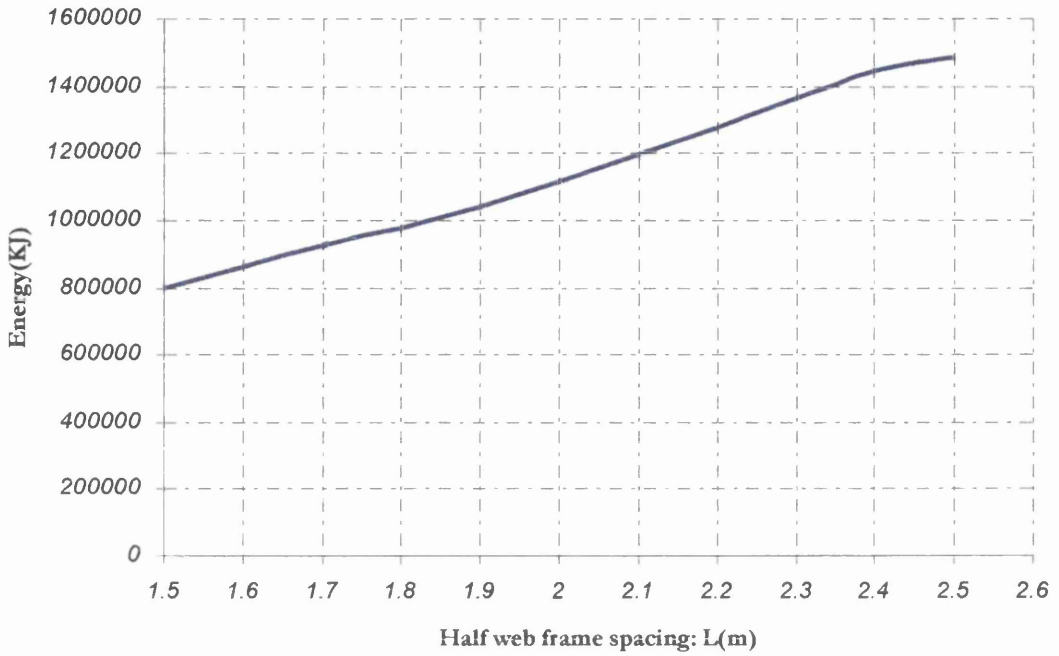


Figure 7.2: Total Energy Absorbed just prior to the rupture of the inner hull of the double-skin tanker plotted for different values of the web frame spacing.

Total Energy Absorbed up to the rupture of the Inner hull

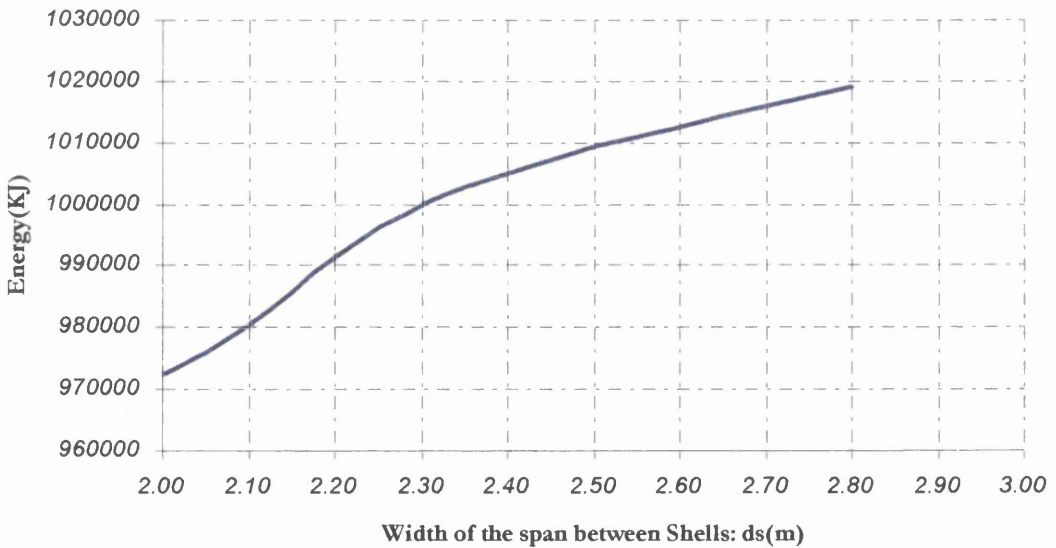


Figure 7.3: Total Energy absorbed by the side structure of the double-skin vessel just prior to the rupture of the inner hull plotted for different values of the distance between the two hulls.

Energy Absorbed up to the rupture of the Inner hull

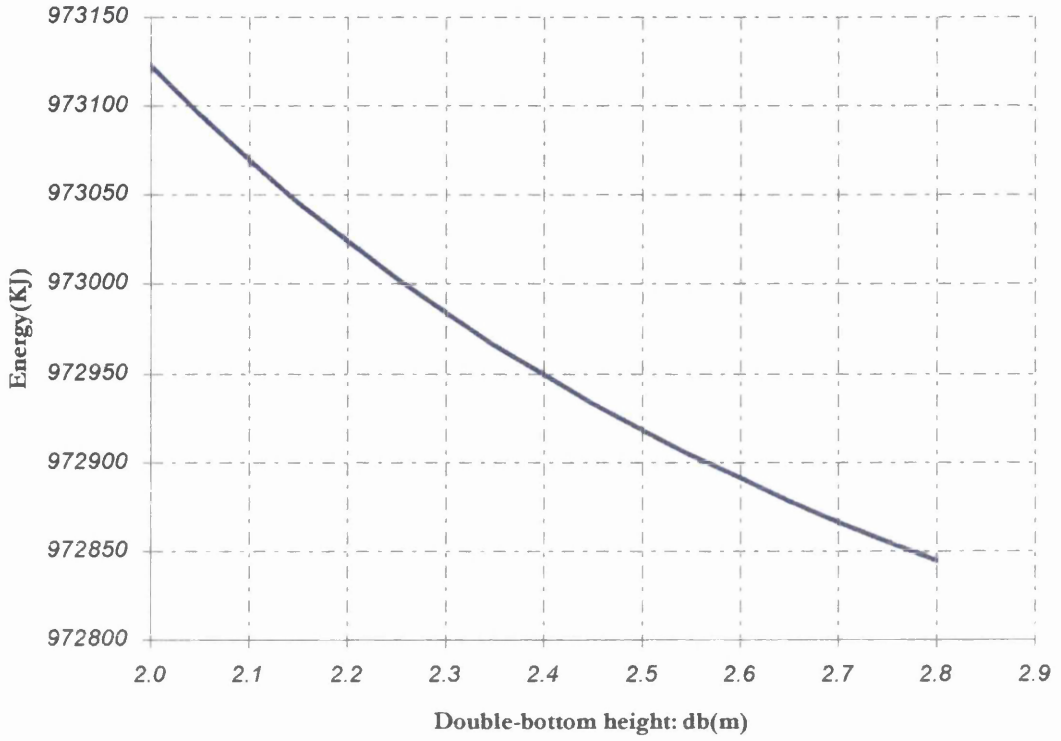


Figure 7.4: Total energy absorbed from the double-skin tanker just prior to the rupture of the inner hull plotted against the double bottom height.

PART TWO: Results obtained by adding a constant extra material to a particular structural member.

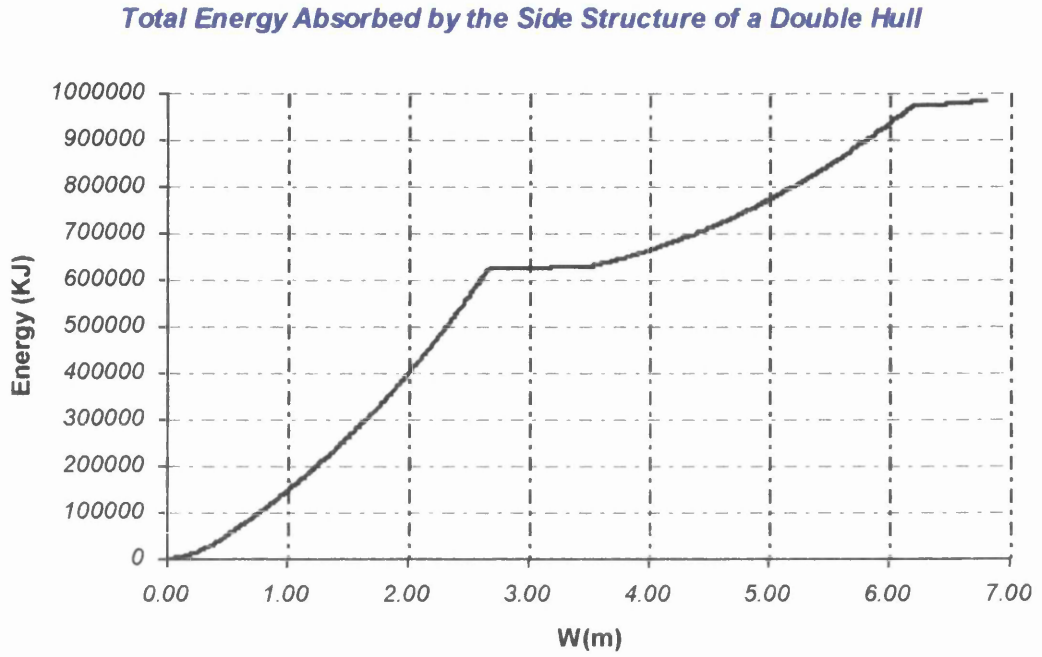


Figure 7.5: Total energy absorbed by the side structure of the double-skin tanker. The vessel is assumed in its original form.

Total Energy Absorbed by the Side Structure of a Double Hull

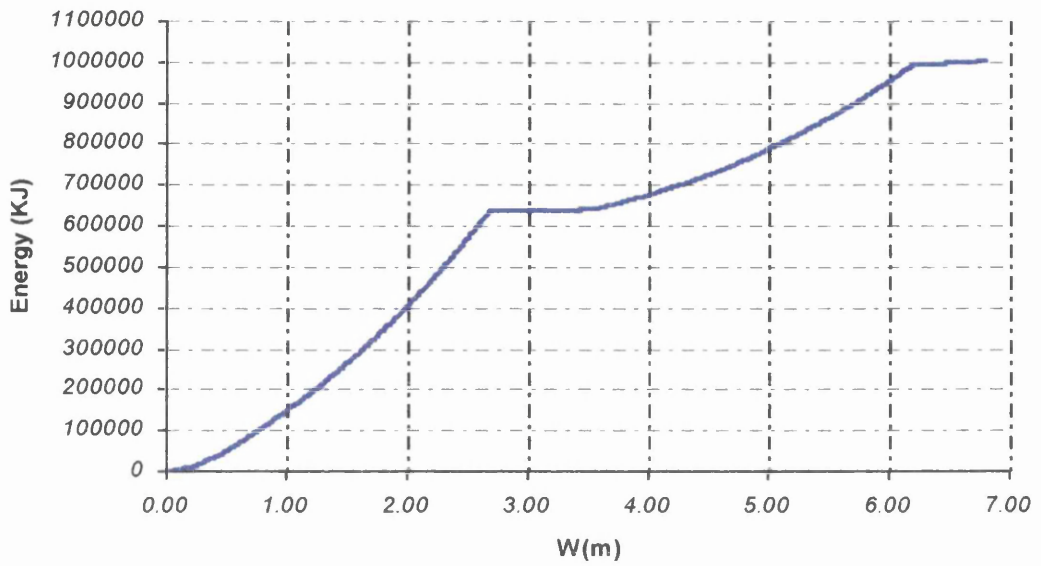


Figure 7.6: Total energy absorbed from the side structure of the struck vessel, when the extra material is placed on the main deck transverse.

Total Energy Absorbed by the side structure

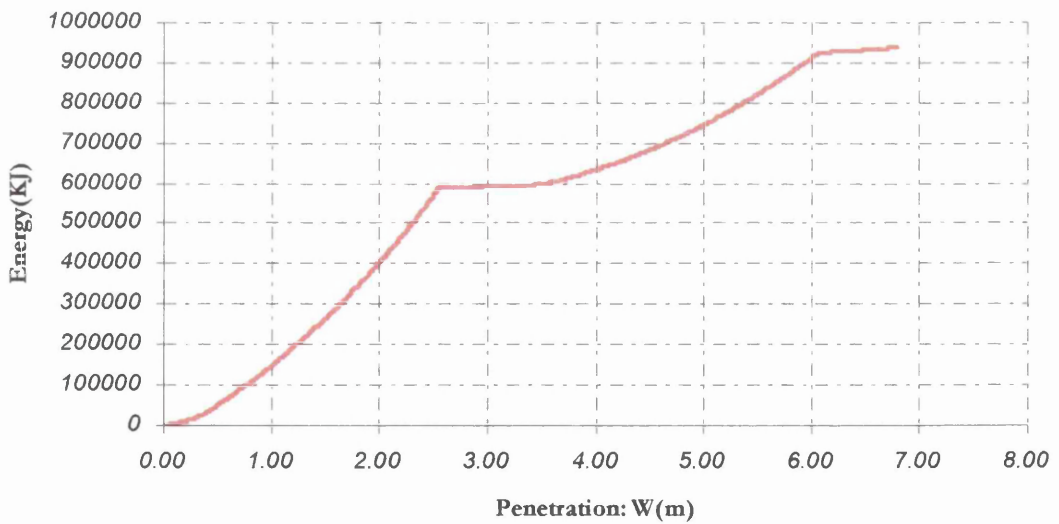


Figure 7.7: Total energy absorbed from the side structure of the struck vessel, when the bottom transverse is enforced with the extra material.

Total Energy Absorbed by the side structure

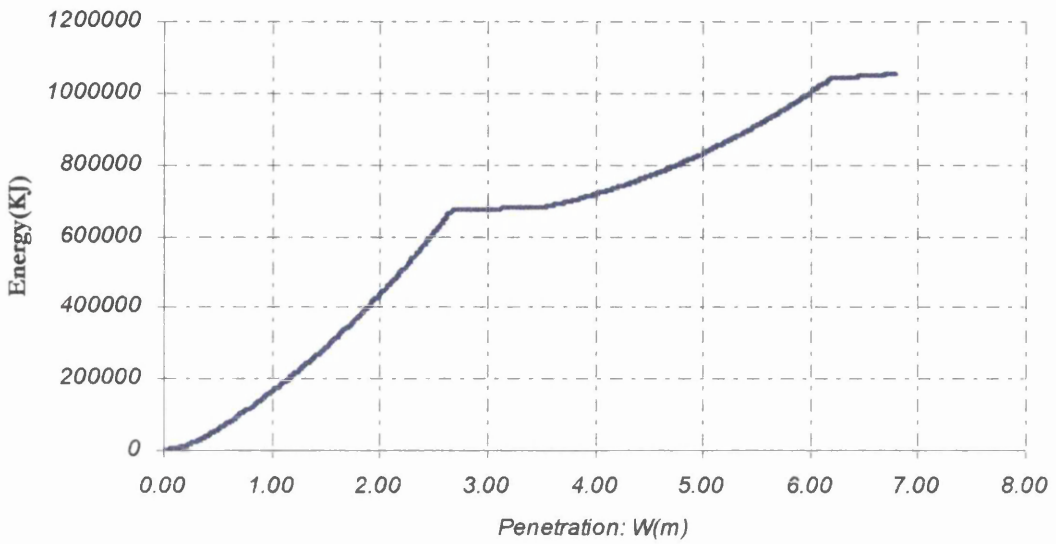


Figure 7.8: Total energy absorbed from the side structure of the double-skin tanker, when the extra material is placed on the main deck plating.

Total Energy Absorbed by the side structure

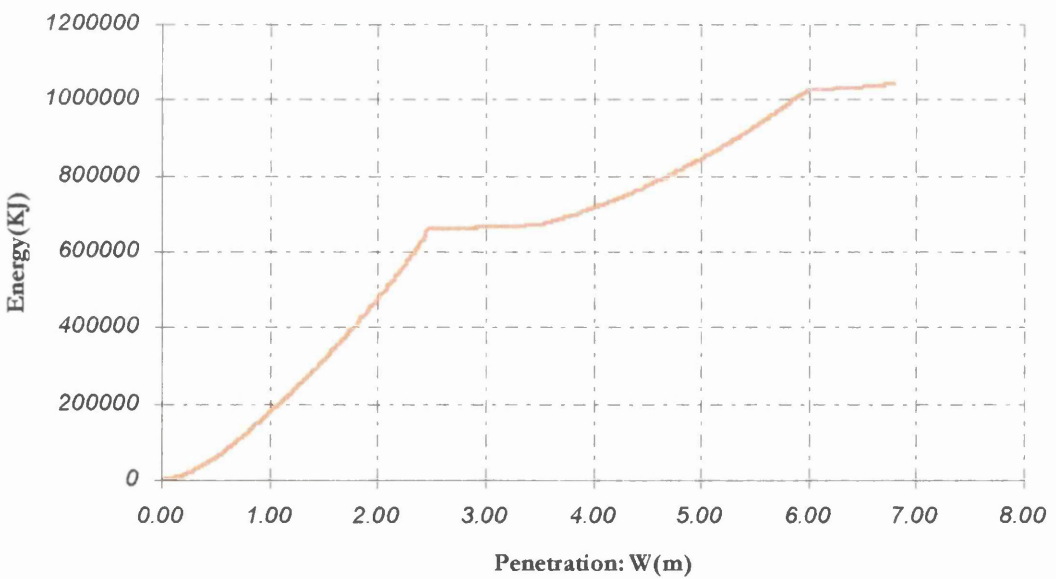


Figure 7.9: Total energy absorbed by the side structure of the struck vessel, when the extra material is placed on the bottom plating.

Total Energy Absorbed by the side structure

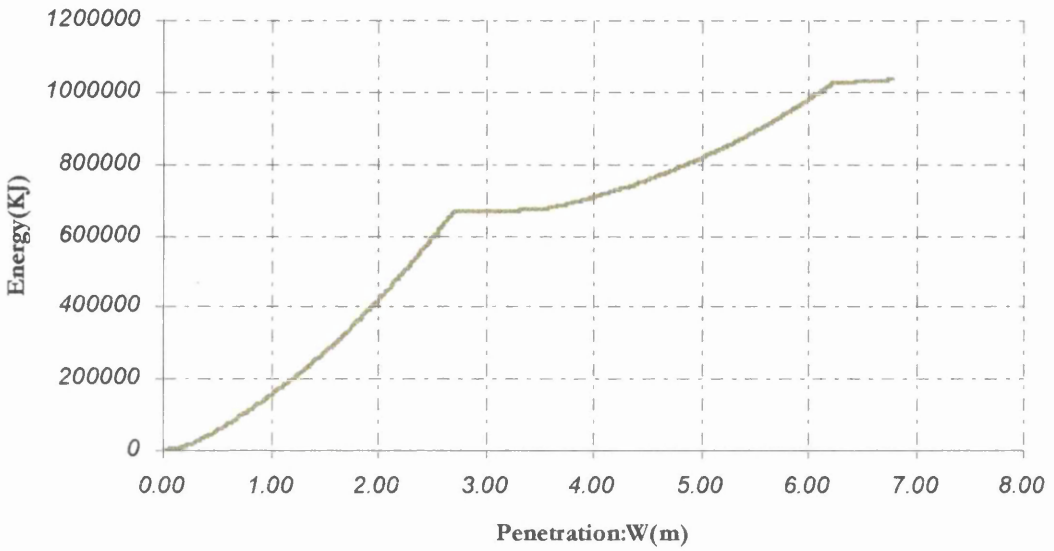


Figure 7.10: Total energy absorbed by the side structure of the double-skin tanker, when the extra material is distributed to the decks between the double-hull.

Total Energy Absorbed by the side structure

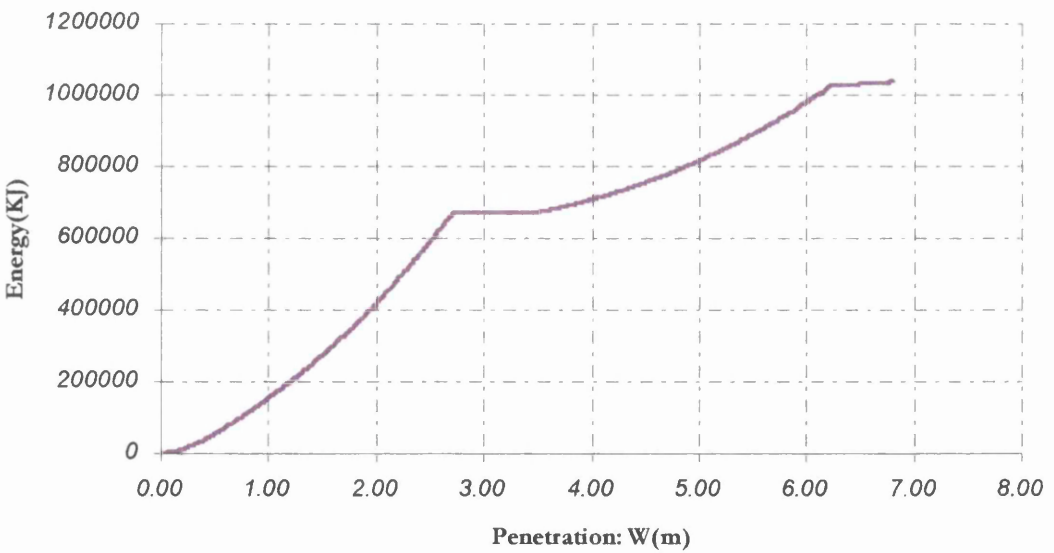


Figure 7.11: Total energy absorbed from the side structure of the double-skin tanker, when the extra material is distributed to the side shell plating.

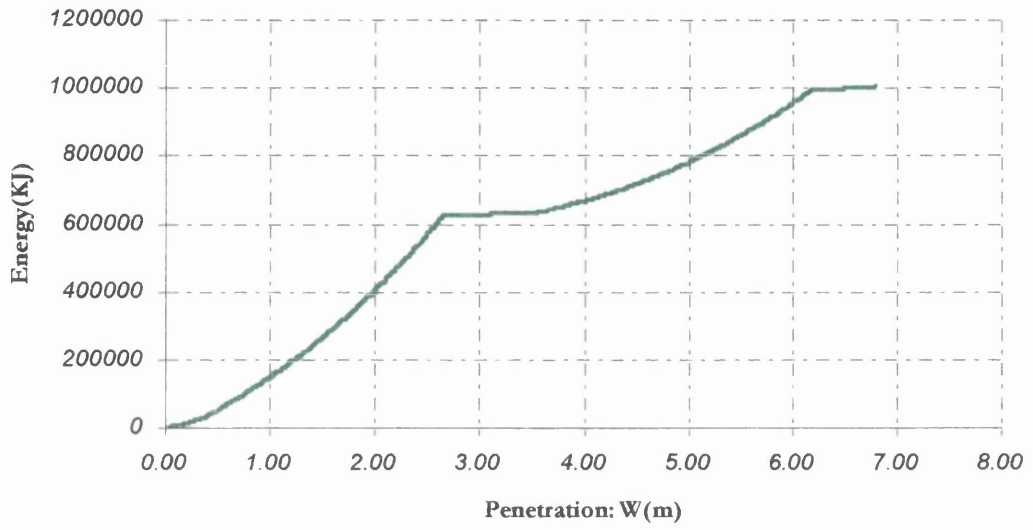
Total Energy Absorbed by the side structure

Figure 7.12: Total energy absorbed from the side structure of the double-skin tanker, when the inner shell plating is enforced with the extra material.

Chapter 8

Conclusions and Proposals

2.1 Assessment and Conclusions of the Work

The initial aims of the thesis were to extend Hegazy's method in a way that would make it applicable to existing structures, to produce results for a particular structure, to modify the method, where possible in order to give better results, and finally to conduct optimization in terms of the energy absorption capacity.

The aims of the project have been reached and furthermore additional work has been carried out than the planned one. The development of the single hull tanker was not planned but became necessary due to the lack of experimental data for comparison, when the results from the double hull were derived. The small oil tanker (chapter 3 and 4) also was thought to be a good idea for the derivation of results and the verification of the Fortran code's soundness due to the simplicity of its midship section.

Conclusions derived from the present study have been cited in each chapter as well as assessment of the results and the assumptions. Herein a general evaluation of the derived results is attempted in order to give a global consideration of the work carried out.

In the first chapter and through the literature review carried out it became evident that in the minor collisions' field the methods, which are known were developed by Rosenblatt (1971, 1972), McDermott et al. (1974), Jones (1978) and Van Mater (1978). The first two methods pertain to the approximate theoretical methods. The other two methods, which are actually one method and its extension to variable location collision cases, pertain to the so-called global methods. The global methods are Minorsky-type methods that relate the energy absorbed with the volume of the damaged material during a collision.

In the major collisions' field the methods, which are most known were developed by Minorsky (1959), NCRE (1967) and Akita et al. (1971, 1972). All the cited methods pertain to the global methods or simple design methods.

In the second chapter the review on the internal mechanics of collision gives the opportunity to understand better the problems and the darkness that there is in some of the subjects involving the theoretical analysis of collisions. The application of the theoretical methods and the finite elements analysis in some new double hull designs have provided us with some results and some intended ways of dealing with the problem.

Some general remarks regarding the way that a structure will follow during collapse due to impact loading, show that the field of the internal collision mechanics is not an easy one. A lot of simplifications have to be made each time and besides the sequence of phenomena occurring during collision could change from one ship to another.

In chapter three a method proposed by Hegazy (1980) is presented. Hegazy (1980) in this study proposed a collapse model, which takes into account every structural member of the struck ship involved in collision. The basic advantages of this method are:

- The method is applicable for analysing structural ships' resistance for both minor and major collisions.
- The collapse model proposed is dependent on the struck ships' structure. Values, which are individual for each ship, are calculated by the method and these are what define the shape of the deformed form of the struck ships' side structure at the end of the collision.

Due to these remarks, Hegazy's method is used in the present work for analysing the side structures of a struck ship during collision. It was found to be a good idea to check how the method works on real ship structures, which do not have the design simplicity of the assumed idealised models.

Furthermore, the developed program is discussed in chapter 3 and results for a small oil tanker are derived. The small oil tanker is considered to be the struck ship in two different scenarios. The results show the difference in absorbed energy due to the difference in the structural members involved in the collision damage.

In chapter four is attempted a modification of the proposed method in order to achieve a better correlation between the experimental tests (Hegazy 1980) and the theoretically calculated values. A discrete beam method is introduced for the calculation of the decks ultimate strength (Pu and Das 1994), when they are transversely framed. When the decks are longitudinally framed overall buckling of the decks is unlikely to occur (Hughes 1988, Hegazy 1980) and a formula for the ultimate strength of the wide plates (Faulkner 1973) between adjacent stiffeners was introduced. The results produced for the small oil tanker design show a

sufficient increase in the total energy absorbed by the struck ship, which compared to the graphs presented from Hegazy (1980) seems to correlate better with the experimental data.

In chapter five a double-skin tanker is presented and the Hegazy's method is applied for the estimation of the crashworthiness of the structure. A lot of further assumptions had to be made in order to calibrate the method to work for the particular structure. The problems are arising when the damage is extended to the adjacent bays (space between two consecutive web frames) due to the difference of the deck's and bottom's transverses critical buckling load. The sloped indentation line at the web frames flanking the strike due to different values of final indentation \overline{W}_1 (see subsection 3.4.6, Fig. 3.2) at the deck and the bottom transverses had to be calculated through geometry. Then the final indentation \overline{W}_1 at each different structural member had to be estimated for the calculation of the energy absorption. Also the relative movement of the inner hull due to the collapse of the web frames flanking the strike was estimated in order to calculate the penetration depth at which the striking ship engages the inner hull.

The results produced for the double hull tanker were found to be rational compared to values obtained through finite element analysis on double-hull vessels by Kitamura (1997).

In chapter 6 a single-skin tanker is developed through preliminary design calculations of its midship section. The form of the midship section was based on other single-skin vessels, which the author had in hand. The aim is to compare the crashworthiness of the double-skin tanker to a single-skin one having the same principal dimensions. The calculations of the developed single hull's midship section properties are shown in Appendix A.

Results have been derived for the energy absorption capacity of the single-hull tanker regarding the same four collision scenarios that were assumed for the double-hull vessel. A comparative table shows the differences in energy absorbed by the side structures of the two ships. The double-skin tanker exhibits much better crashworthiness in three of the cases examined and only in the fourth collision scenario the single hull tanker absorbs more energy due to the larger volume of its main deck's transverses and main deck plating.

Finally in chapter seven a parametric optimization is conducted. General parameters of double hull designs such as double-hull width, double-bottom height and spacing of the web frames have been taken into account in the first part. Then, an assumed constant amount of extra material 20 m^3 is distributed in an individual structural member each time and the energy absorption capacity of the structure is calculated (see subsection 7.4).

This work was done considering the viewpoint of a designer. If there is an extra amount of material where would be better to place it in terms of the crashworthiness of the vessel? The answer for the particular double-skin design is: to the main deck plating. As it was cited above the only collision scenario that the double-skin tanker absorbed less energy than the single-hull one is the scenario where the upper structures of the struck vessels are considered. In the particular area consisting of the main deck plating, the topside tank (double-skinned tanker), the main deck's transverses, the upper part of the side transverse, and the side shell plating, the double-skin tanker seems to be weaker than the single-skin one. Thus, through the optimization procedure the answer is that if an increase of 1.5% of the volume of the material needed for the vessel's construction is placed on the main deck's plating then the result in terms of crashworthiness is a 7% increase in the energy absorbed up to the rupture of the inner hull.

The work carried out in the present thesis is hoped to be a step forward to the understanding of ship to ship collision mechanics.

8.2 Proposals

The author believes that the development of an approximate theoretical method modified through experimental work is the best way for deriving an easy-to-use tool for the preliminary design of ships. The theoretical methods have the capability of being applied on different structures by modifying the mathematical model used due to the different sequence of phenomena occurring for each individual structure.

On the formulae for the strength calculations of decks, beams and side shell plating due to impact loads has been carried out a lot of experimental and theoretical work. This means that the tools for the estimation of the individual structural members exist and besides the small scale tests can provide adequate accuracy in order to optimize the existing formulae.

Experimental small-scale tests are being conducted but the scaling effect does not give the opportunity of full utilization of this area. Full-scale tests are of great interest, but the cost of such tests make them inhibitory. Besides, in full-scale tests there is no opportunity of re-conducting the tests if something goes wrong.

One major problem is the dynamic behavior of the structures during collision accidents. The criterion, when a static approach is adequate and when a dynamic approach is needed, has not been clearly established yet. Furthermore, the magnification factor used by the theoretical methods to take account of dynamic phenomena could be further examined.

It is of course understood that the domination of the finite element methods in the engineering of structures does not leave enough space for the theoretical methods. But the FEA can not provide results without being time and cost consuming. Therefore the author believes that a lot of work has to be carried out for the development of adequate simplified analytical methods.

REFERENCES

Akita, Y., Ando, N., Fujita, Y., and Kitamura, K., Studies on Collision Protective Structures in Nuclear Powered Ships, *First International Conference on Structural Mechanics in Reactor Technology*, Paper J4/6*, Berlin, 20-24 September 1971.

Akita, Y and Kitamura, K., A study on Collision by an Elastic Stem to a Side Structures of Ships, Transaction, *Society of Naval Architects of Japan*, vol. 131, pp.307-317 1972

Aldwinckle, D., S., and Lewis, K., J., Prediction of Structural Damage Penetration and Cargo Spillage due to Ship Collisions with Icebergs, *Report SSC – 345, ICETECH – 84 SNAME ARCTIC SECTION*, April 1984.

Amdahl, J., Mechanics of Ship – Ship Collisions – Basic Crushing Mechanics, Accidental Loading on Marine Structures, Risk and Response, *WEMT '95*, Copenhagen, April 1995.

Amdahl, J., Mechanics of Grounding – Bottom Damage Estimations, Accidental Loading on Marine Structures, Risk and Response, *WEMT '95*, Copenhagen, April 1995.

Amdahl, J., and Kavlie, D., Analysis and Design of Ship Structures for Grounding Collision, *Practical Design of Ships and Mobile Units*, Caldwell & Ward Edition, 1992.

Arita, M., Ando, N., and Akita, K., Study on the Structural Strength of Ships in Collision, *Proc. Conference on Fracture Mechanics and Technology*, Hong Kong, March 1977, pp. 365 – 401.

Belli, V., On the Behaviour of Bow Structures in Collision Tests, *Tecnica Italiana*, March 1970.

Brush, O.,D., and Almroth, O., B., **Buckling of Bars, Plates, and Shells**, McGraw Hill Book Company, 1975.

Corbett, G., G., Reid, R., S., Quasi – Static and Dynamic Local Loading of Monolithic Simply – Supported Steel Plate, *International Journal of Impact Engineering*, Vol. 13, No. 3, 1993, pp. 423 – 441.

Daidola, J., C., «Tanker Structural Behavior During Collision and Grounding», *Marine Technology*, Vol. 32, No. 1, Jan. 1995, pp20 - 32.

Duffey, T.A., Scaling Laws for Fuel Capsules Subjected to Blast, Impact, and Thermal Loading, Soc. of Automotive Engineers, Reprint No. 719107, *Proc Intersociety Energy Conversion*, Eng. Conf., 1971

Discussion on the Report of the Committee V.6, *International Ship and Offshore Structures Congress*, ISSC 1994, Canada.

Faulkner, D., Adamchak, J., C., Snyder, G.J., and Vetter, M. F., *Synthesis of Welded Grillages to Withstand Compression and Normal Loads, Computers and Structures*, vol. 3, pp. 221-246, Pergamon Press, 1973.

Gerard, G., «The Crippling Strength of Compression Elements», *Journal of the Aeronautical Sciences*, 1958.

Glykas A., Samouelides E., Das P., K., «Energy Absorption Capacity of Steel Plates under Lateral Loading», *Proceedings of the 6th International Conference of Offshore and Polar Engineers*, Los Angeles, May 1996.

Glykas, A., Das, P., K., «Energy Conservation During a Tanker Collision», *Journal of Ocean Research*, accepted for publication, March 1998.

Hegazy, E., H., «Loss of Kinetic Energy in the General Case of Collision of Two Ships» *Report*, University of Newcastle, 1979

Hegazy, E., H., «A Method for Estimating the Energy Absorbed by Ship's Structures during Collision», *Report*, University of Newcastle upon Tyne, July 1980.

Hegazy, E., H., «Assessment of Collision Resistance of Ships - A Survey of the State of the Art and new Methodology», *Report*, University of Newcastle upon Tyne, October 1980.

Hodge, G.,P., **Plastic Analysis of Structures**, McGraw Hill series in Engineering Sciences, McGraw Hill, 1959.

Hughes, F., O., **Ship Structural Design**, A Rationally-Based, Computer-Aided Optimization Approach, SNAME, 1988.

Incecik, A., and Samuelides, E., Analytical and Experimental studies on ship-ship and ship-platform collisions, *Proc. of the Dynamic Modelling of Structures*, published jointly by the *Institute of Structural Engineers and Building Research Establishment*, U.K., 1981.

ISSC, «Structural Design against Collision and Grounding», Specialist Panel V.4, *13th International Ship and Offshore Structures Congress 1997*, (ISSC), Trondheim, Norway.

Ito, H., Hayashi, K., «A Comparative Study of Simplified Methods to Analyse the Strength of Double-Hulled Tankers in Collision», *Proceedings of the 4th International Offshore and Polar Engineering Conference*, Osaka, Japan, April 10 - 15, 1994.

Jones, N., Slamming Damage, *Journal of Ship Research*, vol. 17, pp.80-86, 1973

- Jones, N., «Structural Impact for Marine Structures», Impact Research Centre, Report, The University of Liverpool, *Marine Structures 2*, pp.251 - 275.
- Jones, N., «On the Collision Protection of Ships», Report 75 - 3, Massachusetts Institute of Technology, 1975.
- Jones, N., «Plastic Behavior of Ship Structures», *Trans. SNAME 1976*, New York, November 11 -13, 1976.
- Jones, N., A Literature Survey on the Collision and Grounding Protection of Ships, Ship Structure Committee, *Report SSC-283*, 1978.
- Jones, N. and Jouri, W. S., «Study of Plate Tearing for Ship Collision and Grounding Damage», *Journal of Ship Research*, 1987, Vol. 31, pp. 253 - 268.
- Kitamura, O., and Kusuba, S., A Study on the Crashworthiness of Double Side Structure of VLCC, *OMAE 1997*, Safety and Reliability, Vol. II, pp. 181.
- Kitamura, O., Comparative Study on Collision Resistance of Side Structure, *Marine Technology*, Vol. 34, No. 4, Oct. 1997, pp. 293 – 308.
- Kuroiwa, T., Nakamura, T., Kawamoto, Y., «Study on Structural Damage of Ships due to Collision and Grounding», *ISOPE '94*, Vol. IV, April 10 - 15, 1994.
- Lindberg, B., Pedersen, B., J., Plastic Deformation of Impact Loaded Frames, Department of Solid Mechanics, University of Denmark.
- Liu, J., H. and Jones, N., «Dynamic Response of a Rigid Plastic Clamped Beam Struck by a Mass at any Point on the Span», *Int. Journal of Solids and Structures*, 1988, Vol. 24, No. 3, pp251 - 270.
- Marsh, K., J., and Campbell, J., D., «The Effect of Strain Rate on the post - yield Flow of Mild Steel», *Journal of Mechanics and Physics of Solids*, Vol. 11, pp.49 - 63.
- Masuda, Y., Ikeda, H., Tsutsui, Y., Ino, Y., Yasuda, K., «Fracture Mechanics Analysis on Structural Failure of Ships», *Journal of the Society of Naval Architects of Japan*, Vol. 156, Dec. 1984.
- Minorsky, V., U., An Analysis of Ship Collisions With Reference to Protection of Nuclear Power Plants, *Journal of Ship Research*, October 1959.
- McDermott, F., J., Kline, G., R., Emlyn, L., J., Maniar, M., N., Chiang, P., W., *Trans. SNAME 1974*, New York, November 14 - 16.
- NCRE, Plastic and Limit Design, Committee 3e, Proc. Int. Ship Structures Congress, Oslo, 1967, pp. 288 – 290.

Neal, B.G., **The Plastic Methods of Structural Analysis**, Chapman & Hall Ltd., London, 1965.

Ohtsubo, H., and Wang, G., Deformation of Ship Plate Subjected to Very Large Load, *Proceedings of OMAE '97*, Vol. II, Safety and Reliability, ASME 1997.

Ostergaard, C., «Collision and Grounding Mechanics», Proceedings of Ship Safety and Protection of the Environment, *WEMT '95*, Copenhagen, Denmark, 1, 159 - 172.

Paik, J., K., and Pedersen, P., T., Modelling of the Internal Mechanics in Ship Collisions, *Ocean Engineering*, Vol. 23, No 2, pp. 107-142 1996.

Pedersen, T., Valsgard, S., Olsen, D., Spangenberg, S., Ship Impacts : Bow Collisions, *International Journal of Impact Engineering*, Vol. 13, No. 2, 1993, pp. 163 – 187.

Pedersen, P., T., «Collision and Grounding Mechanics», Proceedings of Ship Safety and Protection of the Environment, *WEMT '95*, Copenhagen, Denmark, 1, 125 - 157.

Petersen, E., Assessment of Impact Damage by means of a Simplified non – linear Approach, *Integrity of Offshore Structures*, July 1981.

Rossenblatt, M., and Son and U.S.S. Engineers and Consultants Report No. MR and S 2087 to D.O.T./Coast Guard, “Tanker Structural Evaluation” April 1972.

Rossenblatt, M., and Son, “Tanker Structural Analysis for Minor Collisions”, Report No. CG-D-72-76 to D.O.T./Coast Guard, April 1972.

Samuelides, E., Structural Dynamic and Rigid Body Response Coupling in Ship Collisions, Ph.D. Thesis, Dep. of Naval Architecture and Ocean Eng., University of Glasgow, 1984.

Schroder, K., The Effect of Surface Structure on the Brittle Fracture Strength of Metals, *Journal of the Mechanics of Physics and Solids*, Vol. 11, 1963, pp. 205 – 214.

Shen, W., Q., Jones, N., Dynamic Response of a Grillage under Mass Impact, *International Journal of Impact Engineering*, Vol. 13, No. 4, 1993, pp. 555 – 565.

Soares, G., G., and Soreide, T., H., Behaviour and Design of Stiffened Plates under Predominantly Compressive Loads, *International SB Progress*, Vol. 30, 1983, pp. 13 – 17.

Timoshenko, S., **Theory of Elastic Stability**, McGraw-Hill Limited.

Tsocalis, E.A., T.W. Kowenhoven and A.N. Perakis (1994). A Survey of Classical and New Response Methods for Marine Oil Spill Cleanup. *Marine Technology*, 31, 2, 79 –93.

Van Mater, P.R., and Giannotti, J.G. Critical Evaluation of Low-Energy Ship Collision – Damage Theories and Design Methodologies, Vol. I, *Report SSC-284*, 1978.

Van Mater, P.R., and Giannotti, J.G. Critical Evaluation of Low-Energy Ship Collision – Damage Theories and Design Methodologies, Vol. II, *Report SSC-285*, 1978.

Vredeveltdt, A., V., «Collision and Grounding Mechanics», Proceedings of Ship Safety and Protection of the Environment, *WEMT '95*, Copenhagen, Denmark, 1, 173 -180.

Woisin, G., Instantaneous loss of Energy with Unsymmetrical Ship Collisions, The third symposium on Practical Design of Ships and Mobile Units, Trondheim, Norway, June 22 – 26, 1987.

Zhiliang, Fan, «Load Carrying Mechanism of Restrained Plates at Large Deflections», *Journal of Engineering Mechanics*, Vol. 120, No. 6, June 1994.

Zhu, L., Dynamic Inelastic Behaviour of Ship Plates in Collision, Ph.D. Thesis, Dept. of Naval Architecture and Ocean Engin., University of Glasgow, 1990.

Zhu, L., Faulkner, D., Dynamic Inelastic Behavior of Plates in Minor Ship Collisions, *International Journal of Impact Engineering*, Vol. 15, No. 2, 1994, pp.165 – 178.

Appendix A

Mid-ship Section Design Calculations

Longitudinal Hull – girder Strength of the assumed Single Hull Tanker

In this paragraph will take place calculations of the longitudinal strength of the assumed ship. It is necessary to obtain the wave bending moment and the induced by wave shear force to design the mid-ship section of a ship. For the calculation of these values approximate methods recommended from the classification societies will be used.

Two of those methods are going to be used here. The first originates from ABS in the Steel Vessels Part 3, Section 6 “Longitudinal Strength”. The second one originates from Lloyd’s Register.

▪ **ABS method**

According to the American Bureau of Shipping the maximum bending moment in steel water condition M_s , can be calculated from the following formula:

$$M_s = C_{st} \times L^{2.5} \times B \times (C_B + 0.5) \quad (\text{ton}\cdot\text{m})$$

where:

- $C_{st} = 0.544 \times 10^{-2}$
- $L = 240.00 \text{ m}$
- $B = 41.00 \text{ m}$

- $C_B = 0.855$

From the formula above the steel-water-condition bending moment is calculated to be:

$$M_s = 309486.175 \text{ ton}\cdot\text{m} = 3036059.377 \text{ KNt}\cdot\text{m}$$

Wave Bending Moments:

The additional bending moment induced by wave in the sagging-condition is given by the following formula:

$$M_{ws} = -k_1 C_1 L^2 B (C_B + 0.7) \times 10^{-3} \text{ (KNt}\cdot\text{m)}$$

where:

$$k_1 = 110$$

$$C_1 = 10.75 - ((300-L)/100)^{1.5} = 10.28524$$

By substituting the values in the formula above and calculating the sagging-condition bending moment is found to be:

$$M_{ws} = -4154741.554 \text{ KNt}\cdot\text{m}$$

The additional bending moment induced by wave in the hogging-condition is given by the following formula:

$$M_{wh} = +k_2 C_1 L^2 B C_b \times 10^{-3} \text{ (KNt} \cdot \text{m)}$$

where:

$$k_2 = 190$$

By substituting the values in the formula above the hogging-condition bending moment is found to be:

$$M_{wh} = 3945849.922 \text{ KNt} \cdot \text{m}$$

It can be seen that the bending moment in the hogging-condition is the largest. So the maximum bending moment induced by wave is:

$$\begin{aligned} M_t &= M_s + M_{wh} = 3036059.377 + 3945849.922 = 6981909.299 \text{ KNt} \cdot \text{m} = \\ &= 711713.486 \text{ ton} \cdot \text{m} \end{aligned}$$

▪ *Lloyd's Register method*

The steel water bending moment will be assumed to be the one calculated in the previous section. The additional bending moment induced by wave is calculated from the following formula:

$$\begin{aligned} M_w &= 0.01 C_1 L^2 B (C_b + 0.7) \Rightarrow \\ M_w &= 376236.19 \text{ ton} \cdot \text{m} = 3690877.024 \text{ KNt} \cdot \text{m} \end{aligned}$$

So the maximum bending moment according to Lloyd's regulation is the sum of the still water condition and the wave induced bending moment:

$$M_t = M_s + M_w = 3036059.377 + 3690877.024 = 6726936.401 \text{ KNt} \cdot \text{m}$$

Section Modulus

The required hull-girder section modulus for 0.4L amidships is to be obtained from the following equation:

$$SM = M_t / f_p$$

where:

M_t : total bending moment as obtained from the equation in the previous section.

$$f_p : \text{nominal permissible bending stress} = 17.5 \text{ KNt/cm}^2 = 175000 \text{ KNt/m}^2$$

Finally we obtain the section modulus:

$$SM = 398966.246 \text{ m-cm}^2 = 39.897 \text{ m}^3 \quad (\text{A-1})$$

The minimum hull – girder section modulus amidships is not to be less than obtained from the following equation:

$$SM = C_1 C_2 L^2 B (C_b + 0.7) \text{ m-cm}^2$$

where:

C_1 : as defined in the previous section

C_2 : 0.01 in SI

By substituting and calculating the minimum section modulus is found to be:

$$SM_{\min} = 377703.63 \text{ m-cm}^2 = 37.770 \text{ m}^3 \quad (\text{A-2})$$

According to the regulations the section modulus to be used is the greater value between the (A-1) and (A-2). So the section modulus is **SM = 398966.246 m-cm²**.

Frame Spacing

The standard frame spacing S amidships for vessels with transverse framing may be obtained from the following equation:

$$S_{\max} = 2.08 \cdot L + 438 \text{ mm} \quad \text{for } L \leq 270 \text{ m}$$

$$S_{\max} = (2.08 \cdot 240 + 438) \text{ mm} \Rightarrow S_{\max} = 937.2 \text{ mm}$$

This is the maximum allowable spacing for the frames. A frame spacing in the order of $S = 935 \text{ mm}$ is selected for the ship under study.

The web frames are selected to be every fourth frame. That concludes in a web frame spacing in the order of $S_{\text{web}} = 3740 \text{ mm}$.

Mid - ship Section preliminary design

In the paragraphs below will be conducted the calculations of the structural members which constitute the mid – ship section of a ship. Calculations of the thickness of deck plating, shell plating and bottom plating will take place as well as calculations of the scantlings of stiffeners for the length of 0.4L amidships. These calculations will be conducted under the regulation of the American Bureau of Shipping and the choice of the stiffeners will be such so that the designed ship will have sufficient strength against the foregoing calculated loads.

The form of the mid – ship section is based on similar single hull tankers and presented in figure A1. It must be noted that the framing of the ship is assumed to be multidirectional.

From the previous calculations the section modulus of the mid – ship section is required to be $SM_{req} = 398966.246m\text{-cm}^2$. In the following paragraphs the formulae of Part 3 of the ABS are used to calculate the thickness and scantlings of the structural members.

Calculation of Plating and Girders

Bottom Shell Plating

The term “bottom plating” refers to the plating from the keel to the upper turn of the bilge for 0.4L amidships. The minimum thickness of the bottom plating is not to be less than obtained from the following equation:

$$t = \frac{s}{508} \cdot \sqrt{(L - 62.5) \cdot \frac{d}{D_s}} + 2.5\text{mm} \Rightarrow t = 21.27\text{mm} \quad \text{for } 122 \leq L \leq 305 \text{ m}$$

where:

S: frame spacing = 935mm

L: length of vessel = 240 m

d : design draft = 15.950 m

D_s : depth moulded = 21.200 m

After all other requirements are met, the thickness, t_{min} of shell plating amidships below the upper turn of bilge for ships of unrestricted class and service is not to be less than obtained from the following equation:

$$t_{min} = s \cdot \frac{(L - 18.3)}{(42 \cdot L + 1070)} \text{ mm} \Rightarrow t_{min} = 18.591 \text{ mm} \quad \text{for } L \leq 427 \text{ m}$$

Finally for the bottom plating is selected a thickness in the order of $t_b = 23.000 \text{ mm}$.

Keel Plating

The minimum required thickness of the plate keel is obtained from the thickness of the bottom plating by adding 1.5mm.

$$t_{min} = 21.270 + 1.5 = 22.770 \text{ mm}$$

For the plate keel is selected a thickness in the order of $t_{keel} = 24.000 \text{ mm}$.

Side Shell Plating

The minimum thickness t of the side shell plating for the midship $0.4L$ for vessels having lengths up to 305 m is to be obtained from the following equation:

$$t_{\min} = \frac{s}{645} \cdot \sqrt{(L - 15.2) \cdot \left(\frac{d}{D_s}\right)} + 2.5 \text{mm} \Rightarrow t_{\min} = 18.852 \text{mm}$$

For the side shell plating is selected a thickness in the order of $t_{\text{shell}} = 20.000 \text{mm}$.

Shearstrake

The thickness of the shearstrake is to be not less than the thickness of the side shell plating nor less than required from the following equation:

$$t_{\min} = \frac{24.38 \cdot s_b}{1615.4 - 1.1 \cdot L} \text{mm} \Rightarrow t_{\min} = 17.14 \text{mm} \quad \text{for } 183 \leq L \leq 427 \text{ m}$$

In conclusion the thickness of the shearstrake is selected in the order of $t_{\text{strake}} = 20.000 \text{mm}$.

Deck Plating

The deck plating is to be of the thickness necessary to obtain the required hull-girder section modulus. Also the thickness outside the line of the openings, or completely across the vessel where there are no centreline openings, is not to be less than the maximum of the values obtained from the equations:

$$t = 0.006 \cdot s_b + 4.7 \text{ mm} \Rightarrow t = 10.310 \text{ mm} \quad \text{for } s_b > 760 \text{mm}$$

$$t_{\min} = \frac{24.38 \cdot s_b}{1615.4 - 1.1 \cdot L} \text{mm} \Rightarrow t_{\min} = 17.14 \text{mm} \quad \text{for } 183 \leq L \leq 427 \text{ m}$$

For the deck plating is finally selected a thickness in the order of $t_{\text{deck}} = 20.000\text{mm}$.

Centre Girder

Centre girder plates are to be of the thickness and depths given by the following equations:

Thickness Amidships:

$$t = 0.056 \cdot L + 5.5 \text{ mm} \Rightarrow t = 18.940\text{mm} \quad \text{for } L \leq 427 \text{ m}$$

Depth:

$$d = 32 \cdot B + 190 \sqrt{d} \text{ mm} \Rightarrow d = 2186.83 \text{ mm} \quad \text{for } L \leq 427 \text{ m}$$

So for the centre girder is selected the thickness to be $t = 19.000\text{mm}$ and the depth to be $d = 2200.0\text{mm}$.

Side Girders

The side girder plates are to be of the thickness given by the following equation and depth equal to the value obtained for the centre girder:

$$t = 0.036 \cdot L + 6.2 \text{ mm} \Rightarrow t = 14.840 \text{ mm} \quad \text{for } L \leq 427 \text{ m}$$

For the side girders is selected a thickness in the order of $t = 15.000 \text{ mm}$.

Margin Plating

The minimum thickness of the margin plate is to be obtained from the following equation:

$$t = 0.037*L + 0.009*s + 1.5 \text{ mm} \Rightarrow t = 18.795 \text{ mm}$$

For the margin plating is selected a thickness in the order of $t = 19.000 \text{ mm}$.

Calculation of Stiffeners and Frames

Bottom Plating Stiffeners

The required section modulus for the bottom plating stiffeners is given from the following equation:

$$SM = 7.8 c h s l^2 = 2160.429 \text{ cm}^3$$

where:

$c = 1.3$ for bottom longitudinal stiffeners.

h : distance in m from the keel to the load line (d), or two-thirds of the distance to the bulkhead of freeboard deck whichever is greater, $h=15.950 \text{ m}$

s : spacing of the stiffeners, $s=0.955 \text{ m}$

l : distance in m between the supports but is not to be taken as less than 1.83m,
 $l=3.740\text{m}$

Because of the magnitude of the required section modulus the type of the stiffener was not selected from a table for standard stiffeners. The stiffener selected is a **T-bar stiffener 600x200x18** and the calculated section modulus $SM = 2178 \text{ cm}^3$.

The calculations of the section modulus are shown in Table A1.

Deck Plating Stiffeners

The required section modulus for the deck plating stiffeners is given from the equation:

$$\mathbf{SM = 7.8 c h s l^2 = 652.983 \text{ cm}^3}$$

where: $c = 1.2$ for deck plating stiffeners.

h, s, l , as defined in the previous paragraph.

The stiffener selected for the deck plating is a standard one according to the British Steel Table shown as Table A2. The stiffener is a **bulb stiffener 430x62.5x17** and the section modulus provided from the Table is: **$SM = 700 \text{ cm}^3$** .

Side Shell Stiffeners

The required section modulus for the side shell plating stiffeners is given from the following equation:

$$\mathbf{SM = 7.8 c h s l^2}$$

where:

$c = 0.95$ for longitudinal shell stiffeners.

h, s, l : as defined in the above paragraphs.

Stiffeners	c	h	s	<i>I</i>	SM(cm ³)
Side Upper	0.95	2.620	0.950	3.740	257.980
Side Middle	0.95	6.330	0.950	3.740	623.288
Side Lower	0.95	13.75	0.950	3.740	1353.900

For the upper side shell plate a standard stiffener is selected (Table A2):

Bulb stiffener 320x46x11.5 and SM = 266 cm³.

For the middle part of the side shell plating a standard stiffener is selected (Table A2):

Bulb stiffener 430x62.5x17 and SM = 700 cm³.

For the lower side shell plating a stiffener with very high section modulus is needed.

The stiffener was calculated to be a **T-bar stiffener 550x200x18** and section modulus calculated as shown in Table A1: **SM = 1599 cm³.**

Transverse Frames

The minimum required section modulus of each transverse frame amidships is to be obtained from the following equation:

$$SM = s \cdot l^2 \cdot \left(h + \frac{b \cdot h_1}{33} \right) \cdot \left(7 + \frac{45}{l^3} \right) \text{cm}^3 \Rightarrow SM = 9469.685 \text{cm}^3$$

where:

l: the span in m between the toes of brackets, *l* = 17.000 m

s: frame spacing in m, *s* = 0.935 m

h: vertical distance in m from the middle of *l* to the load line or 0.4*l* whichever is greater, *h* = 5.000 m.

b: horizontal distance in m from the outside of the frames to the first row of deck supports, *b* = 2.000 m.

h_1 : vertical distance in m from the deck at the top of the frame to the bulkhead or freeboard deck, $h_1 = 0.00$ m.

Because of the magnitude of the required section modulus of the frames there was not used a standard beam. The selected beam is calculated to be a **T-bar beam 950x250x18** and section modulus calculated as shown in Table A1: **SM = 10072 cm³**.

Web Frames

Each web frame amidships and aft is to have a section modulus not less than obtained from the following equation:

$$SM = 4.74 \cdot c \cdot s \cdot l^2 \cdot \left(h + \frac{bh_1}{45K} \right) \text{cm}^3 \Rightarrow SM = 38424.573 \text{cm}^3$$

where:

c : 1.5

s : spacing of the web frames in m, $s = 3.740$ m

l : span in m measured from the line of the bottom transverse to the deck at the top of the web frames, $l = 17.000$ m

h : vertical distance in m from the middle of l to the load line, $h = 5.000$ m

h_1 : as explained in the previous paragraph, $h_1 = 0.00$ m

b : as explained in the previous paragraph, $b = 2.000$ m

K : 1.0 where the decks are longitudinally framed and a deck transverse is fitted in way of each web frame.

Because of the magnitude of the required section modulus of the web frames there was not used a standard beam. The selected beam is calculated to be a **T-bar beam 1500x250x20** and section modulus calculated as shown in Table A1: **SM = 41502 cm³**.

Properties of the Mid-Ship Section

Finally, in Table A-3 is illustrated the calculation of the neutral axis of the mid-ship section and of the section modulus. As it can be seen the proposed structure satisfy the requirements imposed by the classification society in terms of the section modulus. The section modulus of the proposed mid-ship section is found to be:

$$\mathbf{SM = 400811.33 \text{ m-cm}^2}.$$

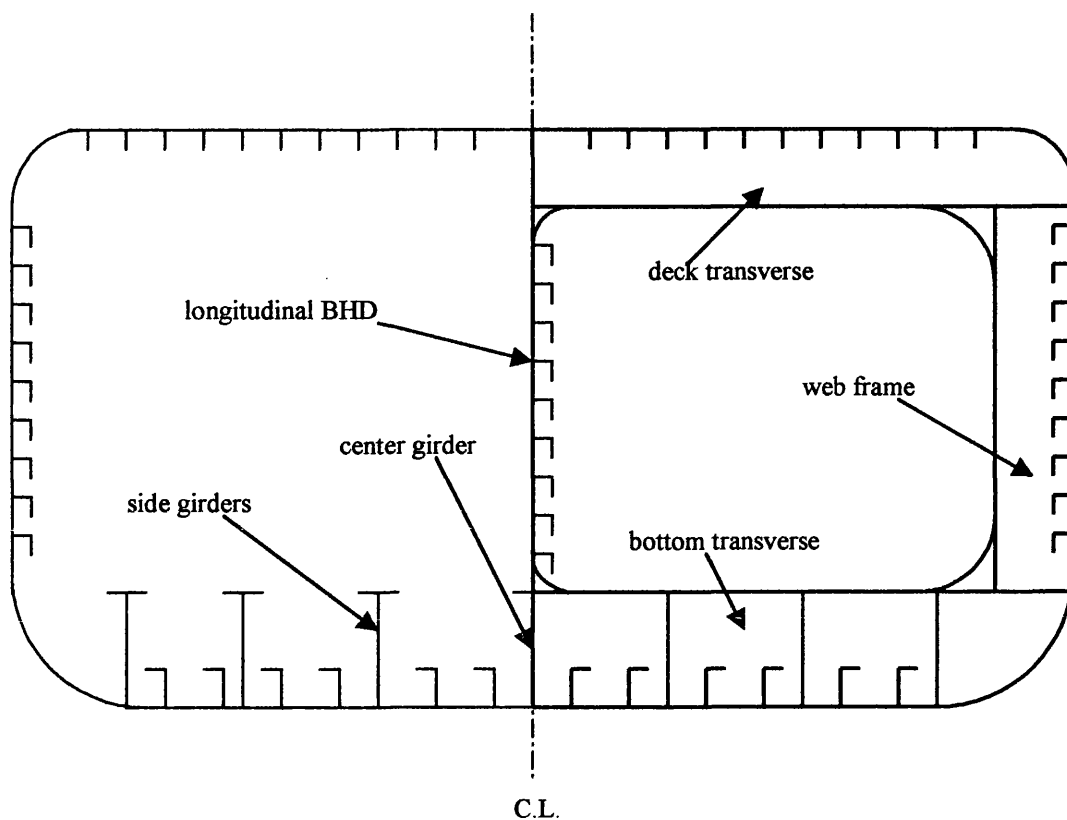
Appendix A - Figures

Figure A1: Typical midship section of a single hull Oil Tanker. Descriptions of some of the above-calculated structural members are also shown.

TABLE A1 : Calculations of the Section Modulus of non-standard stiffeners

Bottom Stiffeners		A/A	l (cm)	t (cm)	A (cm ²)	z (cm)	A*z (cm ³)	A*z ² (cm ⁴)	i (cm ⁴)
Web	1		60,0	1,8	108,0	30,0	3240,0	97200,0	32400,0
T-bar	2		20,0	1,8	36,0	60,9	2192,4	133517,2	9,7
			$\Sigma A =$	$\Sigma A =$	$\Sigma A =$	$\Sigma A^*z =$	$\Sigma A^*z =$	$\Sigma A^*z^2 =$	$\Sigma i =$
			144,0	144,0	144,0	5432,4	5432,4	230717,2	32409,7
<p>z = 37,725 cm from bottom</p> <p>SM_{BOTTOM} = 3084,9 cm³ SM_{TOP} = -3136,3 cm³</p> <p>SM_{req} = 2160,4 cm³</p>									
Side Shell Lower Stiffeners		A/A	l (cm)	t (cm)	A (cm ²)	z (cm)	A*z (cm ³)	A*z ² (cm ⁴)	i (cm ⁴)
Web	1		55,0	1,8	99,0	27,5	2722,5	74868,8	24956,3
T-bar	2		20,0	1,8	36,0	55,9	2012,4	112493,2	9,7
			$\Sigma A =$	$\Sigma A =$	$\Sigma A =$	$\Sigma A^*z =$	$\Sigma A^*z =$	$\Sigma A^*z^2 =$	$\Sigma i =$
			135,0	135,0	135,0	4734,9	4734,9	187361,9	24966,0
<p>z = 35,07 cm from bottom</p> <p>SM_{BOTTOM} = 2637,9 cm³ SM_{TOP} = -2681,3 cm³</p> <p>SM_{req} = 1353,9 cm³</p>									

Frames	A/A	I (cm)	t (cm)	A (cm ²)	z (cm)	A ² z (cm ³)	A ² z ² (cm ⁴)	I (cm ⁴)
Web	1	95,0	1,8	171,0	47,5	8122,5	385818,8	128606,3
T-bar	2	25,0	1,8	45,0	95,9	4315,5	413856,5	12,2
	$\Sigma A =$			216,000	$\Sigma A^2z =$	12438,0	799675,2	128618,4

Z = 57,58 cm from bottom

SM_{BOTTOM} = 7365,7 cm³

SM_{TOP} = -7491,7 cm³

SM_{req} = 9469,7 cm³

Web Frames	A/A	I (cm)	t (cm)	A (cm ²)	z (cm)	A ² z (cm ³)	A ² z ² (cm ⁴)	I (cm ⁴)
Web	1	220,0	2,0	440,0	110,0	48400,0	5324000,0	1774666,7
T-bar	2	30,0	2,0	60,0	221,0	13260,0	2930460,0	20,0
	$\Sigma A =$			500,000	$\Sigma A^2z =$	61660,0	8254460,0	1774686,7

Z = 123,32 cm from bottom

SM_{BOTTOM} = 39332,4 cm³

SM_{TOP} = -40053,4 cm³

SM_{req} = 38424,6 cm³

Deck Transverse	A/A	I (cm)	t (cm)	A (cm ²)	z (cm)	A*z (cm ³)	A*z ² (cm ⁴)	I (cm ⁴)
Web	1	150,0	2,0	300,0	75,0	22500,0	1687500,0	562500,0
T-bar	2	20,0	2,0	40,0	151,0	6040,0	912040,0	13,3
	ΣA =			340,000	ΣA*z =	28540,0	2599540,0	562513,3

Z = 83,94 cm from bottom

SM_{BOTTOM} = 18259,7 cm³

SM_{TOP} = -18596,5 cm³

SM_{req} = 17348,3 cm³

Bottom Transverse	A/A	I (cm)	t (cm)	A (cm ²)	z (cm)	A*z (cm ³)	A*z ² (cm ⁴)	I (cm ⁴)
Web	1	210,0	2,0	420,0	105,0	44100,0	4630500,0	1543500,0
T-bar	2	30,0	2,0	60,0	211,0	12660,0	2671260,0	20,0
	ΣA =			480,0	ΣA*z =	56760,0	7301760,0	1543520,0

Z = 118,25 cm from bottom

SM_{BOTTOM} = 36083,0 cm³

SM_{TOP} = -36741,8 cm³

SM_{req} = 35136,9 cm³

TABLE A2: British Steel Standard Stiffeners.

SIZE mm	WIDTH b mm	THICK t mm	BULB HGHT C mm	BULB RAD r1 mm	AREA OF X SECTION F cm ²	MASS PER UNIT LENGTH G kg/m	SURFACE AREA U m ² /m	CENTROID ex cm	MOMENT OF INERTIA Ix cm ⁴	MODULUS Wx cm ³
120	6	6	17	5	9,31	7,31	0,276	7,2	133	18,4
	7	7	17	5	10,5	8,25	0,278	7,07	148	21,0
	8	8	17	5	11,7	9,19	0,280	6,96	164	23,6
140	6,5	6,5	19	5,5	11,7	9,21	0,319	8,37	228	27,3
	7	7	19	5,5	12,4	9,74	0,320	8,31	241	29,0
	8	8	19	5,5	13,8	10,83	0,322	8,18	266	32,5
	10	10	19	5,5	16,6	13,03	0,326	7,92	316	39,8
160	7	7	22	6	14,6	11,4	0,365	9,66	373	38,6
	8	8	22	6	16,2	12,7	0,367	9,49	411	43,3
	9	9	22	6	17,8	14,0	0,369	9,36	448	47,9
	11,5	11,5	22	6	21,8	17,3	0,374	9,11	544	59,8
180	8	8	25	7	18,9	14,8	0,411	10,9	609	55,9
	9	9	25	7	20,7	16,2	0,413	10,7	663	61,8
	10	10	25	7	22,5	17,6	0,415	10,6	717	67,8
	11,5	11,5	25	7	25,2	19,7	0,418	10,4	799	76,8
200	8,5	8,5	28	8	22,6	17,8	0,456	12,2	902	74,0
	9	9	28	8	23,6	18,5	0,457	12,1	941	77,7
	10	10	28	8	25,6	20,1	0,459	11,9	1020	85,0
	11	11	28	8	27,6	21,7	0,461	11,8	1090	92,3
	12	12	28	8	29,6	23,2	0,463	11,7	1160	99,6
220	9	9	31	9	26,8	21,0	0,501	13,6	1296	95,3
	10	10	31	9	29,0	22,8	0,503	13,4	1400	105
	11	11	31	9	31,2	24,5	0,505	13,2	1500	113
	12	12	31	9	33,4	26,2	0,507	13	1590	122
240	9,5	9,5	34	10	31,2	24,4	0,546	14,8	1800	123
	10	10	34	10	32,4	25,4	0,547	14,7	1860	126
	11	11	34	10	34,9	27,4	0,549	14,6	2000	137
	12	12	34	10	37,3	29,3	0,551	14,4	2130	148
260	10	10	37	11	36,1	28,3	0,593	16,2	2477	153

11	11	37	11	38,7	30,3	0,593	16	2610	162
12	12	37	11	41,3	32,4	0,595	15,8	2770	175
280	10,5	40	12	41,2	32,4	0,636	17,5	3223	184
11	11	40	12	42,6	33,5	0,637	17,4	3330	191
12	12	40	12	45,5	35,7	0,639	17,2	3550	206
13	13	40	12	48,4	37,9	0,641	17	3760	221
300	11	43	13	46,7	36,7	0,681	18,9	4190	222
12	12	43	13	49,7	39,0	0,683	18,7	4460	239
13	13	43	13	52,8	41,5	0,685	18,5	4720	256
320	11,5	46	14	52,6	41,2	0,727	20,2	5370	266
12	12	46	14	54,2	42,5	0,728	20,1	5530	274
13	13	46	14	57,4	45,0	0,730	19,9	5850	294
14	14	46	14	60,6	47,5	0,732	19,7	6170	313
340	12	49	15	58,8	46,1	0,772	21,5	6760	313
13	13	49	15	62,2	48,8	0,774	21,3	7160	335
14	14	49	15	65,5	51,5	0,776	21,1	7540	357
15	15	49	15	69,0	54,2	0,778	20,9	7920	379
370	12,5	53,5	16,5	67,8	53,1	0,839	23,6	9213	390
13	13	53,5	16,5	69,6	54,6	0,840	23,5	9470	402
14	14	53,5	16,5	73,3	57,5	0,842	23,2	9980	428
15	15	53,5	16,5	77,0	60,5	0,844	23	10490	455
16	16	53,5	16,5	80,7	63,5	0,846	22,8	10980	481
400	13	58	18	77,4	60,8	0,907	25,8	12280	476
14	14	58	18	81,4	63,9	0,908	25,5	12930	507
15	15	58	18	85,4	67,0	0,910	25,2	13580	537
16	16	58	18	89,4	70,2	0,912	25	14220	568
430	14	62,5	19,5	89,7	70,6	0,975	27,7	16460	594
15	15	62,5	19,5	94,1	73,9	0,976	27,4	17260	628
17	17	62,5	19,5	103,0	80,6	0,980	26,9	18860	700
20	20	62,5	19,5	115,0	90,8	0,986	26,3	21180	804

Table A-3: Mid-ship Section Properties**Calculation of the Neutral Axis of the Midship Section****Plating**

Member	l (cm)	t (cm)	A (cm ²)	z (m)	A*z (m*cm ²)	A*z ² (m ² *cm ²)	Ix (m ² *cm ²)	
Keel Plate	280,00	2,40	672,0	0,00	0,00	0,00	0,032	
Bottom Plate	1570,00	2,20	3454,0	0,00	0,00	0,00	0,139	
Bilge Plate	370,00	2,20	814,0	1,20	976,80	1172,16	3,142	
Side shel Plate	1575,00	2,00	3150,0	10,20	32130,00	327726,00	65116,406	
Shearstrake	300,00	2,00	600,0	19,70	11820,00	232854,00	450,000	
Main Deck Plate	2050,00	2,00	4100,0	21,20	86920,00	1842704,00	0,137	
Longitudinal BHD	1915,00	2,10	4021,5	11,24	45181,55	507614,74	122897,878	
ΣA =			16811,5	ΣA*z =		177028,35	2912070,90	188467,734

Bottom Stiffeners No. 1 - 22

Member	l (cm)	t (cm)	A (cm ²)	z (m)	A*z (m*cm ²)	A*z ² (m ² *cm ²)	Ix (m ² *cm ²)	
Web	600,00	2,00	26400,0	0,30	7920,00	2376,00	79200,000	
T-bar	200,00	2,00	8800,0	0,61	5359,20	3263,75	0,293	
ΣA =			35200,00	ΣA*z =		13279,200	5639,75	79200,29

Lower Side Shell Stiffeners No. 15 - 20

Member	l (cm)	t (cm)	A (cm ²)	z (m)	A*z (m*cm ²)	A*z ² (m ² *cm ²)	Ix (m ² *cm ²)	
No. 15	55,00	1,80	99,00	6,95	688,05	4781,95	0,003	
	20,00	1,80	36,00	6,85	246,60	1689,21	0,120	
No. 16	55,00	1,80	99,00	6,00	594,00	3564,00	0,003	
	20,00	1,80	36,00	5,90	212,40	1253,16	0,120	
No. 17	55,00	1,80	99,00	5,05	499,95	2524,75	0,003	
	20,00	1,80	36,00	4,95	178,20	882,09	0,120	
No. 18	55,00	1,80	99,00	4,10	405,90	1664,19	0,003	
	20,00	1,80	36,00	4,00	144,00	576,00	0,120	
No. 19	55,00	1,80	99,00	3,15	311,85	982,33	0,003	
	20,00	1,80	36,00	3,05	109,80	334,89	0,120	
No. 20	55,00	1,80	99,00	2,20	217,80	479,16	0,003	
	20,00	1,80	36,00	2,10	75,60	158,76	0,120	
ΣA =			810,00	ΣA*z =		3684,15	18890,48	0,736

Middle Side Shell Stiffeners No. 8 - 14

Member	l (cm)	t (cm)	A (cm ²)	z (m)	A*z (m*cm ²)	A*z ² (m ² *cm ²)	Ix (m ² *cm ²)	
No. 8	43,00	1,70	103,00	13,60	1400,80	19050,88	1,886	
No. 9	43,00	1,70	103,00	12,65	1302,95	16482,32	1,886	
No. 10	43,00	1,70	103,00	11,70	1205,10	14099,67	1,886	
No. 11	43,00	1,70	103,00	10,75	1107,25	11902,94	1,886	
No. 12	43,00	1,70	103,00	9,80	1009,40	9892,12	1,886	
No. 13	43,00	1,70	103,00	8,85	911,55	8067,22	1,886	
No. 14	43,00	1,70	103,00	7,90	813,70	6428,23	1,886	
ΣA =			721,00	ΣA*z =		7750,75	85923,37	13,202

Upper Side Shell Stiffeners No. 1 - 7

Member	l (cm)	t (cm)	A (cm ²)	z (m)	A*z (m ² cm ²)	A*z ² (m ² cm ²)	Ix (m ² cm ²)
No. 1	32,00	1,15	52,60	20,25	1065,15	21569,29	0,537
No. 2	32,00	1,15	52,60	19,30	1015,18	19592,97	0,537
No. 3	32,00	1,15	52,60	18,35	965,21	17711,60	0,537
No. 4	32,00	1,15	52,60	17,40	915,24	15925,18	0,537
No. 5	32,00	1,15	52,60	16,45	865,27	14233,69	0,537
No. 6	32,00	1,15	52,60	15,50	815,30	12637,15	0,537
No. 7	32,00	1,15	52,60	14,55	765,33	11135,55	0,537
ΣA =			368,20	ΣA*z =	6406,68	112805,43	3,759

Main Deck Stiffeners No. 1 - 20

Member	l (cm)	t (cm)	A (cm ²)	z (m)	A*z (m ² cm ²)	A*z ² (m ² cm ²)	Ix (m ² cm ²)
No. 1	43,00	1,80	110,00	20,93	2302,41	48191,74	1,924
No. 2	43,00	1,80	110,00	20,93	2302,41	48191,74	1,924
No. 3	43,00	1,80	110,00	20,93	2302,41	48191,74	1,924
No. 4	43,00	1,80	110,00	20,93	2302,41	48191,74	1,924
No. 5	43,00	1,80	110,00	20,93	2302,41	48191,74	1,924
No. 6	43,00	1,80	110,00	20,93	2302,41	48191,74	1,924
No. 7	43,00	1,80	110,00	20,93	2302,41	48191,74	1,924
No. 8	43,00	1,80	110,00	20,93	2302,41	48191,74	1,924
No. 9	43,00	1,80	110,00	20,93	2302,41	48191,74	1,924
No. 10	43,00	1,80	110,00	20,93	2302,41	48191,74	1,924
No. 11	43,00	1,80	110,00	20,93	2302,41	48191,74	1,924
No. 12	43,00	1,80	110,00	20,93	2302,41	48191,74	1,924
No. 13	43,00	1,80	110,00	20,93	2302,41	48191,74	1,924
No. 14	43,00	1,80	110,00	20,93	2302,41	48191,74	1,924
No. 15	43,00	1,80	110,00	20,93	2302,41	48191,74	1,924
No. 16	43,00	1,80	110,00	20,93	2302,41	48191,74	1,924
No. 17	43,00	1,80	110,00	20,93	2302,41	48191,74	1,924
No. 18	43,00	1,80	110,00	20,93	2302,41	48191,74	1,924
No. 19	43,00	1,80	110,00	20,93	2302,41	48191,74	1,924
No. 20	43,00	1,80	110,00	20,93	2302,41	48191,74	1,924
ΣA =			2200,00	ΣA*z =	46048,20	963834,87	38,480

Longitudinal BHD Stiffeners

The longitudinal bulkhead's stiffeners are assumed to be the same as the side shell's stiffeners.

Calculation of the Neutral Axis, Moment of Inertia and Section Modulus.

Neutral Axis :

Distance from keel :	$z_{\text{bottom}} =$	4,690	m
Distance from deck:	$z_{\text{deck}} =$	16,510	m

Moment of Inertia :

$\Sigma Az^2 =$	4316784,11 m ² *cm ²
-----------------	--

$\Sigma I =$	267741,901 m ² *cm ²
--------------	--

$\Sigma A =$	58009,90 cm ²
--------------	--------------------------

$I_z =$	6617585,1 m ² *cm ²
---------	---

Section Modulus :

$SM_{\text{bottom}} =$	1411141,69 m*cm ²
------------------------	------------------------------

$SM_{\text{deck}} =$	400811,325 m*cm ²
----------------------	------------------------------

$SM_{\text{required}} =$	398966,246 m*cm ²
--------------------------	------------------------------

Appendix B

Energy absorbed due to membrane tension in the stiffened hull of the struck ship

Consider a strip of the (vertical) hull side plating in the struck ship, as a rigid perfectly plastic beam with fully clamped supports across a span $2L$, and subjected to a concentrated load p (see Figure B1). Then it can be shown that:

$$\frac{p}{p_c} = \frac{2W}{t_s} \quad \left(\frac{W}{t_s} \geq \frac{1}{1+2a} \right) \quad (\text{B-1})$$

where,

W = inwards deflection at load point

t_s = plating thickness

$$P_c = \text{collapse load} = \frac{2M_o(2L)}{a \cdot b}$$

$$M_o = \text{yield moment} = \sigma_y \frac{dx \cdot t_s^2}{4}$$

dx = width of strip

$$\alpha = \frac{2 \cdot L \cdot \Delta}{2 \cdot W^2}$$

σ_y = material yield stress

Δ = the displacement of the supports in the original plane of the plating

$\alpha = 0$ for full axial restraint

$\alpha = -0.5$ for zero axial restraint

a and b define the load position as shown in Figure B1.

Substitution gives:

$$P = \sigma_y \cdot t_s \cdot dx \cdot \left(\frac{1}{a} + \frac{1}{b} \right) \cdot W \quad (\text{B-2})$$

The energy absorbed in plastic deformation of this elementary strip of plating is therefore:

$$\delta E_1 = \int_0^W P dW = \frac{1}{2} \sigma_y t_s W^2 \left(\frac{1}{a} + \frac{1}{b} \right) dx \quad (\text{B-3})$$

For a vertical striking bow the indentation W is constant over the vertical depth of damage H (see Figure 1) and the total energy absorbed is therefore:

$$E_1 = \frac{1}{2} \sigma_y t_s W^2 \left(\frac{1}{a} + \frac{1}{b} \right) H \quad (\text{B-4})$$

or,

$$E_1 = \frac{1}{2} \sigma_y \left(\frac{W}{L} \right)^2 R_{T1} B \quad (\text{B-5})$$

where:

$R_T = 2LHt_s =$ the volume of the deformed portion of hull plating.

$$B = \frac{1}{4} \left[\frac{1}{a/2L} + \frac{1}{b/2L} \right] = \frac{L^2}{a \cdot b} \quad (\text{B-6})$$

For mid-span strike, $a = b = L$ and $B = 1$, therefore, the absorbed energy in this case will be:

$$E_1^o = \frac{1}{2} \sigma_y \left(\frac{W}{L} \right)^2 R_{T1} \tag{B-7}$$

It should be pointed out that, from equation (B-2) it follows that the membrane tension force per unit height of shell plating is given by:

$$T_s = \sigma_y \cdot t_s \tag{B-8}$$

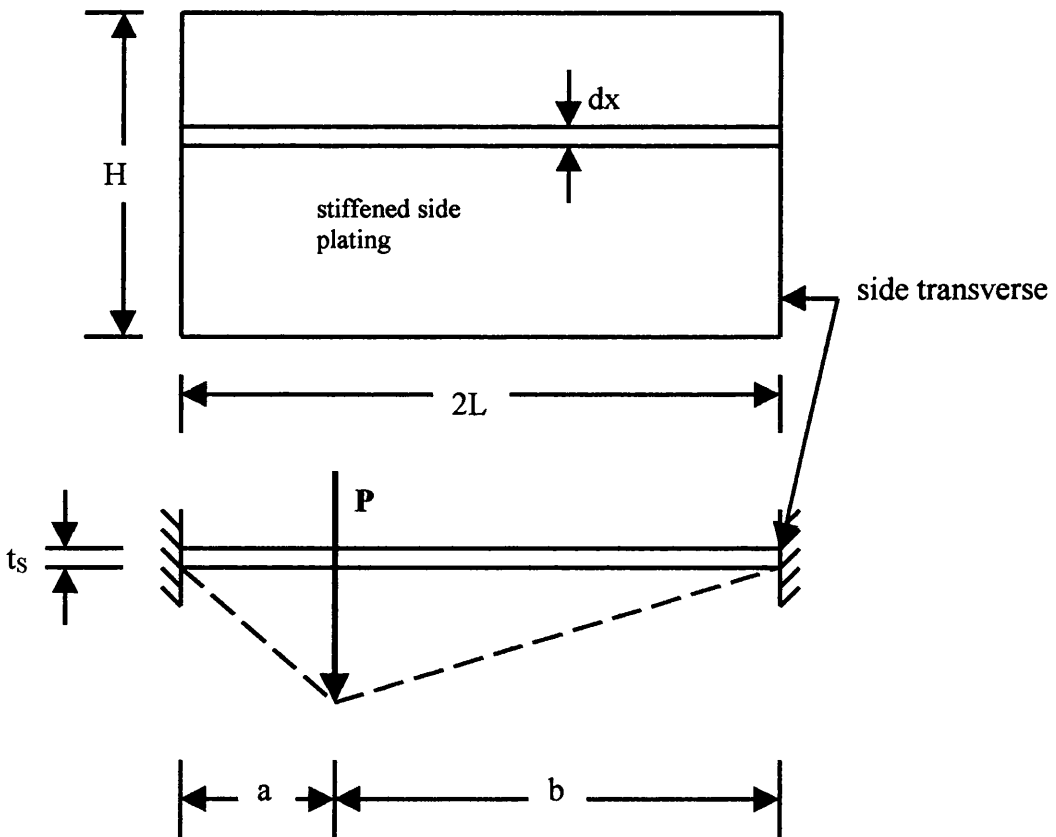


Figure B1: Membrane tension in stiffened side plating.

Appendix C

Energy absorbed due to membrane tension in the stiffened deck of the struck ship

Consider the right side of the distorted area shown in Figure C1. Assuming that the in-plane stress in this zone has reached the yield stress σ_y , the membrane force acting in an increment (dx) of the distorted depth is given by:

$$T_x = \sigma_y \cdot t_d \cdot dx \quad (C-1)$$

The total component T_{d1} of the membrane force in the transverse direction (i.e. in the direction of the strike) is found by integrating the transverse component of T_x over the distorted depth, i.e.,

$$T_{d1} = \int_0^w \sigma_y t_d \sin \psi_x dx \cong \int_0^w \sigma_y t_d \frac{x}{b} dx = \sigma_y t_d \frac{W^2}{2b} \quad (C-2)$$

Similarly, for the other side we get,

$$T_{d2} = \sigma_y t_d \frac{W^2}{2a} \quad (C-3)$$

The total energy absorbed in plastic in-plane stretching of the plating is therefore:

$$E_2 = \int_0^W T_{d1} dW + \int_0^W T_{d2} dW = \frac{1}{6} \sigma_y t_d W^2 \left(\frac{1}{a} + \frac{1}{b} \right) \tag{C-4}$$

With further rearrangement the equation becomes:

$$E_2 = \frac{1}{3} \sigma_y \left(\frac{W}{L} \right)^2 R_{T2} B \tag{C-5}$$

where R_{T2} represents the volume of the distorted part of the deck plating during this phase and is given by:

$$R_{T2} = W t_d L \tag{C-6}$$

$$B = \frac{L^2}{a \cdot b} \text{ as given before in Appendix B.}$$

For mid-span strike, $a = b = L$ and $B = 1$, therefore,

$$E_2^o = \frac{1}{3} \sigma_y \left(\frac{W}{L} \right)^2 R_{T2} \tag{C-7}$$

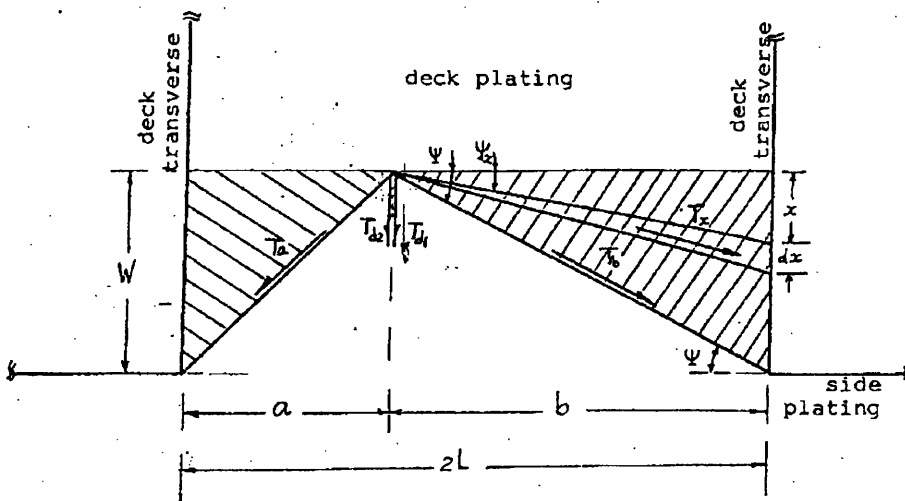


Figure C.1: Membrane tension force in decks.

Appendix D

Buckling Strength of Deck Structures

D1 Energy Absorbed due to Buckling of Deck Structure

Let us assume that at failure the whole deck plating area is subjected to a uniform compressive stress of average value equal to $\Phi_d \sigma_y$, where Φ_d is a strength factor depending on the scantlings of the deck structure and the system of framing used (see subsection D2 below).

Consider the right side of Figure D1. The force T_b in the direction of the strike is given by:

$$T_b = \overline{T}_b \cdot \cos \psi = \Phi_d \sigma_y t_d dx \frac{x}{\sqrt{x^2 + W_x^2}} = \Phi_d \sigma_y t_d dx \frac{1}{\sqrt{1 + \left(\frac{W_x}{x}\right)^2}}$$

Assuming $\frac{W_x}{x}$ is small, then

$$T_b = \Phi_d \sigma_y t_d dx \cdot \left(1 - \frac{1}{2} \frac{W_x^2}{x^2}\right) \quad (D-1)$$

The increment of buckling energy δE_b will be

$$\delta E_b = \int T_b dW_x = \frac{1}{2} \Phi_d \sigma_y t_d \left(W_x - \frac{1}{3} \frac{W_x^3}{x^2} \right) dx$$

Substitute for $W_x = \frac{W}{b} \cdot x$ and integrate over the length b we get:

$$E_b = \frac{1}{4} \Phi_d \sigma_y t_d \frac{W}{b} \left(1 - \frac{1}{3} \frac{W^2}{b^2} \right) b^2 \quad (D-2)$$

Similarly for the other side we have:

$$E_a = \frac{1}{4} \Phi_d \sigma_y t_d \frac{W}{b} \left(1 - \frac{1}{3} \frac{W^2}{a^2} \right) a^2 \quad (D-3)$$

The total energy (E_3) absorbed by buckling of deck structure is therefore,

$$E_3 = E_a + E_b$$

Using equations (D-2) and (D-3) and with further rearrangement we finally get:

$$E_3 = \frac{1}{2} \Phi_d \sigma_y R_{T3} \left(1 - \frac{1}{3} \frac{W^2}{L^2} B \right) \quad (D-4)$$

where,

$$R_{T3} = W t_d L$$

$$B = \frac{L^2}{a \cdot b}$$

For mid-span strike $a = b = L$ and $B = 1$, therefore:

$$E_3^o = \frac{1}{2} \Phi_d \sigma_y \left(1 - \frac{1}{3} \frac{W^2}{L^2} \right) R_{T3} \quad (D-5)$$

D2 Determination of the Ultimate Strength Factor Φ

Considering the idealised models of deck structures with transverse and longitudinal systems of framing given in Table D1. Two modes of failure are to be considered:

- a) Buckling of plate surrounded by stiffeners (local buckling)
- b) Buckling of the whole stiffened panel (overall buckling)

Local buckling of stiffeners is not considered because it has not appeared to be significant in collision tests.

The proposed formulae for calculating the local buckling stress, (σ_{cr}) and overall buckling stress $(\overline{\sigma_{cr}})$ are listed in Table D1 for different systems of deck structures. After the values of (σ_{cr}) and $(\overline{\sigma_{cr}})$ have been calculated the ultimate load which the deck plating can support is obtained in the following manner:

1. In the case of $(\sigma_{cr}) < (\overline{\sigma_{cr}})$ buckling of the plate between stiffeners occurs, but this buckling does not represent a true limit to the load carrying capacity of the deck panel. The load increases until the stress of the effective width of the plate

reaches the yield stress (σ_y). The maximum stress ($\overline{\sigma_m}$) which can be carried by the panel in this case may be estimated using the following formula:

$$\overline{\sigma_m} = \sqrt{\sigma_{cr} \cdot \sigma_y} \quad (D-6)$$

2. In case of ($\overline{\sigma_{cr}} < \sigma_{cd}$), overall buckling of the deck panel occurs and the panel cannot support any more load, i.e.

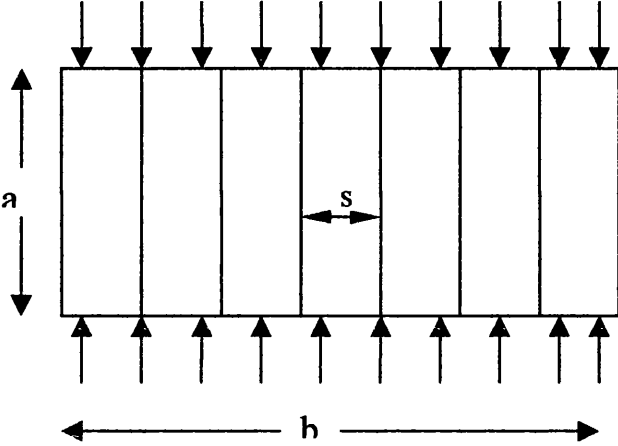
$$\overline{\sigma_m} = \overline{\sigma_{cr}} \quad (D-7)$$

In both cases the ultimate strength factor Φ will be given by:

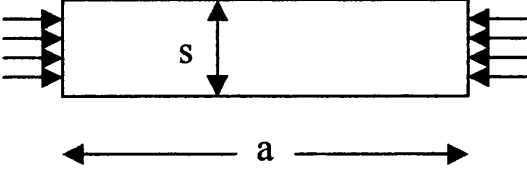
$$\Phi = \frac{\overline{\sigma_m}}{\sigma_y} \quad (D-8)$$

It should be pointed out, that case (1) might apply to a deck structure with longitudinal system of framing (since the overall buckling in this case is so unlikely), while case (2) might apply to a transverse system of framing.

Table D1: Calculation of the critical buckling strength of deck structures.

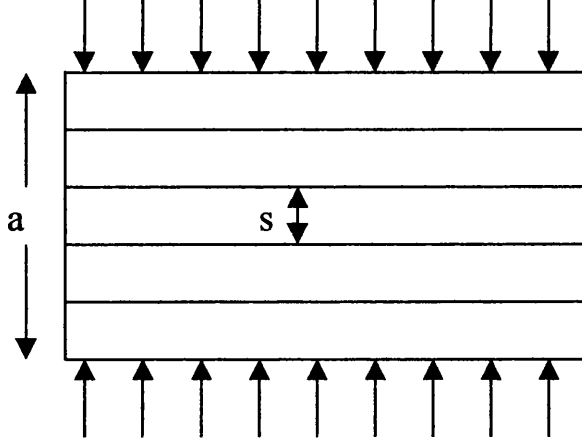
Transverse System of Framing Overall Buckling of Deck Structure	
	
$\bar{\sigma}_{cr} = \min_m \frac{\pi^2}{b^2 \left(t + \frac{A}{s} \right)} \left[D_1 \left(\frac{mb}{a} \right)^2 + 2D_3 + D \left(\frac{a}{mb} \right)^2 \right]$	
<p>m = buckling number</p> <p>$b = 2L$ = distance between web frames</p> <p>a = distance between ship's side and the nearest deck girder</p> <p>A = deck beam cross sectional area</p> $D_1 = \frac{EI_1}{1 - \mu_1 \mu_2} \quad D = \frac{Et^3}{12(1 - \mu^2)} \quad D_3 = \frac{1}{2}(\mu_1 D_2 + \mu_2 D_1) + 2D_t$ $D_t = G_{12} \frac{t^3}{12} \quad G_{12} = \frac{E}{2(1 + \sqrt{\mu_1 \mu_2})}$ <p>t = deck plating thickness</p> <p>I_1 = moment of inertia of deck beam</p> <p>s = spacing between deck beams</p>	

Transverse System of Framing
Local Buckling of Deck Structure



$$\sigma_{cr} = \frac{4\pi^2 D}{ts^2}$$

Longitudinal System of Framing
Overall Buckling of Deck Structure



$$\overline{\sigma}_{cr} = \min_m \frac{\pi^2}{b^2 t} \left[D \left(\frac{mb}{a} \right)^2 + 2D_3 + D_2 \left(\frac{a}{mb} \right)^2 \right]$$

$$D_2 = \frac{EI_2}{1 - \mu_1 \mu_2}$$

I_2 = moment of inertia of deck longitudinal

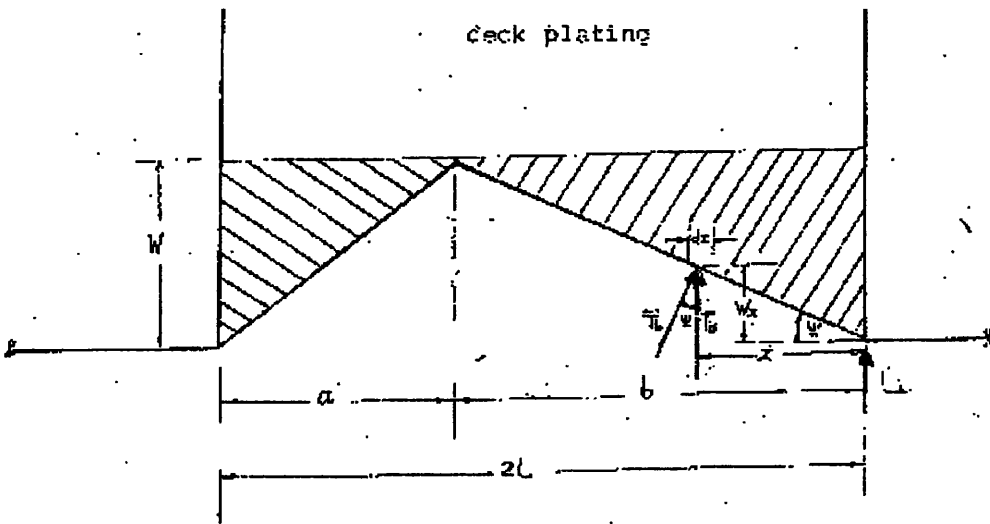
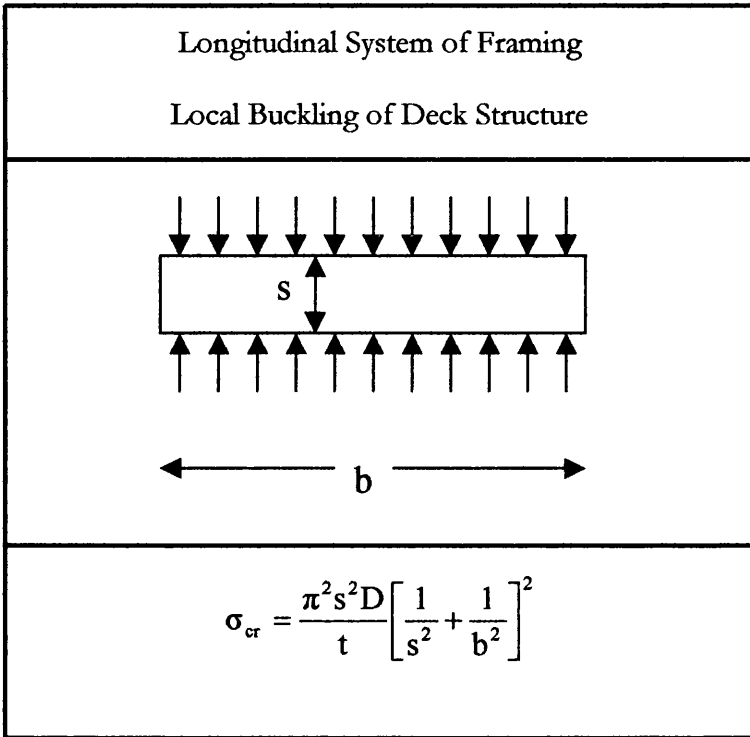


Figure D1: Buckling of deck plating

Appendix E

Calculation of the limiting value of the indentation beyond which rupture of the hull occurs

By assuming that the deflection profile is a triangle and using small deflection geometry McDermott et al. (1974) give the following approximate expression for indentation at rupture:

$$W_L = \sqrt{\frac{2 \cdot a \cdot b}{2 \cdot L} (a \cdot \varepsilon_a + b \cdot \varepsilon_b) + W_b^2} \quad (\text{E-1})$$

where,

$\varepsilon_a, \varepsilon_b$ = strains in legs a and b (see Figure E1)

W_b = maximum deflection during bending phase ($\approx 0.15W_L$, negligible)

On the other hand, from the condition of geometric compatibility the following relations between W , ε_a and ε_b exist (see Figure E1):

$$a^2(\varepsilon_a + 1)^2 - a^2 = W = b^2(\varepsilon_b + 1)^2 - b^2$$

which leads to:

$$\varepsilon_b^2 + 2\varepsilon_b = (\varepsilon_a + 2\varepsilon_a) \cdot \left(\frac{a}{b}\right)^2 \quad (\text{E-2})$$

According to the failure criteria used rupture will occur when the ultimate value of strain (ϵ_u) of the steel is reached. Since the strain in the shorter leg “a” will be greater than that in leg “b”, then:

$$\epsilon_a = \epsilon_u \tag{E-3}$$

By neglecting ϵ_b^2 equation (E-2) will yield:

$$\epsilon_b = \frac{1}{2} \epsilon_u (1 + 2\epsilon_u) \cdot \left(\frac{a}{b}\right)^2 \tag{E-4}$$

Using equations (E-1), (E-3) and (E-4) the value of the limiting indentation (W_L) can be expressed in terms of the ultimate strain ϵ_u .

For mid-span impact the relation between W_L and ϵ_u can be obtained directly from equation (E-1) by neglecting W_b and putting $a = b = L$ and $\epsilon_a = \epsilon_b = \epsilon_u$.

$$W_L = L \cdot \sqrt{2 \cdot \epsilon_u} = 1.414 \cdot L \cdot \sqrt{\epsilon_u} \tag{E-5}$$

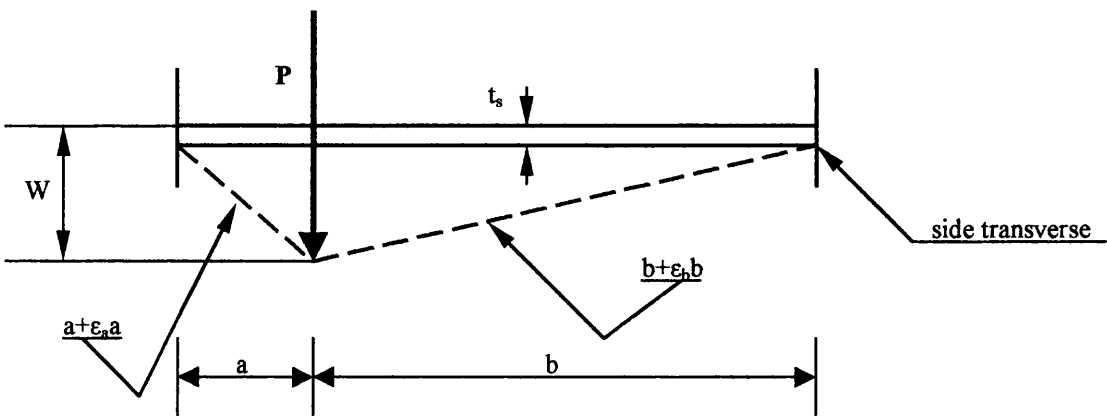


Figure E1: model of the side shell plating during impact.

